Energy, Mines and Resources • *Yukon Geological Survey*

YUKON
EXPLORATION & GEOLOGY

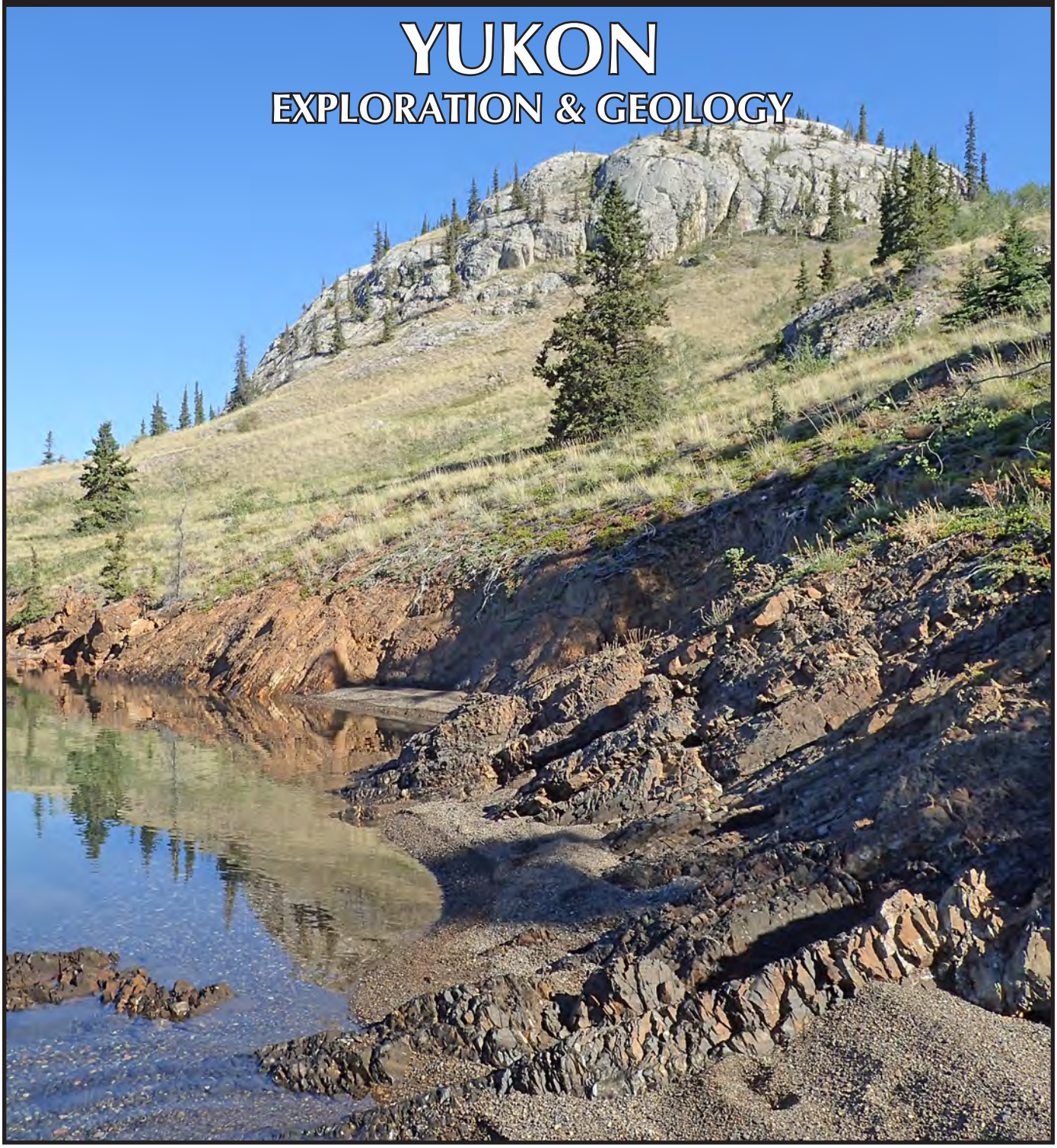

YUKON GEOLOGICAL SURVEY

Yukon
Energy, Mines and Resources

Yukon Geological Survey staff: (standing, left to right): Robert Deklerk, Scott Casselman, Derek Torgerson, Tiffani Fraser, Patrick Sack, Maurice Colpron, Brett Elliot, Karen MacFarlane, Jeff Bond, Kristen Kennedy, Steve Israel, Rosie Cobbett, Julie Minor, Olwyn Bruce, Panya Lipovsky, David Moynihan; (kneeling, left to right) Carolyn Relf, Lara Lewis, Leyla Weston, Sydney van Loon, Midori Kirby
Missing from photo: Bailey Staffen, Esther Bordet, Craig Nicholson, Sue Roy

YUKON
EXPLORATION & GEOLOGY
2017

Edited by

K.E. MacFarlane

Yukon Geological Survey

Energy, Mines and Resources

Government of Yukon

Published under the authority of the Department of Energy, Mines and Resources, Government of Yukon ***http://www.emr.gov.yk.ca*****.**

Printed in Whitehorse, Yukon, 2018.

Publié avec l'autorisation du Ministères de l'Énergie, des Mines et des Ressources du gouvernement du Yukon, ***http://www.emr.gov.yk.ca*****.**

Imprimé à Whitehorse (Yukon) en 2018.

ISSN 1718-8326

This, and other Yukon Geological Survey publications, may be obtained from:
Yukon Geological Survey
102-300 Main Street
Box 2703 (K-102)
Whitehorse, Yukon, Canada Y1A 2C6

phone (867) 667-3201, e-mail ***geology@gov.yk.ca***

Visit the Yukon Geological Survey website at ***www.geology.gov.yk.ca*****.**

In referring to this publication, please use the following citation:
Yukon Geological Survey, 2018. Yukon Exploration and Geology 2017, K.E. MacFarlane (ed.), 2018. Yukon Geological Survey, 163 p.

Front cover photograph: Pale grey limestone of the Upper Triassic Lewes River Group is thrust over brown weathering, thin bedded mudstone of the Lower-Middle Jurassic Laberge Group; east shore of Lake Laberge. Photo by Esther Bordet, Yukon Geological Survey.

PREFACE

Yukon Exploration and Geology (YEG) papers and the Yukon Exploration and Geology Overview continue to be the main publications of the Yukon Geological Survey (Energy, Mines and Resources, Government of Yukon). Individual YEG papers, with colour images, are only available in digital format and can be downloaded from our website. The YEG Overview is available in digital format and in a limited colour print run.

YEG 2017 contains up-to-date information on mining and mineral exploration activity, studies by industry and results of recent geological field studies. Information in this volume comes from prospectors, exploration and government geologists, mining companies and students who are willing to contribute to public geoscience for the benefit of the scientific community, general public and mineral and petroleum industries of Yukon. Their work is appreciated.

Many of the papers submitted have been authored or reviewed by colleagues at the Yukon Geological Survey - thank you for being involved and making production of this publication easier.

Sherry Tyrner of the Queen's Printer ensured that the printing process went smoothly.

We welcome any input or suggestions that you may have to improve future YEG publications. Please contact me at (867) 667-8519, or by e-mail at karen.macfarlane@gov.yk.ca.

Karen MacFarlane

TABLE OF CONTENTS

Bedrock geology of the Teslin Mountain and east Lake Laberge areas, south-central Yukon

E. Bordet
Yukon Geological Survey

Bordet, E., 2018. Bedrock geology of the Teslin Mountain and east Lake Laberge areas, south-central Yukon. *In:* Yukon Exploration and Geology 2017, K.E. MacFarlane (ed.), Yukon Geological Survey, p. 1-24.

ABSTRACT

Mafic volcanic and clastic strata of the Middle Triassic Joe Mountain Formation, east of Lake Laberge, Yukon, represent a juvenile volcanic arc sequence. Mafic volcanic rocks of the Upper Triassic Lewes River Group were formed in the spatial and temporal continuity of Joe Mountain volcanism. Carbonate sedimentation took place in shallow oceanic subbasins adjacent to the arc from the Carnian to Rhaetian; these subbasins were separated by physiographic boundaries inherent to the arc, resulting in lateral stratigraphic variations. Polymictic conglomerate and turbiditic sequences of the Lower-Middle Jurassic Laberge Group unconformably overlie Triassic rocks. Two north-northwest strike-slip faults, the Laurier Creek and the Goddard, control the distribution of units. Joe Mountain Formation rocks are characterized by an east-west structural trend, whereas the Upper Triassic and Jurassic sequences are characterized by north-northwest trending tight folds and thrust faults. At least five post-accretion igneous suites intrude or overlie older stratigraphy, including the Late Cretaceous Open Creek volcanic complex.

* *esther.bordet@gov.yk.ca*

INTRODUCTION

The area located northeast of Whitehorse, east of Lake Laberge, in south-central Yukon, is underlain by arc-related, volcano-sedimentary rocks that are part of Stikinia (Fig. 1), and post-accretion sedimentary rocks and plutons. The Middle Triassic Joe Mountain Formation (Hart, 1997) and Upper Triassic Lewes River Group (Bostock and Lees, 1938; Lees, 1934; Tempelman-Kluit, 1984, 2009; Tozer, 1958; Wheeler, 1961) are unconformably overlain by the Early-Middle Jurassic Laberge Group, which defines the Whitehorse trough (Fig. 1; Wheeler, 1961; White *et al.*, 2012). Several post-accretion, Early to Late Cretaceous plutons intrude older stratigraphy and are locally associated with mineral occurrences.

This paper presents field observations gathered from 2015 to 2017 as part of a 1:50 000-scale bedrock mapping project covering parts of the Teslin Mountain (NTS 105E/2), Lake Laberge (NTS 105E/3) and Lower Laberge (NTS 105E/6) map areas. The project area also includes part the Joe Mountain map sheet (105D/15). Rock units in the Joe Mountain area were reviewed, but no modification was made to the mapping conducted by Hart and Hunt (1994, 2003). Preliminary observations and interpretations from the Teslin Mountain area were presented in Bordet (2016a). Data collected the following year along the east shore of Lake Laberge (NTS 105E/3 and 6) provide a detailed framework for the internal stratigraphy and structure of the Lewes River Group (Bordet, 2017a). This paper provides the latest interpretation of the stratigraphy and relationships between the Joe Mountain Formation, the Lewes River Group and the Laberge Group, as well as new data from samples collected from Early to Late Cretaceous plutons, dikes and volcanic strata.

This paper addresses the following points:

- Five volcanic, volcaniclastic and sedimentary units are defined as part of the Joe Mountain Formation. The units exposed north and northwest of Teslin Mountain were revisited during the summer of 2017. The area displays complex deformation and geology, combined with a lack of exposure along the valley where contacts should be exposed. In particular, a sequence of fine-grained clastic sedimentary rocks underlies the mafic volcanic rocks, suggesting the existence of a basin prior to Joe Mountain volcanism. This clastic sequence also underlies coarse volcanic conglomerate, volcanic sandstone and minor basalt that were originally attributed to the Late Triassic Lewes River Group. Recent reinterpretation of stratigraphic and structural relationships in this area suggests that the coarse volcaniclastic package must be part of the Middle Triassic Joe Mountain Formation. While rock descriptions remain the same as in the previous years, the interpretation presented in this paper supersedes those found in previous work by Bordet (2016a,b and 2017a).
- Nine units are interpreted as part of the Lewes River Group, including by a basal volcanic mafic sequence, and a younger laterally variable carbonate sequence. The internal stratigraphy of the group is now supported by detailed mapping, combined with fossil analyses and detrital zircon geochronology. Lateral variations within the carbonate sequence may result from synchronous sedimentation in isolated subbasins, controlled by the physiography of a central volcanic arc highland.
- Individual dikes with a range of compositions and textures were mapped over the course of three summers. Preliminary investigations of these dikes include petrography, geochemistry and geochronology work. While detailed analyses are not presented here, field descriptions and preliminary results highlight the lithological, compositional and temporal diversity of this discrete, but pervasive igneous system. Results suggest at least three distinct episodes of igneous activity took place in the Early, middle and Late Cretaceous. Some of these intrusions are suspected to be related to mineralizing events.
- The Late Cretaceous Open Creek volcanic complex located north of Teslin Mountain was mapped in detail for the first time. At least four volcanic map units were identified, and samples were collected for petrography, geochemistry and geochronology to better constrain the nature of the volcanic rocks and their relationship with other Late Cretaceous magmatic suites in Yukon. This dominantly silicic pyroclastic volcanic sequence is spatially and temporally associated with the Late Cretaceous Teslin Mountain pluton.

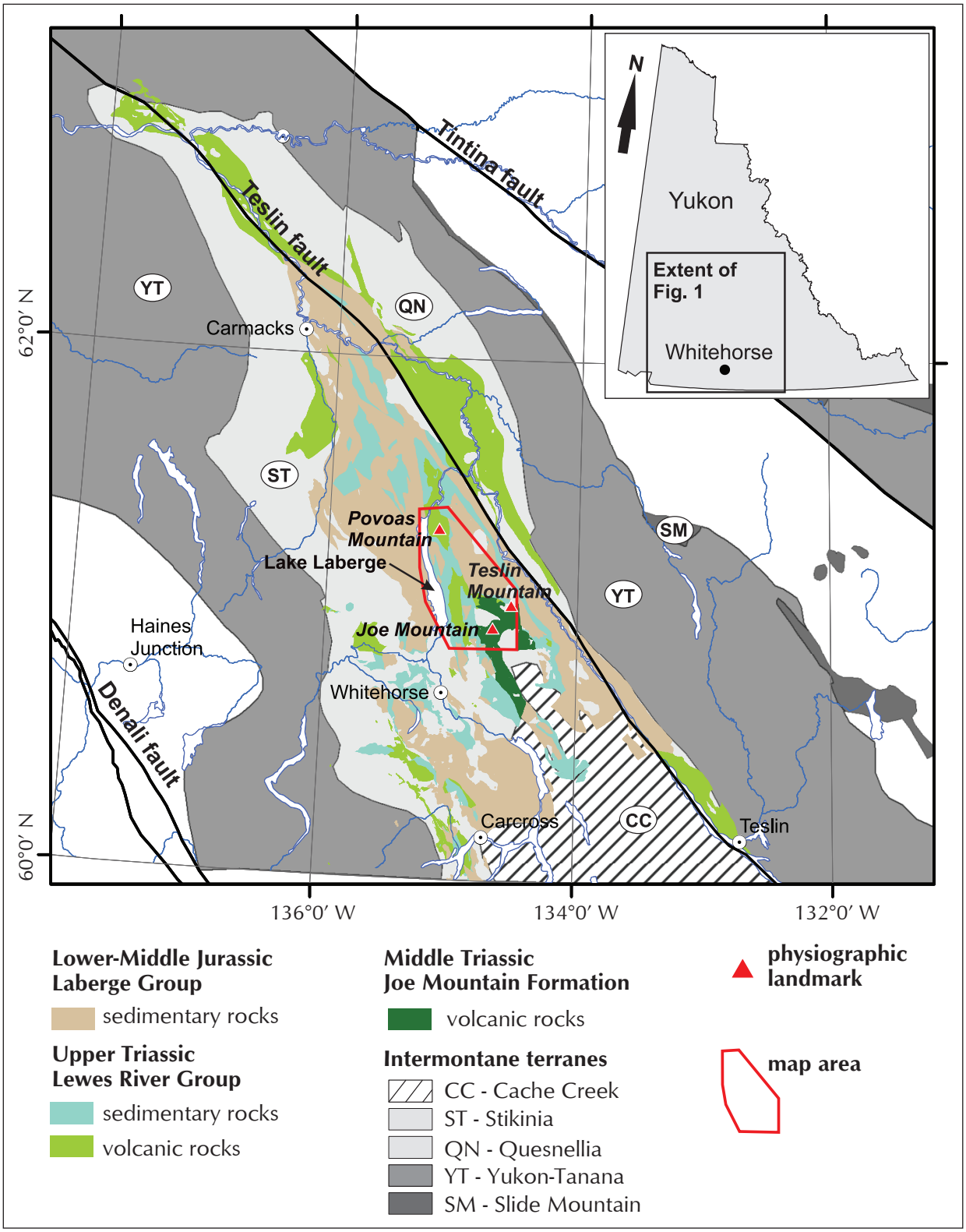

Figure 1. *Terrane map of south-central Yukon showing the distribution of Intermontane terranes and Triassic to Middle Jurassic geology of the Whitehorse trough. Red polygon on figure delineates the mapped area, and includes parts of Teslin Mountain (105E/2), Lake Laberge (105E/3) and Lower Laberge (105E/06) map sheets. Physiographic landmarks referred to in text are indicated. Terrane boundaries after Colpron and Nelson (2011). Laberge Group rocks extent correspond to the Whitehorse trough (after Hutchison, pers. comm., 2015).*

TECTONIC SETTING

The Intermontane terranes underlie most of south-central Yukon and British Columbia southwest of the Tintina fault (Fig. 1). They represent the largest amalgamation of crustal fragments that accreted to the North American margin during the Mesozoic (Coney *et al.*, 1980). In Yukon, the outer margin of the Intermontane terranes is defined by middle Paleozoic (and older) metasedimentary and metavolcanic rocks of the Yukon-Tanana terrane (Fig. 1; Mortensen and Jilson, 1985; Mortensen, 1992). The core and bulk of the Intermontane terranes comprise Mesozoic volcanic arc rocks of Stikinia and Quesnellia (Fig. 1; Colpron and Nelson, 2011; Wheeler *et al.*, 1991), which are juxtaposed along the Teslin fault north of Whitehorse (Fig. 1). Upper Paleozoic to lower Mesozoic accretionary complex rocks of the Cache Creek terrane (*e.g.*, Monger *et al.*, 1991; Struik *et al.*, 2001) are surrounded by Stikinia and Quesnellia (Fig. 1) and extend south of Whitehorse to northern British Columbia. To date, Cache Creek rocks have not been identified north of Whitehorse (Bickerton *et al.*, 2013).

Subduction of the Panthalassa Ocean along the North American margin during the Mesozoic produced volcanic arcs of Stikinia and Quesnellia (Mihalynuk *et al.,* 1994). In south-central Yukon, arc volcanism and arc-related basinal sedimentation are recorded by Middle and Upper Triassic volcanic and sedimentary rocks of Stikinia, namely the Joe Mountain Formation and Lewes River Group (Wheeler, 1961; Hart, 1997).

Erosion of Stikinia and Quesnellia arcs and their plutonic roots from the Early to Middle Jurassic resulted in the deposition of up to 3000 m of sediments of the Lower to Middle Jurassic Laberge Group in the Whitehorse trough (*e.g.*, Wheeler, 1961; White *et al.*, 2012). The Whitehorse trough extends approximately 650 km, from Dease Lake, British Columbia to north of Carmacks in central Yukon. The Whitehorse trough originally developed as a forearc basin and evolved into a northwest-trending, synorogenic, intermontane piggy-back transpressional basin by Middle Jurassic (Colpron *et al.*, 2015; White *et al.*, 2012).

Ongoing eastward subduction of Pacific plates beneath North America during the Cretaceous led to progressive thickening and shortening of the crust, associated with orogen-parallel dextral displacements (Nelson *et al.*, 2013). In this dominantly transpressional and transtensional orogen, corridors of deformation provided pathways for post-accretionary arc-activity and the emplacement of a number of mineral occurrences (Nelson *et al.*, 2013).

REGIONAL GEOLOGY

In south-central Yukon, the Middle Triassic Joe Mountain Formation and Upper Triassic Lewes River Group of Stikinia comprise coherent, massive to flow-banded or pillowed, subalkaline tholeiitic to calc-alkaline basalt and basaltic andesite, as well as a range of volcaniclastic units (Hart, 1997). In addition, the Lewes River Group comprises a thick sedimentary and volcaniclastic sequence, including thick-bedded limestone, calcareous conglomerate, calcareous sandstone/mudstone, and volcaniclastic sandstone, mudstone and conglomerate (Aksala formation; Wheeler, 1961; Hart, 1997; Tempelman-Kluit, 1984, 2009). A summary of regional mapping work and original stratigraphic descriptions of the Joe Mountain Formation and Lewes River Group are provided in Bordet (2016a, 2017a).

The Lower to Middle Jurassic Laberge Group includes shallow marine to fluvial and coal-bearing sandstone, conglomerate and shale of the Tanglefoot formation exposed in the northern part of the Whitehorse trough (Hart, 1997; Lowey, 2005, 2008; Tempelman-Kluit, 1984, 2009). To the south, deep-marine turbidite and mass-flow conglomerate of the Richthofen formation are partly coeval and laterally equivalent to the Tanglefoot formation (*e.g.*, Lowey, 2005; Tempelman-Kluit, 1984, 2009). The Nordenskiöld facies, a distinct crystal-lithic tuff (Tempelman-Kluit, 1984, 2009), occurs at multiple stratigraphic levels in both the Richthofen and Tanglefoot formations, and represents at least three distinct volcanic events between 188 and 186 Ma (Colpron and Friedman, 2008).

The Middle Jurassic Teslin Crossing pluton intrudes the Laberge Group sedimentary strata (Tempelman-Kluit, 1984). Other overlap assemblages include intrusive bodies related to the Whitehorse, Teslin and Rancheria plutonic suites (Colpron *et al.*, 2016; and discussion below). Finally, a few occurrences of the middle Cretaceous Byng Creek volcanic rocks are reported south of Joe Mountain (Hart and Hunt, 1994, 2003; Hart, 1997), and the Upper Cretaceous Open Creek volcanic rocks (Tempelman-Kluit, 1984, 2009) are exposed north of Teslin Mountain.

TRIASSIC STRATIGRAPHY

JOE MOUNTAIN FORMATION (MIDDLE TRIASSIC)

The southeastern part of the map area, east of the Laurier Creek fault, is dominated by coherent pillowed basalt of the Joe Mountain Formation (mTJMb) centered on Joe Mountain and Teslin Mountain, overlain by mafic volcaniclastic deposits (mTJMvc) west of Teslin Mountain (Fig. 2a,b). North of Teslin Mountain, Joe Mountain Formation basalt and fragmental rocks are underlain by clastic, locally thin-bedded and laminated strata (mTJMms). To the north, this clastic sequence is also underlying, or locally thrusted over a volcanic and volcaniclastic assemblage (mTJMbx; Fig. 2a,b). In addition, dark, massive, coarse-grained and locally pegmatitic, pyroxene gabbro and diorite (mTJMg) are reported at Joe Mountain (105D/14; Hart, 1997; Hart and Hunt, 1994, 2003; Fig. 2a,b).

The thickness of the Joe Mountain Formation is estimated at ~3500 m, including an ~1000 m-thick basal sedimentary sequence north of Teslin Mountain, a cumulative thickness of 2000-2300 m for the basalt and volcaniclastic sequence (Bordet, 2016a), and a thickness of at least 500 m for the younger volcaniclastic sequence. Previous thickness estimates indicate at least 3200 m for the Joe Mountain Formation type section at Joe Mountain (Hart and Hunt, 1994, 2003; Hart, 1997).

The Joe Mountain Formation is folded along a consistent E-W structural trend (Fig. 2a). It is locally intruded by middle and Late Cretaceous plutons.

*Coherent basalt (*mTJMb)

The dominant lithology of the Joe Mountain Formation comprises dark grey, grey-green aphyric to microcrystalline coherent basalt and basalt andesite exposed throughout the area between Joe Mountain and Teslin Mountain (Fig. 2a). Coherent mafic rocks overlie thin-bedded clastic strata exposed north of Teslin Mountain, and are overlain by volcaniclastic strata along the western ridge of Teslin Mountain (Fig. 3a, section 1; Bordet, 2016a). The Laurier Creek fault marks the western boundary of the Joe Mountain Formation basalt (Figs. 2a,b and 3b). East of this boundary, the contact between Joe Mountain Formation basalt and the overlying Lewes River Group carbonate sequence is folded (Bordet, 2017a), and is likely a stratigraphic disconformity.

Coherent mafic strata of the Joe Mountain Formation include grey to rusty-brown weathering, dark grey-green, fine to medium-crystalline, locally finely amygdaloidal or vesicular aphyric basalt and basaltic andesite forming thick-bedded (up to 1-2 m), blocky, massive to pillowed lava flows (Bordet, 2016a). The lava is locally plagioclase-phyric (up to 5%), or displays minor pyroxene cumulates. Locally, layers of volcanic breccia and volcaniclastic sandstone are found interbedded with the basalt. Joe Mountain Formation basalt is intruded by several plutons (Fig. 2a), including monzonite and monzodiorite of the middle Cretaceous Laurier Creek pluton (EKgT) and granodiorite of the Late Cretaceous Teslin Mountain pluton (LKgR).

Chlorite alteration is pervasive amongst coherent basalt of the Joe Mountain Formation, and is accompanied by quartz or carbonate veinlets and disseminated pyrite. The unit is magnetite-rich, and the highest magnetic values are measured in layers and clasts of hematite-magnetite iron formation (Figs. 2 and 4; Piercey, 2005).

*Mafic tuff and volcanic breccia (*mTJMvc*)*

To the west and north of Teslin Mountain, an ~100 m thick volcaniclastic sequence includes poorly sorted volcanic conglomerate, volcanic sandstone, and mafic tuff interbedded with minor lenses of calcareous mudstone/sandstone (Figs. 2a and 3a; Bordet, 2016a). This unit overlies the Joe Mountain Formation basalt. Thick-bedded, polymictic, chaotic volcaniclastic conglomerate displays boulder-size clasts (30-50 cm) of quartz-plagioclase-phyric diorite, cherty, glassy, basaltic ash tuff, dark green, finely crystalline basalt, and blocks of red-brick oxidized iron formation (Fig. 4b; Piercey, 2005). The conglomerate is interbedded with orange-brown-grey to tan weathering, pale grey-green, and medium-bedded volcaniclastic sandstone, with angular, dark basalt clasts (2%), and quartz eyes (up to 3%) in a pale grey-green very fine matrix. North of Teslin Mountain, this unit is dominated by south-dipping, pale green weathering, dark green to grey, silicified, laminated, mafic ash tuff (Bordet, 2016a). Mafic ash tuff is interbedded with lenses of pale grey weathered, thin-bedded calcareous mudstone and sandstone. Disseminated pyrite is observed locally.

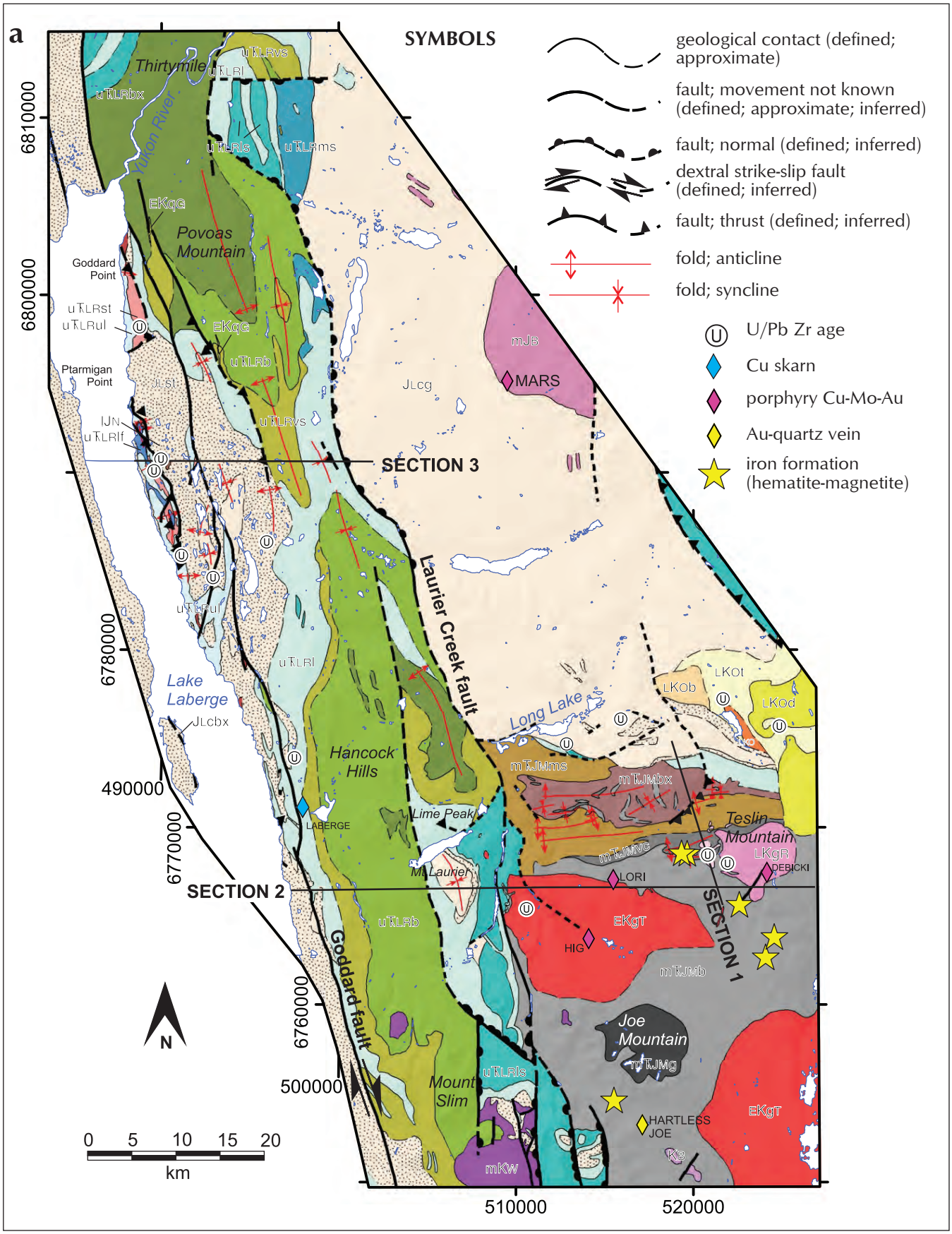
a
SYMBOLS
geological contact (defined; approximate)
fault; movement not known (defined; approximate; inferred)
fault; normal (defined; inferred)
dextral strike-slip fault (defined; inferred)
fault; thrust (defined; inferred)
fold; anticline
fold; syncline
U/Pb Zr age
Cu skarn
porphyry Cu-Mo-Au
Au-quartz vein
iron formation (hematite-magnetite)
Thirtymile
Yukon River
Povoas Mountain
Goddard Point
Ptarmigan Point
MARS
SECTION 3
SECTION 2
SECTION 1
Laurier Creek fault
Goddard fault
Lake Laberge
Hancock Hills
Lime Peak
Mt Laurier
Long Lake
Teslin Mountain
Joe Mountain
Mount Slim
LABERGE
LORI
DEBICKI
HIG
HARTLESS JOE
N
0 5 10 15 20
km
6810000
6800000
6780000
6770000
6760000
490000
500000
510000
520000

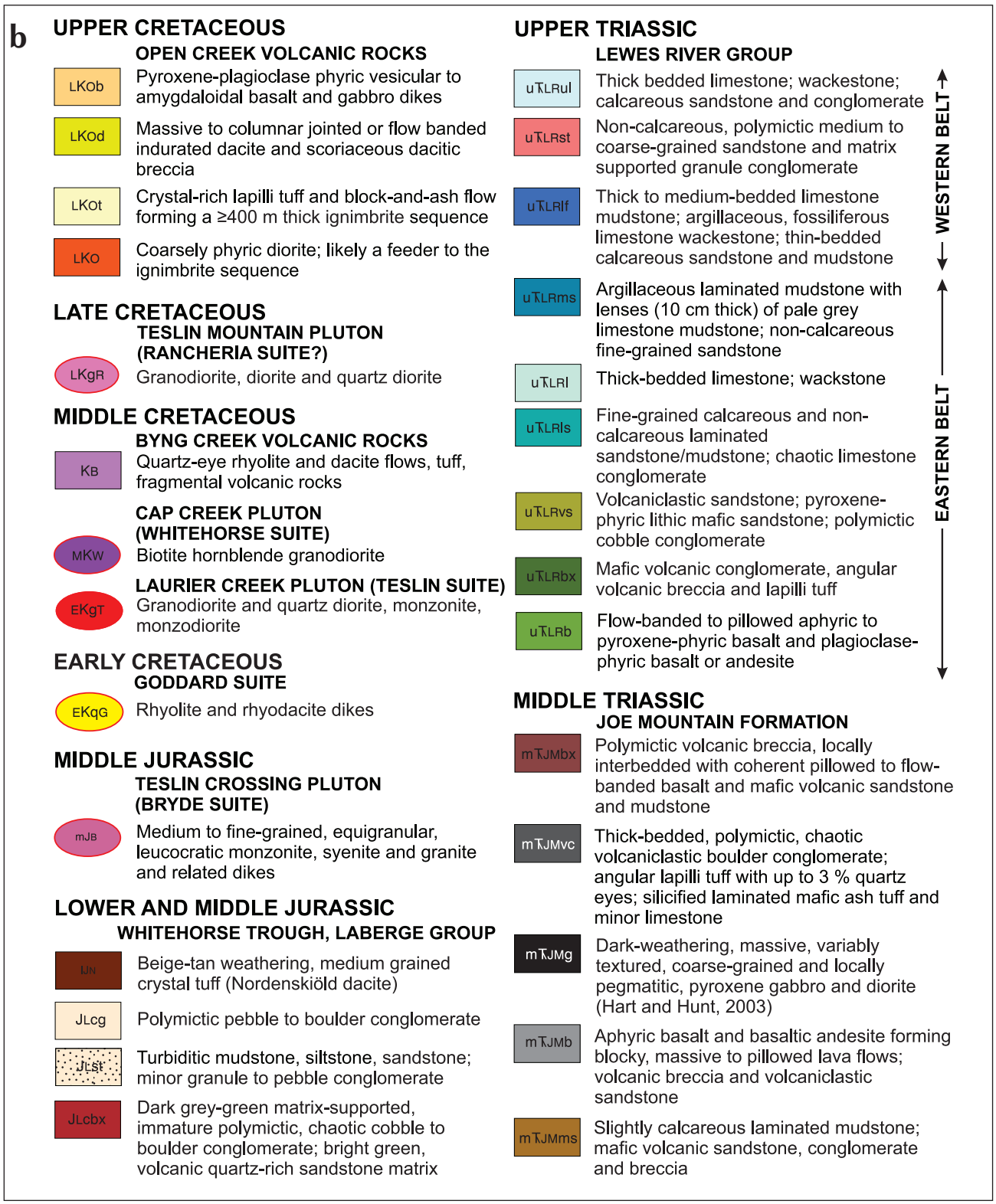

Figure 2. *Geology of parts of the Teslin Mountain (105E/2), Lake Laberge (105E/3) and Lower Laberge (105E/6) areas based on 1:50000-scale mapping conducted during the summers of 2015-2017. Mineral occurrences from Yukon MINFILE (2015). Grid in UTM zone 8, NAD 83.* ***(a)*** *Bedrock geology map; and* ***(b)*** *legend. Sections are on Figure 3.*

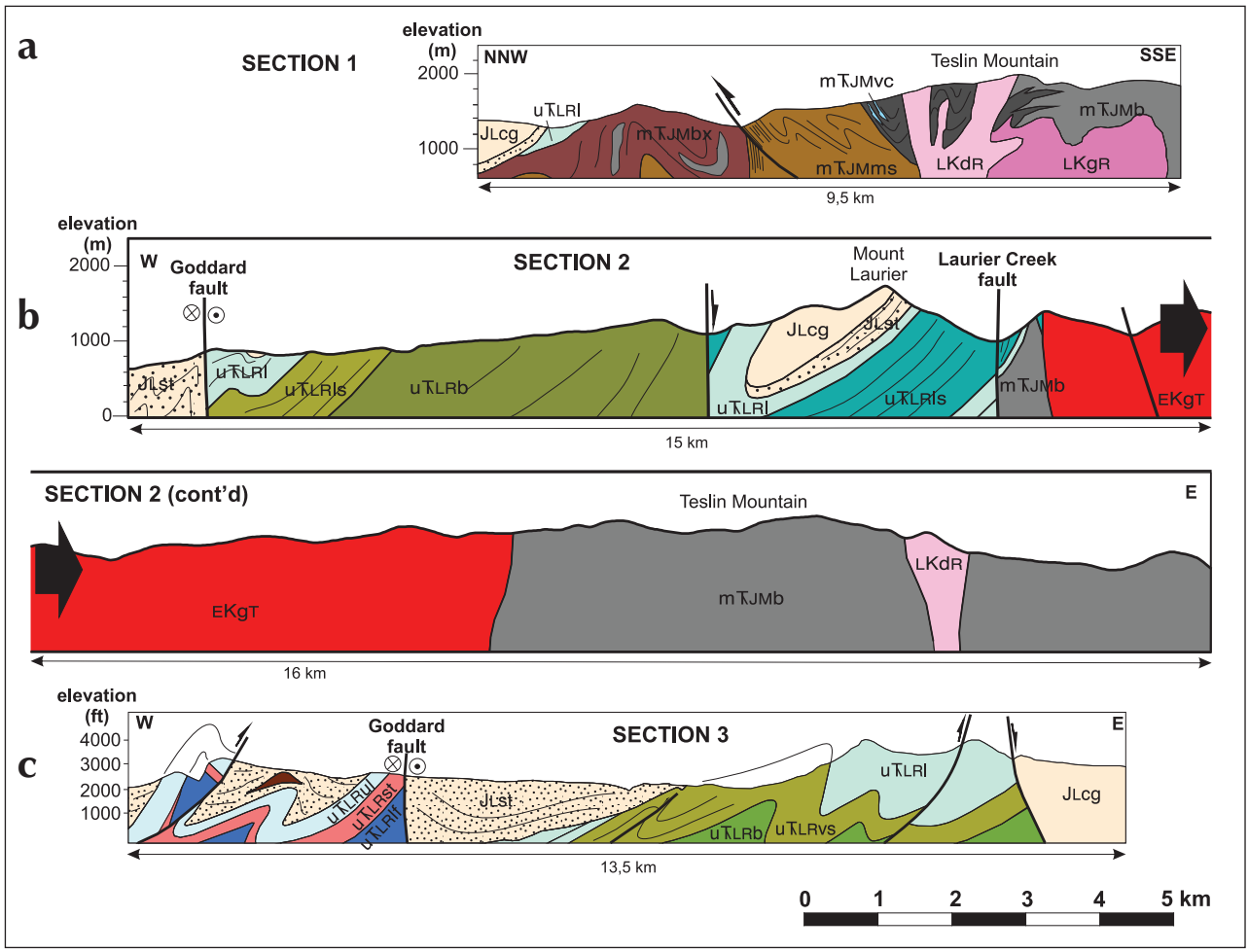

Figure 3. *Schematic geological cross sections illustrating stratigraphic and structural relationships in the map area;* ***(a)*** *section 1 is located across the Joe Mountain Formation at Teslin Mountain (NNW-SSE);* ***(b)*** *section 2 (W-E) is along the Mount Laurier-Teslin Mountain axis (6766440 N); and* ***(c)*** *section 3 (W-E) is located north of the Hancock Hills (6790660 N). See Figure 2a for section lines.*

Clastic sedimentary sequence (mTJMms)

A newly defined, dominantly clastic sedimentary sequence underlies mafic and volcaniclastic strata of the Joe Mountain Formation north of Teslin Mountain (Fig. 2a). North of Teslin Mountain, the clastic sedimentary strata display a consistent southern dip. Contact with mafic volcaniclastic rocks (mTJMvc) to the south is interpreted as conformable, whereas the contact to the north with volcanic conglomerate and breccia (mTJMbx) is interpreted as a thrust fault (Fig. 3a). The sequence is continuously exposed along the northern flank of Teslin Mountain's westernmost ridge, and presumably underlies an east-west trending valley covered by vegetation and thick glacial fluvial terraces. The sequence outcrops again south of Long Lake (Fig. 2a). The Laurier Creek fault marks the westernmost boundary of this sequence, and it is not exposed past Long Lake to the north.

The sequence comprises slightly calcareous, laminated mudstone/sandstone, mafic volcanic sandstone, conglomerate and breccia. A south dipping sequence of rusty-brown weathering, dark grey to pale grey-green, thin to medium-bedded, fine-grained, slightly calcareous laminated mudstone/sandstone is exposed north of Teslin Mountain and is up to 100 m thick. The same thin-bedded, laminated mudstone lithology is exposed along steeply dipping beds south of Long Lake. This lithology contains less than 1% disseminated sulphides. Coarse, matrix-supported, angular volcanic conglomerate made of volcanic clasts and dark brown, very fine mudstone clasts in a sandstone rich matrix, contains thick interbeds of

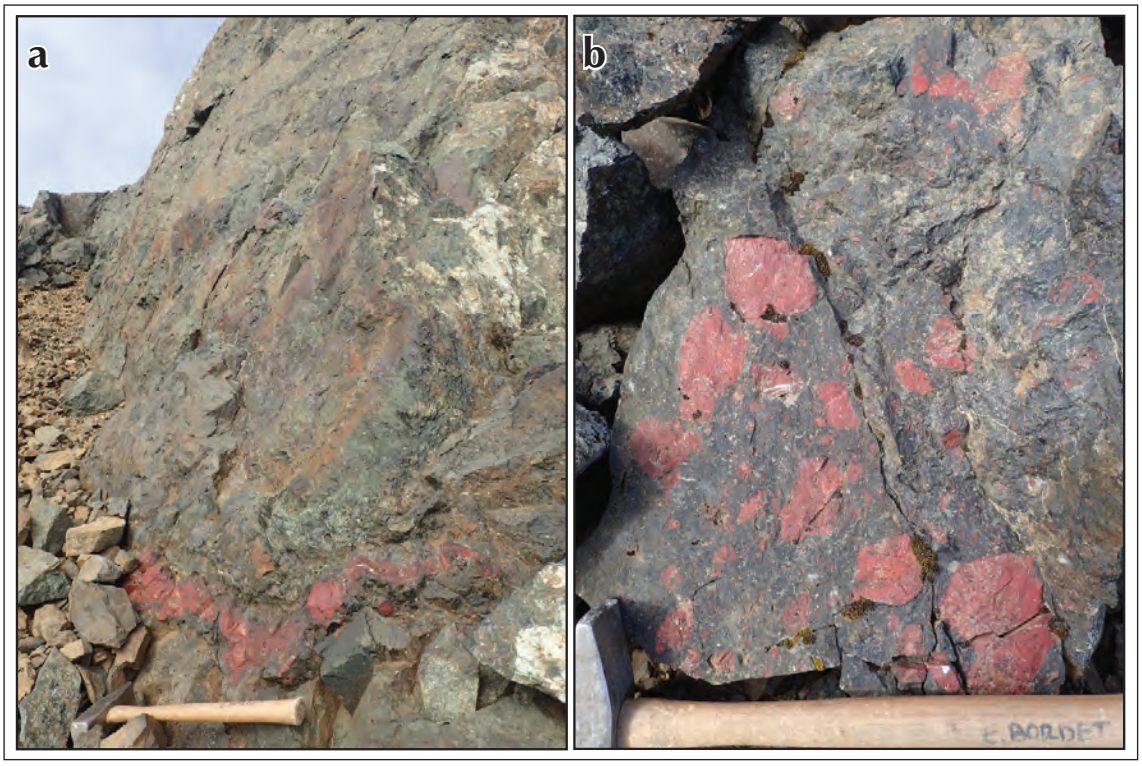

Figure 4. *Iron formation within the Joe Mountain Formation basalt at Teslin Mountain,* ***(a)*** *layer of hematite-magnetite with a coherent basalt sequence; and* ***(b)*** *clasts of the iron formation within the volcaniclastic unit (*mTJMvc*) at Teslin Mountain.*

laminated sandstone. Brown-grey weathering, calcareous sandstone to pebble conglomerate are found immediately north of the contact with Joe Mountain Formation basalt at Teslin Mountain, and contains rounded to subangular clasts of limestone, shell fragments, and fine-grained, dark grey, aphyric or plagioclase-phyric volcanic rock.

This sequence is deformed, as indicated by frequent changes of strike and dip, interpreted as successive, parallel E-W trending folds (Figs. 2a and 3).

*Volcanic breccia and conglomerate (*mTJMbx*)*

A newly defined unit of volcanic conglomerate/breccia, locally interbedded with coherent pillowed to flow-banded basalt and mafic volcanic sandstone/mudstone covers an area ~12 by 4 km on the high alpine ridges between Teslin Mountain and Long Lake (Fig. 2a). This sequence is dominated by thick-bedded (1-5 m), orange-brown-grey weathering, dark green, matrix-supported volcanic breccia and conglomerate. Clasts are subangular to subrounded, range from lapilli to block size, and are poorly sorted. Clast composition is volcanic, but displays textural variability or various degrees of oxidation. They include red oxidized pyroxene or plagioclase-phyric basalt/andesite, vesicular to massive andesite, and lapilli size angular fragments of grey, grey-green to red aphanitic volcanic rock. The conglomerate matrix is a fine-grained, grey to green volcaniclastic sandstone, with ash to lapilli size fragments and disseminated plagioclase and pyroxene crystals. Petrographic observations of the breccia matrix indicate a relatively homogeneous clast composition. Fragmental rocks are locally interbedded with coherent pillowed to flow-banded basalt and mafic volcanic sandstone/mudstone. Frequent changes of dip and a generally consistent east-west bedding strike suggest that this unit is deformed by east-west trending folds similar to those affecting the underlying sedimentary sequence (Figs. 2a and 3).

Gabbro and diorite (mTJMg)

Dark-weathering, massive, variably textured, coarse-grained and locally pegmatitic, pyroxene gabbro and diorite (Fig. 2a) underlies the highest peaks of Joe Mountain (105D/15), where the Joe Mountain Formation was originally defined (Hart and Hunt, 1994, 2003; Hart, 1997). This unit underlies and intrudes microdiorite and basalt flows that form the bulk of the formation (Hart, 1997).

Age and interpretation of the Joe Mountain Formation

Coherent, massive aphyric microcrystalline basalt appears to be underlain by a series of fine-grained, thin-bedded, laminated mudstone/sandstone north of Teslin Mountain. This suggests the existence of a sedimentary basin prior to, or coeval with, Joe Mountain basaltic volcanism. Basalt is generally pillowed, with subaerial, flow-banded, vesicular lava locally observed. Regular lamination within the mafic tuff sequence, interbedded limestone lenses, and the presence of pillows suggests deposition under water for at least part of the formation. A reaction rind surrounds the limestone lenses at the contact with the mafic tuff, suggesting that limestone was incorporated as the tuff was still hot (Bordet, 2016a). The chaotic organization of the volcanic conglomerate and dominant volcanic clast composition indicate that only a minimum amount of reworking took place.

The youngest part of the Joe Mountain Formation is characterized by volcaniclastic conglomerate and breccia, interbedded locally with coherent pillow basalt and volcaniclastic sandstone. Because of similarities to volcaniclastic conglomerate of the Lewes River Group, this unit was originally inferred to be Late Triassic. However, the east-west structural grain reflects deformation observed in the rest of the Joe Mountain Formation, and contrasts with the north-south trend measured in rocks of the younger Lewes River Group. The combined structural relationship, as well as stratigraphic ties, implies that this unit is more likely to represent a volcaniclastic facies of the Joe Mountain Formation.

The Joe Mountain Formation volcanic rocks are dominated by basalt and basaltic andesite. Geochemical signatures are characterized by MORB/BABB and IAT (Bordet, 2017b). Pegmatitic and pyroxene-gabbro and diorite exposed at Joe Mountain likely represent a juvenile subvolcanic intrusion that developed just beneath a volcanic arc centre and was later exposed by erosion.

A preliminary U/Pb zircon age of ~245 Ma (J. Crowley, *pers. comm.,* 2016) was obtained from the laminated mafic tuff of the Joe Mountain Formation volcaniclastic sequence (mTJMvc) at Teslin Mountain. The outcrop comprises brown to grey weathering, fine to coarse-grained, laminated volcanic sandstone/mudstone. This date confirms a Middle Triassic age for the Joe Mountain Formation. It is compatible with Ladinian conodont ages collected at Joe Mountain, about 15 km south of the present study area (Hart and Orchard, 1996; Hart 1997).

LEWES RIVER GROUP (UPPER TRIASSIC)

The Upper Triassic Lewes River Group is exposed along a north-northwest trending belt between Laurier Creek fault and the east shore of Lake Laberge (Fig. 2a). A basal mafic volcanic sequence (~1000 m thick) is overlain by a laterally variable succession of carbonate and clastic sedimentary rocks (~1000-1500 m thick). Nine map units comprising clastic sedimentary, calcareous, volcaniclastic and mafic volcanic strata are defined based on lithology, stratigraphic associations and geographic distribution. Minor adjustment was made to units, but descriptions and the stratigraphic framework for the Lewes River Group remain the same as the one presented in Bordet (2017a).

Limestone strata of the Lewes River Group overlie basalt of the Joe Mountain Formation along Laurier Creek, and volcaniclastic strata of the Joe Mountain Formation south of Long Lake and north of Teslin Mountain (Fig. 2a). The contact between the Lewes River Group and the overlying Laberge Group is marked by an angular unconformity south of Long Lake (Fig. 2a). The overall structural trend in the Upper Triassic sequence is north to north-northwest (Fig. 2a).

The total thickness of the group is >3000 m based on field estimates and map measurements. Previous thickness estimates for the Lewes River Group are from 2100 m (Tozer, 1958) to greater than 3000 m (Hart, 1997).

Mafic volcanic sequence

The volcanic sequence of the Lewes River Group is exposed in the central part of the map area, along a north-south-trending belt extending more than 60 km from

Mount Slim to Povoas Mountain (Fig. 2a). It continues north beyond the limit of the map area past the mouth of the Yukon River. The belt is characterized by a subdued, rolling topography, with extensive and thick tree cover in valleys and rare exposed hill tops in the Hancock Hills. The volcanic sequence is bounded to the east by the Laurier Creek fault and to the west by the Goddard fault. No occurrences of the Lewes River Group volcanic sequence were observed west of the Goddard fault, except for a sliver of coherent, plagioclase-pyroxene-phyric, basalt-andesite in a valley bottom that parallels the inferred trace of the Goddard fault (Bordet, 2017a).

Coherent basalt (uTLRb)

Between the Laurier Creek and Goddard faults, in the Hancock Hills, coherent, flow-banded and pillowed basalt dominate (Bordet, 2016a). The unit comprises coherent, dark green-grey to rusty brown weathering, dark green, flow-banded to pillowed aphyric to pyroxene-phyric basalt and plagioclase-phyric basalt or andesite. Basalt comprises very fine (< 1 mm) plagioclase crystals (1-5%), small brown pyroxene crystals (1%) and minor olivine (<1%) in a finely crystalline aphyric groundmass. Amygdules or sparse small rounded (1-2 mm) to larger irregularly shaped (1-2 cm) vesicles are visible locally. Petrographic observations (Bordet, 2016a) display a porphyritic texture of the basalt, with plagioclase, clinopyroxene and olivine phenocrysts in a microcrystalline, equigranular, plagioclase rich groundmass. Mafic crystals are locally strongly altered to chlorite. Carbonate alteration is pervasive.

*Fragmental facies (*uTLRbx *and* uTLRvs*)*

Coherent basalt is interbedded with various volcanic breccia, volcaniclastic sandstone and conglomerate units. Descriptions of the various volcanic fragmental facies mapped in the Hancock Hills are provided in Bordet (2016a). One distinctive pale green, matrix-supported volcanic breccia with subrounded, pyroxene-phyric basalt blocks forms beds up to 10-20 m thick (Bordet, 2016a). At Povoas Mountain and in the Thirtymile area, angular volcanic breccia and volcaniclastic sandstone dominate (Fig. 5a-c). Brown weathering, red-green, matrix-supported volcanic breccia contains angular, dark green clasts of microcrystalline basalt, in a dark brown, fine-grained plagioclase-rich groundmass.

Carbonate sequence

The region between the Hancock Hills and the east shore of Lake Laberge is underlain by a succession of deformed sedimentary rocks that overlie the basal mafic volcanic sequence. In particular, north to northwest-trending ridges of pale grey weathering, micritic limestone constitute visibly prominent stratigraphic marker beds and structural features. Detailed mapping in 2016 and 2017 allowed the breakdown of a single carbonate sedimentary unit of the Lewes River Group (Hancock member of Tempelman-Kluit, 1984) into six distinct units, distributed in two belts with distinct stratigraphy (Fig. 2a; Bordet, 2017a).

*Eastern carbonate sequence (*uTLRls, uTLRl *and* uTLRlms*)*

A carbonate sequence is exposed on either side of the Lewes River Group mafic volcanic belt (Fig. 2a). The stratigraphic framework includes prominent north to northwest-trending ridges of pale grey micritic limestone east of Mount Laurier, at Lime Peak, and east of Thirtymile (Fig. 2a).

Thin to medium-bedded calcareous mudstone and sandstone (uTLRls) is exposed along the Laurier Creek fault and overlies the Joe Mountain Formation basalt (Bordet, 2017a). Massive to thick-bedded, pale grey weathering, micritic and fossiliferous limestone is particularly well exposed at Lime Peak (uTLRl; Yarnell *et al.,* 1999), as well as along a north-trending belt that extends north and west of the Hancock Hills. It overlies Middle and Upper Triassic volcanic rocks, or is interfingered with other thin-bedded calcareous units. In the centre of the map area, massive limestone is interbedded with tan-grey weathering, clast-supported (locally matrix-supported), non-sorted, pebble to cobble calcareous conglomerate, which also includes lenses of tan-orange weathering, fine-grained calcareous sandstone. The conglomerate comprises subrounded to subangular limestone mudstone clasts in a pale yellow weathering, medium-grained calcareous sandstone matrix. Finally, east of the mouth of the Yukon River at Thirtymile, an east dipping sequence of argillaceous laminated mudstone and fine-grained sandstone is exposed (uTLRms; Fig. 5d-f). It comprises at least three levels of thick–bedded, massive micritic limestone, interbedded with intervals of medium to thin-bedded, brown weathered argillaceous mudstone and fine-grained sandstone.

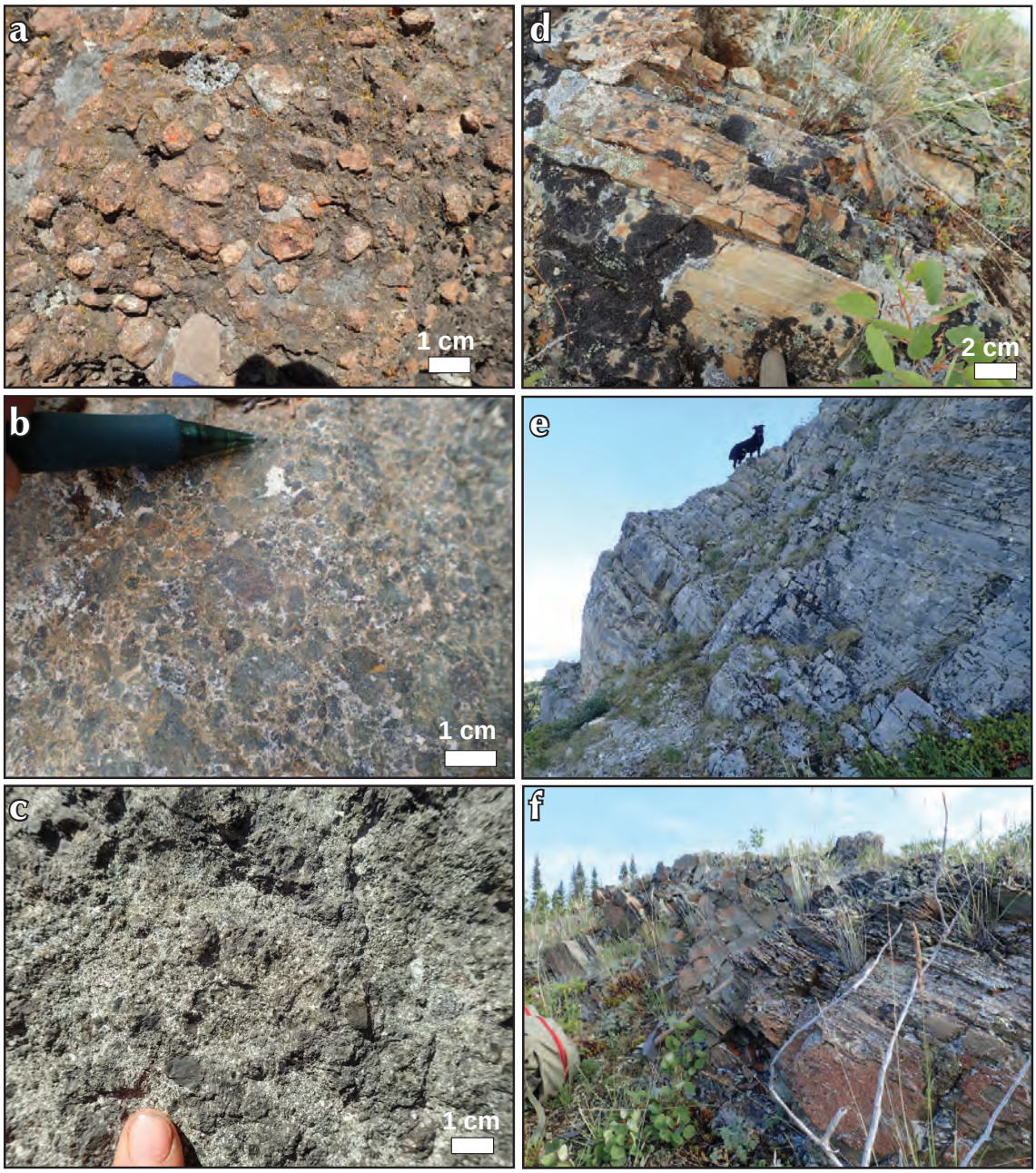

Figure 5. *Field photographs of the Lewes River Group in the Povoas Mountain and Thirtymile area. Fragmental volcanic sequence at Povoas Mountain and east of Thirtymile is illustrated in photos a, b, c. East dipping carbonate sequence east of Thirtymile is illustrated in photos d, e, f.* ***(a)*** *Matrix-supported pebble conglomerate east of Thirtymile. Formed of dark green, mafic matrix and clasts of plagioclase-phyric andesite, limestone mudstone, and red-oxidized volcanic clasts;* ***(b)*** *pale grey-green, matrix-supported, carbonate altered volcanic breccia, clasts are granule to boulder size, angular, made of dark green aphyric lava;* ***(c)*** *matrix-supported, grey-green angular volcanic breccia in the Povoas Mountain area. The matrix is plagioclase-rich and clasts are dark green aphyric to plagioclase-phyric basalt-andesite;* ***(d)*** *east-dipping thinly-bedded, laminated, non-calcareous mudstone;* ***(e)*** *east-dipping medium to thick-bedded, pale grey limestone-mudstone. Lighter colored intervals are very fine grained, argillaceous; and* ***(f)*** *East-dipping, very thin bedded slightly calcareous to non-calcareous mudstone and sandstone.*

*Western carbonate sequence (*uTLRlf, uTLRst, uTLRul*)*

The western part of the map area, exposed along the east shore of Lake Laberge, is characterized by a distinctive carbonate sequence (Fig. 2a,b; Bordet, 2017a). As in the rest of the map area, the stratigraphy includes prominent north to northwest-trending ridges of pale grey micritic limestone.

The following units form the core of an anticlinorium along the east shore of Lake Laberge: a medium-bedded (30-50 cm), argillaceous, fossiliferous (bivalve or brachiopod shells, corals and burrows) limestone wackestone; a thin-bedded, calcareous sandstone and mudstone; and a thick to medium-bedded, pale grey micritic limestone including lenses of rusty weathering, dark grey calcareous mudstone (uTLRlf). These rocks are overlain by 5-10 m of brown to orange weathering, dark grey-green, non-calcareous, medium to coarse-grained sandstone with polymictic, matrix-supported granule conglomerate (uTLRst). A characteristic of this clastic lithology is its high magnetic susceptibility (2-13 S.I.). Overlying this sequence is a very thick bedded, pale grey to orange weathering, dark grey, finely to coarsely crystalline, micritic limestone (uTLRul), which is interbedded with minor bioclastic wackestone (corals, bivalve shells/ brachiopods and crinoids), and minor calcareous sandstone and conglomerate.

Paleoenvironment interpretation

The Lewes River Group comprises a basal mafic volcanic sequence (Povoas formation of Tempelman-Kluit, 1984, 2009), and a carbonate and clastic sedimentary sequence (Aksala formation of Tempelman-Kluit, 1984, 2009). The mafic volcanic sequence is dominated by basalt and basaltic andesite compositions, as well as trachyandesite to tracydacite compositions. Geochemical signatures range from tholeiitic, transitional to calc-alkaline (Bordet, 2017b). This volcanic belt represents an arc sequence developed over and around Middle Triassic volcanic and sedimentary strata of the Joe Mountain Formation. This newer arc formed a significant topographic high, surrounded by a shallow oceanic basin in which carbonate sedimentation took place.

The thick (~2000-2500 m) carbonate sequence overlying mafic volcanic rocks can be divided into at least two belts displaying similar rock types, but spatially distinct stratigraphic successions. Lateral variation in the stratigraphy may result from carbonate sedimentation taking place simultaneously in subbasins separated by natural topographic boundaries controlled by the volcanic physiography. The eastern contact of the western carbonate belt extends to the Goddard fault (Figs. 2a and 3c), suggesting that the rocks originally formed in a shallow subbasin distal from the arc, and were later stacked over and against the eastern carbonate belt during Late Triassic or post Triassic deformation.

Massive micritic limestone strata represent reef buildup structures (Reid, 1980; Yarnell, 1999), whereas calcareous conglomerate likely represents a high-energy zone along the slope in front of the reef. Based on macrofossil analyses, environments of deposition for the carbonate sequence are interpreted as shallow marine (inner platform or shelf) to open marine, with normal salinity and a tropical climate (R. Blodgett, *pers. comm.,* 2017). Other fine-grained, thin-bedded, more argillaceous units are interpreted as forming in deeper parts of the basin, or in shallow lagoons located between the reef and the arc. Continuous erosion of the arc provided a steady supply of volcanic material throughout the Late Triassic.

Age of the Lewes River Group

A new macrofossil collection from the carbonate sequence of the Lewes River Group includes specimens of bivalve and brachiopod shells, gastropods, scleractinian corals, columnal crinoid ossicles, and various sponge and other biotic debris (R. Blodgett, *pers. comm*., 2017). Diagnostic fauna assemblages support a Late Triassic age, with some specimens restricted to the late Middle Norian (bivalves *Halobia* and *Monotis*). Five conodont samples also support a Late Triassic age for the carbonate sequence of the Lewes River Group. Identified specimens of *Mockina cf. englandi* restrict the age of deposition to the Norian-Rhaetian (Golding, 2017).

Two detrital zircon ages from a non-calcareous pebble conglomerate unit (uTLRst) underlying massive micritic limestone (uTLRul) returned a maximum deposition age between 212 and 211 Ma (J. Crowley, *pers. comm.* 2017).

Based on fossil and detrital zircon analyses, the age range for the Lewes River Group is constrained between the Carnian to Rhaetian. The carbonate sequence was deposited during the Late Triassic, dominantly in Norian time (Hoover, 1991; Senowbari-Daryan, 1990; Orchard, 1995; Orchard, *pers. comm.,* 2016; R. Blodgett, *pers. comm*., 2017; Golding, 2017).

OVERLAP ASSEMBLAGES

WHITEHORSE TROUGH – LABERGE GROUP

Early-Middle Jurassic strata of the Laberge Group are dominated by thick-bedded, polymictic pebble to boulder conglomerate (JLcg) in the northeastern part of the map area and along the rugged ridge of Mount Laurier (Figs. 2a and 3). The conglomerate unit is bounded to the west by the Laurier Creek fault, to the south by Long Lake, and to the east by the Teslin River. Fine-grained, thin-bedded clastic sedimentary rocks are exposed along the shore of Lake Laberge (JLst; Fig. 2a). Two additional minor units are reported: a dark green, matrix-supported conglomerate (JLcbx) and one occurrence of the Nordenskiöld dacite (lJN). The contact between Laberge Group and the underlying Lewes River Group is either a disconformity (Mount Laurier), or an angular unconformity (south of Long Lake; Fig. 2a). In fact, Laberge Group unconformably overlies various units of the Upper Triassic Lewes River Group, a relationship described in detail in van Drecht and Beranek (2018). The upper contact of the Laberge Group is not exposed in the Teslin Mountain area, therefore the estimated thickness of 2000 m for the Laberge Group is a minimum. Previous estimates report between 1000 and 3000 m (*e.g.*, Hart, 1997; White *et al.*, 2012) across the Whitehorse trough.

*Polymictic conglomerate (*JLcg*)*

Grey-brown-rusty to tan weathering, thick-bedded, clast to matrix-supported, poorly sorted, polymictic pebble to boulder conglomerate includes rounded to subrounded clasts of fine-grained mudstone, limestone mudstone or cherty limestone, a variety of intrusive clasts, and volcanic mafic clasts (Bordet, 2016a). Bedding thickness ranges from 10 to 30 cm to locally metre-scale. Matrix is a pale yellow weathering, dark grey-green calcareous sandstone rich in biotite, quartz, feldspar and hornblende. Lithic sandstone forms metre-scale interbeds or lenses within the conglomerate. In addition, an ~30 m thick sequence of brown weathering, thin-bedded sandstone and mudstone underlies the polymictic conglomerate and marks the base of the Laberge Group at Mount Laurier and north of Teslin Mountain (Bordet, 2016a).

SANDSTONE/MUDSTONE (JLST)

Fine-grained, thin-bedded clastic sedimentary rocks of the Early to Middle Jurassic Laberge Group are exposed along the west shore of Lake Laberge, on Richthofen Island, and as a discontinuous strip along the east shore of Lake Laberge (Bordet, 2017a). Unit JLst comprises dark grey to brown weathering, thin-bedded, slightly calcareous to non-calcareous, dark grey turbiditic mudstone and siltstone. Dark grey, thin-laminated mudstone displays interbeds of pale yellow weathering sandstone with angular mudstone intraclasts. Load structures are common between sandstone beds and underlying mudstone, and generally indicate a stratigraphic polarity to the west (Bordet, 2017a).

*Dark green conglomerate (*JLcbx*)*

A distinct dark green conglomerate unit is exposed east of Richthofen Island and at several locations on the east shore of Lake Laberge, north of Goddard Point, and at Ptarmigan Point (Bordet, 2017a; Fig. 2a). It is composed of dark grey-green weathering, bright green, thick to medium-bedded, matrix-supported, immature, polymictic, poorly sorted cobble to boulder conglomerate locally interbedded with thin-bedded, lenticular mudstone/sandstone. The matrix is composed of pale green, fine-grained, non-calcareous volcanic sandstone with up to 3-4% quartz eyes. Subrounded clasts include pale grey micritic limestone, plagioclase-phyric rhyolite, andesite and dark grey mudstone.

*Nordenskiöld dacite (*lJN*)*

Beige-tan weathering, medium-crystalline, equigranular crystal tuff was mapped near the eastern shore of Lake Laberge. This unit is interbedded with pebble conglomerate and fine-grained sandstone and mudstone of the Laberge Group. The basal contact with thin-bedded mudstone-sandstone is irregular (Fig. 6a). The unit contains subrounded quartz crystals, hornblende and lithic fragments of plagioclase-phyric andesite in a microcrystalline plagioclase-phyric matrix (Fig. 6a,b). Small centimetre-scale lithic clasts of fine-grained grey mudstone are also reported (Fig. 6b). Magnetic susceptibility for this unit is high (~25 S.I.).

Petrographic observations (Fig. 6c) display a fragmental volcanic texture, with subrounded lithic fragments of plagioclase-phyric andesite (<1%). The matrix is plagioclase-rich. Crystals include quartz (1%), hornblende (3-5%), plagioclase (70%), opaque minerals (3%) and pyroxene (<1%).

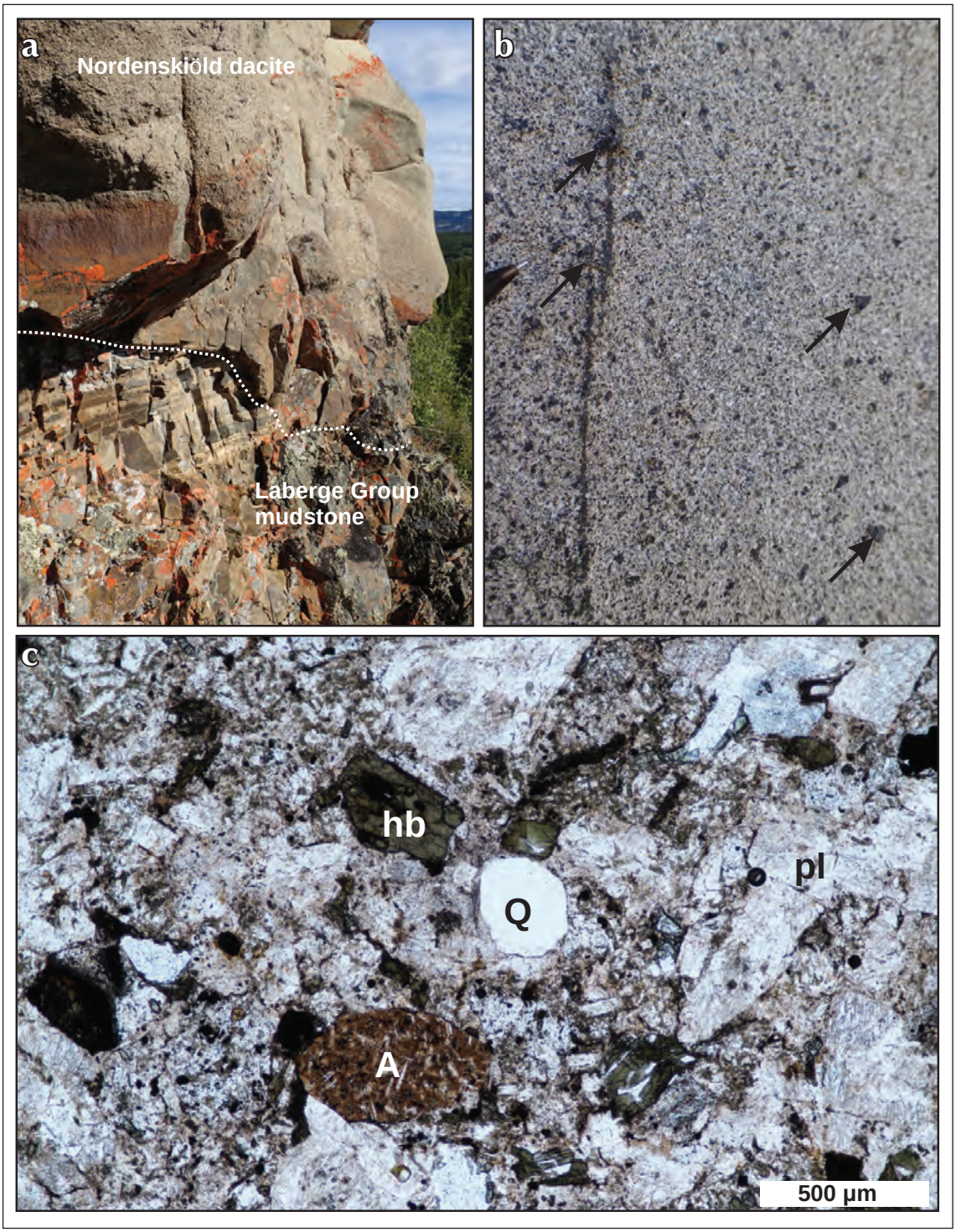

Figure 6. *Occurrence of the Nordenskiöld dacite east of Lake Laberge,* ***(a)*** *irregular basal contact (white dashed outline) of the Nordenskiöld dacite with underlying thin-bedded, laminated mudstone-sandstone of the Laberge Group;* ***(b)*** *macroscopic view of the outcrop of the Nordenskiöld dacite displaying tan weathering, medium crystalline, equigranular crystal tuff; pencil tip for scale. The matrix contains plagioclase and hornblende, and angular lithic clasts are visible (black arrows); and* ***(c)*** *petrographic view (plain light) of the Nordenskiöld dacite, characterized by a fragmental volcanic texture. Includes subrounded quartz crystals (Q), lithic fragments of plagioclase-phyric andesite (A), hornblende (hb), plagioclase (pl).*

Interpretation and age of the Laberge Group

Mapping suggests lateral facies changes within the Laberge Group from west to east. East of the Laurier Creek fault, Laberge Group is dominated by cobble to boulder polymictic conglomerate interpreted to represent submarine fan channel deposits (Dickie and Hein, 1995; Lowey, 2005, 2008). The lithology west of Laurier Creek fault, along Lake Laberge and on Richthofen Island, is dominated by fine-grained, thin-bedded turbiditic mudstone/sandstone, locally interbedded with granule to cobble polymictic conglomerate. This lithology is related to relatively deep-basin sedimentation. Limited conglomerate exposures within the turbiditic sequence to the west may be the result of localized channel activity. Detrital zircon ages within rocks of the Laberge Group range from the Late Triassic to Early Jurassic (~220-180 Ma; Colpron *et al.*, 2015).

The deposition of Laberge Group sediments in the Early Jurassic was likely controlled by pre-existing Triassic topography. Massive micritic limestone beds of the Lewes River Group (uTLRl) constitute present-day, prominent topographic features, and their reefal origin suggests that they were probably already shaping the landscape during the Late Triassic and Early Jurassic. These reefs formed buttresses, constraining the deposition of both Upper Triassic argillaceous sediments, and Laberge Group turbiditic or deltaic fan deposits (JLst).

The Nordenskiöld facies is a distinct crystal-lithic tuff (Tempelman-Kluit, 1984, 2009), occurring at multiple stratigraphic levels in both the Richthofen and Tanglefoot formations. It represents at least three distinct volcanic events between 188 and 186 Ma in the northern Whitehorse trough (Colpron and Friedman, 2008), but was also recognized and dated in the Lake Laberge area (184±4 Ma; Hart, 1997). Samples collected east of Lake Laberge were compared to Nordenskiöld samples collected regionally, and compositional and textural similarity was established based on petrographic observations.

PLUTONIC ROCKS

Igneous rocks in the map area include the Middle Jurassic Teslin Crossing, middle Cretaceous Cap Creek (Hart and Hunt, 1994, 2003; Hart 1997) and Laurier Creek plutons, and Late Cretaceous Teslin Mountain pluton. In addition to these large plutonic bodies, more than 200 dikes were mapped over the course of three summers. Several of these igneous bodies are related to mineral occurrences.

*Teslin Crossing pluton (*mJB*)*

The Teslin Crossing pluton is an ~5 by 10 km body located in the northeastern part of the map area (Fig. 2a). Limited exposures of the pluton are visible along a north-south trending alpine ridge. Contact with Early-Middle Jurassic strata was mapped at the southern edge of the igneous body. The pluton is characterized by medium to coarse-grained monzonite, monzodiorite and syenite. Related dikes of dacite to andesite porphyry with euhedral andesine, hornblende and locally quartz in aphanitic greenish, or grey groundmass are also reported (Colpron, 2011). An age of *ca.* 172 Ma is reported for the Teslin Crossing pluton, and it is therefore interpreted to be part of the Bryde Plutonic suite (Sacks and Colpron, *pers. comm.* 2017). The Teslin Crossing pluton hosts the porphyry Cu-Mo-Au Mars prospect (Fig. 2a; Yukon MINFILE 105E 002).

*Laurier Creek pluton (*EKgT*)*

The Laurier Creek pluton is characterized by grey to tan weathering, white to pale pink, equigranular, medium to coarse-grained granodiorite, monzonite, monzodiorite and quartz diorite that forms an ~5 by 12 km intrusion to the southwest of Teslin Mountain (Figs. 2a and 3). It intrudes Joe Mountain Formation aphyric massive basalt, but also the Lewes River Group sedimentary succession to the west. Detailed descriptions based on recent observations along the northern and western contacts of the intrusion are provided in Bordet (2017a).

A preliminary U/Pb age of ~116 Ma was obtained from granodiorite of the Laurier Creek pluton (J. Crowley, *pers. comm.,* 2017). This is similar to a previous date of *ca.* 118 Ma (K/Ar biotite; Stevens *et al.*, 1982). Therefore, the Laurier Creek pluton is assigned to the middle Cretaceous Teslin Suite (123-115 Ma; Colpron *et al.*, 2016). The Laurier Creek pluton hosts the molybdenum porphyry Hig (Yukon MINFILE 105E 024) and Lori (Yukon MINFILE 105E 025) showings.

*Teslin Mountain pluton (*LKgR *and* LKdR*)*

The Teslin Mountain pluton is an ~4 by 3 km massive, blocky, medium-grained, grey weathering, pale grey to white monzodiorite (LKgR) that intrudes Joe Mountain Formation massive basalt at Teslin Mountain (Figs. 2a and 3b; Bordet, 2016a). It contains plagioclase (40-60%), K-feldspar (up to 15%), biotite (10-15%), hornblende (10-20%) and quartz (1-3%). Another phase (LKdR) comprises tan to grey weathering, massive, blocky, fine-grained, dark grey-green diorite (1-2% quartz) and quartz diorite (up to

5-10% quartz), which contain plagioclase (10-15% and locally up to 50%), biotite or hornblende (5-15%).

A preliminary U/Pb zircon age of ~78 Ma was obtained for the Teslin Mountain pluton as part of this study (J. Crowley, *pers. comm.,* 2016). Based on geographic proximity and geological context, an association with the Rancheria plutonic suite exposed at Red Mountain (Yukon MINFILE 105C 009) east of the Teslin fault (81-79 Ma, Ar/Ar; Joyce *et al.*, 2015) is proposed. The Open Creek volcanic complex (*see* below) constitutes likely volcanic equivalents of this intrusive suite.

The Teslin Mountain pluton hosts the Debicki occurrence (Yukon MINFILE 105E 050).

Dikes

More than 200 dikes crosscut the Triassic to Jurassic stratigraphy in the map area. Petrography and geochemical analyses identified a variety of textures and compositions (Bordet, 2016a, 2017a; Fig. 7). Dikes locally display a magmatic foliation and are generally oriented N-S. At least three different dike compositions are reported:

- Brown weathering, conchoidally fractured, dark grey-green gabbro dikes with pyroxene (1-2%) and plagioclase (5%) in a fine-crystalline, dark grey groundmass are less common (~8% of all dikes; Fig. 7a,b). They are spatially concentrated along the east shore of Lake Laberge, and crosscut massive micritic limestone of the Lewes River Group, as well as thin-bedded mudstone at the base of the Laberge Group (Bordet, 2017a). These gabbro dikes appear to be folded along with the Upper Triassic-Jurassic sequence.
- Grey to beige weathering, grey, porphyritic dacite and rhyodacite dikes are widespread (~36% of all the dikes; Fig. 7c,d). They display a grey-green, aphanitic to finely crystalline equigranular groundmass. Phenocrysts include plagioclase (5 mm to 2 cm; 10-15%, and up to 25%), hornblende (1-5%, and up to 10%; laths up to 1 cm) and quartz (<1%).
- Pale pink/orange/beige to tan weathering, massive to blocky or locally foliated rhyolite quartz-phyric dikes are most common (~56% of all the dikes; Fig. 7e,f). They display a fine to medium-crystalline, pale pink to grey groundmass, and contain up to 10-60% plagioclase. Phenocrysts include K-feldspar (5-25%), quartz (1-10%) and hornblende or biotite (1-5%).

Three dikes were selected for U/Pb zircon geochronology. Preliminary results returned one middle Cretaceous age for a gabbro dike (~106 Ma; J. Crowley, *pers. comm.* 2017) which can be related to magmatic activity of the Whitehorse plutonic suite (112-98 Ma; Colpron *et al.*, 2016).

Two Early Cretaceous ages were obtained for a quartz-phyric rhyolite and a rhyodacite dike (ca. 138-136 Ma; J. Crowley, *pers. comm*. 2017). Early Cretaceous igneous ages are rare in the Yukon, and no igneous suite is defined so far that includes 138-136 Ma ages (Colpron *et al.*, 2016). Considering the pervasive nature of felsic dikes such as those that were dated, and the increased frequency of these dikes along the Goddard fault zone, the Goddard plutonic suite (EKqG) is newly defined here (Fig. 2).

VOLCANIC ROCKS

Open Creek volcanic complex

Dark grey to brown weathering dacite lava and tephra and chaotic volcanic breccia are exposed northeast of Teslin Mountain and west of Open Creek (Fig. 2a). These rocks were previously described by Tempelman-Kluit (1984, 2009), and informally named "Open Creek volcanics". They cover an area of at least 5 by 10 km and are best exposed along the eastern flank of a north-south trending ridge, which also marks the boundary of a landslide scarp. Open Creek volcanic rocks are in unconformable contact with the underlying Laberge Group and Joe Mountain Formation, but contacts are not exposed.

Crystal-rich lapilli tuff and block and ash flow form a ≥400 m thick ignimbrite sequence (LKOt), overlain by indurated dacite lava and breccia (LKOd; Fig. 8a-c). Grey to rainbow weathering, beige-tan colored, lithic-crystal lapilli ash tuff (Fig. 8d) has up to 15% crystals (quartz, biotite, plagioclase), 5-10% angular and rounded lithic clasts (plagioclase phyric andesite or dacite), and 2-5% pumice lapilli (Fig. 8g). Elongated vesicles are visible in the upper part of the ignimbrite below the contact with overlying dacite lava. The block-and-ash flow (Fig. 8e) has a white-pale green silicic ash matrix containing crystals (biotite, plagioclase and hornblende) and lapilli size lithic fragments. Blocks are up to 1 m in size, subrounded, of intermediate-silicic composition. Composition of the ignimbrite sequence is rhyodacite to rhyolite.

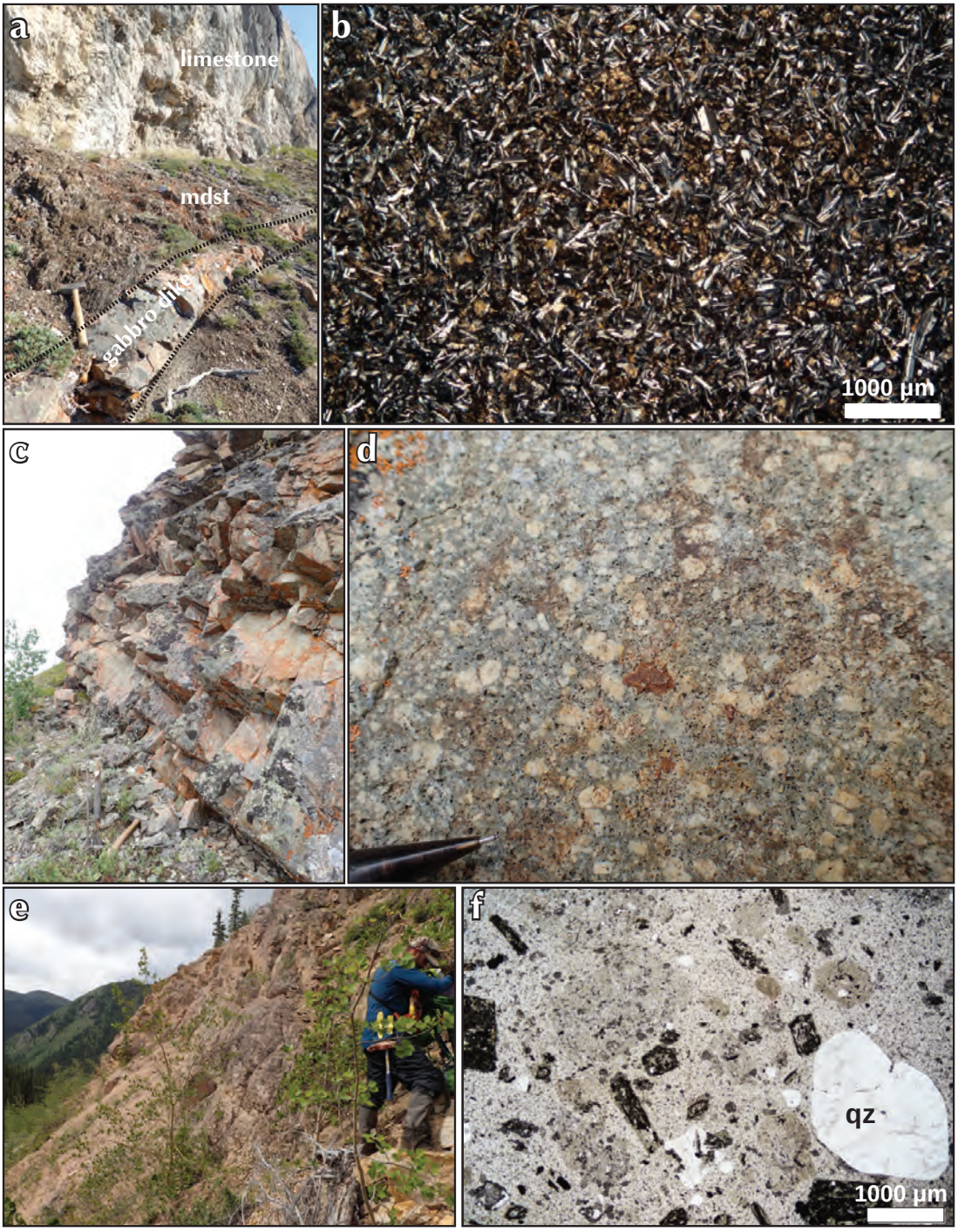

Figure 7. *Dikes textures and compositions,* ***(a)*** *outcrop photograph of an ~30 cm thick gabbro dike. At this location, Upper Triassic limestone is thrust over Early-Middle Jurassic mudstone of the Laberge Group. The dike intrudes the Jurassic sequence and is parallel to bedding;* ***(b)*** *petrographic view (cross-polar light) of the gabbro dike. Texture is equigranular, microcrystalline, essentially composed of plagioclase and pyroxene crystals;* ***(c)*** *outcrop photograph of an ~5 m wide rhyodacite dike intruding sedimentary strata of the Laberge Group;* ***(d)*** *macroscopic field photograph of the rhyodacite dike. Texture is porphyritic, with plagioclase phenocrysts, and biotite and hornblende microcrystals, in a pale grey aphanitic groundmass;* ***(e)*** *outcrop photograph of an ~10 m thick plagioclase-quartz-phyric rhyolite dike intruding mudstone of the Laberge Group; and* ***(f)*** *petrographic view (polarized light) of a quartz-plagioclase-biotite phyric rhyolite dike. The groundmass is pervasively carbonate altered.*

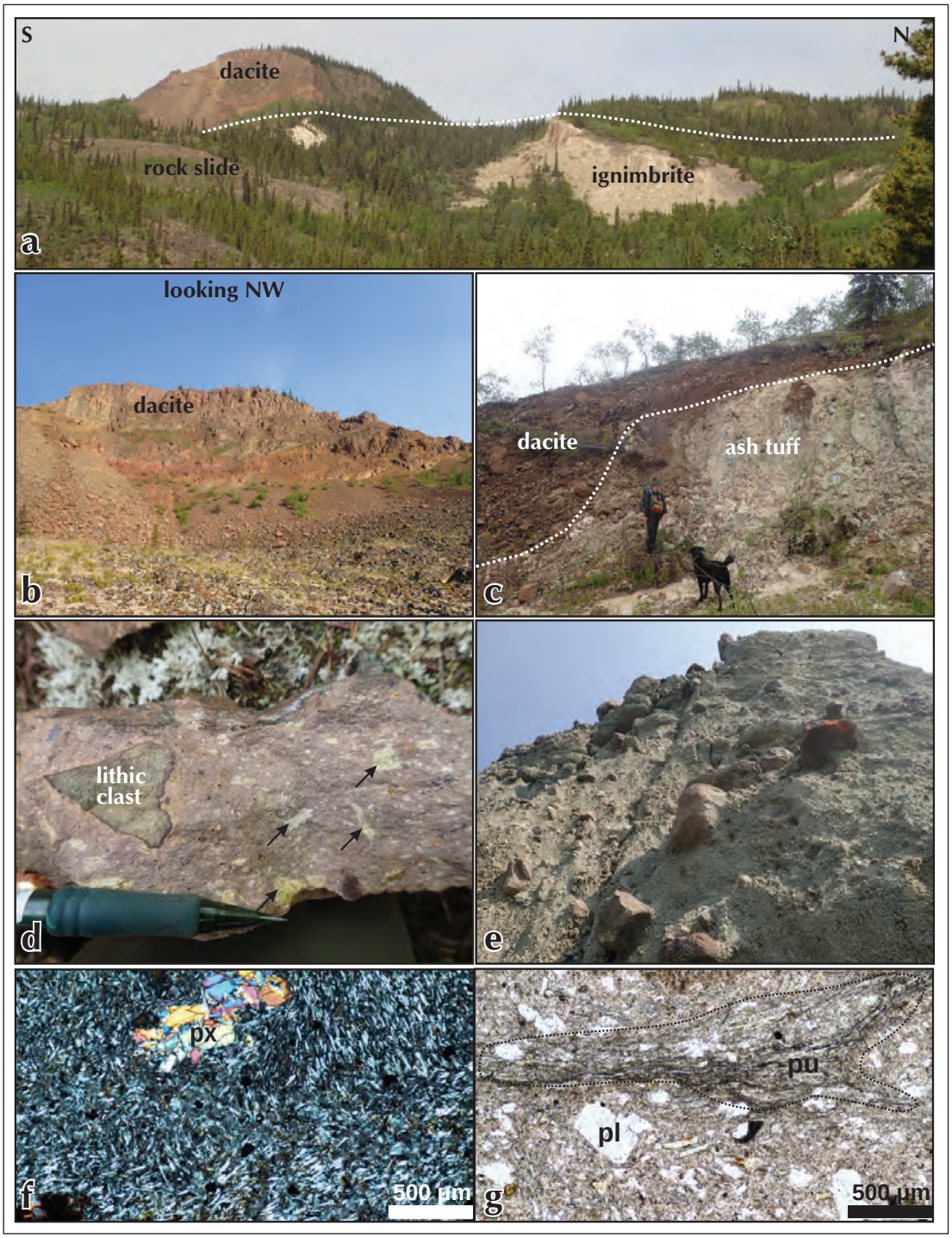

Figure 8. *Late Cretaceous Open Creek volcanic complex.* ***(a)*** *View looking west of the Open Creek volcanic complex. Indurated dacite lava and breccia cap an ~400 m thick ignimbrite sequence. Several landslides and rock slides occur in the area, due the ash tuff matrix of the ignimbrite forming a weak clay layer when altered;* ***(b)*** *a close up photograph of the indurated dacite cap, looking NW;* ***(c)*** *the contact between the basal clay-altered ignimbrite and overlying dacite lava;* ***(d)*** *a macroscopic view of the lapilli-ash tuff forming the ignimbrite. Pumice clasts indicated with black arrows;* ***(e)*** *block and ash flow sequence containing metre-sized blocks of dacitic lava in an ash-tuff matrix;* ***(f)*** *petrographic view of the dacite lava. The groundmass comprises microcrystalline plagioclase crystals, rare pyroxene phenocrysts are observed (px); and* ***(g)*** *petrographic view of the lapilli-ash tuff forming part of the ignimbrite sequence. Crystals include, plagioclase (pl), quartz. A pumice clast is outlined and labelled (pu).*

Brown-grey weathering, brown, aphyric to plagioclase (1-2%), pyroxene (2-3%), ±hornblende (1%) phyric, massive to columnar jointed or flow-banded indurated dacite (Fig. 8f) caps the ignimbrite sequence. It includes brown to rusty weathering, matrix-supported scoriaceous dacite breccia and autobreccia.

Isolated exposures of brown weathering, dark grey-brown, pyroxene-plagioclase phyric vesicular to amygdaloidal basalt and gabbro dikes (LKOb) are mapped to the west of the ignimbrite sequence, but their relationship with the rest of the stratigraphy is unclear. Grey-brown weathering, massive, grey, plagioclase (20%), biotite (1-3%), hornblende (7-10%) coarsely phyric diorite (LKO) sits at the base of the volcanic complex, and is likely a feeder to the volcanic sequence.

Interpretation and age of the Open Creek volcanic rocks

The nature of the Open Creek volcanic succession suggests a period of explosive volcanism, leading to the deposition of an ignimbrite sequence at least 400 m thick. The ignimbrite comprises block and ash flow deposits, as well as crystal-lithic rich lapilli-ash tuff. Metre-sized dacite blocks in the block and ash flow sequence, as well as very primary textures in the rest of the ignimbrite sequence, suggest that these deposits are relatively proximal to a volcanic centre (deposition within a few kilometres). The dacitic sequence capping the ignimbrite displays a range of textures from lava to monomictic breccia. Once again, the texture of the lava and breccia suggest they were emplaced proximally relative to a volcanic center.

The Open Creek volcanic rocks were originally dated at ~80 Ma (whole rock, K/Ar; Tempelman-Kluit, 2009). Two preliminary U/Pb dates conducted as part of this project returned similar ages of 79 Ma (J. Crowley, *pers. comm.*, 2017) for the ignimbrite sequence. The timing of volcanism is therefore coeval to the emplacement of the Teslin Mountain pluton, located just a few kilometres to the south. The felsic lithology, similar ages, and spatial proximity suggest that the Teslin Mountain pluton and Open Creek volcanic rocks are part of a same magmatic complex and probably share a common magmatic source.

The area where Open Creek volcanic rocks are exposed displays signs of active landslide and rockslide activity (Fig. 8a). In fact, the highly porous, ash matrix of the ignimbrite sequence is altered into clay-rich soil, creating an unstable slippery layer responsible for the collapse of the upper dacite lava.

STRUCTURE

A detailed structural review of the map area is provided in Bordet (2017a). In summary, two major north-northwest-trending strike-slip faults dissect the Triassic to Jurassic stratigraphy, the Goddard and Laurier Creek faults. Two dominant structural trends are identified in rocks exposed along these faults. North to northwest-striking thrust and normal faults, and east-verging tight folds dominate in the Lewes River Group, between the east shore of Lake Laberge and Laurier Creek fault (Fig. 2a). East of the Laurier Creek fault, bedding measurements consistently indicate an east-trending structural fabric and tight east-west folds within the Middle Triassic Joe Mountain Formation.

Deformation affects the entire Triassic to Jurassic sequence. Most of the thrusting, as well as strike-slip motion along the Goddard and Laurier Creek faults, must have at least a syn or post-Jurassic component. However, the contrasting east-west structural grain in rocks of the Joe Mountain Formation at Teslin Mountain, compared to the dominant north-northwest structural trends west of the Laurier Creek fault, suggest evidence for a pre-Late Triassic event that occurred prior to deposition of the Lewes River Group.

In addition, the structures in the map area contrast with those of the northern Whitehorse trough, characterized by northwest-striking, southwest-verging folds and thrust faults that are dissected by northwest and north-striking strike-slip faults (White *et al.*, 2012).

SUMMARY AND CONCLUSIONS

The Teslin Mountain and Lake Laberge areas in south-central Yukon were investigated from 2015 to 2017 as part of a 1:50 000 scale bedrock mapping project. The area is underlain by mafic volcanic, volcaniclastic and clastic sedimentary strata of the Middle Triassic Joe Mountain Formation, mafic volcanic and sedimentary strata of the Upper Triassic Lewes River Group, and polymictic conglomerate and thin-bedded turbiditic sequences of the Lower-Middle Jurassic Laberge Group. At least five post-accretion igneous suites are recognized, as well as one Late Cretaceous volcanic complex.

TRIASSIC STRATIGRAPHY

- Five volcanic, volcaniclastic and sedimentary units are now defined as part of the Middle Triassic Joe Mountain Formation, and nine units as part of the Upper Triassic Lewes River Group. Unit descriptions

presented in this paper generally supersede previous subdivisions described by Bordet (2016a, 2017a).

- The nature of the northern contact of the Joe Mountain Formation basalt was revised in 2017, and the relationships with volcaniclastic and sedimentary units exposed northwest of Teslin Mountain were reinterpreted. In conclusion: 1) clastic sedimentary rocks (mTJMms) underlying the Middle Triassic mafic sequence represent a basin that existed prior to Joe Mountain volcanism; 2) coarse volcanic conglomerate, volcanic sandstone and minor basalt (mTJMbx) overlying the clastic sedimentary sequence must be part of the Middle Triassic Joe Mountain Formation in order explain structural and stratigraphic relationships with underlying strata.
- Joe Mountain volcanism is dated at ~245 Ma (J. Crowley, *pers. comm.*, 2016). The age range for the Lewes River Group is constrained between the Carnian and Rhaetian, based on combined fossil and U/Pb detrital zircon ages.
- The Joe Mountain Formation and Lewes River Group volcanic rocks are dominated by basalt and basaltic andesite compositions. The Joe Mountain Formation is characterized by MORB/BABB and IAT signatures, whereas Lewes River Group signatures range from tholeiitic, transitional to calc-alkaline. Geochemical analysis of the Triassic volcanic rocks indicates similar tectonic settings for both suites, with internal variations within each suite. However, the Joe Mountain Formation seems to represent a more juvenile end-member of the Triassic volcanic rocks sample suite. It is proposed that the Joe Mountain Formation represents the onset of arc magmatism in the Middle Triassic, and that the Lewes River group represents a temporal and spatial continuity of this arc throughout the Late Triassic.
- The Lewes River Group is interpreted to have developed on the margin of a volcanic arc forming a topographic highland. This arc constituted a natural break in a shallow oceanic basin, leading to synchronous but dissimilar carbonate sedimentation on either side of the arc. As a result, lateral stratigraphic variations occur throughout the Lewes River Group carbonate sequence.

OVERLAP ASSEMBLAGES

Interfingering between Triassic and Jurassic strata suggests that the deposition of Laberge Group sediments was controlled by pre-existing Triassic topography. This pattern was further emphasized by later deformation that thrusted sheets of Triassic rocks over younger Jurassic strata.

At least five distinct post-accretionary plutonic suites ranging from the Middle Jurassic to the Late Cretaceous are identified in the map area, as well as one Late Cretaceous volcanic complex. Igneous activity occurred at ~172 Ma (Teslin Crossing pluton), between 138 and 136 Ma (felsic dikes part of the newly defined Goddard Suite), between 116 and 106 Ma (Cap Creek pluton, Laurier Creek pluton, gabbro dike), and at ~79-78 Ma (Open Creek volcanic complex, Teslin Mountain pluton).

At least four map units were identified as part of the Late Cretaceous Open Creek volcanic complex. Field observations combined with preliminary analytical results suggest that a series of pyroclastic eruptions led to the deposition of a thick ignimbrite sequence around 79 Ma (J. Crowley, *pers. Comm.*, 2017), and subsequent dacitic lava flows capped the ignimbrite. The layered volcanic sequence is spatially and temporally associated with the nearby Late Cretaceous Teslin Mountain pluton.

A number of individual dikes showing a range of compositions and textures were mapped. Preliminary analytical results highlight the lithological, compositional and temporal diversity of this discrete, but pervasive igneous system. A new magmatic episode was identified with at least two of the dacite-rhyolite dikes returning ages between 138 and 136 Ma (J. Crowley, *pers. comm.,* 2017). This is newly defined as the Goddard suite, since most of the dikes occurrences are aligned with the Goddard fault zone.

The map area includes several styles of mineral occurrences: Cu or Mo porphyry associated with large middle Cretaceous plutons (*e.g.*, Hig showing, Yukon MINFILE 105E 024); quartz vein related gold and polymetallic veins (*e.g.*, Hartless Joe prospect, Yukon MINFILE 105D 051, Fig. 2a); and Cu or Mo skarn where the Upper Triassic carbonate sequence is intersected by numerous dikes (*e.g.*, Laberge prospect, Yukon MINFILE 105E 006). The middle Cretaceous Teslin Mountain pluton may be temporally and genetically related to the Red Mountain Cu-Mo-Au-porphyry deposit (Yukon MINFILE 105C 009) located about 45 km to the east. This relationship will be investigated during summer 2018.

STRUCTURE

Two north-northwest trending regional-scale faults crosscut the map area: the Goddard and Laurier Creek faults.

- The Goddard fault is regionally interpreted as a dextral strike-slip structure, but locally displays a thrust motion. Changes of strata strike and dip and an increased concentration of dikes occur in the vicinity of the fault.
- The Laurier Creek fault constitutes a major geological and structural boundary in the map area. The Middle Triassic Joe Mountain Formation is only exposed east of the fault, and characterized by an east-west structural grain. West of the fault, units of the Upper Triassic Lewes River group dominate, and they are characterized by north-northwest trending fold axes and thrust faults.

ACKNOWLEDGEMENTS

Galena Roots' and Alexina Boileau's help in the field was much appreciated. Heli Dynamics Ltd. provided safe helicopter support throughout the field season. The GSC GEM-2 program is thanked for supporting part of the analytical and logistical expenses for this project. Discussions with Steve Israel and Maurice Colpron helped in developing a better understanding of the complex geology in the Teslin Mountain area. Jim Crowley at Boise State University provided very precise U/Pb igneous and detrital ages. Robert Blodgett conducted fossil identification on 16 macrofossil samples collected during mapping. Martyn Golding conducted analyses and identification of 25 (5 productive) conodont samples.

REFERENCES

Bickerton, L., Colpron, M. and Gibson, D.W., 2013. Cache Creek terrane, Stikinia, and overlap assemblages of eastern Whitehorse (NTS 105D) and western Teslin (NTS 105C) map areas. *In:* Yukon Exploration and Geology 2012, K.E. MacFarlane, M.G. Nordling and P.J. Sack (eds.), Yukon Geological Survey, p. 1-17.

Bordet, E., 2016a. Preliminary results on the Middle Triassic-Middle Jurassic stratigraphy and structure of the Teslin Mountain area, southern Yukon. *In:* Yukon Exploration and Geology 2015, K.E. MacFarlane and M.G. Nordling (eds.), Yukon Geological Survey, p. 43-61.

Bordet, E., 2016b. Bedrock geology map of the Teslin Mountain and East Lake Laberge areas, parts of NTS 105E/2, 3 and 6. Yukon Geological Survey , Open File 2016-38, scale 1:50 000.

Bordet, E., 2017a. Updates on the Middle Triassic-Middle Jurassic stratigraphy and structure of the Teslin Mountain and east Lake Laberge areas, south-central Yukon. *In:* Yukon Exploration and Geology 2016, K.E. MacFarlane and L.H. Weston (eds.), Yukon Geological Survey, p. 1-24.

Bordet, E., 2017b. Geochemical characterization of Triassic volcanic arc rocks of Stikinia in Yukon. Abstract, Cordilleran Tectonic Workshop, Vancouver, BC, February 2017.

Bostock, H.S. and Lees, E.J., 1938. Laberge map-area, Yukon. Geological Survey of Canada, Memoir 217, 33 p.

Colpron, M., 2011. Geological compilation of Whitehorse trough - Whitehorse (105D), Lake Laberge (105E), and part of Carmacks (115I), Glenlyon (105L), Aishihik Lake (115H), Quiet Lake (105F) and Teslin (105C). Yukon Geological Survey, Geoscience Map 2011-1, scale 1:250 000.

Colpron, M. and Friedman, R.M., 2008. U-Pb zircon ages for the Nordenskiöld formation (Laberge Group) and Cretaceous intrusive rocks, Whitehorse trough, Yukon. *In:* Yukon Exploration and Geology 2007, D.S. Emond, L.R. Blackburn, R.P. Hill and L.H. Weston (eds.), Yukon Geological Survey, p. 139-151.

Colpron, M. and Nelson, J.L., 2011. A Digital Atlas of Terranes for the Northern Cordillera. Accessed online from Yukon Geological Survey, www.geology.gov.yk.ca [accessed Nov. 2015].

Colpron, M., Israel, S. and Friend, M. (compilers), 2016. Yukon Plutonic Suites. Yukon Geological Survey, Open File 2016-37, scale 1:750 000.

Colpron, M., Crowley, J.L., Gehrels, G., Long, D.G.F., Murphy, D.C., Beranek, L. and Bickerton, L., 2015. Birth of the northern Cordilleran orogen, as recorded by detrital zircons in Jurassic synorogenic strata and regional exhumation in Yukon. Lithosphere, vol. 7, p. 541-562, doi:10.1130/l451.1.

Coney, P.J., Jones, D.L. and Monger, J.W., 1980. Cordilleran suspect terranes. Nature, vol. 288, p. 329-333.

Dickie, J.R. and Hein, F.J., 1995. Conglomeratic fan deltas and submarine fans of the Jurassic Laberge Group, Whitehorse trough, Yukon Territory, Canada - Fore-arc sedimentation and unroofing of a volcanic island-arc complex. Sedimentary Geology, vol. 98, p. 263-292.

Golding, M., 2017. Report on 25 (5 productive) microfossil samples submitted for analysis by E. Bordet, Yukon Geological Survey (2016), Laberge (105E) map area. Geological Survey of Canada, Paleontological report 2-MG-2017, 12 p.

Hart, C.J., 1997. A transect across northern Stikinia: geology of the northern Whitehorse map area, southern Yukon Territory (105D/13-16). Indian and Northern Affairs Canada, Exploration and Geological Services Division, Yukon Region, Bulletin 8, 77 p.

Hart, C.J.R. and Hunt, J.A., 1994. Geology of the Joe Mountain map area (105D/15), southern Yukon Territory. *In:* Yukon Exploration and Geology 1993, C.F. Roots and D.S. Emond (eds.), Exploration and Geological Services Division, Yukon Region, Indian and Northern Affairs Canada, p. 47-66.

Hart, C.J.R. and Hunt, J.A., 2003. Geology of Joe Mountain map area (105D/15), southern Yukon (1:50 000 scale). Yukon Geological Survey, Energy, Mines and Resources, Yukon Territorial Government, Geoscience Map 2003-4.

Hart, C.J.R. and Orchard, M.J., 1996. Middle Triassic (Ladinian) volcanic strata in southern Yukon Territory, and their Cordilleran correlatives. Geological Survey of Canada, Current Research 1996-A, p. 11-18.

Hoover, P.R., 1991. Late Triassic cyrtinoid spiriferinacean brachiopods from western North America and their biostratigraphic and biogeographic implications. Bulletins of American Paleontology, vol. 100, p. 63-109.

Joyce, N.L., Ryan, J.J., Colpron, M., Hart, C.J.R. and Murphy, D.C., 2015. A compilation of $^{40}Ar/^{39}Ar$ age determinations for igneous and metamorphic rocks, and mineral occurrences from central and southeast Yukon. Geological Survey of Canada, Open File 7924, 229 p.

Lees, E.J., 1934. Geology of the Laberge area, Yukon. Transactions, Royal Canadian Institute, vol. 20, p. 1-48.

Lowey, G.W., 2005. Sedimentology, stratigraphy and source rock potential of the Richthofen formation (Jurassic), northern Whitehorse Trough, Yukon. *In:* Yukon Exploration and Geology 2004, D.S. Emond, L.L. Lewis and G. Bradshaw (eds.), Yukon Geological Survey, p. 177-191.

Lowey, G.W., 2008. Summary of the stratigraphy, sedimentology and hydrocarbon potential of the Laberge Group (Lower-Middle Jurassic), Whitehorse trough, Yukon. *In:* Yukon Exploration and Geology 2007, D.S. Emond, L.R. Blackburn, R.P. Hill and L.H. Weston (eds.), Yukon Geological Survey, p. 179-197.

Mihalynuk, M.G., Nelson, J. and Diakow, L.J., 1994. Cache Creek terrane entrapment: Oroclinal paradox within the Canadian Cordillera. Tectonics, vol. 13, p. 575-595.

Monger, J.W.H., Wheeler, J.O., Tipper, H.W., Gabrielse, H., Harms, T., Struik, L.C., Campbell, R.B., Dodds, C.J., Gehrels, G.E. and O'Brien, J., 1991. Part B. Cordilleran terranes, Upper Devonian to Middle Jurassic assemblages (Chapter 8). *In:* Geology of the Cordilleran orogen in Canada, H. Gabrielse and C.J. Yorath (eds.), Geological Survey of Canada, Geology of Canada 4, p. 281-327; *also Geological Society of America, The Geology of North America, vol. G-2*.

Mortensen, J.K., 1992. Pre-Mid-Mesozoic tectonic evolution of the Yukon-Tanana terrane, Yukon and Alaska. Tectonics, vol. 11, p. 836-853.

Mortensen, J.K. and Jilson, G.A., 1985. Evolution of the Yukon-Tanana terrane: evidence from southeastern Yukon Territory. Geology, vol. 13, p. 806-810.

Nelson, J.L., Colpron, M. and Israel, S., 2013. The Cordillera of British Columbia, Yukon, and Alaska: Tectonics and metallogeny. *In:* Tectonics, Metallogeny and Discovery: The North American Cordillera and Similar Accretionary Settings, M. Colpron, T. Bissig, B.G. Rusk and J.F.H. Thompson (eds.), Society of Economic Geologists, Inc., Special Publication 17, p. 53-103.

Orchard, M.J., 1995. Report on conodonts and other microfossils from the Whitehorse (105D) and Lake Laberge (105E) map areas. Geological Survey of Canada, unpublished report MJO-1995-32.

Piercey, S.J., 2005. Reconnaissance geological and geochemical studies of the Joe Mountain Formation, Joe Mountain region (NTS 105D/15), Yukon. *In:* Yukon Exploration and Geology 2004, D.S. Emond, L.L. Lewis and G.D. Bradshaw (eds.), Yukon Geological Survey, p. 213-226.

Reid, R.P., 1980. Report of field work on the Upper Triassic reef complex of Lime Peak, Laberge map area, Yukon. *In:* Geology and Exploration 1979-80, D.J. Tempelman-Kluit (ed.), Indian and Northern Affairs Canada/ Department of Indian and Northern Development: Exploration and Geological Services Division, p. 110-114.

Senowbari-Daryan, B., 1990. Die systematische Stellung der thalamiden Schwämme und ihre Bedeutung in der Erdgeschichte. Münchner Geowissenschaftliche Abhandlungen, vol. A 21, p. 5-326.

Stevens, R.D., Delabio, R.N. and Lachance, G.R., 1982. Age Determinations and Geological Studies, K-Ar Isotopic Ages. Geological Survey of Canada, Report 16, Paper 82-2, 56 p.

Struik, L.C., Schiarizza, P., Orchard, M.J., Cordey, F., Sano, H., MacIntyre, D.G., Lapierre, H. and Tardy, M., 2001. Imbricate architecture of the upper Paleozoic to Jurassic oceanic Cache Creek Terrane, central British Columbia. Canadian Journal of Earth Sciences, vol. 38, p. 495-514.

Tempelman-Kluit, D.J., 1984. Geology, Laberge (105E) and Carmacks (115I), Yukon Territory. Geological Survey of Canada, Open File 1101, 10 p. and 2 maps, scale 1:250 000.

Tempelman-Kluit, D.J., 2009. Geology of Carmacks and Laberge map areas, central Yukon: Incomplete draft manuscript on stratigraphy, structure and its early interpretation (*ca.* 1986). Geological Survey of Canada, Open File 5982, 399 p.

Tozer, E., 1958. Stratigraphy of the Lewes River Group (Triassic), central Laberge area, Yukon Territory. Geological Survey of Canada, Bulletin 43, 28 p.

Wheeler, J.O., 1961. Whitehorse map area, Yukon Territory. Geological Survey of Canada, Memoir 312, 156 p.

Wheeler, J.O., Brookfield, A.J., Gabrielse, H., Monger, J.W.H., Tipper, H.W. and Woodsworth, G.J., 1991. Terrane map of the Canadian Cordillera. Geological Survey of Canada, Map 1713A, scale 1:2 000 000.

White, D., Colpron, M. and Buffett, G., 2012. Seismic and geological constraints on the structure and hydrocarbon potential of the northern Whitehorse trough, Yukon, Canada. Bulletin of Canadian Petroleum Geology, vol. 60, p. 239-255.

Yarnell, J.M., Stanley, G. and Hart, C.J.R., 1999. New paleontological investigations of Upper Triassic shallow-water reef carbonates (Lewes River Group) in the Whitehorse area, Yukon. *In:* Yukon Exploration and Geology 1998, C.F. Roots and D.S. Edmond (eds.), Exploration and Geological Services Division, Yukon, Indian and Northern Affairs Canada, p. 179-184.

Yukon MINFILE, 2015. Yukon MINFILE – A database of mineral occurrences. Yukon Geological Survey, http://data.geology.gov.yk.ca [accessed May 2015].

Clast fabric analysis of glacial diamict at the Allan Creek section and its implication for paleo-ice flow of Liard Lowland, southeastern Yukon

S.H. Ellis
Palmer Environmental Consulting Group, Vancouver, BC

N.J. Roberts
Simon Fraser University, Burnaby, BC

K.E. Kennedy
Yukon Geological Survey, Whitehorse, Yukon

A.V. Reyes and B.J.L. Jensen
University of Alberta, Edmonton, AB

Ellis, S.H., Roberts, N.J., Kennedy, K.E., Reyes, A.V. and Jensen B.J.L., 2018. Clast fabric analysis of glacial diamict at the Allan Creek section and its implication for paleo-ice flow of Liard Lowland, southeastern Yukon. *In:* Yukon Exploration and Geology 2017, K.E. MacFarlane (ed.), Yukon Geological Survey, p. 25-36.

ABSTRACT

The Allan Creek section was identified and briefly described during reconnaissance mapping of the Watson Lake map area (NTS 105A) several decades ago and provides southeastern Yukon's most complete known record of glaciation. The region supported ice sheets during multiple Quaternary glaciations, with landforms in Liard Lowland recording the ice flow toward the southeast during the Last Glacial Maximum (LGM). Inference of earlier ice-flow patterns requires sedimentologic characterization of glacial deposits underlying Liard Lowland. We expand macro-scale descriptions of the sequence of four diamict units exposed in the Allan Creek section to provide further insight on paleo-ice flow in southeastern Yukon. Pebble fabrics were measured from each diamict unit to compare with known LGM ice-flow directions and previously reported clast orientations. Three of the diamict units record ice-flow along the NW-SE trend of Liard Lowland. The second highest diamict in the sequence may record ice-flow directions both parallel and transvers to the basin's trend. Only the lowest diamict unambiguously indicates unidirectional ice-flow; it suggests southeastward paleo-flow during early glaciation of southeastern Yukon, similar to that during the LGM.

* *kristen.kennedy@gov.yk.ca*

INTRODUCTION

Most of the Yukon landmass was overridden by continental and montane ice during multiple Quaternary glaciations, but stratigraphic sections with evidence for multiple glacial intervals are relatively rare. One such site is the Allan Creek section (Fig. 1: 60.47823°N, 129.68341°W), which was previously described by Klassen (1978; 1987) during regional surficial mapping of southeastern Yukon (Klassen and Morison, 1982). The site consists of multiple sections along an ~85-m-high river bluff (Fig. 2) spanning several hundred metres of lateral exposure on the east bank of Liard River, ~4.5 km downstream of its confluence with Allan Creek. The Allan Creek site is the most important of four sites used by Klassen (1987; Fig. 1) to establish a stratigraphic succession for Liard Lowland and to reconstruct the advance and retreat of Quaternary ice sheets. Klassen's (1987) regional stratigraphic framework includes four diamict units of interpreted glacial origin. The Allan Creek section is the only known location where all four diamict units are present, making it the reference locality for regional glacial records.

Klassen's pioneering work focused on describing the succession of Tertiary-Pleistocene sediments in the Liard River basin, with the main conclusions that at least four southeast flowing glaciations are recorded, ranging in age from mid to late-Pleistocene, and nourished mainly by ice from the Cassiar and Pelly mountains. This study expands upon the initial macro-scale descriptions of glacial sediments from this key section. We report additional pebble fabrics to compare with Klassen's (1978, 1987) previous work, as well as the first ice-flow data for the oldest glacial unit in the section. Our preliminary interpretations provide insight on the variability of paleo-ice flow between multiple glaciations in southeastern Yukon.

REGIONAL SETTING AND GLACIAL HISTORY

Liard River in southeastern Yukon is entrenched into a broad plain of glacial and pre-glacial sediments known as Liard Lowland (Mathews, 1986) or by other authors as Liard Plain (Bostock, 1948; Klassen, 1987). Liard Lowland

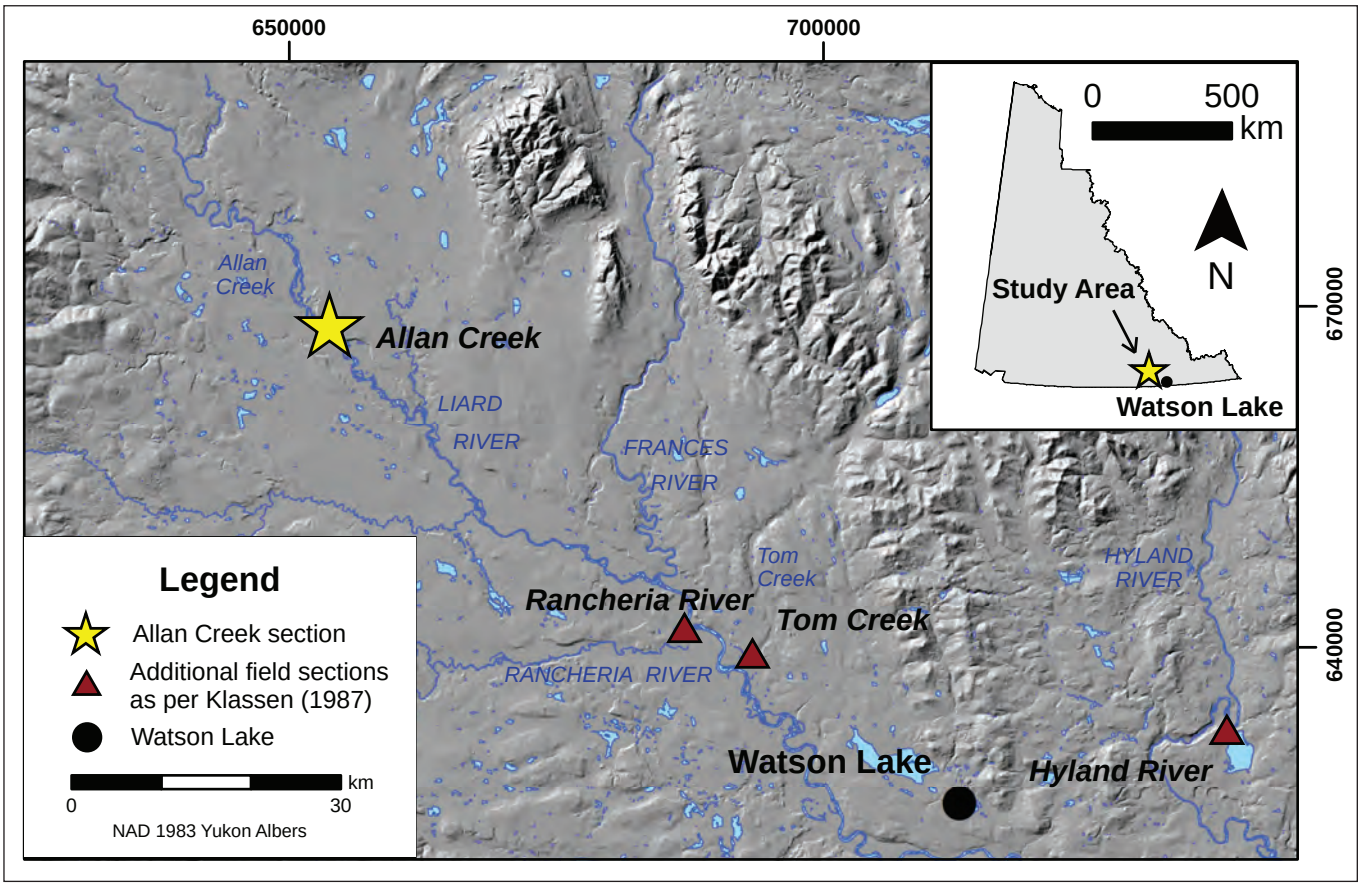

Figure 1. *Location of the study area in southeastern Yukon. The Allan Creek section, along with sections at Tom Creek, Rancheria River, and Hyland River, is the basis for Klassen's (1987) Quaternary stratigraphic framework of Liard basin.*

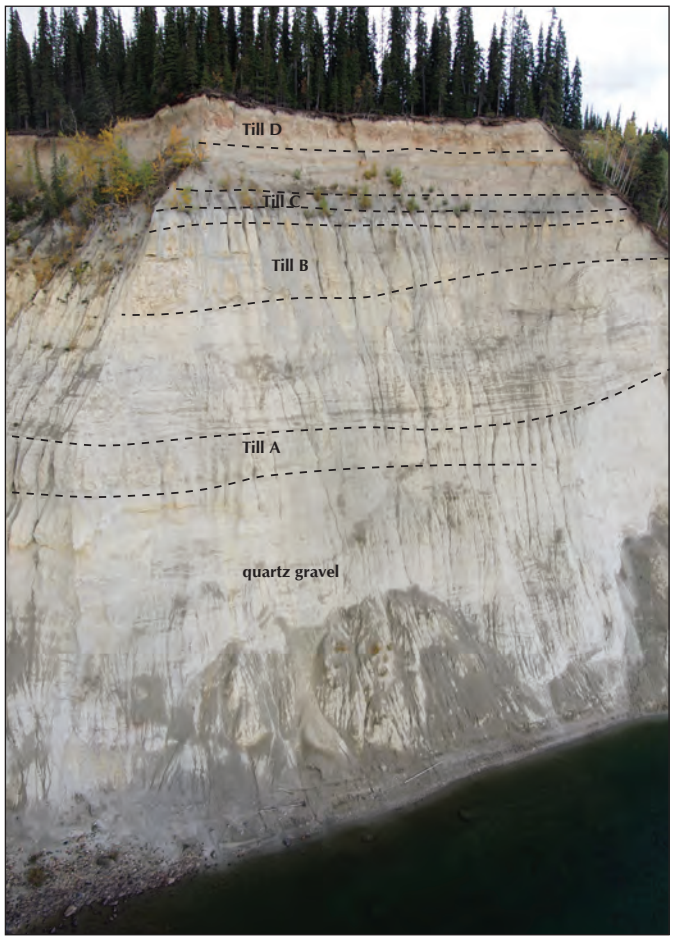

Figure 2. *Aerial view of the Allan Creek section. Tills A through D were initially identified by Klassen (1987) and are further examined in this study.*

is an intermontane basin comprising low hills and broad plains, surrounded by mountain ranges and elevated plateaus: Cassiar Mountains to the southwest; Selwyn Mountains and Hyland Highland to the northeast; and Pelly Mountains to the northwest. The basin is ~175 km long by 50 km wide and lies within Tintina Trench, a major lineament associated with the Tintina fault. Right-lateral strike-slip displacement along this fault, with associated or subsequent dip-slip movement, created several fault-bounded basins, including Liard Lowland (Roddick, 1967). Fault slip continued at least into the Eocene (Hughes and Long, 1980) and may be ongoing today (Leonard *et al.*, 2008). Pre-glacial basin fills include Paleocene-Eocene coal-bearing sediments (claystone, siltstone, shale, sandstone and pebble conglomerate), Tertiary or Pleistocene volcanic rocks, and widespread flat-lying quartz gravel of inferred Miocene age (Dawson, 1898; Hughes and Long, 1980; Klassen, 1987).

Southeastern Yukon was repeatedly glaciated by local montane and regional ice during the Quaternary, although the number of glacial events and most of their ages are unknown. Bostock (1966) recognized four glaciations in central Yukon, and magnetostratigraphy of sediment sequences along Tintina Trench demonstrates at least ten Pliocene and Pleistocene glaciations (Duk-Rodkin *et al.*, 2010; Barendregt *et al.*, 2010). The most recent ice advance in Liard Lowland occurred during the Last Glacial Maximum (LGM) of the Cordilleran Ice Sheet (CIS) *ca.* 25,000-18,000 years ago (Marine Isotope Stage 2). During that time, ice accumulated in the Pelly and Cassiar mountains and flowed southeast across the study area before coalescing with the Laurentide Ice Sheet ~200 km farther east (Hughes *et al.*, 1972; Klassen and Morison, 1982; Jackson *et al.*, 1991; Duk-Rodkin, 1999; Clague and Ward, 2011). Radiocarbon ages on plant macrofossils from the upper (23,900 ± 1140 ^{14}C yr BP; GSC-2811) and lower (>30,000 ^{14}C yr BP; GSC-2949) parts of an ~3.5-m-thick silt unit underlying the uppermost till at Klassen's (1987) Tom Creek section (Fig.1) provide the only chronologic constraint for the onset of LGM ice cover of the study area.

The broad valley bottom of Liard Lowland preserves extensive ice-flow features, most notably a drumlinized till plain that indicates a predominantly southeastern flow direction for the Liard lobe during the LGM (Klassen and Morison, 1982; Duk-Rodkin, 1999). An ice divide over Cassiar Mountains separated the predominantly westward-to-northwestward-flowing Cassiar lobe of the CIS from the southeastward-to-eastward-flowing Liard lobe (Jackson *et al.*, 1991; Fig. 3a). Flow of the Liard lobe was broadly fan-like, spreading from accumulation centres in the Pelly and Cassiar mountains and largely constrained by regional topography, although ice thickness was locally sufficient to overtop regional topographic barriers (Klassen and Morison, 1982; Jackson *et al.*, 1991; Margold *et al.*, 2013).

PREVIOUS WORK

Detailed ice-flow reconstruction of the Liard lobe from glacial landforms (Margold *et al.*, 2013) supports the overall southeastward-to-eastward flow suggested by earlier reconnaissance mapping (Klassen and Morison, 1982). However, several crosscutting sets of glacial lineations near Frances River also record both N-S and WSW-ENE flow, which were later overprinted by lineations recording southeastward-to-eastward flow (Fig. 3b). Margold *et al.* (2013) suggest that this overprinting

may be the result of changing dominance of late-glacial dispersal centres, or that earlier lineations were formed by ice advancing out of Selwyn Mountains prior to the LGM. Klassen (1987) reports the general stratigraphy of the Allan Creek section and clast fabric measurements from the upper three diamict units (Fig. 4). His report states the fabric for the highest diamict aligns with the generally NW-SE orientation of drumlins and streamlined landforms. Klassen (1978, 1987) correlates this diamict with the highest diamict unit at the Tom Creek section, suggesting both were emplaced during the LGM. The lower three diamict units predate *ca.* 30,000 ^{14}C yr BP, but their ages are otherwise unconstrained. Clast fabrics range from SSW-NNE ("Till B") to W-E ("Till C") for the two lowest units measured by Klassen (1987); they are thus oblique to the main trend of landforms attributed to LGM flow of the Liard lobe.

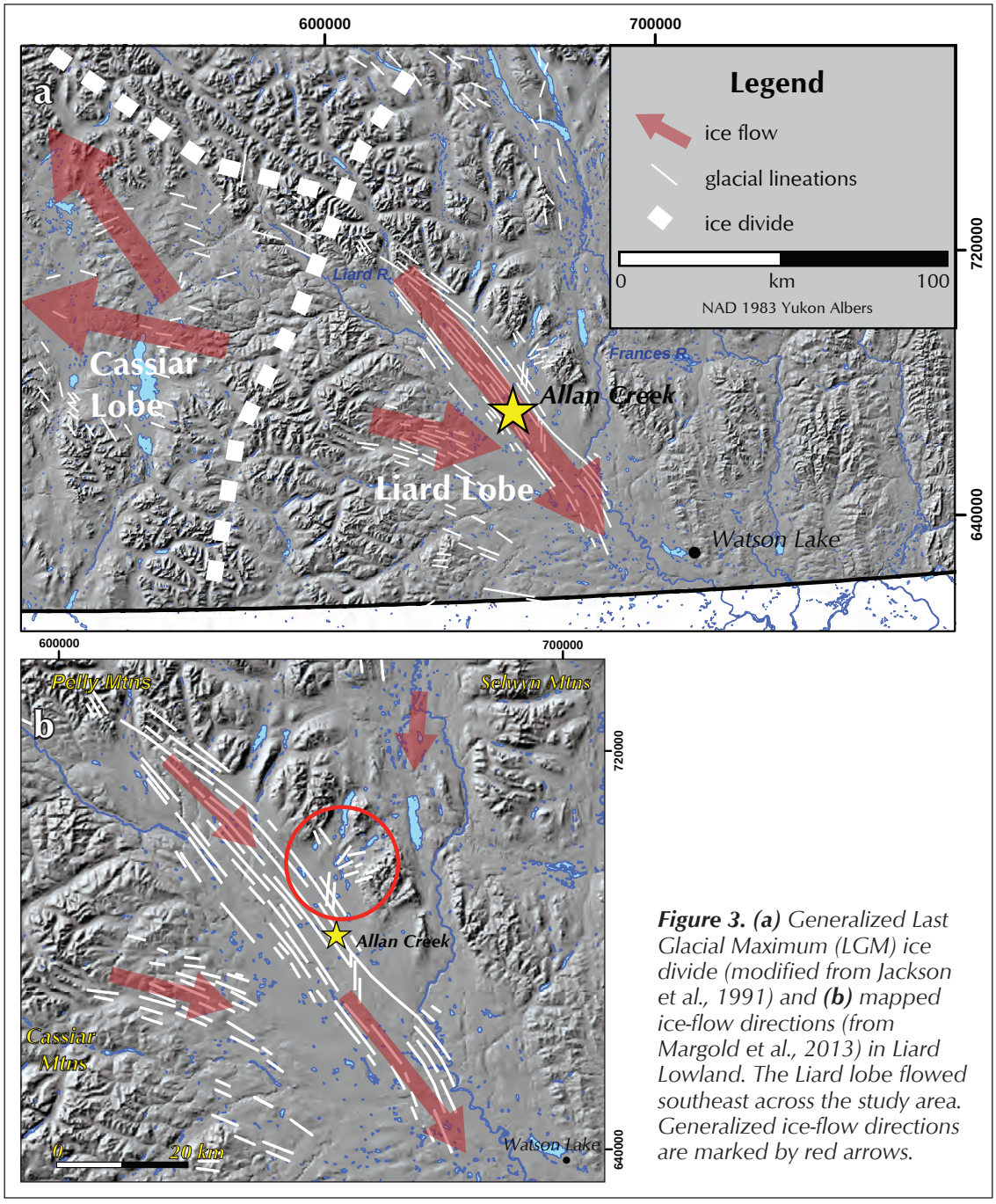

Figure 3. (a) *Generalized Last Glacial Maximum (LGM) ice divide (modified from Jackson et al., 1991) and* ***(b)*** *mapped ice-flow directions (from Margold et al., 2013) in Liard Lowland. The Liard lobe flowed southeast across the study area. Generalized ice-flow directions are marked by red arrows.*

METHODS

Following Klassen's (1987) stratigraphic framework (Fig. 4) we differentiate four diamict units in the Allan Creek section – from base to top Till A, Till B, Till C and Till D – separated by fine-grained, horizontally bedded inter-till units. Clast fabrics were measured in each of the four diamict units, where exposure and access was safe and possible, across a longitudinal span of ~100 m (Fig. 5).

Location information was acquired using a handheld GPS set to a NAD83 datum. Elevations were measured in metres above Liard River using a TruPulse 200 Laser Range Finder. Bulk samples (~5 kg) were collected and screened at 2 mm, 500 μm and 63 μm for more accurate grain-size distribution analysis.

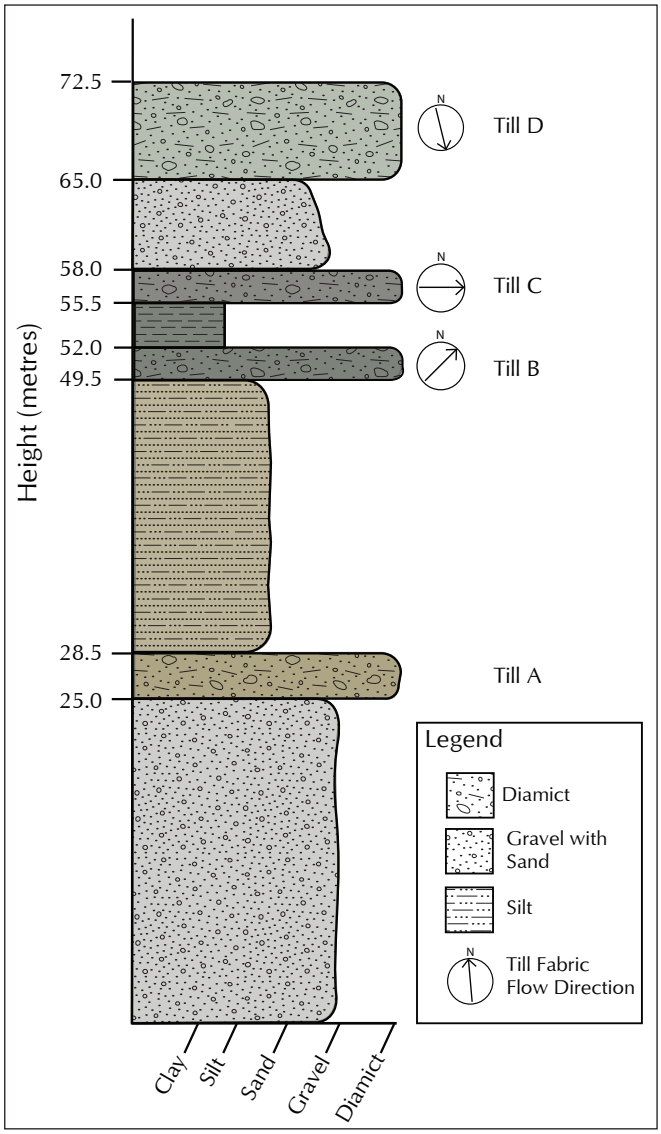

Figure 4. *Summary of the stratigraphy of the Allan Creek section as presented by Klassen (1987). Fabrics were measured only in the three uppermost diamict units (Klassen's "Till B", "Till C", and "Till D").*

Pebble fabric measurements were collected from each diamict unit by clearing two 1 by 1 m vertical exposures with similar elevations. These faces were cleared to fresh surfaces and general observations were recorded, including colour, texture, clast percentage, fissility, and any macro-scale deformation. With the exception of Till C, cleaned faces were oriented perpendicular to each other to reduce aspect bias in the measured clast orientations.

Clasts selected for fabric measurements included rod-shaped, bladed, and platy pebbles (2-6 cm in maximum dimension) with ideal length to width ratios of 2:1, and minimum ratios of 3:2. The trend and plunge of 25 pebbles were measured on each cleared face, yielding 50 clast orientations from each diamict unit. Clast dimensions, lithology, and any glaciogenic wear features were also recorded. Two-dimensional and three-dimensional representations of the pebble fabric for each unit were plotted using Stereonet (v 9.9.4) software as, respectively, rose diagrams and stereo plots. Principal eigenvectors and normalized eigenvalues calculated in the software were subsequently used to plot unit characteristics (glaciogenic sediment flow, lodgment till, or subglacial melt out till) on a May diagram.

RESULTS

TILL D

Till D is a weakly compact, matrix-supported, medium-grey, silty sand boulder diamict (Fig. 6). It is 7 m thick with its base at 78 m above Liard River. The lower contact is planar and gradational, transitioning from a sandy matrix at the base of the unit to a silty matrix towards the top of the unit. Till D forms the surface expression of the landscape at the study area and is discontinuously mantled by up to ~0.5 m of cliff-top loess. The exact nature of the diamict-loess contact is uncertain because of limited clean exposure and a lack of access; cleared faces for fabric measurements were located at the base of the unit ~10 m apart.

The matrix (~70% by volume) comprises 6% silt and clay, and 94% sand (36% coarse, 32% medium, 26% fine sand). Clasts range from pebble to boulder, although boulders are rare; most clasts are striated and faceted. Zones of rusty-purple oxidation occur in horizontal layers. Till D contains abundant oxidized fractures and highly weathered clasts.

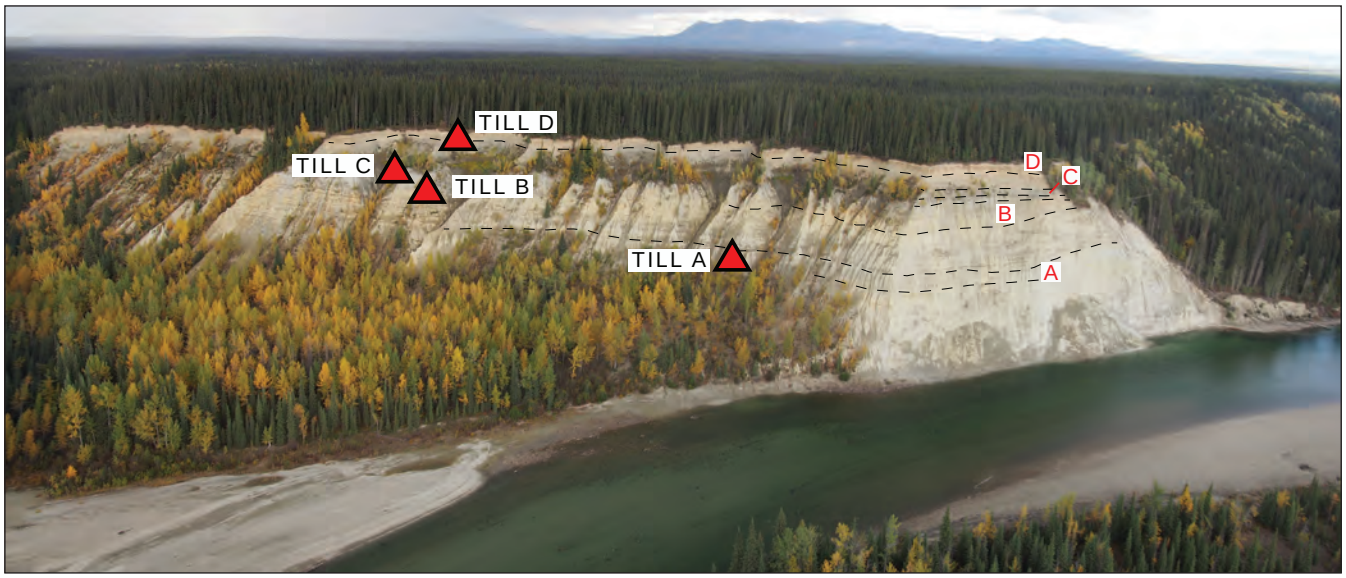

Figure 5. *Site locations of clast fabric measurements (triangles). The ~85-m-tall bluff on the east bank of Liard River is cut by deep gullies that provide fairly continuous lateral exposure and access to each of the units.*

The clast fabric of Till D has a NW-SE trend (Fig. 7). Long-axis clast plunge is generally shallow (<30°) and roughly equally concentrated to the NW and SE. The principal eigenvector has a trend and plunge of 087°/58°, but is not a useful indicator of preferred clast direction given the high dispersion of orientations around the great circle, despite having a strong S1 eigenvalue. The S1 and S3 eigenvalues for Till D are 0.6003 and 0.0543, respectively.

TILL C

Till C is a very compact, matrix-supported dark-blue-grey, silty clay pebble diamict (Fig. 8). The unit is poorly exposed in most locations at the Allan Creek section, so a trench was excavated to provide a fresh surface for sedimentologic

Figure 6. *Till D is a weakly compact medium-grey silty-sand diamict. It contains fewer clasts than stratigraphically lower diamict units, with a diverse variation in grain size. The contact (dashed line) between Till D and underlying glaciofluvial sand is marked.*

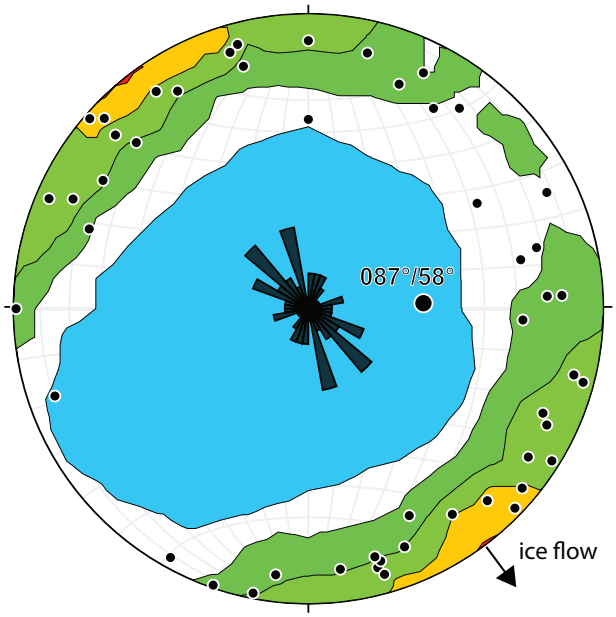

Figure 7. *Stereonet and rose diagram for Till D showing a NW-SE orientation. Each contour represents 2 sigma and the large black dot is the trend/plunge of the eigenvector. The stereonet is plotted on the lower hemisphere of a Schmidt diagram.*

and stratigraphic characterization. The unit is ~4 m thick, coarsening upward in the upper ~2 m from a fine silty-clay matrix to a sandy-silt matrix. The base of the unit is 69 m above Liard River. Till C has a distinctly different colour than tills A, B, and D. A sharp contact separates Till C from the underlying inter-till sediments. The upper contact is sharp and undulating, with concentrations of bright orange-red oxidized clasts.

In the coarser facies at the top of the unit (where the sample was taken), the matrix (~70% by volume) comprises 6% silt and clay and 94% sand (43% coarse, 28% medium, 22% fine sand). Clasts are finer than in the other four till units, with a marked absence of boulders. They range in size from granule to cobble and are predominantly subrounded, striated pebbles. Clasts are predominantly basalt and other volcanic rocks, with some quartzite and foliated metamorphic rocks. The matrix of Till C has oxidized veins and fractures and some clasts are heavily oxidized and weathered orange. In contrast to the other diamict units, joints and fissility were absent in the limited exposures of Till C.

The clast fabric for Till C is bimodal, with two trends oriented NW-SE and WSW-ENE (Fig. 9). The steepness of long-axis plunge is more varied than for the other three diamict units. The principal eigenvectors have a trend and plunge of 064°/31° and 146°/42° for, respectively, the primary and secondary trends. The primary clast trend is roughly WSW-ENE but is dispersed over ~40°. The NW-SE trend, although comprising fewer clasts, is more tightly clustered. The S_1 and S_3 eigenvalues for the entire population of clasts are 0.4627 and 0.2219, respectively.

Figure 8. *Typical appearance of Till C. It is a very compact dark-blue-grey, silty-clay diamict which coarsens in the upper ~2 m from a silty-clay matrix (pictured) to a sandy-silt matrix. The unit is not well exposed and has a distinctly different colour than tills A, B, and D.*

TILL B

Till B is a compact, matrix-supported medium-grey-brown, sandy-silty boulder diamict (Fig. 10). The unit is ~7.3 m thick with its base roughly 60 m above Liard River. It is densely jointed and fissile, with oxidation concentrated along fracture surfaces. The lower contact is sharp and erosive whereas the upper contact is sharp and conformable with overlying inter-till sediments.

The Till B matrix (~60%) comprises 15% silt and clay and 85% sand (31% coarse, 35% medium, 20% fine sand). Clasts range from granules to cobbles, with few boulders. Clasts are predominantly quartzite and basalt, with lesser contributions of granodiorite and foliated metamorphic rocks. Clasts are mainly subrounded, and less commonly rounded or subangular; many are bulleted or faceted. Reddish brown/rusty sand lenses are present throughout the unit and are considerably more cemented than surrounding material. Till B erodes as large vertical spires, making it easy to access different aspects of the unit.

The clast fabric is dominated by a well-defined NNW-SSE trend (Fig. 11). Clast plunges are roughly evenly distributed between the NNW and SSE. The principal eigenvector trend and plunge is 340°/37°. The S_1 and S_3 eigenvalues are 0.7152 and 0.0742, respectively.

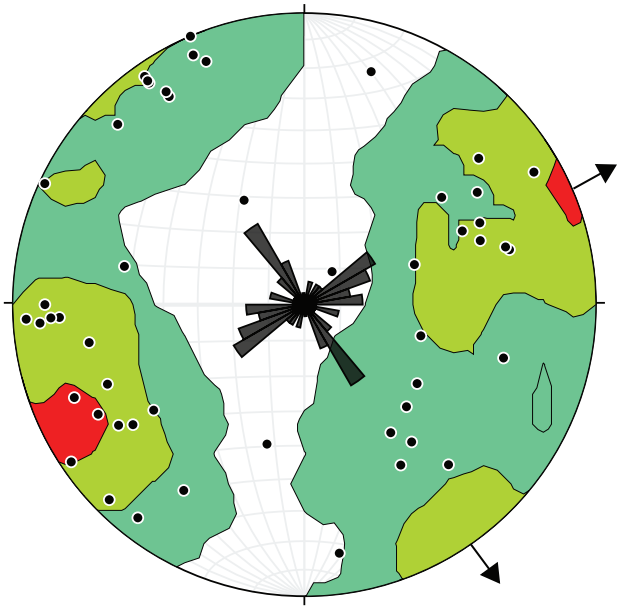

Figure 9. *Stereonet and rose diagram for Till C showing a bimodal trend, with a stronger WSW-ENE trend, and a weaker NW-SE component. Each contour represents 2 sigma. The stereonet is plotted on the lower hemisphere of a Schmidt diagram.*

Figure 10. *Typical appearance of Till B. It is a compact, medium-grey-brown, sandy-silty cobble diamict with weak stratification. Reddish brown/rusty sand lenses occur throughout the unit and are considerably more cemented than surrounding matrix.*

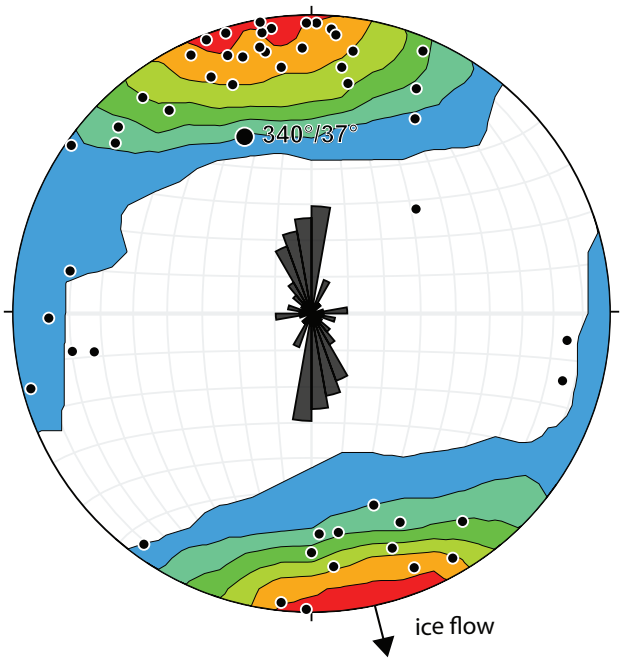

Figure 11. *Stereonet and rose diagram for Till B showing a well-defined NNW-SSE orientation. Each contour represents 2 sigma and the large black dot is the trend/plunge of the eigenvector. The stereonet is plotted on the lower hemisphere of a Schmidt diagram.*

TILL A

Till A is a compact matrix-supported, medium-brown, silty-sandy boulder diamict (Fig. 12) varying from 3.5 to 5.0 m thick. Both the upper and lower contacts are sharp and undulating, suggesting that they are erosive. The unit overlies at least 35 m of pre-glacial, quartz-rich bedded sand and gravel. It is densely jointed and fissile with oxidation concentrated on fracture surfaces, and erodes as large vertical spires providing variable exposure aspects (Fig. 13). Cleared faces for fabric measurements were located near the base of the unit ~4.5 m apart.

The matrix (60%) of Till A comprises 19% silt and clay, and 85% sand (22% coarse, 39% medium, 23% fine). Clasts range from granules to boulders (up to 1 m), and consist of quartzite, quartz, granite, and a minor component of basalt and foliated metamorphic rocks. Clasts are subrounded to subangular and are commonly striated, faceted or bullet-shaped. Striations on bullet-shaped clasts are parallel to the long axis. Granitic pebbles are abundant and distinctly bladed. Most of the potassium feldspar minerals are heavily weathered to orange.

The clast fabric measured in Till A has a strong, well-defined NW-SE trend (Fig. 14). The majority of clasts plunge toward the NW. The principal eigenvector has a trend and plunge of 319°/37°. The S_1 and S_3 eigenvalues are 0.6981 and 0.0731, respectively.

Figure 12. *Typical appearance of Till A. It is a compact medium-brown, silty-sandy cobble diamict. Abundant quartz, quartzite and granite pebbles in the unit are well-rounded, and many granitic pebbles are highly weathered.*

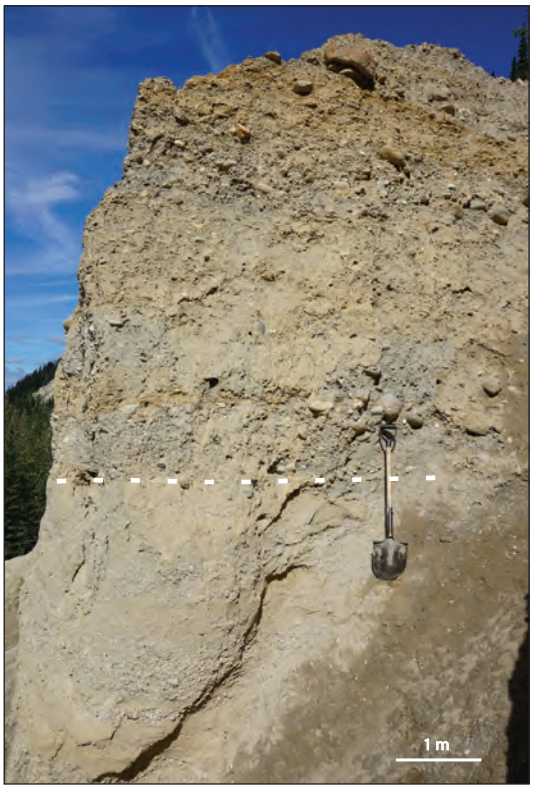

Figure 13. *Lower contact between inferred Tertiary sediments and Till A (marked with dashed line). It is heavily oxidized, horizontal, slightly undulating, and sharp.*

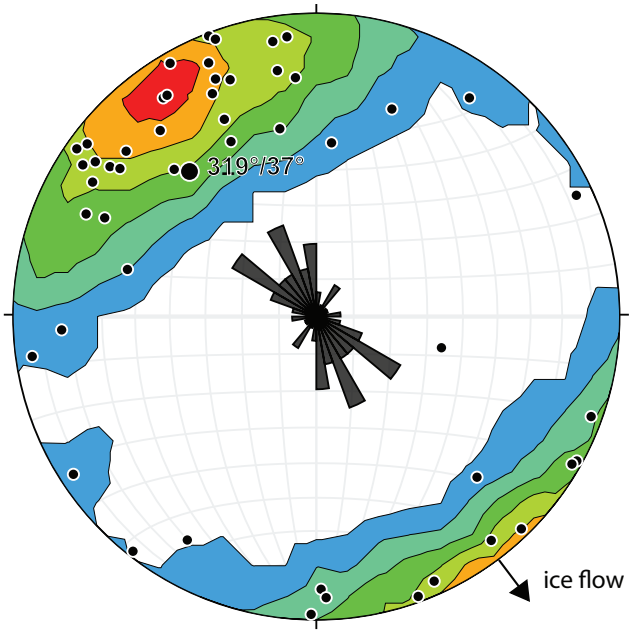

Figure 14. *Stereonet and rose diagram for Till A showing a strongly defined NW-SE orientation. Each contour represents 2 sigma, and the large black dot is the trend/plunge of the eigenvector. The stereonet is plotted on the lower hemisphere of a Schmidt diagram.*

DISCUSSION

Unit elevations, thicknesses and characteristics reported here (Fig. 15) generally agree with the stratigraphy reported by Klassen (1978, 1987; Fig. 4). New flow direction interpretations from clast fabrics measured in this work support the original fabrics measured by Klassen (1987) for the upper two diamict units. The uppermost diamict (Till D) records LGM glaciation of the Liard basin. The NW-SE clast fabric reported here for this unit is consistent

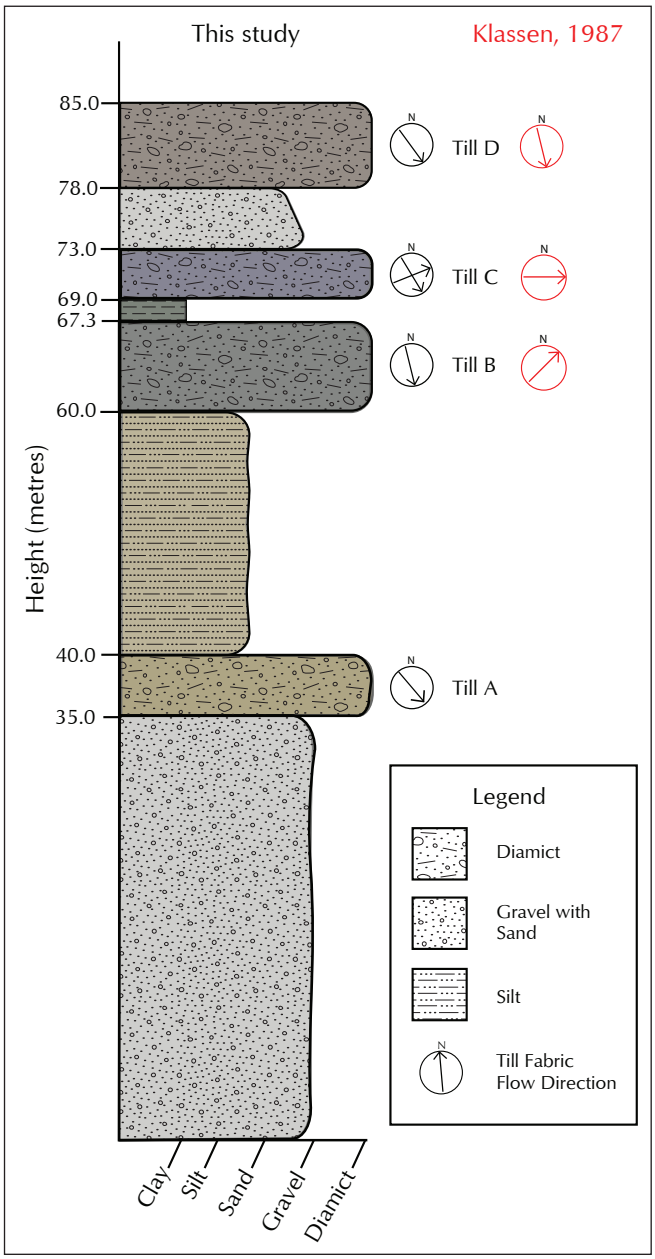

Figure 15. *Stratigraphy for the Allan Creek section measured in this study closely resembles the original stratigraphy presented by Klassen (1987; Fig. 4).*

with previously reported fabrics (Klassen, 1987) as well as streamlined landforms across the Liard Lowland (Klassen, 1987; Margold *et al.*, 2013). The presence of glaciogenic wear features on clasts of all four diamict units suggests their lodgement beneath ice (*cf*. Lian and Hicock, 2010).

Till D plots in between the 'lodgement till' and 'glaciogenic sediment flow' classification of the May diagram (Fig. 16). The physical characteristics of Till D, along with the unidirectional flow shown in the contoured stereonets and rose diagrams, suggest it was deposited as a lodgement till. The NW-SE trend of this unit's clast fabric supports southeastward ice flow suggested by streamlined landforms that dominate the geomorphic grain of Liard Lowland.

The second highest diamict at the Allan Creek section (Till C) differs from the other three glacial units. It has a finer matrix, finer clasts, and overall lower clast content. Unlike the other diamict units, it does not display typical characteristics of a lodgement till (Fig. 16) such as clast long-axes clustered around a single orientation (Evans *et al.*, 2007) and prevalent signs of abrasion on clast surfaces (Benn and Evans, 2010). Thus, Till C may not accurately record ice-flow direction. Its clast fabric reveals concentration about two orientations and the unit plots in the 'glaciogenic sediment flow' classification of the May diagram (Fig. 16). The use of a May diagram with bimodal clast fabrics is problematic because this diagram was designed to work with unimodal fabrics. Therefore interpreting this unit as a glaciogenic sediment flow may not accurately represent the depositional environment (Hicock *et al.*, 1996). Our clast fabric concentrations (064°/31°) and (146°/42°) are similar to, respectively, Klassen's W-E fabric trend and the NW-SE trend of the basin. Both directions align with streamlined landforms in the vicinity of the Allan Creek section (Margold *et al.*, 2013; Klassen, 1987), although W-E landforms are rare (*see* Fig. 3).

The specific mode of emplacement of Till C, and thus the significance of its clast fabrics, is uncertain. Given the close alignment of this unit's fabric with W-E oriented landforms that Margold *et al.* (2013) interpret as having been overprinted during the LGM by a NW-SE geomorphic grain, it is tempting to interpret Till C as lodgement till recording basal ice-flow directions. The W-E orientations might record pediment or valley-bound glaciation emanating from the Selwyn Mountains that followed the Frances River valley.

Till B, the second lowest diamict in the sequence, plots in the 'lodgement till' classification of the May diagram (Fig. 16). The orientation of clast long-axes subparallel to the NW-SE trend of Liard Lowland (160°/37°; Fig. 11) as well as the physical characteristics of this unit, particularly extensive evidence of abrasion on clasts, further support an interpretation of a lodgement till. Although long-axes of clasts dip both to the northwest and southeast, the S1 eigenvector and strong S1 eigenvalue indicate a more dominant north-northwesterly plunge. Since the long-axes of elongate clasts typically plunge up-flow in lodgement tills (Evans *et al.*, 2007), Till B suggests ice flow toward the south-southeast. In contrast, Klassen (1987) reports a clast fabric with a SSW-NNE trend, roughly transverse to the trend of the Liard Lowland.

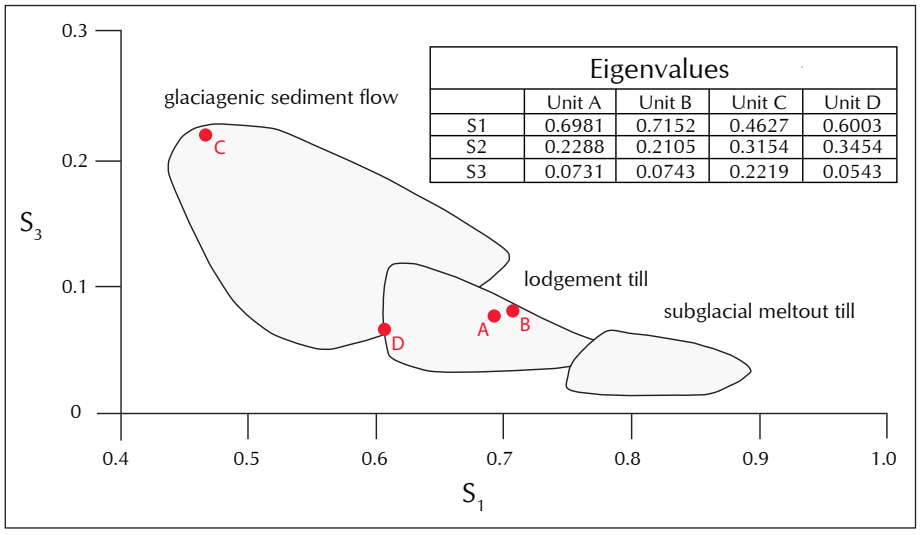

Eigenvalues

	Unit A	Unit B	Unit C	Unit D
S1	0.6981	0.7152	0.4627	0.6003
S2	0.2288	0.2105	0.3154	0.3454
S3	0.0731	0.0743	0.2219	0.0543

Figure 16. *May diagram with principal eigenvalues for Units A, B, C, and D. Base diagram modified from Hicock et al., (1996).*

The lowest and oldest till in the Allan Creek section (Till A) is of particular importance because Klassen (1978, 1987) did not report fabric measurements for it. This unit shows a strong NW-SE fabric (139°/37°). Till A plots in the 'lodgement till' classification of the May diagram (Fig. 16). The physical characteristics of Till A, including the prevalence of striated and faceted clasts, as well as the close alignment of its clast fabric (Fig. 14) with the trend of Liard Lowland suggest deposition as a lodgement till. Given the predominance of plunge of long-axes of elongate clasts to the northwest, the earliest ice flow recorded at the Allen Creek section was most likely from northwest to southeast (*cf.,* Evans *et al.*, 2007).

If fabric measurements of diamict units in the Allan Creek section faithfully record paleo-ice flow directions in Liard Lowland, at least three of the four glacial diamict units represent basal deposition and record glacial events with ice flow toward the NW or the SE. This is consistent with previously published descriptions of LGM glaciation in Liard Lowland, which indicate southeasterly flow. Our new measurements of NW to SE flow in Till A suggest ice flow during early glaciation of the region was similar to that during the LGM.

Limitations of clast fabric analysis include sample bias when choosing clasts and localities of sampling area as well as the potential for sampling material that has been influenced by post-depositional processes. Unimodal distributions for two-dimensional clast directions for three units – Tills A, B and D – suggest ice flow trending roughly parallel to the trend of Liard Lowland. Additional details enable interpretation of unidirectional ice-flow patterns for these three glacial diamict units. Concentrations of clast plunge directions reported here suggest ice flow to the southeast and south-southeast during emplacement of, respectively, Till A and Till B. Previous studies of LGM landforms indicate that Till D was similarly emplaced by southeast-flowing ice.

CONCLUSIONS

The Allan Creek section records four glacial events – possibly representing four separate glaciations – alternating with periods when fine-grained, non-diamict units were deposited. Clast fabrics from Tills A, B, and D suggest that regional ice-flow was along the NW-SE trend of Liard Lowland, although only Till A and B suggest a clear down-valley flow direction. Till C has a bimodal WSW-ENE and NW-SE fabric. The NW-SE fabric seen in these glacial diamict units aligns with known ice-flow direction during the LGM in Liard Lowland and is consistent with the orientation of streamlined landforms in the basin. The WSW-ENE component recorded by Till C, which was also noted during previous work at the site, aligns with rare crosscutting lineations in the region, but the depositional environment of this unit remains uncertain.

Sedimentologic and stratigraphic details reported here generally agree with previously reported reconnaissance studies including descriptions of unit thicknesses, and clast fabrics for the upper two glacial diamict units. Furthermore, plotting clast fabric eigenvalues on the May diagram provides support for environmental interpretation of all four glacial diamict units in this sequence. Our addition of clast orientations for Till A provides the first details on ice flow for the earliest glaciation of Liard Lowland, and likely one of the earliest glaciations of southeastern Yukon. Ice flow during this earliest glaciation, along with the second glaciation recorded in the region (Till B) and the most recent LGM (Till D), appears to have paralleled the trend of Liard Lowland.

ACKNOWLEDGEMENTS

Kaska Dene Council and Liard First Nation are acknowledged for their support of this work in their Traditional Territory. We thank Rudy Klassen for his considerable insight during the planning stages of this research. S.E. would like to thank the Yukon Geological Survey for providing the opportunity to undertake this study during a summer field position, and for the good company, insightful discussions and support from fellow crew members. Capable helicopter support was provided by TRK Helicopters and accommodations in Watson Lake were provided by the Air Force Lodge.

REFERENCES

Barendregt, R.W., Enkin, R.J., Duk-Rodkin, A. and Baker, J., 2010. Paleomagnetic evidence for multiple late Cenozoic glaciations in the Tintina Trench, west-central Yukon, Canada. Canadian Journal of Earth Science, vol. 47, p. 987-1002.

Benn, D. I. and D. J. A. Evans (2010). Glaciers and Glaciation, 2nd ed. Hodder Education, 816 p.

Bostock, H.S., 1948. Physiography of the Canadian Cordillera, with special reference to the area north of the fifty-fifth parallel. Geological Survey of Canada, Memoir 247.

Bostock, H.S., 1966. Notes on glaciation in central Yukon Territory. Geological Survey of Canada, Paper 65-56, 18 p.

Clague, J.J. and Ward, B., 2011. Pleistocene glaciation of British Columbia. *In:* Quaternary glaciations – extent and chronology, a closer look, J. Ehlers, P.L. Gibbard and P.D. Hughes (eds.). Developments in Quaternary Science, vol. 15, p. 563-573.

Dawson, G.M., 1898. Report on the exploration in the Yukon District, N.W.T. and adjacent northern portion of British Columbia, 1887. Geological and Natural History Survey of Canada, Annual Report, Vol 3, Part 1, 1887-88. Montreal, William Foster Brown & Co, Montreal, 277 p. and 3 maps.

Duk-Rodkin, A., 1999. Glacial Limits Map of Yukon. Yukon Geological Survey, Geoscience Map 1999-2, scale 1:1 000 000, 1 sheet; *also known as GSC Open File 3694*.

Duk-Rodkin, A., Barendregt, R.W., Froese, D.G., Weber, F., Enkine, R., Smith, R., Zazula, G.D., Waters, P. and Klassen R., 2004. Timing and extent of Plio-Pleistocene glaciations in north-western Canada and east-central Alaska. *In*: Developments in Quaternary glaciation – extent and chronology, vol. 2, J. Ehlers and P.L. Gibbard (eds.). Developments in Quaternary Science, vol. 2b, p. 313-345.

Duk-Rodkin, A., Barendregt, R.W. and White, J.M., 2010. An extensive late Cenozoic terrestrial record of multiple glaciations preserved in the Tintina Trench of west-central Yukon: Stratigraphy, paleomagnetism, paleosols, and pollen. Canadian Journal of Earth Science, vol. 47, p. 1003-1028.

Evans, D.J.A., Hiemstra, J.F. and O'Cofaigh, C., 2007. An assessment of clast macrofabrics in glacigenic sediments based on A/B plane data. Geografiska Annaler, vol. 89 A, p. 103–120.

Hicock, S.R., Goff, J.R., Lian, O.B. and Little, E.C., 1996. On the interpretation of subglacial till fabric. Journal of Sedimentary Research, vol. 66, p. 928-934.

Hughes, J.D. and Long, D.G.F., 1980. Geology and coal resource potential of Early Tertiary strata along Tintina Trench, Yukon Territory. Geological Survey of Canada, Paper 79-32, 21 p.

Hughes, O.L., Rampton, V.A. and Rutter, N.W., 1972. Quaternary geology and geomorphology, southern and central Yukon. *In:* Guidebook for field excursion A11, XXIV International Geological Congress, Montreal, Que., p. 30-36.

Jackson, L.E., Ward, B., Duk-Rodkin, A. and Hughes, O.L., 1991. The Last Cordilleran Ice Sheet in Southern Yukon Territory. Geographie physique et Quaternaire, vol. 453, p. 341-354.

Klassen, R.W., 1978. A unique stratigraphic record of late Tertiary-Quaternary events in southeastern Yukon. Canadian Journal of Earth Science, vol. 15, p. 1884-1886.

Klassen, R.W., 1987. The Tertiary Pleistocene stratigraphy of the Liard Plain, southeastern Yukon Territory. Geologic Survey of Canada, Paper 86-17, 21 p.

Klassen, R.W. and Morison, S R., 1982. Surficial Geology, Watson Lake, Yukon Territory. Geological Survey of Canada, Preliminary Map 21-1981, scale 1:250 000, 1 sheet.

Leonard, L.J., Mazzotti, S. and Hyndman, R.D., 2008. Deformation rates estimated from earthquakes in the northern Cordillera of Canada and eastern Alaska. Journal of Geophysical Research, vol. 113, B08406.

Lian, O.B. and Hicock, S.R., 2010. Insight into the character of palaeo-ice-flow in upland regions of mountain valleys during the last major advance (Vashon Stade) of the Cordilleran Ice Sheet, southwest British Columbia, Canada. Boreas, vol. 39, p. 171-186.

Mathews, W.H., 1986. Physiography of the Canadian Cordillera. Geological Survey of Canada, Map 1701A, scale 1:5 000 000, 1 sheet.

Margold, M., Jansson, K.N., Kleman, J. and Stroeven, A.P., 2013. Late glacial ice dynamics of the Cordilleran Ice Sheet in northern British Columbia and southern Yukon Territory: Retreat pattern of the Liard Lobe reconstructed from the glacial landform record. Journal of Quaternary Science, vol. 28, p. 180-188.

Roddick, J.A., 1967. Tintina Trench. Journal of Geology, vol. 75, p. 23-33.

An overview of shale studies in Yukon during the 2017 field season

T.A. Fraser, P.J. Sack
Yukon Geological Survey

I. Crawford, D. Layton-Matthews
Queen's University, Ontario

M.G. Gadd, J.M. Peter
Geological Survey of Canada, Ottawa

K. Henderson
McGill University, Quebec

M. Melchin
St. Francis Xavier University, Nova Scotia

E. Sperling
Stanford University, California

J. Strauss
Dartmouth College, New Hampshire

Fraser, T.A., Crawford, I., Gadd, M.G., Henderson, K., Layton-Matthews, D., Melchin, M., Peter, J.M., Sack, P.J., Sperling, E. and Strauss, J., 2018. An overview of shale studies in Yukon during the 2017 field season. *In:* Yukon Exploration and Geology 2017, K.E. MacFarlane (ed.), Yukon Geological Survey, p. 37-45.

ABSTRACT

Summer 2017 fieldwork in Yukon's lower Paleozoic shale basins (Selwyn basin and Richardson trough) involved participants from government geological surveys (Yukon Geological Survey, Geological Survey of Canada) and several universities (Queen's, McGill, St. Francis Xavier, Stanford and Dartmouth College). Research interests include: 1) shale chemostratigraphy and biostratigraphy, and pyrite trace element geochemistry to characterize shale units and assess lower Paleozoic paleoenvironmental conditions and depositional controls; and 2) an assessment of hyper-enriched black shales, specifically the colloquial 'Nick' or 'Ni-Mo' mineralized Ni-Zn-Mo-PGE deposit, in order to develop internally consistent genetic and exploration models for these types of deposits. This paper describes individual research projects underway and summarizes fieldwork in summer 2017.

* *tiffani.fraser@gov.yk.ca*

INTRODUCTION

Recent academic interest in shale deposits in Yukon led to a busy summer of fieldwork in Yukon's Paleozoic shale basins. In late 2016, the Yukon Geological Survey (YGS) invited current shale researchers to join an informal shale working group to share research ideas and to coordinate field-related logistics. This paper summarizes the current state of shale research in Yukon and activities during the 2017 field season.

PALEOZOIC SHALE BASINS

Cambrian to Middle Devonian shale basins (Selwyn basin and Richardson trough; Fig. 1) characterized the northwestern margin of ancestral North America (Laurentia). These were sites of deposition of thick shale sequences situated outboard of an extensive carbonate platform known as the Mackenzie platform. The lower Paleozoic tectonic setting consisted of relatively quiescent passive margin sedimentation with intermittent extension and mafic volcanism in the Cambrian, Early to Middle Ordovician, Silurian and Middle to Late Devonian (Nelson *et al.*, 2013). Richardson trough was the main focus of field studies in 2017, along with minor work in Selwyn basin (Fig. 1). Figure 2 displays the generalized stratigraphy of the Paleozoic shale units in Richardson trough and Selwyn basin that are mentioned in this paper.

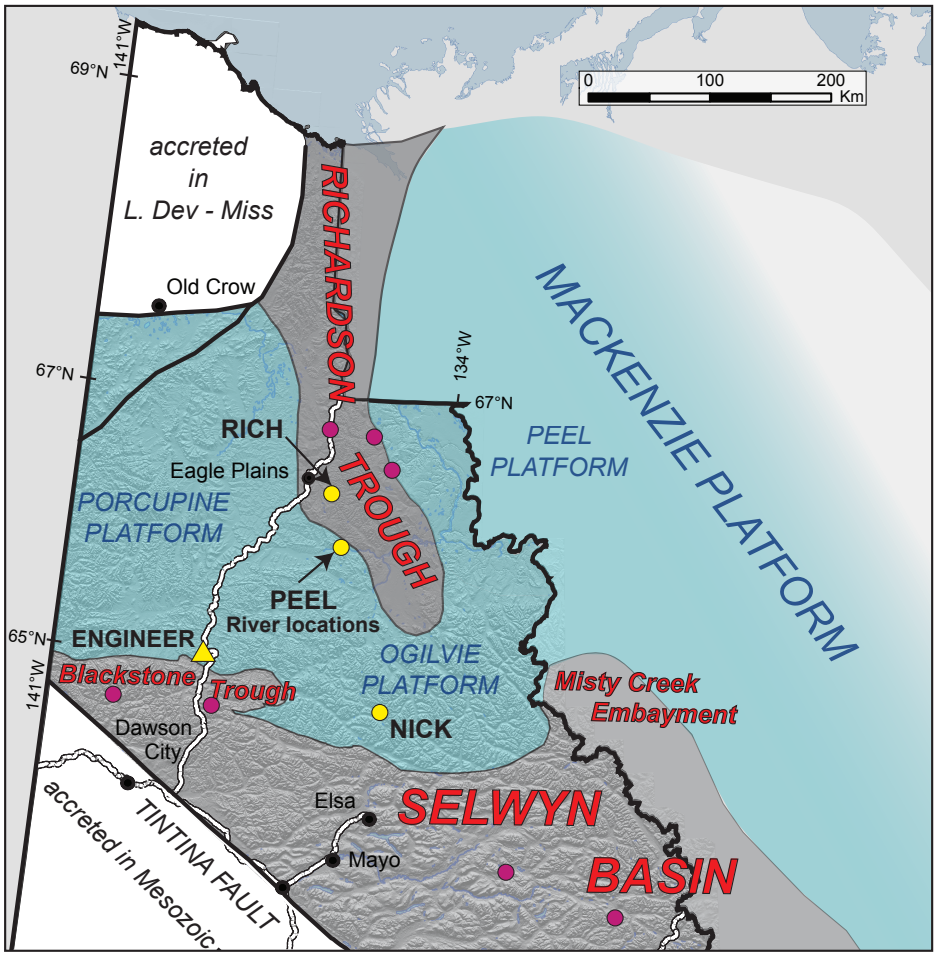

Figure 1. *Generalized map of North Yukon with location of major lower Paleozoic carbonate platforms (blue) and basins (grey). All circle markers (yellow and purple) indicate locations of Nick-style or Ni-Mo mineralization (also, hyper-enriched black shales: HEBS) with yellow denoting locations mentioned in the paper. The purple dots are Ni-Mo horizon outcrops noted from other sources (e.g., Yukon MINFILE 2017, Fraser and Hutchison, 2017). The yellow triangle marks the location of a shale outcrop of indeterminate Paleozoic age measured by YGS in summer 2017.*

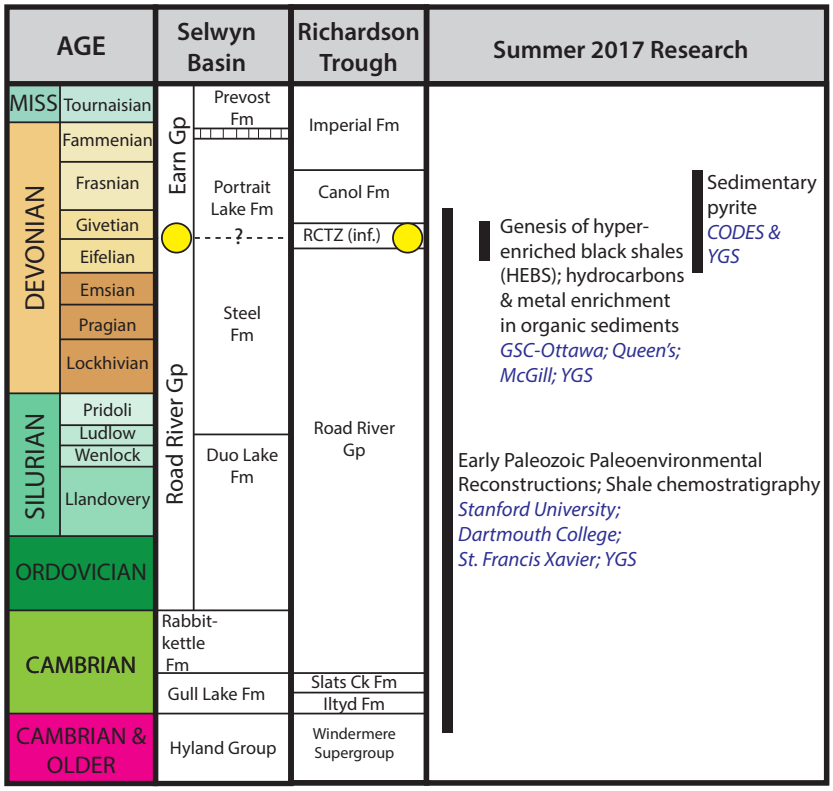

Figure 2. *Generalized stratigraphy for the lower Paleozoic sections in Selwyn basin (NTS 105 I,J,K map areas; after Gordey and Anderson, 1993; Gordey, 2013) and Richardson trough (after Fraser and Hutchison, 2017) alongside the 2017 shale research programs in Yukon. The yellow dot denotes the position of the Nick or Ni-Mo mineralized zone referred to in the text.*

SHALE CHEMOSTRATIGRAPHY

With some notable exceptions, including seminal work on lower Paleozoic stratigraphy (*e.g.*, Lenz and Pedder, 1972; Cecile *et al.*, 1982; Pugh, 1983; Norris, 1985, 1997; Gordey and Anderson, 1993; Morrow, 1999; Gordey, 2013) and bedrock mapping (*e.g.*, Norris 1981; 1982a,b,c,d; Cecile *et al.*, 1982), lower Paleozoic fine-grained sedimentary rocks (*i.e.*, mudstone, siltstone, shale) in north and central Yukon have been largely overlooked in the past. Detailed studies have been restricted to petroleum source rock generative potential (*e.g.*, Feinstein *et al.*, 1988; Link *et al.*, 1989) or mineral potential (*e.g.*, SEDEX deposits; *e.g.*, Goodfellow, 1987; Gadd *et al.*, 2016). Missing from the Yukon dataset are systematic and comprehensive lithogeochemical analyses of these fine-grained rocks, which would facilitate the differentiation and correlation of these commonly thick, regionally distributed units that were deposited over long time periods. To fill this void, the YGS has been identifying and evaluating fine-grained sedimentary rocks in the traditional oil and gas regions of North Yukon for several years (*e.g.*, Allen, 2010; Fraser *et al.*, 2012; Fraser, 2014; Fraser and Reinhardt, 2015; Fraser and Hutchison, 2017). As these units can be difficult to differentiate in drill core, YGS is using a combination of field studies and chemostratigraphy to provide lithofacies interpretations and a sequence stratigraphic framework for the shales. These studies not only provide detailed lithogeochemical markers that can be used for identification and correlation, but have also been useful in characterizing paleoenvironmental conditions such as redox, hydrography, eustasy, and in fossil poor sections have provided a proxy for age control (*see* Fraser and Hutchison, 2017).

In 2017, Tiffani Fraser (YGS) continued work on the Cambrian-Middle Devonian Road River Group and overlying Middle-Upper Devonian Canol Formation (Richardson trough) or Earn Group (Selwyn basin; Fig. 2), with a particular interest in determining the sequence stratigraphic framework for the mineralized contact zone between the two. This interval is known as either the "Nick" zone, after a mineral property of the same name 133 km north of Mayo (Fig. 1), or alternatively as the "Ni-Mo" horizon (herein) for its metal enrichment (percentage level concentrations of Ni and thousands of ppm of Mo). At the Nick property, the Ni-Mo horizon is a thin, stratiform, ≤3 cm thick metalliferous unit with anomalous concentrations of Ni, Zn, PGE, Se, As, Mo, Pb, Ba, U (Hulbert *et al.*, 1992) that has an extensive distribution through north and central Yukon. Two exceptional outcrop exposures of this interval occur along the Peel River, upstream of Aberdeen Canyon, in the former Richardson trough (Figs. 3 and 4). Tiffani, along with Patrick Sack (YGS), investigated the south bank exposure in July; and in August, Tiffani continued the investigation on the north bank with Leyla Weston (YGS) and a contingent from the Geological Survey of Canada (GSC; Mike Gadd and colleagues, project described below). A similar stratigraphic sequence was also visited in the eastern Richardson Mountains, along a creek exposure on the Rich property (Fig. 1). As part of a long-standing project on characterizing the extensive shale

deposits of North Yukon, Tiffani and Leyla also evaluated several indeterminate shale outcrops along the Dempster Highway, in the vicinity of Engineer Creek (Fig. 1) with a goal of defining their age and stratigraphic position.

SEDIMENTARY PYRITE

The upper Road River Group from the Peel River south bank section, previously mentioned (Fig. 3), was also systematically sampled in summer 2017 by Patrick Sack for sedimentary pyrite. This work is part of an ongoing study in conjunction with the Centre for Ore Deposit Research (CODES) at the University of Tasmania. The study involves determining the trace element content of syngenetic and early diagenetic pyrite (herein sedimentary pyrite) that can be used as a proxy for paleo-ocean chemical conditions at the time of formation (*e.g.*, pH, alkalinity and oxygenation level of coeval seawater; *see* Large *et al.*, 2017). The trace element content of sedimentary pyrite in the Road River Group samples will be determined at CODES using laser ablation inductively coupled plasma mass spectrometry (LA-ICPMS). The study will compare results of this technique to other paleo-ocean chemistry proxies (*e.g.*, bulk geochemical compositions) currently being conducted on the same rocks by other research teams.

EARLY PALEOZOIC PALEOENVIRONMENTAL RECONSTRUCTIONS

Summer 2017 marked a third and final field season for a research team composed of Erik Sperling (Stanford University, California), Justin Strauss (Dartmouth College, New Hampshire), and Michael Melchin (St. Francis Xavier University, Nova Scotia), in collaboration with Tiffani Fraser (YGS), studying the Road River Group along the Peel River (Fig. 3). The Road River Group at this locality preserves an essentially continuous deep marine record

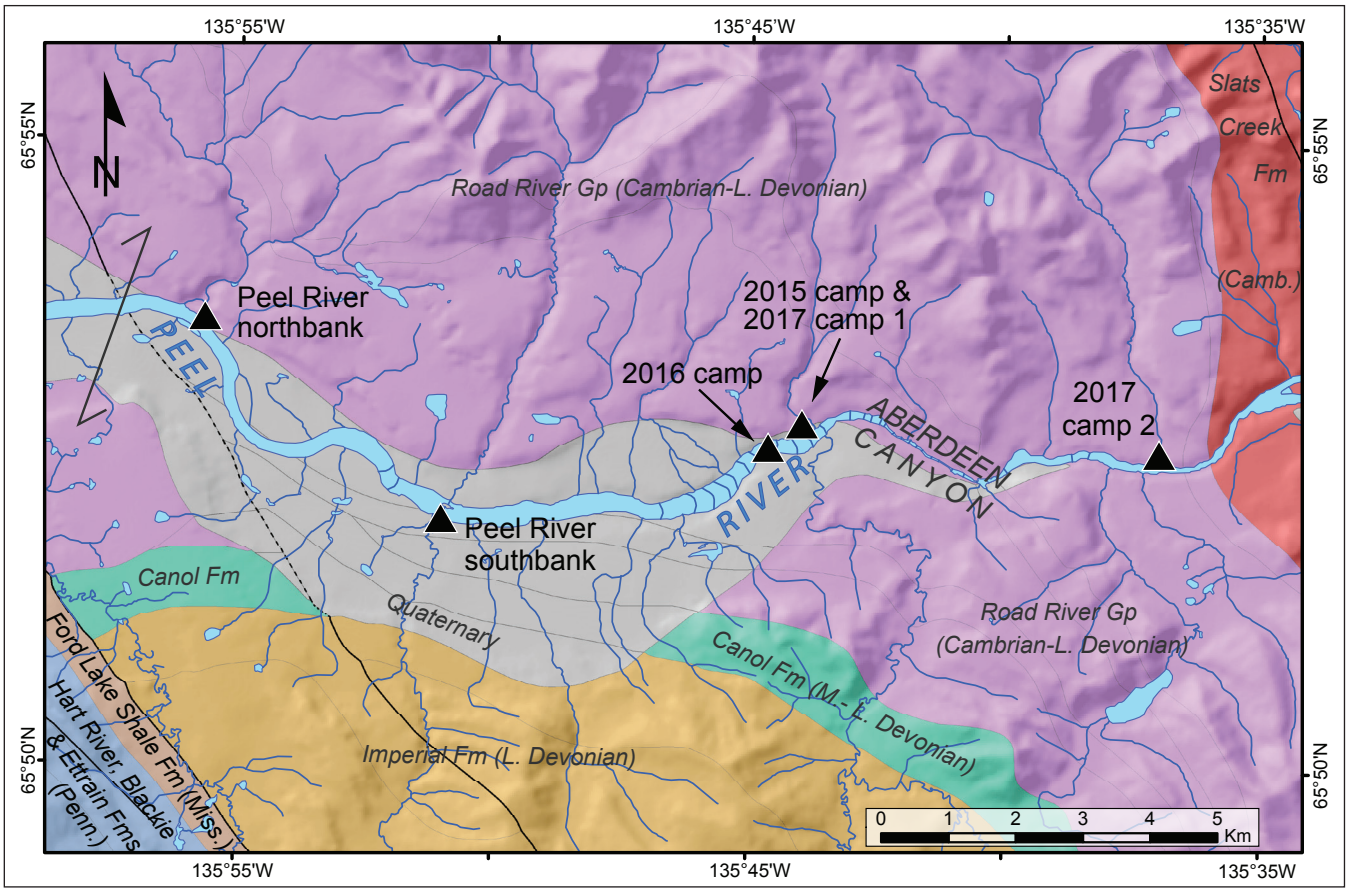

Figure 3. *Bedrock geology map of study area showing shale research stations (black triangles) along the Peel River mentioned in the text. The 2015, 2016 and 2017 sites were camping locations for the Stanford University and Dartmouth College teams in respective years. Geology after Yukon Geological Survey (2015). Black lines denote faults (solid=actual; dashed=inferred). Light grey lines are mapped formation/group subdivisions.*

Figure 4. *Erik Sperling (Stanford University) at the Peel River south bank section. The Ni-Mo horizon (position marked by red dashed line) sits at the contact between the Road River Group and overlying Canol Formation. At this and other locations, large carbonate concretions characterize the uppermost strata of the Road River Group (brown/orange resistant masses between Erik's head and waist region).*

of late Cambrian through Middle Devonian time in a single, unmetamorphosed and well-exposed stratigraphic section along the Peel River (Lenz and Pedder, 1972). This work has shown that the rocks do not support the premise that the stratigraphic record is "more gap than record". The detailed re-examination of this section led by Erik and Justin will provide a unique opportunity to build an ~120-million-year record of early Paleozoic Earth history. Overall, the study goals are to: 1) provide a detailed sedimentological framework for the Peel River section of the Road River Group; 2) produce a detailed age model for the section based on U-Pb geochronology and multiple lines of biostratigraphic evidence; and 3) analyze multiple geochemical proxies to determine how local and global paleoenvironmental conditions changed during this interval.

This research began in 2015 on the north side of the Peel River with systematic measuring and sampling of the Middle Ordovician through Upper Silurian part of the Road River Group (2015 camp; Fig. 3). In 2016, focus was on the south side of the river from the Upper Silurian through to the Peel River south bank section of the Ni-Mo horizon currently being studied by other research groups summarized in this paper (2016 camp; Fig. 3). Finally, in summer 2017 there were two camps (2017 camp 1 and 2; Fig. 3). The first was to re-visit the 2015 camp with the goal of completing detailed graptolite biostratigraphic and carbon isotope chemostratigraphic studies of Upper Ordovician and Lower Silurian strata. The second camp was located below (east of) Aberdeen Canyon, and work here focused on measuring and sampling Upper Cambrian through Middle Ordovician strata.

With a complete composite stratigraphic section of the Road River Group completed, the focus is now on biostratigraphic, geochronological, and geochemical analyses. With respect to age control, four Ordovician ash beds have been analyzed using high-precision chemical abrasion isotope dilution thermal ionization mass spectrometry (CA-ID-TIMS) methods on zircon (Fig. 5). In combination with two new ash beds sampled in 2017, these ages provide anchor points for the Road River Group and will help revise the global Ordovician timescale. Graptolite biostratigraphic studies (Fig. 6) in combination with organic carbon isotope chemostratigraphy have precisely located the position of key Ordovician and Silurian stratigraphic boundaries, and all of the major Silurian positive carbon isotope excursions have been identified. This is the first time these carbon cycle perturbations have been recognized in Yukon shale successions. Ongoing graptolite and conodont biostratigraphic study in the previously undated Devonian portion of the Road River Group should improve time resolution in strata preceding the Ni-Mo horizon. Finally, shale samples have been collected throughout the section at ~2 m stratigraphic intervals and are being analyzed for iron speciation, redox-sensitive trace metal abundance, organic carbon contents and isotopes, and pyrite sulphur isotopes. Ultimately, this high-resolution dataset should provide new insight into many aspects of early Paleozoic paleoenvironmental change.

Figure 5. *Tom Boag (Stanford University) and Justin Strauss (Dartmouth College) collecting samples from Lower Ordovician ash beds (red dashed lines) in the Road River Group below (immediately east of) Aberdeen Falls, Peel River.*

Figure 6. *Graptolite impressions in Lower Ordovician (Tremadocian) strata below Aberdeen Falls, Peel River. The large impression on the left is Kiaerograptus. The larger one on the right is Clonograptus. Centimetre scale at bottom of photograph.*

HYPER-ENRICHED BLACK SHALES

Through the Targeted Geoscience Initiative (TGI) of the Geological Survey of Canada, Mike Gadd and Jan Peter (GSC-Ottawa) are researching the origin of, and processes responsible for, hyper metal-enriched black shales (HEBS), including the Ni-Mo horizon, contained within Devonian stratigraphy of North Yukon. HEBS are thin (<10 cm) and geographically widespread (10 000s of km^2), and are an important global repository for Zn, Ni, Cu, Mo, Se, U, V, ± Cr, Co, Ag, Au, platinum group elements (PGE) and rare earth elements (Jowitt and Keays, 2011). The HEBS layers consist of semi-massive to massive sulphides hosted in carbonaceous shales, that are intercalated with 'background' carbonaceous shales (*i.e.*, not hyper-enriched). Yukon hosts some of the best examples of HEBS globally (*e.g.*, Nick Ni-Zn-Mo-PGE deposit (Ni-Mo horizon); Hulbert *et al.*, 1992) and there is significant potential for further discovery of deposits. Indeed, several HEBS occurrences have been documented in the Richardson trough area of North Yukon (Fig. 1), and these are surmised to have been deposited at the same stratigraphic interval as at the Nick property (*i.e.*, at the Middle Devonian contact of the Road River Group and Canol Formation; Figs. 3 and 4).

Fieldwork in 2017 focused on lesser known examples of HEBS deposits along the north and south banks of the Peel River (Fig. 3) and on the west side of the Richardson Mountains at the Rich property (Fig. 1). At the Peel River localities, we documented for the first time up to three discrete HEBS layers that are not structural repetitions. We have identified abundant biogenic debris — conodont elements and petrified wood (Fig. 7) — within these metalliferous shale layers. Whereas the uppermost HEBS layer at Peel River has been constrained biostratigraphically to the Givetian stage (Gadd and Peter, 2018), the underlying HEBS layers have not yet been dated. However, the stratigraphically lower HEBS layers also contain biogenic debris, and we aim to characterize this as well. This will fulfill one of the salient research goals, to constrain the duration of HEBS mineralizing events. A critical aspect of this research is to understand the processes responsible for HEBS deposit formation. Preliminary data indicate that the metals and metalloids were scavenged from seawater, the efficiency of which was enhanced by extremely low rates of clastic sedimentation (*i.e.*, condensed sedimentation; *see* Fraser and Hutchison, 2017) and highly efficient organic matter remineralization (Gadd and Peter, in press). Ultimately, we aim to develop internally consistent genetic and exploration models for HEBS deposits in Yukon.

Affiliated with the TGI HEBS study, is research by Isobel Crawford. Her MSc graduate research at Queen's University (Ontario) is being conducted under the supervision of Dan Layton-Matthews. Isobel is investigating the ambient paleoenvironmental redox conditions of Richardson trough during deposition of the HEBS Ni-Zn-Mo-PGE horizon (Ni-Mo horizon) and adjacent stratigraphy, using Mo, Tl and U isotopes. Fieldwork in August focused on

Figure 7. *Pyritized plant fragments on a bedding surface of the Ni-Mo horizon at the Peel River north bank section.*

systematic collection of samples collected from outcrop and short drillcores from the Peel River north and south bank sections (Fig. 3). The study aims to contribute to the greater research goal of developing genetic and exploration models for HEBS in the Ogilvie and Richardson mountains in Yukon.

HYDROCARBONS AND METAL ENRICHMENT IN ORGANIC-RICH SEDIMENTS

Complementary to the Ni-Mo work previously described, Kyle Henderson, PhD graduate student at McGill University (Quebec) under Anthony Williams-Jones' supervision, is investigating the role of organic material and related hydrocarbons in the metal enrichment processes that were responsible for this horizon. It has long been known that microbial activity in oxidizing environments and organic matter in anoxic environments play a critical role in enriching sediments in a wide variety of trace elements. As well, there is a large volume of research dedicated to the processes that affect organic matter accumulation, preservation and trace metal uptake by organic-rich sediments (Algeo and Maynard, 2004; Brumsack, 2006; Calvert and Pedersen, 1993; Pedersen and Calvert, 1990; Piper and Calvert, 2009; Tribovillard *et al.*, 2006). These sediments are source beds for liquid hydrocarbons (*i.e.*, crude oil), metalliferous hydrothermal fluids, and they may host base-metal ore deposits. Based on this previous work, Kyle will be studying the relationship between the thermal maturity of the organic matter, trace metal mobility and hydrocarbon generation with the objective of understanding the role (if any) that liquid hydrocarbons may have played in metal concentration. A longer-term objective of the project is to improve understanding of atmosphere-biosphere-lithosphere interactions through time. Kyle collected bitumen samples from the Ni-Mo horizon and associated shale along the Peel River (north and south bank sections; Fig. 3), and at the Rich property in summer 2017 (Fig. 1).

WHAT'S NEXT?

All shale research teams in Yukon in 2017 anticipate several years of investigation into samples collected, with publications forthcoming. Continued fieldwork in summer 2018 is anticipated by geologists from YGS, GSC-Ottawa, and Queen's and McGill universities. These shale studies may prove useful to base metal exploration in Yukon. With renewed interest in base metal exploration, the research described here may help differentiate thick, prolonged shale intervals, facilitate correlation of shale intervals within and between basins, and ultimately refine the stratigraphic column with enhanced age, lithologic, and genetic data. The YGS plans to extend detailed shale studies into Selwyn basin in future years.

REFERENCES

Algeo, T.J. and Maynard, J.B., 2004. Trace-element behavior and redox facies in core shales of Upper Pennsylvanian Kansas-type cyclothems. Chemical Geology, vol. 206, p. 289-318.

Allen, T.L., 2010. Field notes on the Upper Devonian Imperial Formation (NTS map sheet 106L), Tetlit Creek, east Richardson Mountains, Yukon. *In:* Yukon Exploration and Geology 2009, K.E. MacFarlane, L.H. Weston and L.R. Blackburn (eds.), Yukon Geological Survey, p. 1-21.

Brumsack, H.J., 2006. The trace metal content of recent organic carbon-rich sediments: Implications for Cretaceous black shale formation. Palaeogeography, Palaeoclimatology, Palaeoecology, vol. 232, p. 344-361.

Calvert, S.E. and Pedersen, T.F., 1993. Geochemistry of Recent oxic and anoxic marine sediments: Implications for the geological record. Marine Geology, vol. 113, p. 67-88.

Cecile, M.P. 1986. The Lower Paleozoic Misty Creek Embayment, Selwyn Basin, Yukon and Northwest Territories. Geological Survey of Canada, Bulletin 335, 78 p.

Cecile, M.P., Hutcheon, I.E. and Gardner, D. 1982. Geology of the northern Richardson Anticlinorium. Geological Survey of Canada, Open File 875, 1 map and legend.

Feinstein, S., Brooks, P. W., Gentzis, T., Goodarzi, F., Snowdon, L. R. and Williams, G. K. 1988. Thermal maturity in the Mackenzie Corridor, Northwest and Yukon Territories; Canada. Geological Survey of Canada, Open File 1944.

Fraser, T. 2014. Field descriptions of the Middle–Upper Devonian Canol Formation on Trail River, east Richardson Mountains, Yukon. *In:* Yukon Exploration and Geology 2013, K.E. MacFarlane, M.G. Nordling and P.J. Sack (eds.), Yukon Geological Survey, p. 53-68.

Fraser, T.A., Allen, T.L., Lane, L.S. and Reyes, J.C., 2012. Shale gas potential of Devonian shale in north Yukon: Results from a diamond drillhole study in western Richardson Mountains. *In:* Yukon Exploration and Geology 2011, K.E. MacFarlane and P.J. Sack, (eds.), Yukon Geological Survey, p. 45-74.

Fraser, T.A. and Hutchison, M.P. 2017. Lithogeochemical characterization of the Middle-Upper Devonian Road River Group, Canol and Imperial formations on Trail River, east Richardson Mountains, Yukon: age constraints and a depositional model for fine-grained strata in the Lower Paleozoic Richardson trough. Canadian Journal of Earth Sciences, vol. 54, p. 731-765.

Fraser, T.A. and Reinhardt, L., 2015. Stratigraphy, geochemistry and source rock potential of the Boundary Creek Formation, North Slope, Yukon and a description of its burning shale locality. *In:* Yukon Exploration and Geology 2014, K.E. MacFarlane, M.G. Nordling and P.J. Sack (eds.), Yukon Geological Survey, p. 45-71.

Gadd, M.G., Layton-Matthews, D., Peter, J.M. and Paradis, S.J., 2016. The world-class Howard's Pass SEDEX Zn-Pb district, Selwyn Basin, Yukon. Part I: trace element compositions of pyrite record input of hydrothermal, diagenetic and metamorphic fluids to mineralization. Mineralium Deposita, vol. 51, p. 319-342.

Gadd, M.G. and Peter, J.M., in press. Field observations, mineralogy and geochemistry of Middle Devonian Ni-Zn-Mo-PGE hyper-enriched black shale deposits, Yukon. *In:* Targeted Geoscience Initiative – 2017 Report of Activities: Volume 1, N. Rogers (ed.), Geological Survey of Canada, Open File.

Goodfellow, W.D, 1987. Anoxic stratified oceans as a source of sulphur in sediment-hosted stratiform Zn-Pb deposits (Selwyn Basin, Yukon, Canada). Chemical Geology (Isotope Geoscience Section), vol. 65, p. 359-382.

Gordey, S.P., 2013. Evolution of the Selwyn Basin region, Sheldon Lake (105J) and Tay River (105K) map areas, central Yukon Territory. Geological Survey of Canada, Bulletin 599, 190 p.

Gordey, S.P. and Anderson, R.G., 1993. Evolution of the northern Cordilleran miogeocline, Nahanni map area (105I), Yukon and Northwest Territories. Geological Survey of Canada, Memoir 428, 214 p.

Hulbert, L.J., Gregoire, D.C., Paktunc, D. and Carne, R.C. 1992. Sedimentary nickel, zinc and platinum group element mineralization in Devonian black shales at the Nick Property, Yukon, Canada: a new deposit type. Exploration Mining Geology, vol. 1, p. 39-62.

Jowitt, S. M. and Keays, R. R., 2011. Shale-hosted Ni-(Cu-PGE) mineralisation: a global overview. Transactions of the Institution of Mining and Metallurgy Section B-Applied Earth Science, vol. 120, p. 187-197.

Large, R.R., Mukherjee, I., Gregory, D.D., Steadman, J.A. and Meffre, S. 2017. Ocean and atmosphere geochemical proxies derived from trace elements in marine pyrite: Implications for ore genesis in sedimentary basins. Economic Geology, vol. 112, p. 423-450.

Lenz, A.C. and Pedder, A.E.H. 1972. Lower and middle Paleozoic sediments and paleontology of Royal Creek and Peek River, Yukon, and Powell Creek, Northwest Territories. International Geological Congress XXIV Field Excursion Guidebook A14.

Link, C.M., Bustin, R.M. and Snowdon, L.R., 1989. Petroleum source potential and depositional setting of Phanerozoic strata in northern Yukon and northwestern District of Mackenzie. Bulletin of Canadian Petroleum Geology, vol. 37, p. 293-315.

Morrow, D.W., 1999. Lower Paleozoic stratigraphy of northern Yukon Territory and northwestern District of Mackenzie. Geological Survey of Canada, Bulletin 538, 202 p.

Nelson, J.L., Colpron, M. and Israel, S., 2013. The Cordillera of British Columbia, Yukon, and Alaska: Tectonics and metallogeny. *In:* Tectonics, Metallogeny and Discovery: The North American Cordillera and Similar Accretionary Settings, M. Colpron, T. Bissig, B.G. Rusk and J.F.H. Thompson (eds.), Society of Economic Geologists, Special Publication 17, p. 53-103.

Norris, A.W., 1985. Stratigraphy of Devonian outcrop belts in northern Yukon Territory and northwestern District of Mackenzie (Operation Porcupine area). Geological Survey of Canada, Memoir 410, 81 p.

Norris, D.K., 1997 (ed.). Geology and Mineral and hydrocarbon potential of northern Yukon Territory and northwestern District of Mackenzie. Geological Survey of Canada, Bulletin 422, 401 p.

Norris, D.K., 1981. Geology, Trail River, Yukon-Northwest Territories. Geological Survey of Canada, Map 1524A, 1:250 000 scale.

Norris, D.K., 1982a. Geology, Ogilvie River, Yukon Territory. Geological Survey of Canada, Map 1526A, 1:250 000 scale.

Norris, D.K., 1982b. Geology, Hart River, Yukon Territory. Geological Survey of Canada, Map 1527A, 1:250 000 scale.

Norris, D.K., 1982c. Geology, Wind River, Yukon Territory. Geological Survey of Canada, Map 1528A, 1:250 000 scale.

Norris, D.K., 1982d. Geology, Snake River, Yukon-Northwest Territories. Geological Survey of Canada, Map 1529A, 1:250 000 scale.

Pedersen, T.F. and Calvert, S.E., 1990. Anoxia vs. productivity: what controls the formation of organic carbon-rich sediments and sedimentary rocks? American Association of Petroleum Geologists Bulletin, vol. 74, p. 454-466.

Piper, D.Z. and Calvert, S.E., 2009. A marine biogeochemical perspective on black shale deposition. Earth-Science Reviews, vol. 95, p. 63-96.

Pugh, D.C., 1983. Pre-Mesozoic geology in the subsurface of Peel River map area, Yukon Territory and District of Mackenzie. Geological Survey of Canada, Memoir 401, 61 p.

Tribovillard, N., Algeo, T.J., Lyons, T. and Riboulleau, A., 2006. Trace metals as paleoredox and paleoproductivity proxies: An update. Chemical Geology, vol. 232, p. 12-32.

Yukon MINFILE, 2017. Yukon MINFILE – A database of mineral occurrences. Yukon Geological Survey, http://data.geology.gov.yk.ca [accessed 1 September 2015].

Yukon Geological Survey, 2015. Yukon Digital Bedrock Geology. Yukon Geological Survey, http://www.geology.gov.yk.ca/update_yukon_bedrock_geology_map.html [accessed 1 September 2015].

New contributions to the bedrock geology of the Mount Freegold district, Dawson Range, Yukon (NTS 115I/2, 6 and 7)

M.A. Friend, M.M. Allan and C.J.R. Hart
Mineral Deposit Research Unit, University of British Columbia

Friend, M.A., Allan, M.M. and Hart, C.J.R., 2018. New contributions to the bedrock geology of the Mount Freegold district, Dawson Range, Yukon (NTS 115I/2, 6 and 7). *In:* Yukon Exploration and Geology 2017, K.E. MacFarlane (ed.), Yukon Geological Survey, p. 47-68.

ABSTRACT

The Mount Freegold district is an ideal natural laboratory to evaluate the structural and magmatic framework for porphyry, skarn and epithermal mineralization in the Dawson Range. The district is located within a major extensional relay zone of the Big Creek fault system, a regionally significant dextral strike-slip structure in which localized extension facilitated the emplacement of mid to Late Cretaceous magmatic rocks. New mapping defines a previously unrecognized granite pluton at Mount Freegold, as well as the *ca*. 77 Ma Stoddart pluton, which represents the magmatic roots of hypabyssal intrusive rocks at the Revenue Cu-Mo-Au-Ag deposit and Nucleus Au-Ag-Cu deposit. The relay zone in the Big Creek fault system is partly plugged by the *ca*. 70 Ma Seymour Creek stock, which is cut by a southern strand of the fault system. Episodic fault movement took place over a minimum 35 m.y. interval during which at least three distinct epochs of magmatic-hydrothermal mineralization occurred.

* *mfriend@eoas.ubc.ca*

INTRODUCTION

The Dawson Range of west-central Yukon contains economically significant porphyry, epithermal and related styles of mineralization in a regionally extensive belt that stretches approximately 150 km from the Casino porphyry Cu-Mo-Au deposit to the town of Carmacks (Fig. 1). Three main magmatic episodes that span mid to Late Cretaceous time each generated magmatic-hydrothermal mineralization that contributes to this northwest-trending polymetallic belt, suggesting several pulses of fertile magma generation (Allan *et al.*, 2013). The concentration of mineral occurrences along the northern margin of the Dawson Range batholith, and especially along the Big Creek fault system, suggests a close link between magma emplacement and the structural evolution of the Dawson Range.

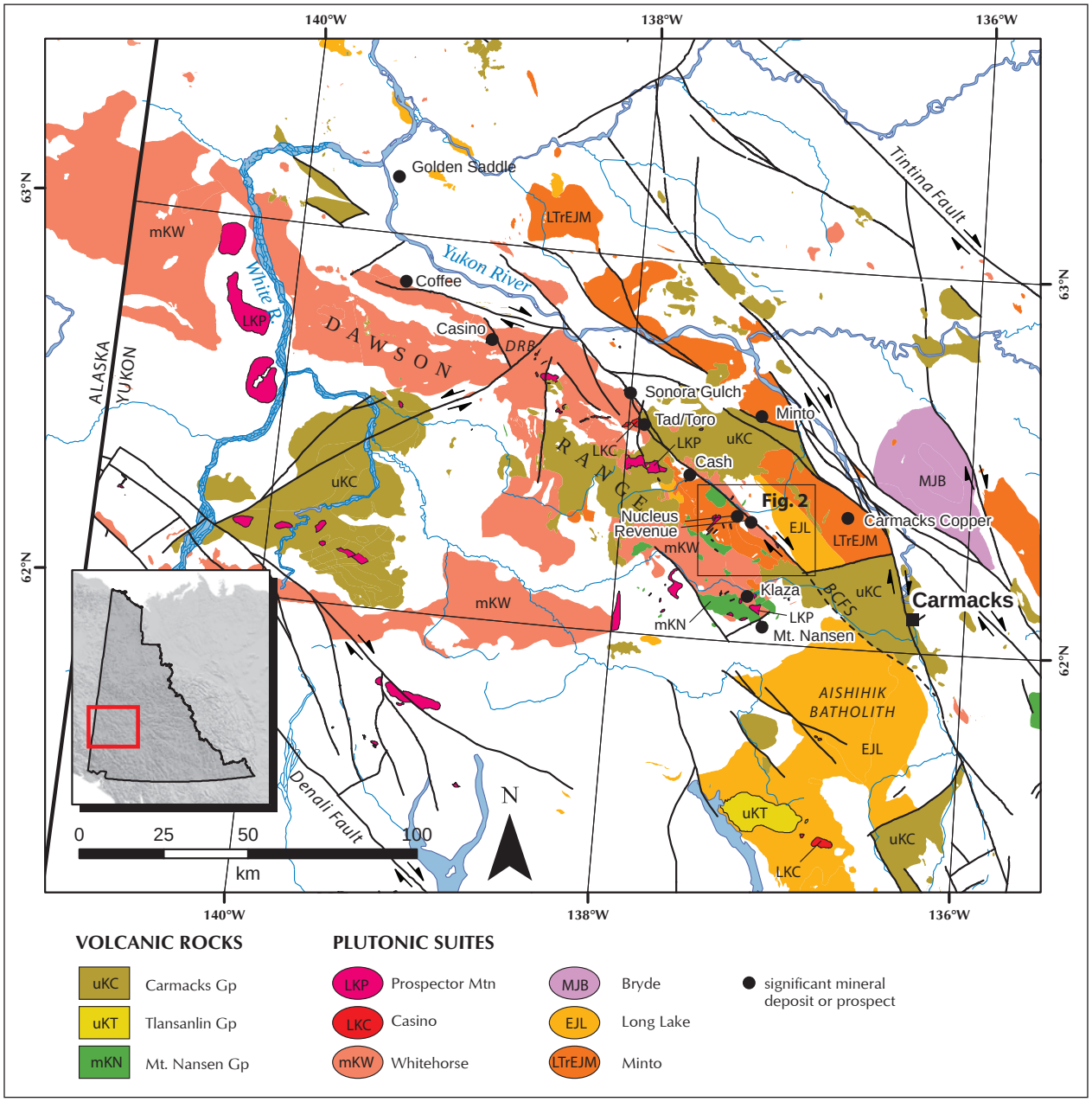

Figure 1. *Simplified regional geologic map of the Dawson Range showing plutonic suites and volcanic packages relative to significant mineral occurrences. Location of study area and Figure 2 is indicated by the black box. DRB = Dawson Range batholith. BCFS = Big Creek fault system. Inset map shows location of the map in Yukon. Geological information from Yukon Geological Survey (2017).*

The Big Creek fault system (BCFS) is a regionally significant dextral strike-slip deformation corridor that exerts a structural control on Cretaceous magmatic-hydrothermal mineralization in the Dawson Range (*e.g.*, Bennett *et al.*, 2010; Nelson *et al.*, 2013; Ryan *et al.*, 2013a,b). The Mount Freegold district in the eastern Dawson Range contains a dense cluster of mineral occurrences along the BCFS, and is herein defined as the area of historic and current bedrock and placer exploration and mining activity that includes, from northwest to southeast: the Klazan (Nitro) occurrence and Nucleus and Revenue deposits south of Big Creek; the numerous mineral occurrences north of Seymour Creek and south of Stoddart Creek in the vicinity of Mount Freegold; and the Tinta Hill occurrence southwest of Granite Mountain (Fig. 2). The Mount Freegold district represents an ideal natural laboratory to test the relationships between structural elements of the BCFS, magmatism and hydrothermal mineralization. Various mineral occurrences and three NI 43-101 compliant resources in the Mount Freegold district are interpreted to be associated with episodes of Cretaceous magmatism: (1) porphyry-related Revenue Cu-Au-Ag-Mo and Nucleus Au-Ag-Cu deposits, and Stoddart and Ridge Zone Cu-Au-Mo prospects; (2) Tinta Hill polymetallic precious-base metal vein deposit; (3) Laforma, Irene, Goldy, Whale, and Emmons Hill Au-Ag-enriched vein systems; (4) Margarete and Augusta Au magnetite skarn systems; and (5) Antoniuk breccia-hosted Au deposit (Yukon MINFILE, 2017; Fig. 2).

Recent studies have improved geochronological constraints on Cretaceous magmatism in the Mount Freegold district (*e.g.*, Bineli Betsi and Bennett, 2010; Allan *et al.*, 2013), but the petrogenetic and geochemical attributes of the causative intrusions have not been established on a systematic basis.

Here we present field descriptions of geologic units of the Mount Freegold district, based primarily on observations made during the 2017 field season, with unit assignments facilitated by previously published and yet unpublished U-Pb geochronological data obtained as part of this study. This report accompanies a new 1:25 000-scale map of the area (Allan and Friend, in press.; Fig. 2). Ongoing petrological, geochemical and geochronological studies will provide additional insights into the character and fertility of magmatic rocks in the Mount Freegold district, augmenting the field-based observations and interpretations presented herein.

PHYSIOGRAPHY

The Mount Freegold district is located in the Dawson Range, and is characterized by moderately mountainous terrain with typically gentle north-facing slopes and steep south-facing slopes. North-facing slopes are typically characterized by permafrost, thick moss accumulations, and stunted trees, whereas south-facing slopes are draped in an active layer of colluvium and have better outcrop exposure (Carlson, 1987). Lack of glacial scouring and minimal erosion in this region has resulted in deep penetrative weathering of near-surface rocks; however, fresh rocks are exposed in subalpine areas (Tempelman-Kluit, 1974; Carlson, 1987).

The Mount Freegold district is accessed via the Freegold Road, an 80-km-long maintained gravel road that extends northwest from the town of Carmacks. Rock exposures in the area are enhanced by exploration trenches and roadcuts along the extensive network of exploration roads. Most of the area is accessible by 4x4 truck or all-terrain vehicle, although the area west of the Nucleus deposit is only accessible by helicopter.

REGIONAL GEOLOGIC SETTING

The Mount Freegold district is partly underlain by poly-deformed metasedimentary, metavolcanic and metaplutonic rocks of the composite pericratonic Yukon-Tanana terrane (YTT), and by post-accretionary Mesozoic plutonic and volcanic rocks. The oldest tectonostratigraphic unit of the YTT is the pre-Late Devonian Snowcap assemblage, a dominantly clastic assemblage deposited during passive margin sedimentation along the ancient Pacific margin of Laurentia. The Snowcap assemblage is interlayered with mafic to intermediate metavolcanic rocks, most likely of the Devonian to Mississippian Finlayson assemblage, an arc assemblage that was likely erupted on top of Snowcap assemblage rocks in a submarine environment (Colpron *et al.*, 2006b; Nelson *et al.*, 2013). These rocks are also interlayered with felsic to intermediate orthogneiss of the Early Mississippian Simpson Range suite, representing continental arc magmatism accompanying subduction beneath the rifted away Snowcap assemblage.

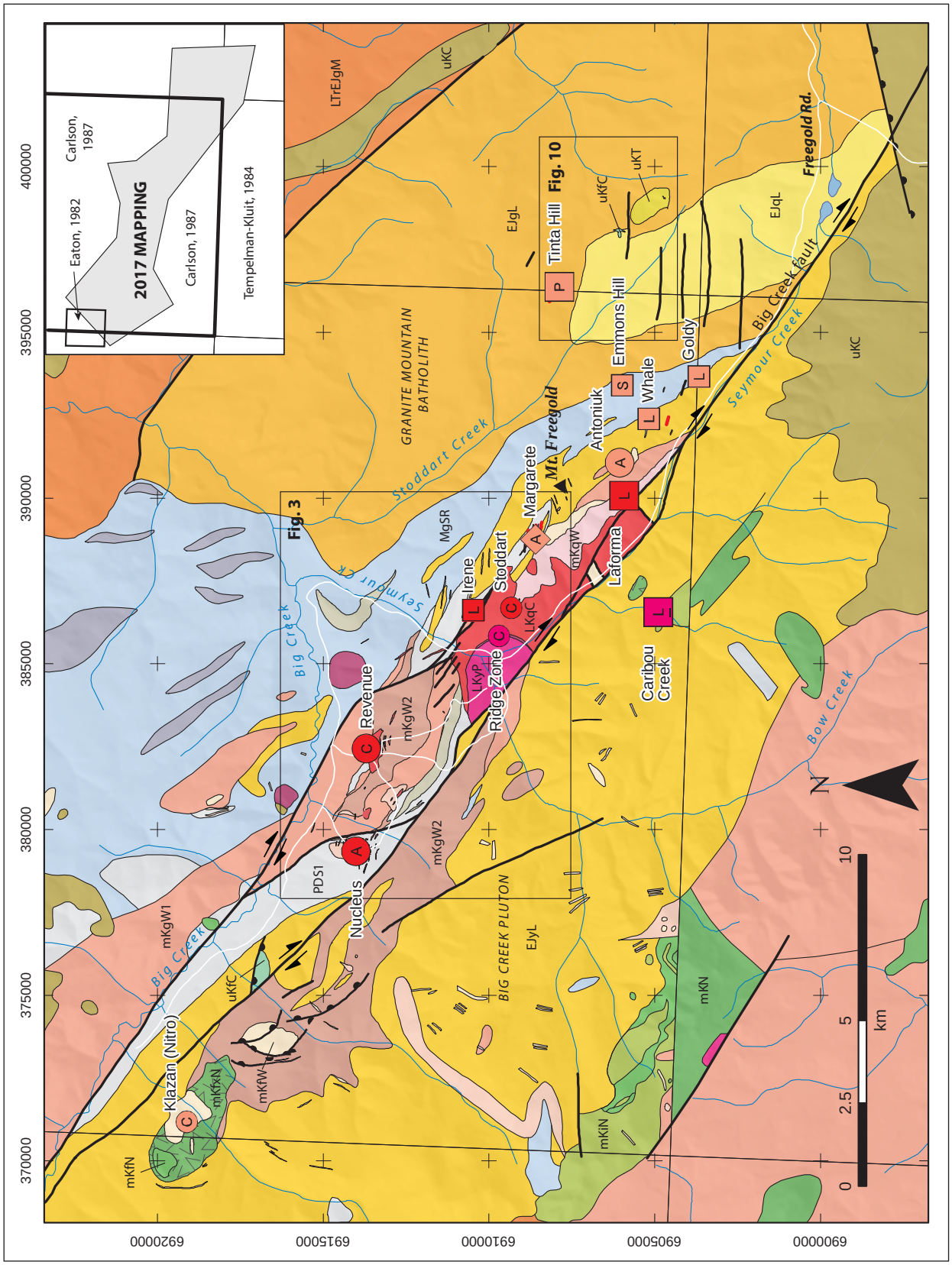

Figure 2. *Bedrock geology map of the Mount Freegold district and Big Creek fault system based on 2017 field work, showing the distribution of significant mineral deposits and occurrences as referenced in the text. Geology is interpreted beyond the limit of mapping and incorporates previous mapping from Carlson (1987), Eaton (1982), and Tempelmen-Kluit (1984) (see inset). The datum for this and all subsequent map figures is NAD83, UTM Zone 8N. Refer to legend for units and mineral occurrence symbology.*

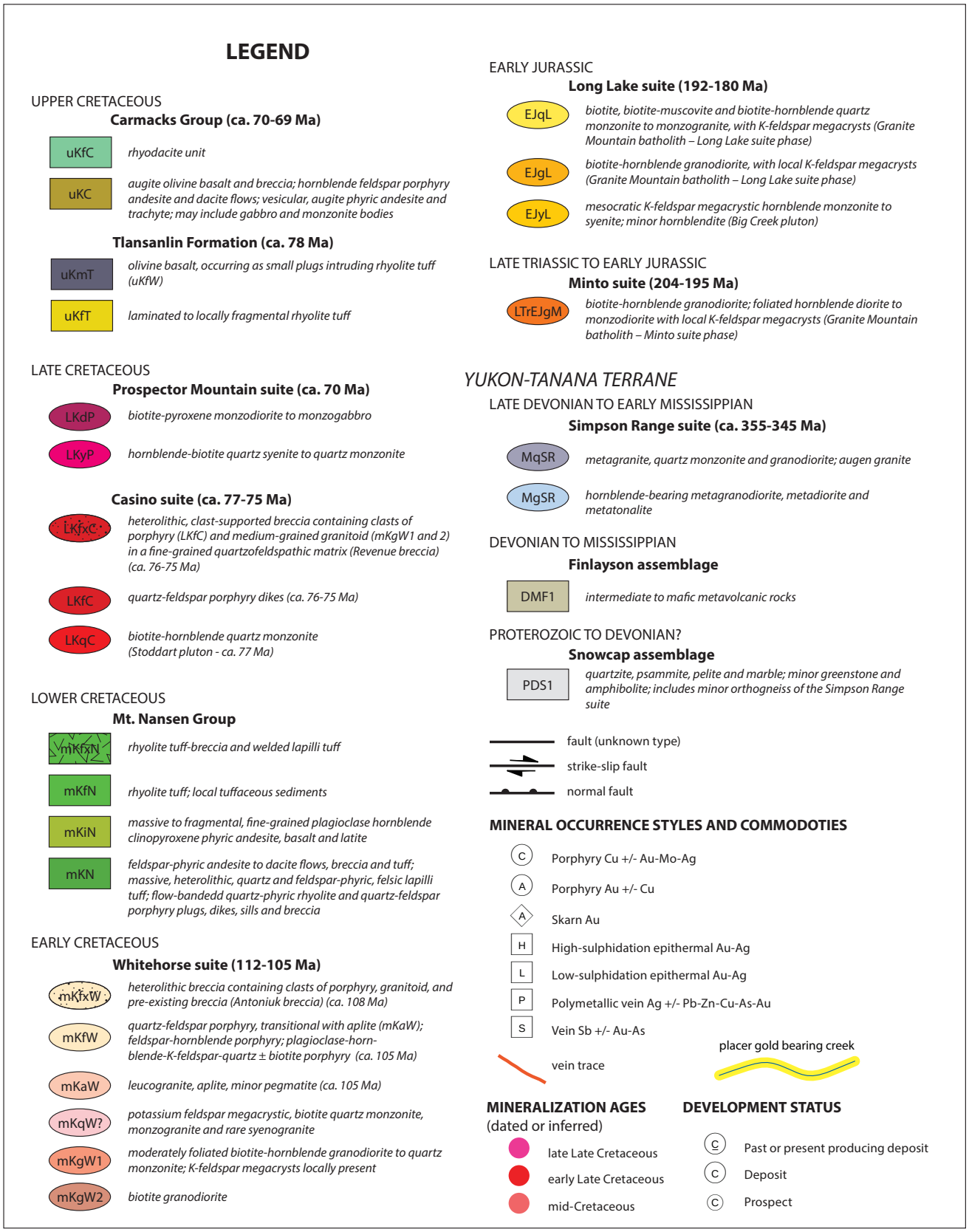

Figure 2 (cont'd). *Legend for Figure 2 and subsequent map figures.*

Yukon-Tanana terrane metamorphic rocks in the Freegold district are intruded by several generations of syn to post-accretionary plutonic rocks, including Early Jurassic Long Lake suite, mid-Cretaceous Whitehorse suite, early Late Cretaceous Casino suite, and late Late Cretaceous Prospector Mountain suite. Plutonic rocks of the Long Lake suite (EJL) include granodiorite, quartz monzonite, and granite of the Granite Mountain batholith, as well as monzonite to syenite of the Big Creek pluton and related intrusions (Tempelman-Kluit, 1984). Granodiorite, quartz monzonite, and granite of the mid-Cretaceous Whitehorse plutonic suite (mKW) occur as large plutons, and hypabyssal equivalents occur as dikes, sills, small stocks and intrusive breccia bodies. Whitehorse suite rocks represent a pulse of post-accretionary magmatism potentially associated with subduction outboard of the YTT. Mount Nansen Group volcanic rocks (mKN) are the eruptive equivalents of the Whitehorse suite (Klöcking *et al.*, 2016), and have been mapped at the Klazan occurrence (Eaton, 1982; Carlson, 1987) and in the Mt. Nansen area south of the Mount Freegold district (Tempelman-Kluit, 1984; Fig. 2).

Calc-alkaline rocks of the early Late Cretaceous Casino suite are exposed as a discontinuous belt of intrusions in the Dawson Range that is largely coincident with the Big Creek fault system (Ryan *et al.*, 2013a,b). Rocks of this suite are represented in the Mount Freegold district by plutons, dikes, and intrusive breccia bodies. This pulse of magmatism was followed in the late Late Cretaceous by eruption of Carmacks Group volcanic rocks and intrusion of plutons and high-level stocks of the Prospector Mountain suite (Tempelman-Kluit, 1984). Exposures of Carmacks Group volcanic rocks surrounding the Mount Freegold district are the erosional remnants of laterally extensive volcanic cover that lies unconformably over all older rock units (Tempelman-Kluit, 1984; Johnston *et al.*, 1996). Proposed mechanisms for generation of these typically high-K mafic melts include mantle melting driven by slab break off (Ciolkiewicz *et al.*, 2012), lithospheric delamination (Mortensen and Hart, 2010), or plume-related magmatism (Johnston *et al.*, 1996).

The dextral strike-slip Big Creek fault system has a prominent northwest-trending topographic and aeromagnetic expression along its entire strike length. In the Freegold district, a major step-over in the Big Creek fault system results in an area of structural complexity that was investigated during mapping (Figs. 2 and 3).

METHODS

Geologic map units established during 1:25 000-scale field mapping were correlated to regionally defined bedrock units based on rock composition and age constraints, either from previously published and unpublished sources, or from new high-resolution U-Pb zircon data obtained as part of this study (Fig. 3; Colpron *et al.*, 2016a). All rock units and descriptions presented here are based on field observations, and will be further refined using petrography, feldspar staining, lithogeochemistry and geochronology. Outcrop observations are supplemented by observations of diamond drill core where available, and of locally derived subcrop and colluvium. Geologic contacts were established in areas of poor rock exposure with the aid of detailed aeromagnetic data provided by Triumph Gold Corp. Topographic features, such as linear valleys and slope breaks, were also utilized in combination with aeromagnetic data to establish geologic contacts and faults in covered or inaccessible areas.

GEOLOGIC UNITS

The Mount Freegold district is underlain by metamorphic rocks of the Yukon-Tanana terrane; plutonic rocks of the Long Lake suite, Whitehorse suite, Casino suite, and Prospector Mountain suite; and volcanic rocks of the Mount Nansen Group and Carmacks Group. Each map unit is described below, in decreasing order of age.

YUKON-TANANA TERRANE

Snowcap assemblage

The Mount Freegold district is partly underlain by greenschist facies metamorphic rocks of the Proterozoic to Devonian Snowcap assemblage, which are intruded by plutonic rocks of the Long Lake suite, Whitehorse suite, Casino suite, and Prospector Mountain suite. The Snowcap assemblage is dominated by siliciclastic rocks, including psammitic to pelitic schist, interlayered locally with marble, felsic orthogneiss, and intermediate to mafic metavolcanic rocks.

Quartz-biotite schist (PDS1)

Quartz-biotite schist is the most abundant rock of the Snowcap Assemblage in the Mount Freegold district. This unit occurs as coherent belts forming ridges as well as blocky enclaves or pendants within the granodiorite to quartz monzonite of the Whitehorse suite (Figs. 2 and 3).

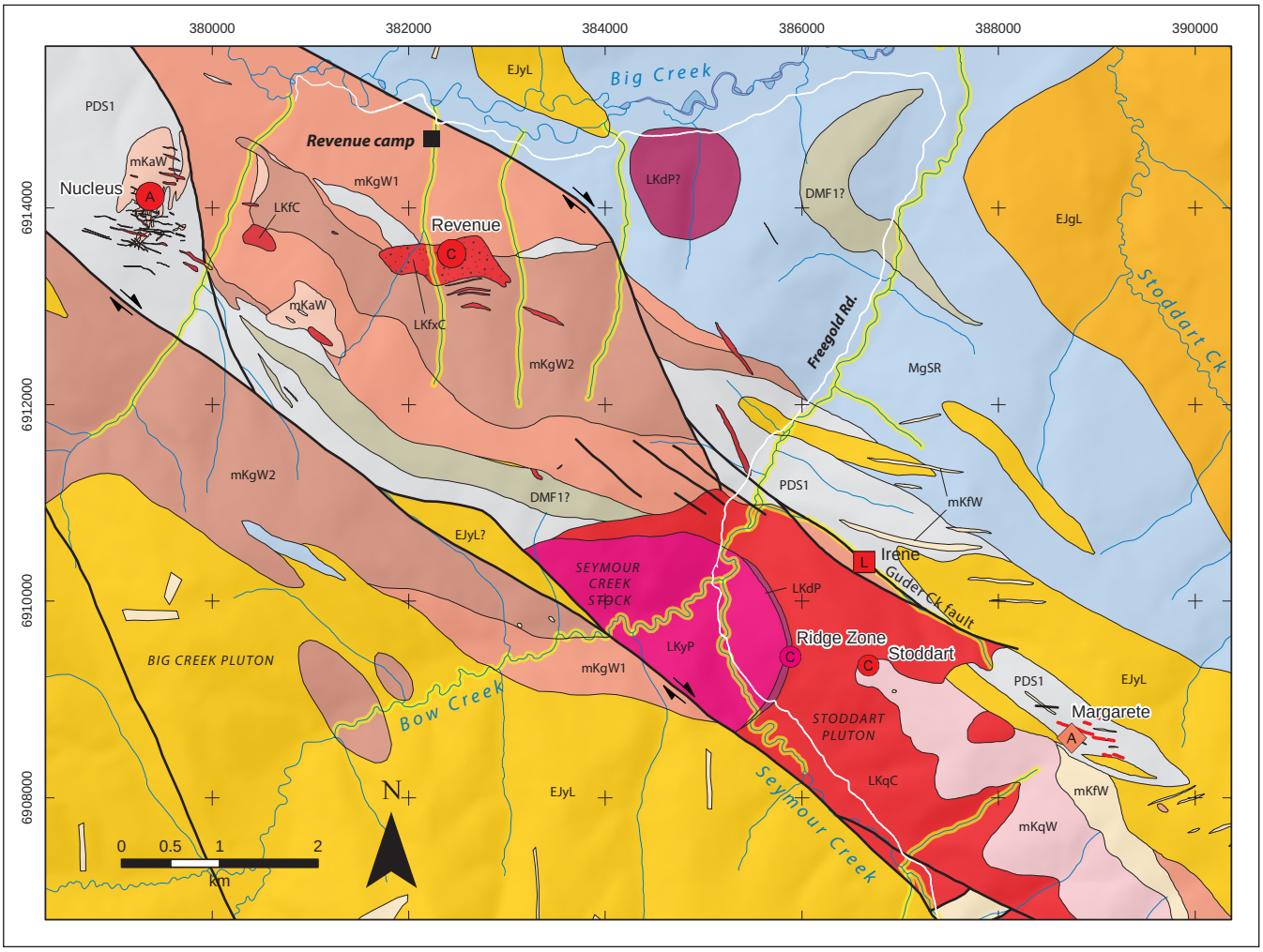

Figure 3. *Bedrock geology map focused on the area between Big Creek and the confluence of Bow and Seymour creeks, showing the distribution of significant mineral deposits and occurrences as referenced in the text. Refer to Figure 2 legend for lithologic and symbol descriptions.*

Locally it occurs as centimetre to metre-scale xenoliths (Fig 4a). The schist is brown weathered and locally gossanous, dark grey fresh, fine to fine-medium-grained, thinly foliated quartz-biotite-schist and quartz-feldspar-biotite schist. Locally the schist contains up to 40% biotite, which defines a well-developed foliation that is locally crenulated. Where the unit has been hornfelsed, it occurs as more prominent spurs on ridges. In proximity to the Revenue and Nucleus deposits, the schist is variably affected by pervasive silica alteration in which metamorphic fabrics are locally obliterated (Fig. 4b). This unit includes minor marble lenses and local garnet-pyroxene skarn in the Mount Freegold area (*e.g.*, Margarete occurrence, Yukon MINFILE 115I 053; Fig. 3), and layers of amphibolite (Finlayson assemblage?) and orthogneiss of the Simpson Range suite (below).

Amphibolite schist to amphibolite gneiss (DMF1?)

Massive to foliated, intermediate to mafic amphibolite occurs in ridge-forming belts south and east of the Revenue deposit, and is locally interlayered with metasedimentary rocks of the Snowcap assemblage and orthogneiss of the Simpson Range suite (Figs. 2 and 3). The amphibolite is dark grey-green to black weathered, cream-green fresh, fine to medium-grained, and composed predominantly of actinolite ± hornblende and plagioclase. Locally the rock is medium to coarse-grained and has a gneissic texture. The gneissic variant typically contains feldspar augen 0.5 to 2 cm in length and locally developed hornblende augen up to 3 cm in length (Fig. 4c). The unit is tentatively assigned to the Finlayson assemblage based on analogous belts of amphibolite elsewhere along the northern margin of the Dawson Range batholith (Ryan *et al.*, 2013a,b).

Felsic to intermediate orthogneiss (MgSR)

Felsic to intermediate gneissic metaplutonic rocks form a coherent belt in the eastern part of the map near Mount Freegold (Fig. 3), but also occurs as narrow layers within packages otherwise dominated by Snowcap assemblage siliciclastic rocks. The gneissic rocks are cut by plutonic rocks of both the Early Jurassic Long Lake suite and mid-Cretaceous Whitehorse suite (Figs. 2 and 3). The orthogneiss forms minor ridges and boulder rubble of pale orange to pink weathered, fine to medium-grained, biotite hornblende granodiorite to quartz monzonite orthogneiss, with local diorite gneiss (Fig. 4d). Locally quartz monzonite orthogneiss contains potassium feldspar augen up to 3 cm. A sample of the orthogneiss collected near the Whale gold occurrence (Yukon MINFILE 115I 112) yielded a U-Pb zircon age of 354.9±4.6 Ma (Allan, unpublished data, 2016).

PLUTONIC ROCKS

Long Lake suite

Plutonic rocks of the Early Jurassic Long Lake suite (EJL) are present in the eastern part of the Mount Freegold district, where they form large spires and prominent tors (Fig. 2). These rocks vary from massive to foliated. Foliations generally strike west-northwest and have either northeast or southwest dips. Both magmatic and tectonic fabrics are present. The age of the Long Lake suite ranges from 192-178 Ma (Joyce *et al.*, 2016). Three compositionally distinct phases are mapped in the Mount Freegold area: granodiorite (EJgL) and granite (EJqL) of the Granite Mountain batholith, and monzonite (EJyL) of the Big Creek pluton and satellite intrusions.

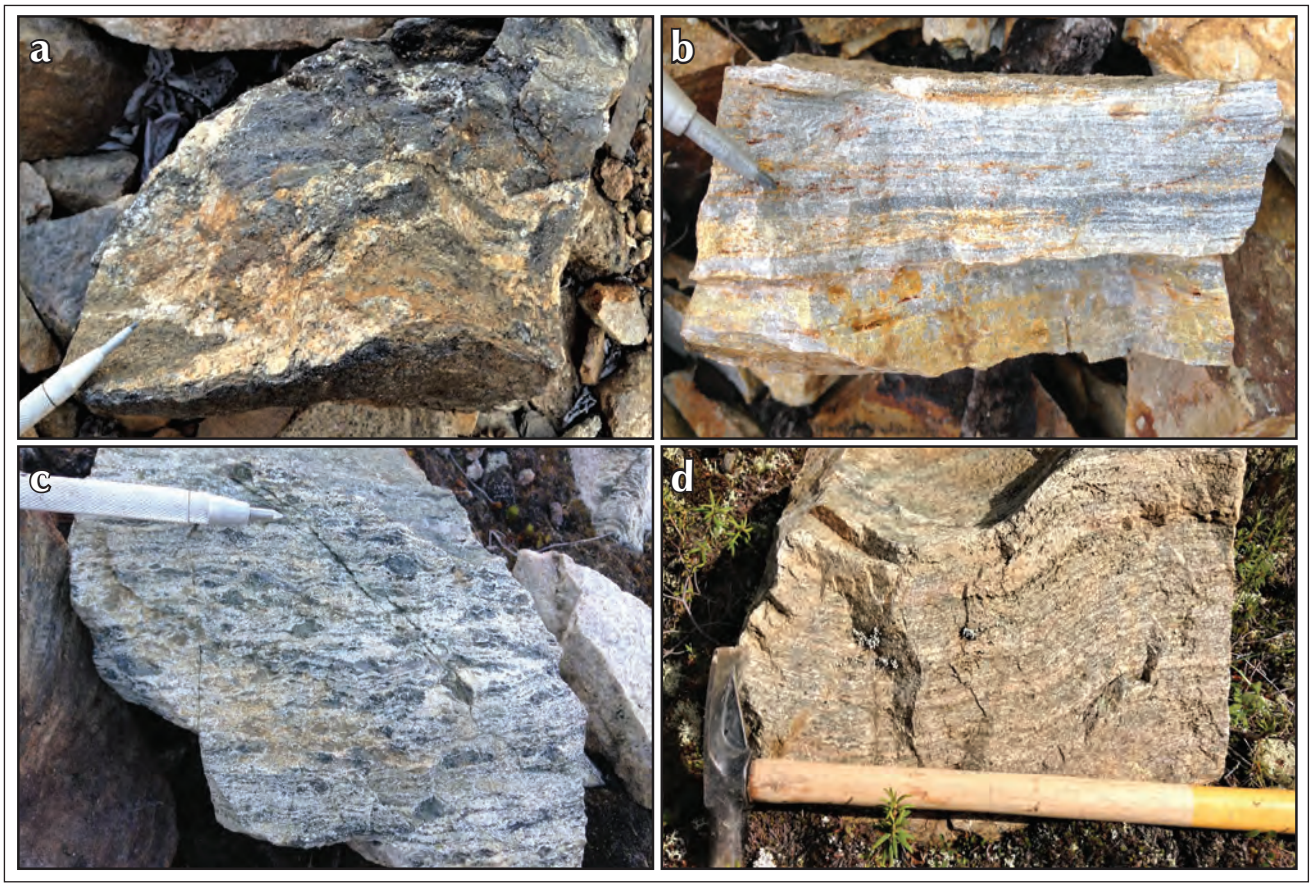

Figure 4. *Metamorphic rocks of the Yukon-Tanana terrane.* ***(a)*** *Xenolith of Snowcap assemblage quartz-biotite schist being digested by mid-Cretaceous granodiorite (mKgW2);* ***(b)*** *pervasive silica alteration and recrystallization of quartz-biotite schist of the Snowcap assemblage;* ***(c)*** *chalky weathered amphibolite gneiss with hornblende augen; and* ***(d)*** *granitic orthogneiss of the Simpson Range suite.*

Biotite hornblende granodiorite (EJgL)

Biotite hornblende granodiorite of Long Lake suite (EJgL) underlies the eastern part of the Mount Freegold district, where it forms part of the southern lobe of the Granite Mountain batholith (Fig. 2). This phase outcrops as spires and tors (Fig. 5a) of buff to white weathered, white fresh, medium-grained, biotite hornblende granodiorite (Fig. 5b). Rocks of this phase typically possess a weak to moderate tectonic foliation. Magnetic susceptibility of the unit ranges from 8.7 to 21.8 x 10^{-3} SI units (Table 1).

Biotite hornblende quartz monzonite to monzogranite (EJqL)

Biotite hornblende quartz monzonite to monzogranite of the Long Lake suite (EJqL) occurs in a part of the southern lobe of the Granite Mountain batholith, where it is the main host rock of the Tinta Hill polymetallic Au-Ag-Pb-Zn-Cu vein system (Yukon MINFILE 115I 058). It outcrops as prominent tors and subdued outcrops of white to pink weathered, sparsely potassium feldspar megacrystic, medium-grained biotite hornblende quartz monzonite to monzogranite (Fig. 5c). Potassium feldspar megacrysts are typically tabular, opaque pink, and 1 to 4 cm in length. A quartz monzonite sample from an adit at the Tinta Hill occurrence yielded a U-Pb zircon date of 188.7 ± 1.2 Ma (Mortensen, J.K., unpublished data, 2011). Magnetic susceptibility of the unit is slightly less magnetic than EJgL, with values ranging from 8.0 to 13.3 x 10^{-3} SI units (Table 1).

K-feldspar megacrystic hornblende monzonite (EJyL)

K-feldspar megacrystic hornblende monzonite of the Long Lake suite (EJyL) is the main phase of the Big Creek pluton, which occurs south of the Big Creek fault system in the Mount Freegold district. The same unit occurs as numerous, narrow plutons that intrude metamorphic rocks of the YTT semi-conformably with the regional fabric (Fig. 2). The unit forms resistant, blocky to subrounded ridges of pink weathered, greenish pink fresh, coarse to very coarse grained hornblende monzonite to quartz monzonite, typically containing a high modal abundance of tabular potassium feldspar megacrysts (Fig. 5d). Historically, the unit has been referred to as the 'Big Creek syenite' in recognition of its high K-feldspar content, but field estimates of modal mineralogy suggest the bulk composition is generally monzonitic.

Rocks of this unit contain 5-15% interstitial blebby quartz (Fig. 5e). Locally, a fine-grained phase is in gradational contact with the more typical coarse-grained phase. Dark green to brown weathered, dark green fresh, coarse-grained, massive to moderately foliated hornblendite occurs as centimetre to metre-thick zones (Fig. 5f), and in one locality, as an approximately 75 m thick sequence interpreted as hornblende cumulate. The main fabric in the Big Creek syenite is defined by cumulate layering of potassium feldspar and hornblende; however, local overprinting tectonic foliations and shear fabrics are well developed. Analysis of a sample collected near Mount Freegold yielded a U-Pb zircon date of 182.84 ± 0.05 Ma (J. Crowley, unpublished data, 2015). This result implies the unit is part of the Long Lake suite, in contrast with previous assignments of the 'Big Creek syenite' to the older Minto suite. This phase is strongly magnetic with values up to 40.5 x 10^{-3} SI units (Table 1).

mid-Cretaceous Whitehorse suite

Plutonic rocks of the Whitehorse suite intrude metamorphic rocks of the Yukon-Tanana terrane (YTT) in the Mount Freegold area, south of Big Creek, and southwest of Seymour Creek (Fig. 2). Rocks of this suite form low positive relief outcrops and are otherwise mapped through exposures of rubble along roads or in exploration trenches. Rocks of this suite are typically buff weathered, white fresh, equigranular monzogranite, quartz monzonite, granodiorite, monzodiorite and lesser syenogranite. The low relief outcrop and presence of enclaves or roof pendants of country rock distinguishes intrusive rocks of the Whitehorse suite from the Long Lake suite. The age of the Whitehorse suite is constrained to 112 to 105 Ma (Colpron *et al.*, 2016b).

Figure 5. *Plutonic rocks of the Long Lake suite.* ***(a)*** *Tor of buff to white weathered biotite hornblende granodiorite;* ***(b)*** *foliated biotite hornblende granodiorite (EJgL);* ***(c)*** *medium-grained hornblende quartz monzonite (EJqL);* ***(d)*** *coarse-grained potassium feldspar megacrystic hornblende monzonite (EJyL), historically termed the 'Big Creek syenite' in recognition of its high K-feldspar content;* ***(e)*** *interstitial quartz and minor hornblende in potassium feldspar dominated Big Creek syenite (EJyL); and* ***(f)*** *cumulate segregations in the Big Creek syenite (EJyL); dark green is hornblende cumulate, pale pink is dominantly potassium feldspar. Abbreviations: qtz=quartz; hbl=hornblende; Kfs=K-feldspar.*

Table 1. *Selected samples and their magnetic susceptibilities.*

Rock Unit	Locality	Latitude	Longitude	Magnetic Susceptibility ($x10^{-3}$ SI units)	Sample
uKfC	Locality 88	62.272727	-136.963687	9.1 ± 2.0 (n = 12)	MF17-DRP52
LKyP	Locality 14	62.295776	-137.207378	8.2 ± 2.0 (n = 6)	MF17-DRP13
	Locality 181	62.306324	-137.227990	10.5 ± 2.3 (n = 10)	*N/A*
	Locality 453	62.302970	-137.231427	8.61 ± 0.82 (n = 10)	*N/A*
LKdP	Locality 443	62.309015	-137.214983	43.4 ± 8.0 (n = 10)	*N/A*
LKqC	Locality 8	62.280623	-137.173829	19.3 ± 5.4. (n = 10)	MF17-DRP9
	Locality 9	62.294258	-137.202347	23.7 ± 6.7 (n = 10)	MF17-DRP10
	Locality 24	62.292342	-137.163861	40.1 ± 5.2 (n = 10)	MF17-DRP20
uKmT	Locality 100	62.26068	-136.943365	11.0 ± 2.7 (n = 8)	*N/A*
uKfT	Locality 96	62.268946	-136.953976	0.34 ± 0.33 (n = 6)	*N/A*
mKfW	Locality 42	62.284817	-137.114611	17.8 ± 5.6 (n = 8)	MF17-DRP35
	Locality 335	62.28819	-136.998635	8.8 ± 3.4 (n = 10)	MF17-DRP86
	Locality 490	62.267223	-137.096439	0.54 ± 0.26 (n = 10)	*N/A*
mKaW	Locality 291	62.347361	-137.421616	0.24 ± 0.15 (n = 10)	*N/A*
	Locality 419	62.341176	-137.322944	0.04 ± 0.01 (n = 10)	*N/A*
mKqW?	Locality 20	62.296745	-137.180937	16.9 ± 3.0 (n = 10)	MF17-DRP21
	Locality 49	62.284040	-137.144230	19.0 ± 16.3 (n = 6)	MF17-DRP41
mKgW2	Locality 283	62.340271	-137.457920	16.0 ± 3.0 (n = 10)	*N/A*
	Locality 320	62.325366	-137.348657	18.5 ± 2.1 (n = 10)	*N/A*
	Locality 471	62.327050	-137.221718	0.04 ± 0.02 (n = 10)	*N/A*
mKgW	Locality 46	62.278267	-137.121602	21.8 ± 2.8 (n = 10)	MF17-DRP38
	Locality 173	62.315100	-137.240800	31.4 ± 11.4 (n = 10)	*N/A*
	Locality 256	62.383475	-137.471920	15.9 ± 9.2 (n = 10)	MF17-DRP76
EJqL	Locality 73	62.245130	-136.942107	13.3 ± 4.0 (n = 12)	*N/A*
	Locality 333	62.245089	-136.973366	8.0 ± 1.8 (n = 10)	*N/A*
EJgL	Locality 92	62.266226	-136.962096	8.7 ± 2.7 (n = 8)	*N/A*
	Locality 118	62.220381	-136.887677	21.8 ± 4.3 (n = 10)	*N/A*
EJyL	Locality 321	62.329185	-137.349618	40.5 ± 11.4 (n = 10)	*N/A*
	Locality 6	62.259460	-137.128655	39.9 ± 7.5 (n = 10)	MF17-DRP7

Biotite hornblende quartz monzonite to granodiorite (mKgW1)

Biotite hornblende quartz monzonite to granodiorite of the Whitehorse suite intrudes YTT rocks north of the Big Creek fault in the central part of the Mount Freegold district (Fig. 2), where it forms blocky outcrops of buff weathered, pinkish grey fresh, medium-grained biotite hornblende granodiorite to quartz monzonite and lesser monzodiorite. Euhedral blocky hornblende and dark, fine-grained diorite autoliths inclusions are characteristic of this suite of rocks within the map area (Fig. 6a). Sparse white to pink potassium feldspar megacrysts are typical in the granodiorite to quartz monzonite. The unit is locally foliated, which distinguishes this phase from the separate biotite granodiorite phase (mKgW2, below; Fig. 6b). A sample of a monzodiorite member of this unit exposed in Revenue Creek was dated at 107.1 ± 0.6 Ma (Bineli Betsi and Bennett, 2010). Magnetic susceptibility of this unit is variable from 15.9 to 31.4 x 10^{-3} SI units (Table 1).

Biotite granodiorite (mKgW2)

Massive, biotite granodiorite of the Whitehorse suite occurs as a mappable unit south of the Revenue deposit, and as a large body intruding the Big Creek pluton south of the Big Creek fault system (Fig. 3). Rocks of this unit form low relief outcrops and subcrop of white to pink weathered, white fresh, medium-grained equigranular, biotite granodiorite with distinctive euhedral plagioclase grains. Rare megacrysts of potassium feldspar are observed (Fig. 6c). Enclaves and xenoliths of metamorphic wall rock are common in this phase, which preserve the attitude of metamorphic layering (Fig. 6d). A diamond drill core sample of this unit from the Revenue deposit yielded a U-Pb zircon age of 102.5 ± 2.7 Ma (Mortensen and Allan, unpublished data, 2012). Magnetic susceptibility of this phase is variable from <1 to 18.5 x 10^{-3} SI units (Table 1).

K-feldspar megacrystic biotite quartz monzonite and minor monzogranite to syenogranite (mKqW)

A previously unmapped body of coarse-grained granitoid is exposed on the southern slope of Mount Freegold, and is one of the host rocks of the Laforma high-sulphidation epithermal vein system (Yukon MINFILE 115I 054). The unit intrudes the monzonite phase of the Long Lake suite (EJyL) and is cut along the south by Late Cretaceous granitoid rocks (Fig. 3). The unit forms saddles and topographic lows of buff to grey weathered, greyish pink fresh, coarse to very coarse grained, potassium feldspar megacrystic biotite quartz monzonite, monzogranite and rare syenogranite (Fig. 6e,f). The unit is tentatively assigned to the mid-Cretaceous Whitehorse suite, but absolute age control is pending U-Pb zircon analysis. Magnetic susceptibility of this phase ranges from 16.9 to 19 x 10^{-3} SI units (Table 1).

Leucogranite (mKaW)

A leucogranite phase of Whitehorse suite occurs in in the far west, near Klazan (Nitro) and in the Mount Freegold area as plugs, sills and dikes that intrude YTT metamorphic rocks and mid-Cretaceous granitoid rocks (Figs. 2 and 7). The leucogranite is locally transitional with the mid-Cretaceous granitoid rocks. At the Nucleus deposit, field evidence and drill data suggest that this leucogranite unit is a swarm of sills intruding the Yukon-Tanana country rocks rather than a single intrusive body. Rocks assigned to this unit form hillocks of low relief outcrop to blocky rubble that are white to beige weathered. This unit is texturally variable, and includes (1) a very fine grained, aplitic phase (Fig. 7a); (2) a fine to medium-grained equigranular phase; (3) a fine-grained phase that contains sparse phenocrysts of feldspar and quartz; and (4) a rare coarse-grained to pegmatitic phase. The quartzofeldspathic groundmass is locally granophyric and exhibits a magmatic fabric with alternating laminae of quartz and feldspar. Locally the unit is cut by bluish-grey quartz veinlets (Fig. 7b). These quartz veins, along with granophyric textures and local flow banding are interpreted to reflect the rapid quenching of wet, silicic magma cooling during deformation (Campbell *et al.*, 2010). Textural changes in the unit are gradational and typically subtle, and the unit is texturally transitional with granodiorite of the Whitehorse suite (mKgW2), suggesting the units are co-magmatic. Overall, the unit is leucocratic and contains less than 10% mafic minerals. A sample of leucogranite hosting mineralization at the Nucleus deposit yielded a U-Pb zircon age of 104.3 ± 3.5 Ma (Allan, unpublished data, 2012). Magnetic susceptibility of this phase ranges from 16.9 to 19 x 10^{-3} SI units (Table 1).

Porphyritic rocks (mKfW)

Hypabyssal porphyritic rocks occur in the vicinity of Mount Freegold, Nucleus and Klazan (Nitro) as dikes, sills and plugs that intrude granitoid rocks of the Whitehorse and Long Lake suites, and YTT metamorphic rocks (Figs. 2 and 3). Where exposed at surface, the porphyritic rocks generally form subcrop or rubble with rare angular to blocky outcrop.

Figure 6. *Plutonic rocks of the Whitehorse suite.* ***(a)*** *Biotite hornblende granodiorite; note the fine-grained dioritic autolith (dashed circle), a characteristic feature of this phase (mKgW1);* ***(b)*** *foliation observed in granodiorite (mKgW1); note this is a feature that distinguishes it from the biotite granodiorite (mKgW2);* ***(c)*** *equigranular, biotite granodiorite with rare megacrysts of potassium feldspar (mKgW2);* ***(d)*** *biotite granodiorite (mKgW2) with xenoliths of metamorphic wall rock that give it a foliation (white arrow); note the distinctive euhedral plagioclase grains;* ***(e)*** *coarse-grained, potassium feldspar megacrystic biotite quartz monzonite (mKqW); and* ***(f)*** *left: weathered surface of the coarse-grained biotite quartz monzonite, note the abundance of potassium feldspar megacrysts (mKqW); right: buff weathered quartz feldspar porphyry dike (mKfW) that cuts the quartz monzonite (mKqW).*

The main phase of this unit is blocky, grey to orange weathered, dark grey to pink fresh, crowded feldspar-hornblende to quartz-feldspar-hornblende porphyry with a greenish pink granular granitic to monzogranitic groundmass (Fig. 7c). Strong silicification and potassium feldspar alteration is common. Less abundant is a pink to grey weathered, densely porphyritic, plagioclase-hornblende-potassium feldspar ± quartz-biotite porphyry in a fine-grained granite to monzonite groundmass (Fig. 7d). Quartz phenocrysts are rounded and embayed. Potassium feldspar phenocrysts up to 8 mm in diameter locally contain inclusions of plagioclase and hornblende. Rocks of this unit are constrained to *ca.* 105-102 Ma (M. Allan, unpublished data, 2016). Magnetic susceptibility of this phase ranges from 0.54 to 17.8 x 10^{-3} SI units (Table 1).

Late Cretaceous Casino Suite

Within the Mount Freegold district, rocks of the Casino suite include small plutons, dikes, and intrusive breccia complexes that intrude YTT metamorphic rocks and plutonic rocks of the Long Lake and Whitehorse suites. A pluton of this suite outcrops north of Seymour Creek where it forms blocky outcrops with trapezoidal joint patterns, whereas dikes and intrusive breccia complexes are exposed as strongly altered rubble in the Revenue and Nucleus deposit area (Fig. 8). Plutonic rocks of the Casino suite are typically beige weathered, equigranular monzogranite.

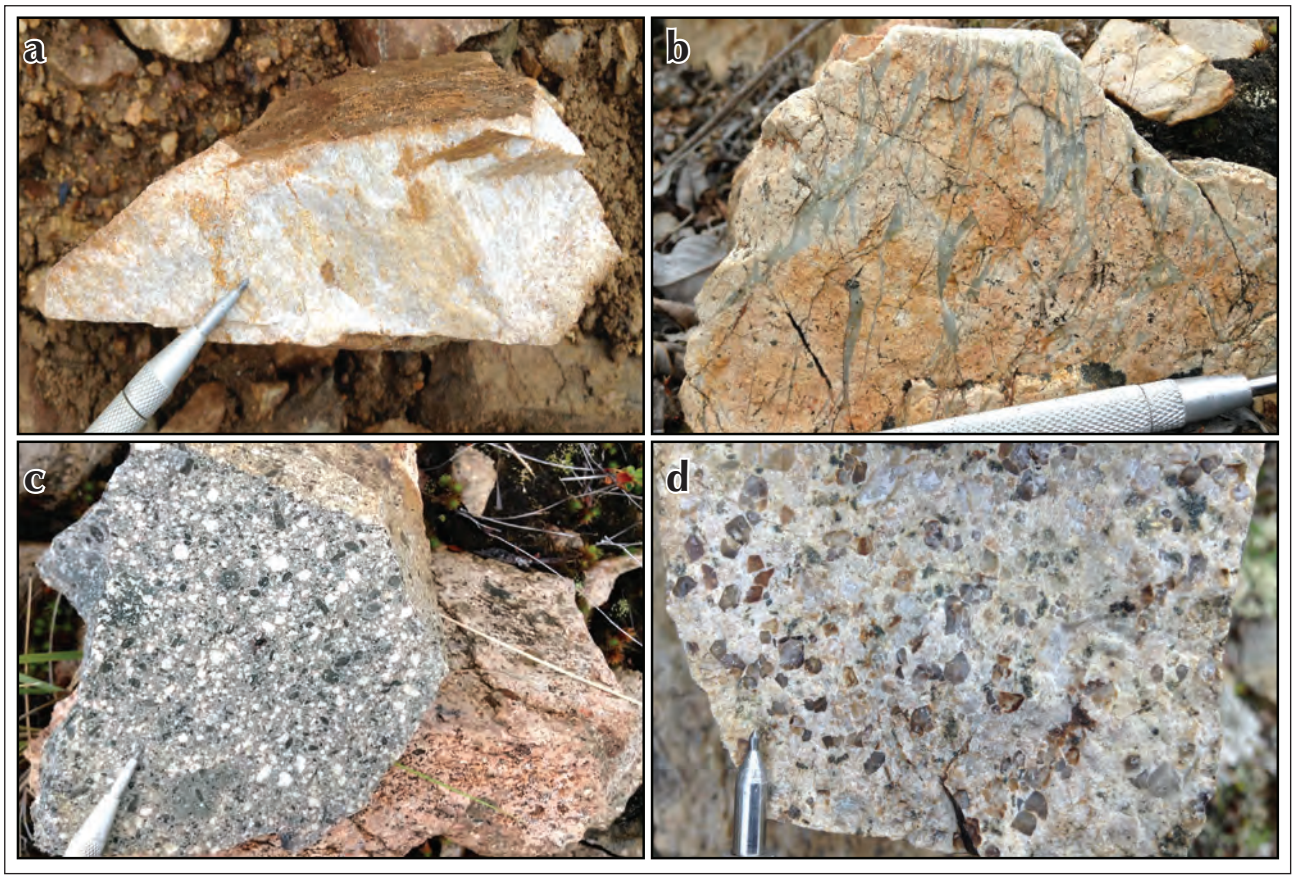

Figure 7. *Hypabyssal rocks of the Whitehorse suite.* ***(a)*** *Aplitic phase of the ca. 105 Ma leucogranite at Nucleus (mKaW);* ***(b)*** *bluish-grey quartz veinlet swarm cutting the sparsely porphyritic phase of the leucogranite;* ***(c)*** *crowded feldspar-hornblende porphyry typical of the Whitehorse suite (mKfW); and* ***(d)*** *plagioclase-hornblende-potassium feldspar ± quartz-biotite porphyry with distinctive smoky grey embayed quartz phenocrysts (mKfW).*

Biotite hornblende quartz monzonite (LKqC)

The largest intrusion of the Casino suite in the Mount Freegold district is the previously unmapped Stoddart pluton, which occurs north of Seymour Creek (Figs. 2 and 3). This unit is exposed on outcropping ridges and in roadcuts of blocky, massive, beige weathered, pink to pinkish grey fresh, medium-grained biotite hornblende quartz monzonite (Fig. 8a; LKqC). This unit is characterized by sparse tabular bluish-grey potassium feldspar megacrysts and greenish saussuritized plagioclase grains in a hypidiomorphic groundmass. Biotite phenocrysts are black and euhedral. Locally the unit is cut by widely spaced (one per metre), subvertical quartz-chalcopyrite-pyrite veinlets with narrow potassium feldspar haloes, and weathered to limonite and malachite. The unit also hosts Cu-Mo-Au mineralization at the Stoddart prospect (Yukon MINFILE 115I 121). The age of the Stoddart pluton is *ca.* 77 Ma (J. Crowley, pers. comm., 2017). The unit is highly magnetic, with susceptibilities ranging from 20 to 40×10^{-3} SI units (Table 1).

Porphyritic rocks (LKfC)

Variably Cu-Au-Ag-Mo mineralized porphyritic dikes of early Late Cretaceous age are common in the vicinity of the Revenue and Nucleus deposits (Allan *et al.*, 2013), where they occur in west to northwest-striking swarms that cut mid-Cretaceous granitoid rocks and Paleozoic basement rocks (Fig. 3). Where dikes are exposed at surface, they rarely outcrop and instead form rubble of orange-beige weathered, crowded feldspar quartz to quartz feldspar porphyry containing 5-10% phenocrysts in a fine-grained groundmass (Fig. 8b). The groundmass is typically silicified in the Nucleus deposit (Fig. 8c). Feldspar phenocrysts are typically sericite altered and rare tabular remnants of potassium feldspar phenocrysts weather to orange clay. A sample of feldspar quartz porphyry dike that cuts leucogranite at the Nucleus deposit yielded a U-Pb zircon age of 75.0 ± 0.4 Ma. (Allan and Mortensen, unpublished data, 2012).

Figure 8. *Plutonic and hypabyssal rocks of the Casino suite.* ***(a)*** *Biotite hornblende quartz monzonite of the ca. 77 Ma Stoddart pluton (LKqC);* ***(b)*** *feldspar quartz porphyry dike of the Casino suite at surface; potassium feldspar phenocrysts are weathered to clay (LKfC);* ***(c)*** *diamond drill core sample of the crowded feldspar quartz porphyry dike (LKfC) with a medium-grey silicified groundmass; dike cuts the leucogranite at the Nucleus deposit; and* ***(d)*** *intrusive breccia at the Revenue deposit (LKfxC).*

Intrusive breccia (LKfxC)

The Revenue Cu-Au-Ag-Mo deposit is hosted primarily by an east-west elongate intrusive breccia complex that intrudes along the contact of biotite hornblende granodiorite (mKgW) to the north, and biotite granodiorite (mKgW2) to the south. The unit is exposed at surface in exploration roadcuts and trenches as buff to pink weathered clast-supported breccia with sand to pebble-sized igneous clasts in a strongly altered and weathered very fine grained matrix (Fig. 8d). The breccia is cut by dikes (LKfC) and is locally transitional with porphyritic rocks, consistent with a magmatic-hydrothermal origin. The breccia body narrows with depth and potentially represents a diatreme (T. Barresi, pers. comm., 2017).

Late Cretaceous Prospector Mountain suite

Biotite hornblende quartz syenite (LKyP)

The Late Cretaceous Prospector Mountain suite is represented in the Mount Freegold district by the Seymour Creek stock, a one kilometre diameter intrusion that is exposed at the confluence of Bow Creek and Seymour Creek (Figs. 2 and 3). The stock intrudes metamorphic rocks of the YTT as well as granitoid rocks of the Long Lake, Whitehorse, and Casino suites, and is cut to the south by the Big Creek fault, as indicated by field mapping and interpretations of aeromagnetic data (Fig. 3). The unit also hosts polymetallic Au-Ag-Pb-Cu mineralization of the Ridge zone east of Stoddart Creek (Fig. 3). The most common phase of the Seymour Creek stock outcrops as angular blocks of white weathered, pink fresh, fine to medium-grained biotite hornblende quartz syenite to quartz monzonite and lesser syenogranite with glomerophyric hornblende ± biotite in an equigranular hypidiomorphic groundmass (Fig. 9a; LKyP). A sample of the Seymour Creek stock collected near the confluence of Bow Creek and Seymour Creek yielded a U-Pb zircon age of 69.99 ± 0.02 Ma (J. Crowley, pers. comm., 2017). Magnetic susceptibility of this unit is consistently in the range of 8 to 11×10^{-3} SI units (Table 1).

Biotite monzodiorite to monzogabbro (LKdP)

The eastern margin of the Seymour Creek stock is characterized by a 5 to 20 m-wide, intermediate to mafic border phase (LKdP) that is in sharp, but locally texturally transitional, contact with the main quartz syenite to monzonite phase (Figs. 3 and 9b,c). This recessive unit is exposed in roadcuts and trenches as rounded, brown black weathered, medium-grained biotite monzodiorite to monzogabbro that weathers largely to grus (Fig. 9d,e). Sparse, disseminated blebs of copper limonite after chalcopyrite occur in the monzogabbro, and are interpreted as a magmatic sulphide phase (Fig. 9d). Magnetic susceptibility of this phase of the Prospector Mountain suite is $43.4 \pm 8.0 \times 10^{-3}$ SI units (Table 1).

A small, circular intrusion of monzogabbro flanked by mafic volcanic rocks of the Carmacks Group was mapped by Carlson (1987) north of Big Creek, and is interpreted here as age-equivalent to Prospector Mountain suite (Fig. 3). A similar circular feature characterized by a prominent negative magnetic anomaly is present northeast of the Revenue deposit (Fig. 3). The feature is not expressed in outcrop, but is also tentatively interpreted as an intermediate to mafic stock of the Prospector Mountain suite.

VOLCANIC ROCKS

Volcanic rocks are present locally in the Mount Freegold district, most notably in the Klazan (Nitro) area south of Big Creek (Fig. 2), and south of the Tinta Hill deposit (Fig. 10).

mid-Cretaceous Mount Nansen Group (mKN)

The Klazan (Nitro) occurrence located at the far western end of the Mount Freegold district (Fig. 2) is located within an exposure of rhyolite tuff (mKfN) and rhyolite tuff-breccia (mKfxN) cored by an intrusive complex that includes felsic porphyry and intrusive breccia (mKfW; Eaton, 1982). Fragmental volcanic rocks exposed as rubble in trenches are buff weathered, white to green fresh, and contain subangular coarse sand to pebble-sized, clay-altered lapilli in a crystal rich groundmass (Fig. 11a). Fine-grained angular quartz crystals occur in the groundmass. Locally lapilli are flattened and define volcanic layering. The volcanic unit is tentatively assigned to the mid-Cretaceous Mount Nansen Group according to previous mapping (Eaton, 1982; Tempelman-Kluit, 1984; Carlson, 1987), but absolute age control is pending U-Pb zircon analysis.

Figure 9. *Plutonic rocks of the Prospector Mountain suite.* ***(a)*** *Typical biotite hornblende quartz syenite of the ca. 70 Ma Seymour Creek stock; note the glomerophyric aggregates of hornblende ± biotite (white arrows);* ***(b)*** *malachite and azurite stained shear and carbonate vein at the contact between the biotite quartz syenite (LKyP) and the biotite monzogabbro (LKdP) in the Ridge zone (refer to Fig. 3);* ***(c)*** *biotite-hornblende quartz syenite (LKyP) dikelet cutting biotite monzogabbro (LKdP) in the Ridge zone (refer to Fig. 3);* ***(d)*** *equigranular biotite monzodiorite phase at the eastern margin of the Seymour Creek stock;* ***(e)*** *biotite monzogabbro with sparse dark red blebs of copper limonite after chalcopyrite (white arrows); and* ***(f)*** *left to right: biotite monzogabbro, biotite monzodiorite, and biotite quartz syenite of the Seymour Creek stock. cp = chalcopyrite, cb = carbonate, bt = biotite.*

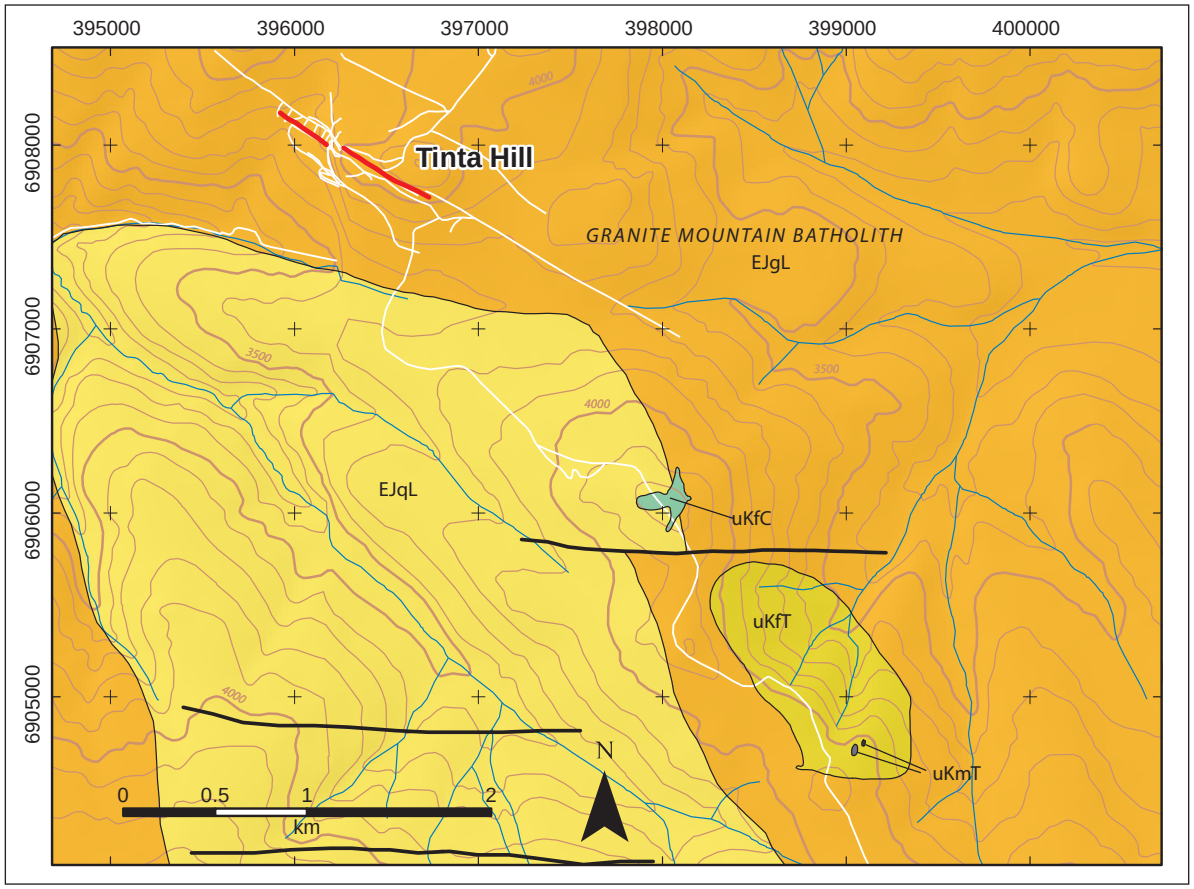

Figure 10. *Bedrock geology map of the Tinta Hill deposit area, showing felsic flow-dome complexes of the Tlansanlin Formation (uKfT) and Carmacks Group (uKfC). Refer to Figure 2 legend.*

Upper Cretaceous Tlansanlin Formation (uKfT and uKmT)

An elliptical, approximately one square kilometre exposure of felsic flows and tuffs occurs north of Seymour Creek along the Tinta Hill road (Figs. 2 and 10). Volcanic rocks unconformably overlie granodiorite of the Long Lake suite and occur as splintery to flaggy subcropping rubble of pale pink weathered, laminated to locally fragmental rhyolite tuff (uKfT) with 1 to 2% quartz phenocrysts and trace disseminated pyrite (Fig. 11b). The southwestern margin of the exposure consists of whitish pink to maroon weathered, clast-supported pyroclastic breccia to volcanic sandstone dominated by subrounded clasts of rhyolite with lesser jasper and altered granitoid (EJgL; Fig. 11c). Two small plugs of columnar jointed, dark brown weathered, olivine pyroxene phyric basalt (uKmT) with rare granitic xenoliths intrude rhyolite near the southeastern margin of the volcanic exposure (Fig. 11d). On the basis of the elliptical map pattern, felsic volcanic rocks are interpreted as the extrusive facies of a flow-dome complex. The marginal breccia phase is interpreted to be a basal facies as the contact appears to be depositional. This rhyolite yielded a U-Pb zircon age of 78.18±0.03 Ma (J. Crowley, pers. comm., 2017), suggesting correlation with the Tlansanlin Formation – the extrusive equivalent of the Casino suite. Magnetic susceptibilities of the volcanic rocks range from 0.34 to 11 x 10^{-3} SI units (Table 1).

Upper Cretaceous Carmacks Group (uKC)

Two exposures of rhyodacite tuff were mapped in the Mount Freegold district: one south of Big Creek and west of the Nucleus deposit (Fig. 2); and one along Tinta Hill Road north of the previously described rhyolite flow dome (Fig. 10). The latter forms a prominent hillock of splintery to flaggy rhyodacite that locally unconformably overlies Early Jurassic granitoid rocks of the Granite Mountain batholith (Figs. 10 and 11e). The unit is a pale grey to mauve, plagioclase biotite quartz phyric rhyodacite tuff with locally developed dark glassy laminae (Fig. 11f). The eastern exposure of this unit along Tinta Hill Road

has a massive core compared to laminated, tuffaceous margins, suggesting a flow dome architecture. A sample of rhyodacite at this locality yielded a U-Pb zircon age of 70.04±0.02 Ma, which demonstrates age equivalence to the Seymour Creek stock (J. Crowley, pers. comm., 2017). Magnetic susceptibility of the rhyodacite is $9.1 \pm 2.0 \times 10^{-3}$ SI units (Table 1). The unit is broadly contemporaneous with mafic volcanic rocks of the Upper Cretaceous Carmacks Group (UKC) that are exposed north and west of Big Creek, and in the Seymour Creek drainage southeast of the Mount Freegold area (Fig. 3).

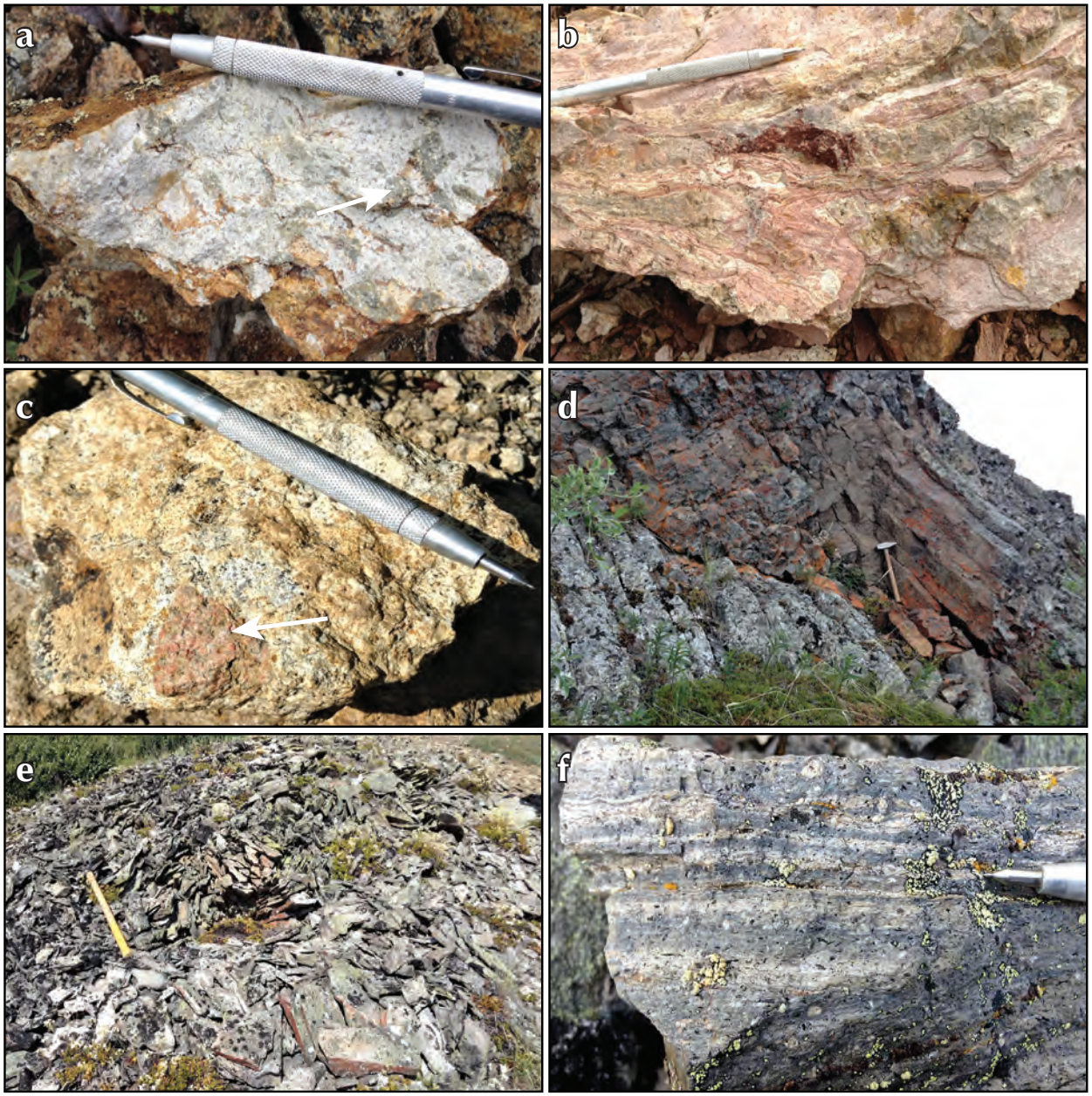

Figure 11. *Volcanic rocks in the Mount Freegold district.* ***(a)*** *Altered lapilli tuff tentatively assigned to the Mount Nansen Group from the Klazan (Nitro) occurrence (Yukon MINFILE 115I038); white arrow points to lapilli;* ***(b)*** *laminated rhyolite flow of the Tlansanlin formation near Tinta Hill (uKfT);* ***(c)*** *basal pyroclastic breccia to rhyolite tuff at the margin of the rhyolite flow-dome complex of the Tlansanlin formation;* ***(d)*** *columnar jointed basalt plug (uKmT) that intrudes the southeastern margin of the rhyolite flow-dome complex;* ***(e)*** *small hillock of splintery rubble of ca. 70 Ma rhyodacite (uKfC); and* ***(f)*** *plagioclase biotite quartz-phyric rhyodacite tuff with well-developed laminae (uKfC).*

STRUCTURE

The Mount Freegold district coincides with a right-stepping duplex in the dextral strike-slip Big Creek fault system. The duplex is bound to the north by a fault strand that tracks the southeast-trending segment of the Big Creek valley, and to the south by a fault strand that follows the Seymour Creek valley and traverses the north-facing slope south of the Nucleus and Revenue deposits (Fig. 2). The trace of the northern fault strand is interpreted from aeromagnetic data to bend southeastward approximately 1 km northeast of the Revenue deposit. Mapping demonstrates this fault strand to be plugged by both the 77 Ma Stoddart pluton and the 70 Ma Seymour Creek stock near the confluence of Seymour Creek and Bow Creek (Fig. 3). This northern fault strand thus records pre-77 Ma movement. A series of low-displacement, southeast-trending dextral strike-slip faults that are mapped or inferred from aeromagnetic data cut the northern intrusive contact of the Stoddart pluton, the most northerly of which defines the Guder Creek fault and controls epithermal mineralization of the Irene occurrence (Fig. 3). These faults thus define post-77 Ma movement. The Seymour Creek strand of the Big Creek fault system cuts both the Stoddart pluton and Seymour Creek stock to the south, thus defining post-70 Ma movement. The trace of this fault to the northwest is defined by geology, aeromagnetic data, and recessive topography, and appears to converge with the northern fault strand northwest of the Klazan occurrence (Fig. 2). A secondary north-northwest-trending linking fault is inferred between the Nucleus and Revenue deposits on the basis of geology and aeromagnetic data. Overall, no apparent strike-slip movement on the northern strand of the Big Creek fault system is recorded after Late Cretaceous emplacement of the Stoddart pluton, whereas movement on the southern strand outlasted emplacement of the 70 Ma Seymour Creek stock.

DISCUSSION

BIG CREEK FAULT SYSTEM AND MAGMATISM

The right-stepping duplex of the Big Creek fault system defines an extensional regime that accommodated emplacement of magmas, and localized magmatic-hydrothermal mineralization in the Mount Freegold district. Based on new field observations and mapping, the influence of the Big Creek fault system on the emplacement of three plutonic suites is considered: the mid-Cretaceous Whitehorse suite, early Late Cretaceous Casino suite, and late Late Cretaceous Prospector Mountain Suite.

The three plutonic units of the Whitehorse suite recognized in the Mount Freegold district (mKgW1, mKgW2, mKqW) intrude, and occur inboard of, Early Jurassic plutonic rocks. Mid-Cretaceous plutonic rocks surrounding the Revenue deposit were likely emplaced into a zone of extension facilitated by dextral movement on the right-stepping northern and southern strands of the Big Creek fault system. Furthermore, it is likely that the northwest-trending belt of mid-Cretaceous granitoid rocks exposed on the southern slope of Mount Freegold also intruded into an early strand of the Big Creek fault system. Mid-Cretaceous dikes and intrusive breccia at the Antoniuk gold deposit in the Mount Freegold area are hypabyssal expressions of these granitoid rocks at higher crustal level, and were also likely controlled by the Big Creek fault system.

Plutonic to hypabyssal rocks of the Casino suite are apparently contained entirely within the right-stepping duplex of the Big Creek fault system, strongly suggesting their emplacement into local zones of extension accommodated by dextral strike-slip movement on the main fault system. The spatial association of the Seymour Creek stock and related Prospector Mountain suite intrusions with the Big Creek fault system is also conspicuous, and likely suggests a fundamental structural control on pluton emplacement.

CRUSTAL LEVEL AND IMPLICATIONS FOR MINERALIZATION

Mid-Cretaceous dikes and a stock of felsic porphyry (mKfW) on Mount Freegold are present at a higher structural and topographic level than the coarse-grained quartz monzonite to monzogranite unit (mKqW), suggesting they are potentially hypabyssal equivalents. A similar relationship is observed in the western part of the Mount Freegold district, where transitional relationships among plutonic rocks (mKgW2), aplite (mKaW), and felsic porphyry (mKfW) indicate that the current erosional level exposes the carapace of an upper crustal magma chamber (Fig. 3).

Similarly, the Stoddart pluton (LKqC) that outcrops north of Seymour Creek locally exhibits transitional textures with aplite, pegmatite, and Cu-Mo bearing quartz veins at the Stoddart porphyry prospect. These relationships indicate a crustal level near the hydrous carapace of the magma chamber. In contrast, west of Seymour Creek,

hypabyssal intrusions of the Revenue deposit, with no known exposures of Casino suite plutonic rocks, indicates a somewhat high level of crustal exposure. However, widespread high-temperature hydrothermal alteration and mineralization surrounding the Revenue deposit may indicate the presence of a laterally extensive Casino suite pluton at depth.

Elsewhere in the Mount Freegold district, the present-day erosional surface is equivalent to the Late Cretaceous unconformity, as indicated by *ca.* 78 Ma and 70 Ma flow domes built on Early Jurassic granitoid rocks south of the Tinta Hill deposit (Fig. 3).

CONCLUSIONS

Three distinct pulses of magmatism associated with mineralization are recognized in the Mount Freegold district that were, at least in part, controlled by episodic movement on the long-lived Big Creek fault system. An extensional relay zone in the Big Creek fault system controlled magmatism of the Casino and Prospector Mountain suites and associated magmatic-hydrothermal mineralization in the district. This dextral transtensional environment may also have had similar control on the emplacement of plutonic and hypabyssal phases of the mid-Cretaceous Whitehorse suite.

Ongoing investigations include systematic characterization of mid and Late Cretaceous plutonic and hypabyssal rocks, through lithogeochemistry, mineral staining, petrographic analysis, U-Pb dating and trace element chemistry of zircon.

ACKNOWLEDGEMENTS

This project is supported by the Yukon Geological Survey. We are grateful to Triumph Gold Corp. for logistical support, the use of camp facilities during the field season, permission to sample drill core, and access to company data. Ryan Burke is thanked for providing excellent field assistance. The authors are grateful to Tony Barresi, Jesse Halle, Steve Israel, Jim Crowley and Maurice Colpron for stimulating discussions that have strengthened our field observations and interpretations. Helicopter support was provided by Trans North Helicopters. This manuscript benefited from critical review by Steve Israel of the Yukon Geological Survey.

REFERENCES

Allan, M.M., Mortensen, J.K., Hart, C.J.R., Bailey, L.A., Sanchez, M.G., Ciolkiewicz, W., McKenzie, G.G. and Creaser, R.A., 2013. Magmatic and metallogenic framework of west-central Yukon and eastern Alaska. Society of Economic Geologists, Special Publication 17, p. 111-168.

Allan, M.M. and Friend, M.A., in press. Bedrock geology of the Mount Freegold district, Dawson Range, Yukon Territory (NTS 115I/2, 6, 7). Yukon Geological Survey, Open File.

Bennett, V., Schulze, C., Ouellette, D. and Pollries, B., 2010. Deconstructing complex Au-Ag-Cu mineralization, Sonora Gulch project, Dawson Range: A Late Cretaceous evolution to the epithermal environment. *In:* Yukon Exploration and Geology 2009, K.E. MacFarlane, L.H. Weston and L.R. Blackburn (eds.), Yukon Geological Survey, p. 23-45

Bineli Betsi, T. and Bennett, V., 2010. New U-Pb age constraints at Freegold Mountain: Evidence for multiple phases of polymetallic mid- to Late Cretaceous mineralization. *In*: Yukon Exploration and Geology 2009, K.E. MacFarlane, L.H. Weston and L.R. Blackburn (eds.), Yukon Geological Survey, p. 57-84.

Campbell, J., Armitage, A. and Barnes, W., 2010. Technical report on the Nucleus property, Freegold Mountain project, including an updated mineral resource estimate: Northern Freegold Resources Ltd., 89 p., http:// www.northernfreegold.com/i/pdf/TechnicalReport-NucleusZone.pdf [accessed November 29, 2017].

Carlson, G.G., 1987. Geology of Mount Nansen (115I/3) and Stoddart Creek (115I/6) map areas Dawson Range, Central Yukon. Exploration and Geological Services Division, Yukon Region, Indian and Northern Affairs Canada, Open File 1987-2, 181 p., two map sheets, scale 1:30 000.

Ciolkiewicz, W., Mortensen, J., Ryan, J. and Hart, C., 2012. Space-time composition patterns of the Late Cretaceous magmatism in west-central Yukon and east-central Alaska: Insights into the tectonic evolution of the northern Cordillera. Cordilleran Tectonics Workshop, Victoria, February 24–26, 2012, Schedule and abstracts, 15 p.

Colpron, M., Nelson, J.L., and Murphy, D.C., 2006b. A tectonostratigraphic framework for the pericratonic terranes of the northern Cordillera. *In*: Paleozoic Evolution and Metallogeny of Pericratonic Terranes at the Ancient Pacific Margin of North America, Canadian and Alaskan Cordillera, M. Colpron and J.L. Nelson (eds.), Geological Association of Canada, Special Paper, Volume 45, p. 1-23.

Colpron, M., Israel, S., Murphy, D., Pigage, L. and Moynihan, D., 2016a. Yukon Bedrock Geology Map. Yukon Geological Survey, Open File 2016-1, 1:1 000 000 scale map and legend.

Colpron, M., Israel, S., Murphy, D., Pigage, L. and Moynihan, D., 2016b. Yukon Bedrock Geology Legend. Yukon Geological Survey, Open File 2016-1, 1:1 000 000 scale map and legend.

Eaton, W.D., 1982. Nat Joint Venture, geological and geochemical report, Nitro 1-24 Claims (Archer, Cathro & Associates (1981) Ltd.). Yukon Energy, Mines and Resources Assessment Report 091438, 26 p.

Johnston, S.T., Wynne, P.J., Francis, D., Hart, C.J.R., Enkin, R.J. and Engebretson, D.C., 1996. Yellowstone in Yukon: The Late Cretaceous Carmacks Group. Geology, vol. 24, p. 997-1000.

Joyce, N.L., Colpron, M., Allan, M.M., Sack, P.J., Crowley, J.L. and Chapman, J.B., 2016. New U-Pb ziron dates from the Aishihik batholith, southern Yukon. *In:* Yukon Exploration and Geology 2015, K.E. MacFarlane and M.G. Nordling (eds.), Yukon Geological Survey, p. 131-149.

Klöcking, M., Mills, L., Mortensen, J. and Roots, C., 2016. Geology of mid-Cretaceous volcanic rocks at Mount Nansen, central Yukon, and their relationship to the Dawson Range batholith. Yukon Geological Survey, Open File 2016-25, 37 p. plus appendices.

Mortensen, J.K. and Hart, C.J.R. 2010. Late and postaccretionary Mesozoic magmatism and metallogeny in the northern Cordillera, Yukon and east central Alaska. *In:* Geological Society of America, Program with Abstracts, vol., 42, p. 676.

Nelson, J.L., Colpron, M. and Israel, S., 2013. The Cordillera of British Columbia, Yukon, and Alaska: Tectonics and metallogeny. *In:* Tectonics, Metallogeny and discovery: The North American Cordillera and similar accretionary settings, M. Colpron, T. Bissig, B.G. Rusk and J.F. Thompson (eds.), Society of Economic Geologists, Special Publication No. 17, p. 53-109.

Ryan, J.J., Zagorevski, A., Williams, S.P., Roots, C., Ciolkiewicz, W., Hayward, N. and Chapman, J.B., 2013a. Geology, Stevenson Ridge (northeast part), Yukon. Geological Survey of Canada, Canadian Geoscience Map 116 (2nd edition, preliminary), scale 1:100 000. doi:10.4095/292407.

Ryan, J.J., Zagorevski, A., Williams, S.P., Roots, C., Ciolkiewicz, W., Hayward, N. and Chapman, J.B., 2013b. Geology, Stevenson Ridge (northwest part), Yukon. Geological Survey of Canada, Canadian Geoscience Map 117 (2nd edition, preliminary), scale 1:100 000. doi:10.4095/292408.

Tempelman-Kluit, D.J., 1974. Reconnaissance geology of Aishihik Lake, Snag and part of Stewart River map areas, west-central Yukon. Geological Survey of Canada, Paper 73-41, 3 maps (scale 1:250 000) and 97 p.

Tempelman-Kluit, D., 1984. Geology, Laberge and Carmacks, Yukon Territory. Geological Survey of Canada, Open File 1101, scale 1:250 000, 2 sheets.

Yukon MINFILE, 2017. Yukon MINFILE – A database of mineral occurrences. Yukon Geological Survey, http://data.geology.gov.yk.ca [accessed November, 2017].

An appraisal of Devonian-Mississippian shale strata in Yukon's Liard basin

M.P. Hutchison
Yukon Geological Survey

Hutchison, M.P., 2018. An appraisal of Devonian-Mississippian shale strata in Yukon's Liard basin. *In:* Yukon Exploration and Geology 2017, K.E. MacFarlane (ed.), Yukon Geological Survey, p. 69-88.

ABSTRACT

This study presents the first shale gas appraisal of Devonian-Mississippian shale strata in Yukon's Liard basin. Assessed volumes of 68 Tcf gas-in-place and 7.6 Tcf marketable gas are contained within two shale plays identified from an integrated wireline log and geochemical evaluation: the Devonian (Givetian-Frasnian) Horn River shale and the Devonian-Mississippian (Famennian-Tournaisian) Exshaw-Patry shale. Average burial depths of 3018 mTVD and net pay thicknesses of 73 m for the Horn River, and 2688 mTVD and 89 m for the Exshaw-Patry plays are interpreted. Both plays are dominated by black, organic-rich, siliceous mudstones, and exhibit: elevated TOC contents (0.6-6.9 wt %); maturities within or past the dry gas window (2.1-4.6 %R_o); very high biogenic silica proportions (averaging 80.2-90.3%); high mineralogical stiffness (0.80-0.87); and average porosities of 1.2% for the Horn River and 4.2% for the Exshaw-Patry play. Resource distribution models indicate 50% of Yukon's marketable gas will be found in 30% of its assessed area, with the best potential for significant volumes located in the very southeast of the territory where play depth and thickness increases.

* *matt2016ygs@gmail.com*

INTRODUCTION

In 2012, Yukon Geological Survey entered a multi-jurisdictional, collaborative research study of unconventional shale gas potential of the Liard basin. The project was initiated due to increasing industry exploration interests in Liard basin and the adjacent Horn River basin in northeast British Columbia (BC), where organic-rich Upper Devonian-Mississippian black shale formations comprise world-class, regionally extensive unconventional exploration targets (Adams *et al.*, 2015).

Previous work has focused on outcrop field studies of the Besa River Formation in BC (Ferri *et al.*, 2011, 2012, 2013), Yukon (Fraser *et al.*, 2012) and the Northwest Territories (*e.g.*, Rocheleau *et al.*, 2014; Pyle *et al.*, 2016). In 2016, a basin-wide shale resource assessment was published by the National Energy Board (NEB, 2016; Johnson *et al.*, 2016), together with the supporting detailed analytical methodologies and non-interpretative compilation of outcrop and subsurface data specific to Yukon's part of the basin by Hutchison (2016). To date, no interpretative unconventional subsurface analysis has been undertaken specifically on Yukon's well material or wireline data, and no correlation has been attempted with the more robustly differentiated stratigraphy in northeast BC (*e.g.*, Ferri *et al.*, 2013, 2015). This paper reports the first quantitative appraisal of frontier shale strata not only in Yukon's Liard basin, but also in the territory itself.

REGIONAL PETROLEUM GEOLOGY

Liard basin is located in southeastern Yukon straddling the border with BC and Northwest Territories (NWT), and constitutes the northernmost extension of the Western Canada Sedimentary basin (Fig. 1). In Yukon, it is approximately 6500 km^2 in area, and contains a sedimentary fill of >6000 m consisting of broadly folded Paleozoic and Mesozoic strata comparable to that of northeastern BC and northeastern Alberta (NEB, 2001). In the territory, 13 conventional wells have been drilled to date in the basin, and are focused in the Beaver River and Kotaneelee fields (Fraser and Hogue, 2007). Of these 13 wells, only three were put on production until eventual suspension of the Kotaneelee field in 2012 due to excessive water coning.

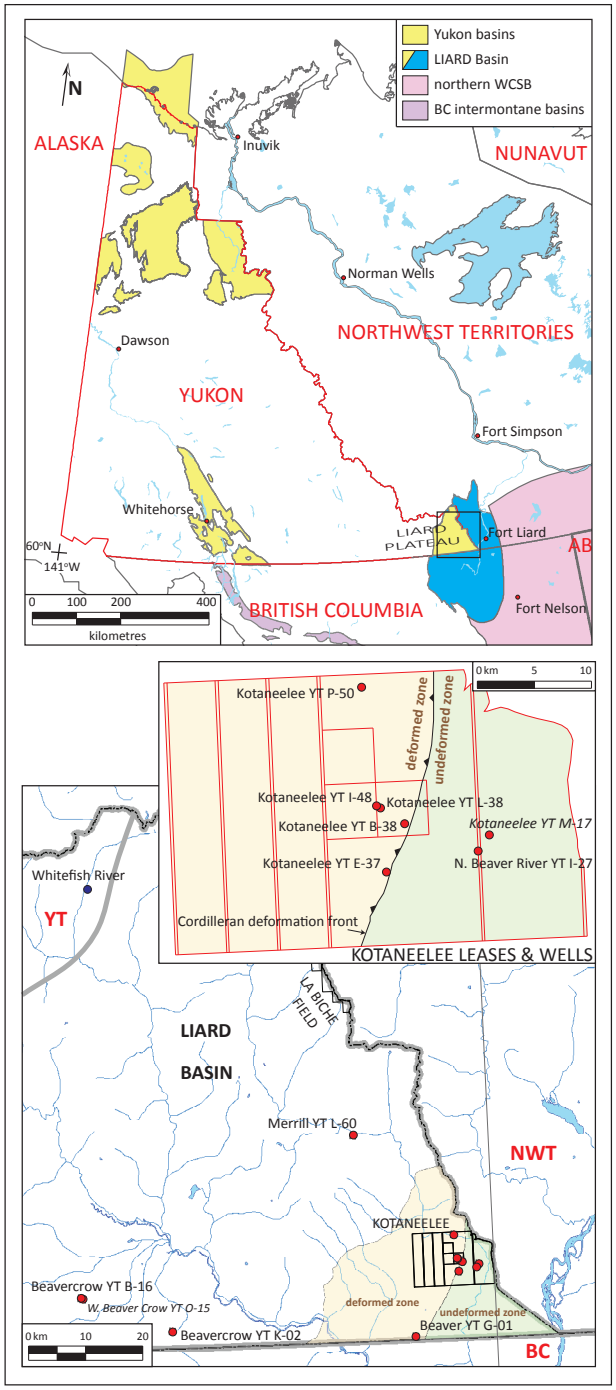

Figure 1. *Location of Liard basin in northwest Canada, with the Yukon portion shaded in yellow (after Hutchison, 2016, with basin margins from Mossop et al., 2004). The box on Liard Plateau in the upper map represents the area of the basin zoomed in below. Wells in italics in the lower map were not used in this study. The green and brown coloured 'zones' in the lower map refer to those areas assessed in the NEB (2016) resource calculations, with the boundary between the two representing the Cordillera deformation front. The red lines in the inset demark the Kotaneelee lease outlines.*

The strata of interest for this study are fissile, grey to black marine shales of the Devonian to Carboniferous Besa River Formation (Fig. 2): a generic unit used during surface mapping to describe thick successions of undifferentiated black shale (*e.g.*, Fallas *et al.*, 2014). These shales conformably overly the conventional gas-producing Cambrian through Middle Devonian platformal carbonate reservoirs of the Nahanni Formation (*see* Hutchison, 2016, for further detail). Stable organic carbon isotope data from Kotaneelee YT I-48 (see Hutchison, 2016), in conjunction with regional correlations and faunal and isotopic data from elsewhere in the WCSB (*e.g.*, Noble and Ferguson, 1971; Nadjiwon, 2001; Creaser *et al.*, 2002; Richards *et al.*, 2002; Selby and Creaser, 2005; Ferri *et al.*, 2015) have helped constrain the depositional age of the Horn River-Exshaw succession in Liard basin to Givetian to early Tournaisian (N. Sullivan *et al.*, in prep.).

In addition to the immature, proven conventional gas plays in the basin (NEB, 2001), unconventional play potential exists in two high quality source rocks within this Devonian-Mississippian basinal shale succession: the Exshaw-Patry and Horn River shale plays (NEB, 2016). The Exshaw-Patry play comprises shales of the Exshaw Formation and Ferri *et al.*'s (2015) underlying informal 'Patry member', and the Horn River play comprises shales of the Horn River Group in its entirety.

MATERIALS AND METHODS

Detailed sampling and analytical methods, re-interpreted formation tops, depths, gross thicknesses and net unconventional pay thicknesses and index data, together with Yukon's entire Liard basin sample database, are available for reference and digital download in Hutchison (2016). Sample data are summarized in Table 1 and methods are described briefly below (*see* Figure 1 for outcrop/well location map).

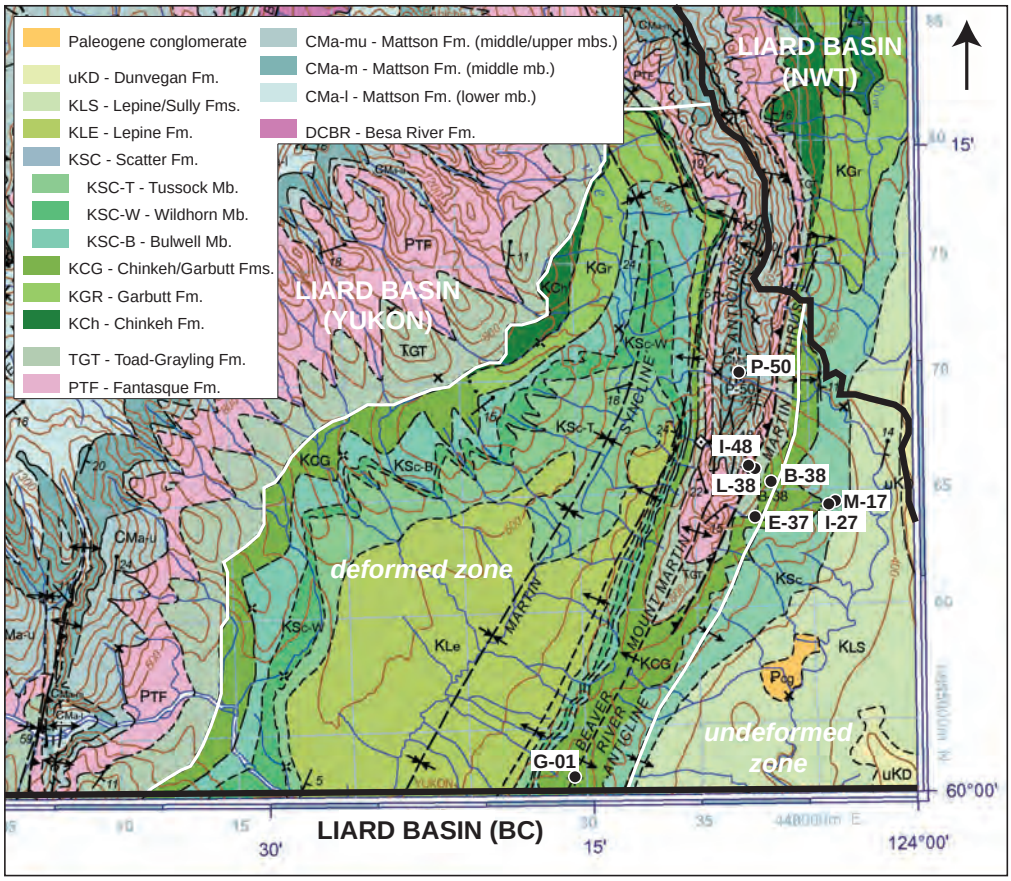

Figure 2. *Geology map of the southeastern part of Liard basin in Yukon with the undeformed and deformed assessment areas indicated. The Fort St John Group that defines the assessment area is composed of Chinkeh to Levine/Sully formations. Map modified from Fallas et al. (2014).*

Table 1. *Outcrop and well sample database for Yukon's Liard basin, reprinted from Hutchison (2016). Note that sample depth ranges for Kotaneelee YT I-48 are presented in post-shift measured depth (see text for discussion).*

Section/well ID	UWI	Easting	Northing	UTM zone	Elevation (KB asl)	Deviated?	TD (mMD)
Beaver YT G-01	300/G-01-6010-12415/0	429467	6652839	10	797.60	yes	4499.50
Beavercrow YT B-16	300/B-16-6010-12515/0	371896	6663005	10	1152.40	no	2288.40
Beavercrow YT K-02	300/K-02-6010-12500/0	387353	6656330	10	1133.90	no	3976.10
Kotaneelee YT B-38	300/B-38-6010-12400/1	438289	6665340	10	685.80	yes	3898.10
Kotaneelee YT E-37	300/E-37-6010-12400/2	437588	6663894	10	621.20	yes	4191.00
Kotaneelee YT I-48	300/I-48-6010-12400/4	437308	6666031	10	832.70	yes	4430.00
Kotaneelee YT I-48A	300/I-48-6010-12400/5	437308	6666031	10	832.70	yes	3915.00
Kotaneelee YT L-38A	300/L-38-6010-12400/0	437710	6666092	10	810.40	yes	4124.00
Kotaneelee YT M-17	300/M-17-6010-12400/1	441087	6664393	10	419.10	no	1333.00
Kotaneelee YT P-50	300/P-50-6010-12400/0	437108	6670086	10	454.20	yes	4410.50
Merrill YT L-60	300/L-60/6020-12415/0	420757	6688450	10	594.40	no	1634.30
North Beaver River YT I-27	300/I-27-6010-12540/3	440735	6664293	10	1445.80	yes	4418.10
West Beaver Crow YT O-15	300/O-15-6010-12515/0	372211	6662860	10	1147.90	yes	4418.10
Whitefish River	outcrop	378293	6734735	10			254.00

Section/well ID	SAMPLE RANGES (mMD)														
	Rock-Eval/TOC			Vitrinite reflectance			ICP-ES/MS			$\delta^{13}C_{org}$ (+TOC)			Porosity		
	No.	Top	Base	No.	Top	Base	No.	Top	Base	No.	Top	Base	No.	Top	Base
Beaver YT G-01	241	124.70	4395.52	69	125.00	4396.00	76	3529.58	4123.94				4	3608.83	4099.56
Beavercrow YT B-16	78	1189.00	1710.00	1	1505.71	1505.71	17	1453.90	1563.62						
Beavercrow YT K-02	53	935.74	1423.42	5	1018.30	1402.08	50	972.31	1423.42						
Kotaneelee YT B-38															
Kotaneelee YT E-37	86	3413.76	3958.44										5	3478.68	3883.30
Kotaneelee YT I-48	232	801.72	3640.00	5	3207.00	3634.00	114	3030.00	3697.00	184	2982.00	3684.00	1	3225.00	3225.00
Kotaneelee YT I-48A															
Kotaneelee YT L-38A															

Section/well ID	SAMPLE RANGES (mMD)															
	Rock-Eval/TOC			Vitrinite reflectance			ICP-ES/MS			$\delta^{13}C_{org}$ (+TOC)			Porosity			
	No.	Top	Base	No.	Top	Base	No.	Top	Base	No.	Top	Base	No.	Top	Base	
Kotaneelee YT M-17																
Kotaneelee YT P-50																
Merrill YT L-60	27	1024.13	1514.86	1	1136.90	1136.90										
North Beaver River YT I-27	95	963.17	3819.00	42	45.72	3816.80	19	3611.88	3712.46				1	3621.02	3621.02	
West Beaver Crow YT O-15																
Whitefish River	94	0.00	254.00	2	0.00	254.00	94	0.00	254.00							
	906			**125**			**370**			**184**			**11**			

blank cells = not sampled

SAMPLES

Outcrop samples were collected from the Whitefish River locality (378293E, 6734735N, UTM zone10) in the summer of 2012 (Fraser *et al.*, 2012), and consisted of homogenized, 2 m intervals of rock chips collected from fresh exposures. Yukon well cuttings were sampled at the GSC-C's core repository during December 2014 and transported to the Yukon Geological Survey in Whitehorse for subsequent preparation (washing, picking and weighing). Cuttings were sampled approximately every third bag (30 ft/9 m) in the wells selected, with every bag (10 ft/3 m) sampled in Kotaneelee YT I-48 from top Banff Formation into the Nahanni Formation (Table 1). Cuttings were also sampled every 500 ft (156 m) over the entire penetrated stratigraphy in North Beaver River YT I-27 to build a complete thermal maturation profile for this well based on vitrinite reflectance analysis. Six further cuttings samples and five core plug samples were collected for mercury porosimetry and helium stress porosity analyses respectively (Table 1).

The bulk of outcrop and cuttings samples were sent to Bureau Veritas Laboratories Ltd. (BVL; formerly Acme Analytical Laboratories Ltd.) in Whitehorse and then to Vancouver to be crushed. The resultant pulps were riffle-split, with half remaining with BVL in Vancouver for lithogeochemical analysis, and half shipped to the Geological Survey of Canada in Calgary's (GSC-C) Organic Petrology Laboratory for Rock-Eval/TOC analysis. Vitrinite reflectance and porosity samples were sent directly to the GSC-C and Trican Geological Solutions Ltd. in Calgary respectively.

WIRELINE DATA

Digital wireline data were available for 10 of the 13 Yukon wells, with a standard log suite consisting of gamma ray (GR), resistivity (ILD), density/neutron and sonic logs. Existing stratigraphic picks from Fraser and Hogue (2007) were reinterpreted using wireline signatures correlated using outcrop and core (Apache well b-023-K/094-O-05) from the basin in northeastern BC (*e.g.*, Ferri *et al.*, 2011, 2012, 2015). Formation tops in Yukon were picked using wireline logs only, except for the top Patry shale, which was picked based on its distinctive geochemical 'kick' signature (*see* EfMo, EfU, Th, TIP and Zr logs in Fig. 4).

Net pay thicknesses for the Horn River and Exshaw-Patry shales were calculated using cut-off values agreed to by the NEB (2016) project team for resistivity (>10 Ωm) and GR (>100 API), together with visual conditioning of the

results where the density log approaches or crosses the neutron porosity log. The net pay connectivity index (see method in Hutchison, 2016) provides an initial indication of how vertically connected pay zones in the reservoir may be, and therefore how heterogeneous the reservoir may be to produce. Net pay indices approaching 1.00 indicate increasing pay homogeneity. Log data were plotted in metres in measured depth (mMD), due to analytical samples being collected in and referenced to measured rather than true vertical depth (TVD), using version 5.1 of ALT's WellCAD® software, and geoSCOUT® software was used to generate equivalent depth and thickness data in mTVD.

GRID DATA

Depth, net pay thickness and TOC grid data for the Horn River and Exshaw-Patry shales (presented in map format in the results section) were provided courtesy of the National Energy Board (M. Johnson, personal communication, 2016). These grid maps use the geographically sparse Yukon well data to generate and condition a tract-by-tract map of these parameters for the entire assessment area (*see* NEB, 2016, for further details on tract sizes) that was then used to calculate marketable resource (for the Exshaw-Patry) in the NEB (2016) resource assessment. As the stratigraphy and resource is basin-wide, these maps also rely on data from BC and the Northwest Territories with which to interpolate areas of missing data in Yukon, such as the far southeast of Yukon's portion of the basin. Results presented in this report refer to actual, known Yukon well data; however, these grid maps should be viewed with the caveat that the gridded data extent used here to illustrate general trends in Yukon will therefore show some differences to actual Yukon data outside of areas with well control.

RESULTS

Reinterpreted wireline log and new cuttings geochemical analyses have facilitated correlation of the Besa River Formation in Yukon's subsurface to more robustly differentiated shales farther to the southeast (Fig. 3), including the Horn River Group (Evie, Otter Park and Muskwa formations), and Fort Simpson, Kotcho (Patry member: *c.f.*, Ferri *et al.*, 2015), Exshaw and Banff formations (*e.g.*, Hutchison, 2016; Hutchison and Fraser, 2016; Ferri *et al.*, 2015; NEB, 2016).

LITHOLOGY & WIRELINE SIGNATURE

The Horn River Group in Yukon is identified based on its tripartite gamma ray signature (Fig. 4) which is also recognized in northeastern BC's subsurface (*e.g.,* well a-067-D in Fig. 3) and in BC outcrop from the Caribou and Stone Mountains (Ferri *et al.*, 2012, their Figure 15). In the Horn River Group, lower radioactivity shales of the Otter Park Formation separate typically higher radioactive shales of the underlying Evie and overlying Muskwa formations. In the latter two formations, GR logs often experience scale 'wrap-round' (*i.e.*, log values greater than 150 API), and this is seen in the upper Muskwa Formation in Kotaneelee YT I-48 in Figure 4, and in all wells with penetrated Horn River Group in Figure 3.

The Fort Simpson Formation is divided into three informal members (lower, middle and upper) in Yukon, and the formation potentially correlates into the Tetcho-Redknife platform carbonate stratigraphy observed in the Horn River basin and on the platform to the east (*see* Fig. 3). Two informal members of the Exshaw Formation were recognized, the wireline characters of which correlate robustly with the upper and lower Exshaw markers of Ferri *et al.* (2015). Two members were also observed in the Banff Formation: a lower, thin carbonate-predominant unit (possibly equivalent to one of the Banff Formation Member B mixed carbonate/siliclastic units that overly the Exshaw Formation in southwestern Northwest Territories' subsurface; Richards *et al.*, 1994); and an upper, thick, shale-dominated unit equivalent to Member A of the same region (Richards *et al.*, 1994).

Lithological cyclicity was observed in cuttings logs within the overall succession (Fig. 4), with units alternating between dark grey to black, pyritic chert and siliceous shale (Horn River Group, middle Fort Simpson and Patry-lower Exshaw intervals), and brown to light grey dolomitic shales (lower and upper Fort Simpson, upper Exshaw and Banff shale intervals). Units of black pyritic chert are characterized by high GR, higher resistivity, overlapping or narrowly-separated density/neutron, and slower sonic log signatures. Intervals of dolomitic shale typically display the opposite response, exhibiting a distinctive, wide density/neutron separation (especially in the lower and upper Fort Simpson Formation) that greatly facilitated correlation of the overall stratigraphic succession between wells.

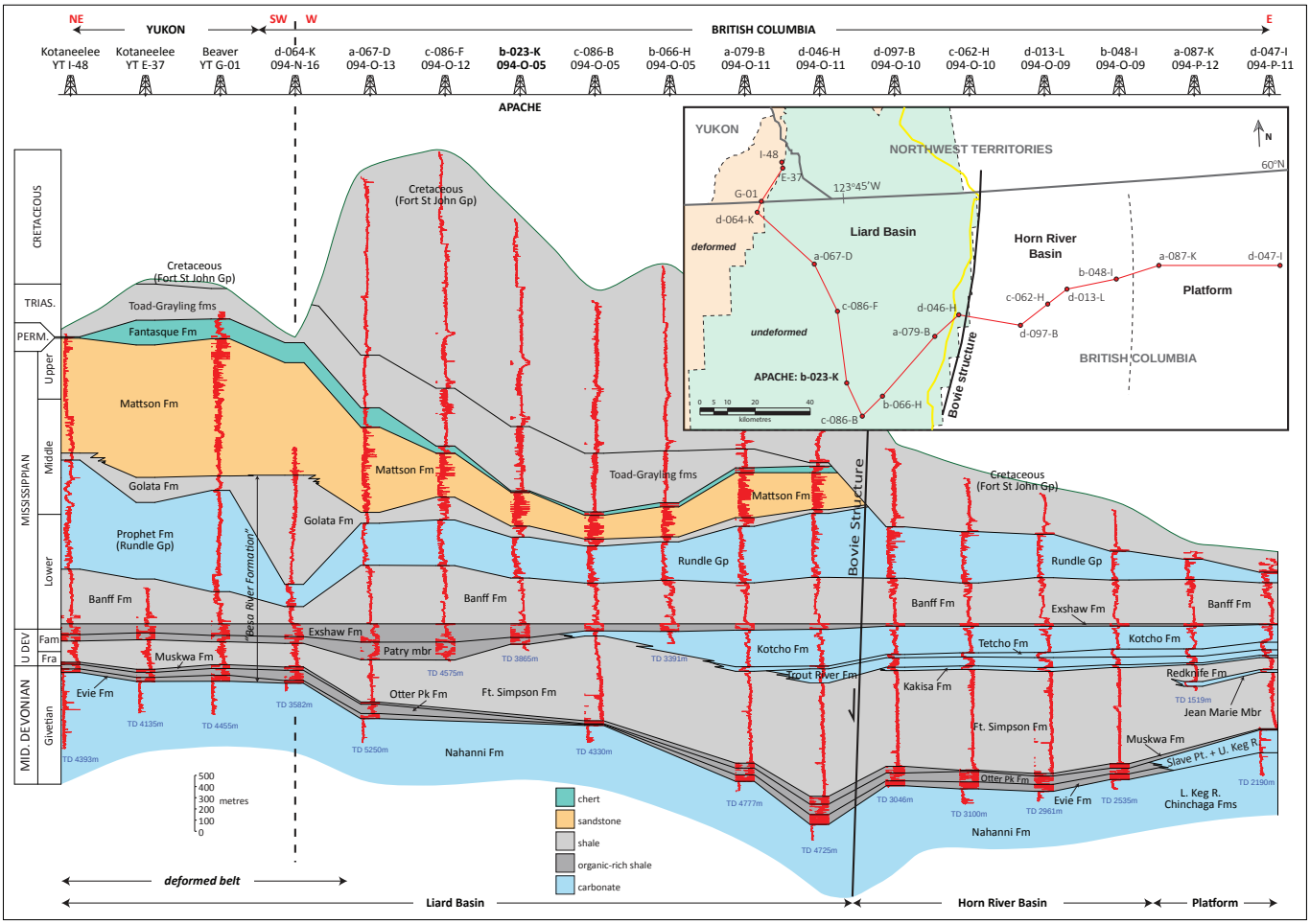

Figure 3. *Stratigraphic relationships of the Middle Devonian to Mississippian carbonate platform to shale basin succession in the northwestern WCSB. Inset map shows east to west correlation section. Note location of Apache's Patry well b-023-K in BC (referred to in text). The section datum is hung the top Exshaw Formation. Gamma ray logs are shown in red, with a log scale of 0-150 API (increasing to right). After Ferri et al. (2015).*

In core from Kotaneelee YT E-37, the Patry shale is black, siliceous, lacks sedimentary structure and exhibits disseminated pyrite blebs and rare pyritized radiolaria visible in hand specimen (Fig. 4). However, in cuttings logs the shale is also locally dolomitic, and is interbedded with rare dolostone beds (ranging from 1.4-4.7 mTVD in thickness) and 'marlstone'. Also of note is that the Otter Park Formation exhibits lithological and petrophysical characteristics more similar to those of the under and overlying Evie and Muskwa formations (Fig. 4), despite it typically being characterized in BC in the Liard and Horn River basins as calcareous (*e.g.*, Johnson and Johnson, 2012) and clay-rich (*e.g.*, Ayranci *et al.*, 2015; Harris *et al.*, 2017).

AREA, DEPTH & NET PAY THICKNESS

Prospective Horn River and Exshaw-Patry shale reservoirs were only assessed in the southeastern corner of the basin where structural deformation due to Cordilleran thrusting is anticipated to be of relatively minimal expression in the basin (*see* Fig. 2). The overall assessment area (657 km^2) also corresponds to the limit of Cretaceous Fort St John Group outcrop in the basin (Fig. 2). This was considered by the NEB (2016) project team to provide the minimum overburden thickness to generate sufficient Devonian-Carboniferous reservoir pressures at depth in Yukon and BC.

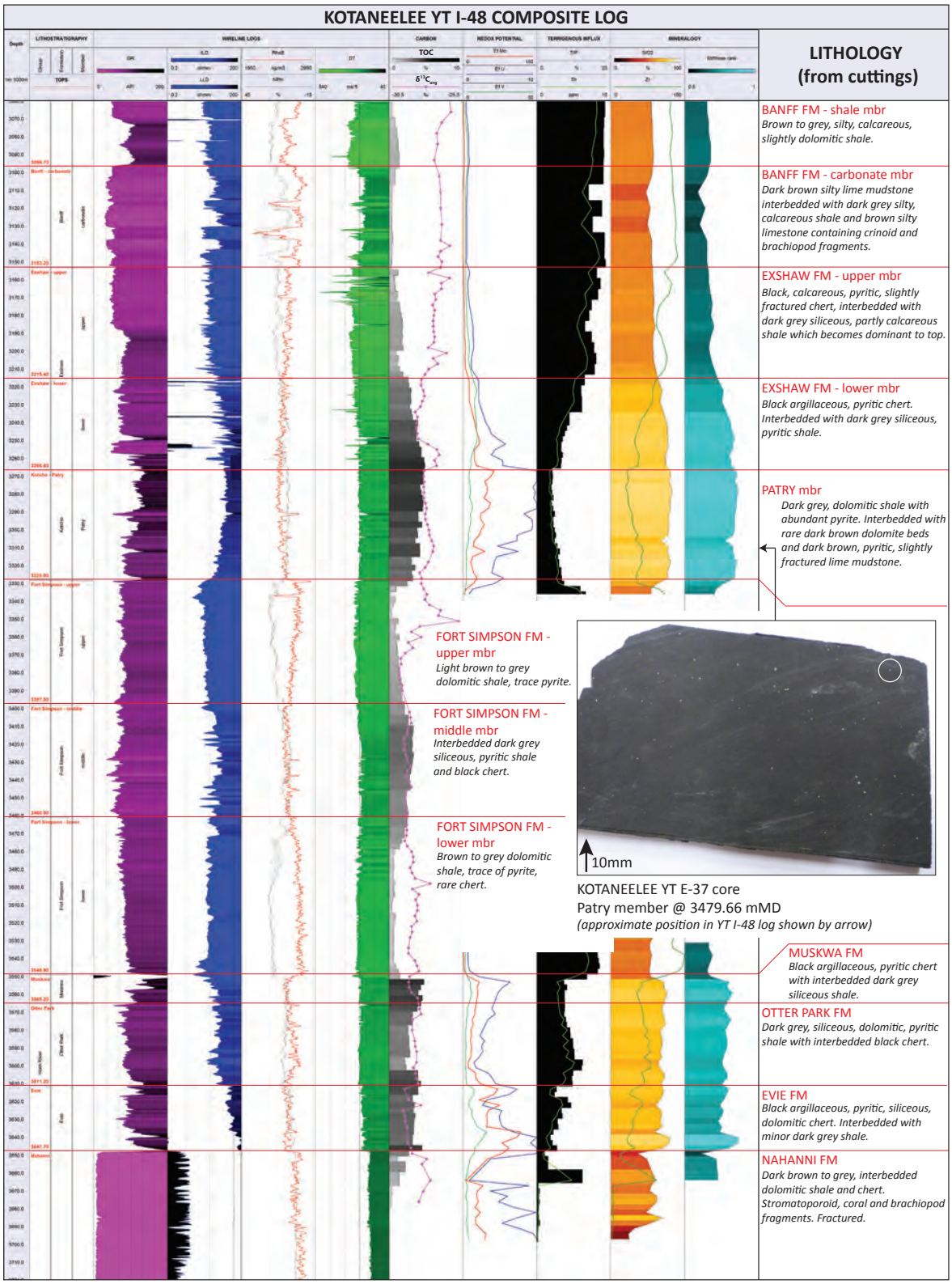

Figure 4. *Composite wireline, geochemistry and cuttings-based lithology log for the Kotaneelee YT I-48 well. The core photo is from an equivalent Patry member section in Kotaneelee YT E-37 (the white blebs are pyrite, sometimes pyritised radiolaria - circled). Depths are plotted in mMD, of which a full log suite is presented in this figure for completeness (see Hutchison, 2016, for data and methodology: Ef=enrichment factor, TIP=terrigenous input profile).*

The depth to the top Horn River Group ranges from 1273.3 mTVD (Beavercrow YT K-02) to 4208.9 mTVD (Kotaneelee YT P-50), and averages 3017.9 mTVD (Fig. 5; Table 2). Burial depths decrease towards the north and west in association with the transition from undeformed to uplifted/deformed zones within the basin (Fig. 6a). Average gross play thicknesses range from 88.5-161.4 m, and net pay thickness typically increases with depth towards the southeast of the basin (Fig. 6b) where comparable Horn River shale thicknesses occur in BC wells d-064-K and a-067-D (*see* Fig. 3). The Otter Park Formation is the thickest constituent shale of this play (102.4 m in Kotaneelee YT L-38A) and averages 55.1 m across the basin. The formation therefore exhibits the maximum net pay thickness (45.7 m) and thickest average net pay interval (30.1 m) of the Horn River Group.

The Exshaw-Patry shale is shallower and thicker than the Horn River shale, with depths to the top of the Exshaw Formation ranging from 980.5 mTVD (Beavercrow YT K-02) to 4012.7 mTVD (Kotaneelee YT P-50) and averaging 2687.9 mTVD (Fig. 5; Table 2). The play averages 127.1 mTVD in total thickness, with the greatest thicknesses occurring in the southeast of the basin adjacent to the BC border (*e.g.*, 178.7 mTVD in Beaver YT G-01). As in the Horn River Group, burial depths (Fig. 6c) and gross and net pay thicknesses (Fig. 6d) decrease towards the northwest of the basin, and the shales start to outcrop substantially west of 124° 50′ W (Fallas *et al.*, 2014; *see* Fig. 2). Both the Patry member and the Exshaw Formation exhibit net pay thicknesses exceeding 40 m (Table 2), and combined play net pay thicknesses average 88.74 m (ranging from 46.2 m in North Beaver River YT I-27 to 116.8 m where the unit is thickest in Beaver YT G-01).

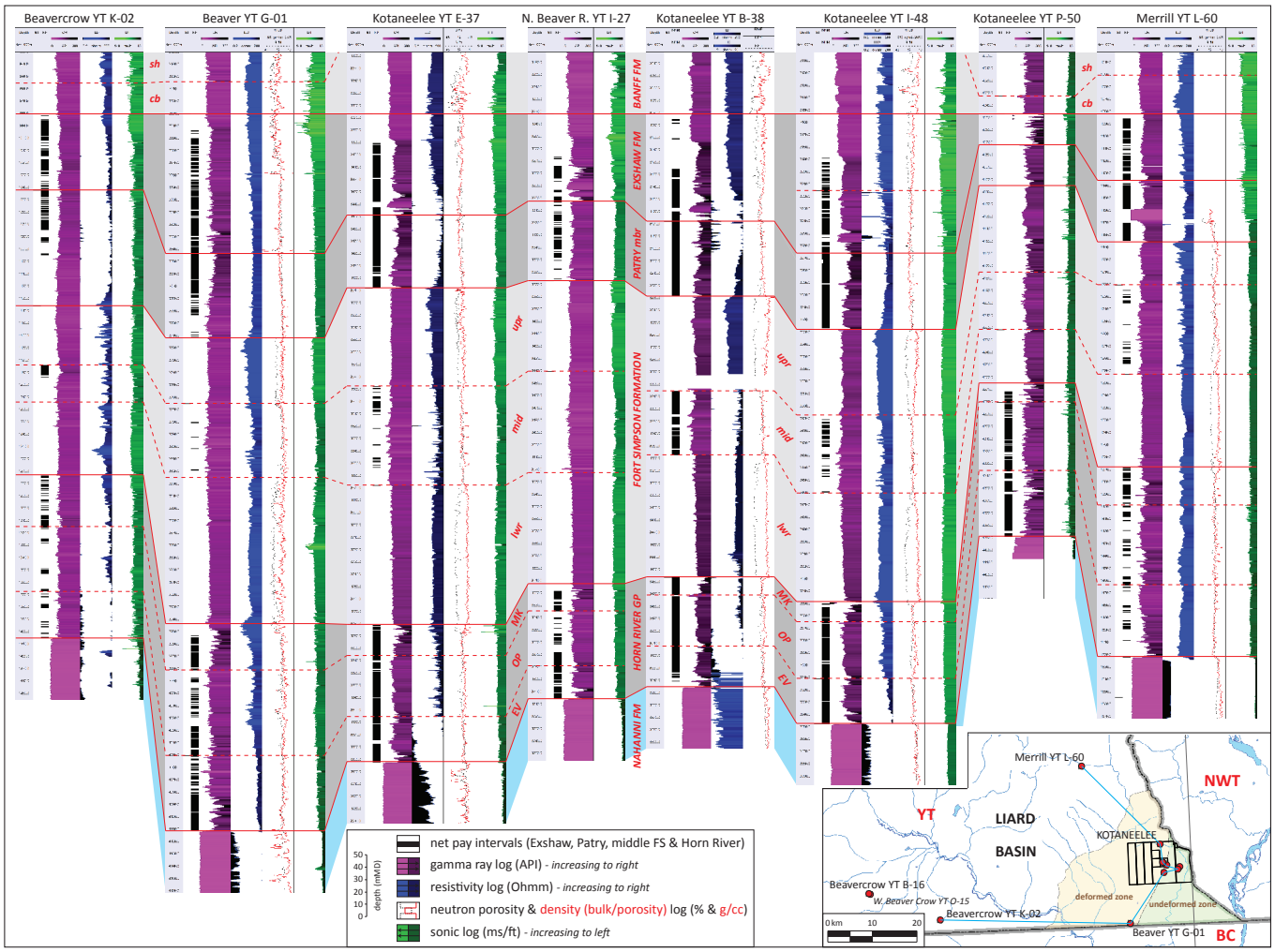

Figure 5. *Wireline log correlation panel across Yukon's Liard basin. Horizontal datum is the top of the Exshaw Formation and data extend 50 m into the Banff and Nahanni formations. The Exshaw-Patry and Horn River shale correlation is shaded in dark grey. Abbreviations: middle FS – middle member of the Fort Simpson Formation; EV – Evie Formation; OP – Otter Park Formation; MK – Muskwa Formation.*

Table 2. *Horn River and Exshaw-Patry shale play characteristics in Yukon's Liard basin. Note that upper values are averages and lower italicized values in parentheses are ranges. Also note that mineralogical data, except stiffness rank, are presented as ternary diagram proportional percentages (for actual concentration data refer to Hutchison, 2016).*

		Evie	Otter Park	Muskwa	HORN RIVER	Patry	Exshaw	EXSHAW-PATRY
Depth (mTVD)		3097.92 *(1368 - 4273)*	3042.83 *(1315 - 4223)*	3017.88 *(1273 - 4209)*	3017.88 *(1273 - 4209)*	2760.02 *(1042 - 4035)*	2687.91 *(981 - 4013)*	2687.91 *(981 - 4013)*
Thickness (mTVD)		41.05 *(26.70 - 58.40)*	55.09 *(34.90 - 102.38)*	24.95 *(13.70 - 42.00)*	121.08 *(88.50 - 161.40)*	57.95 *(29.80 - 93.90)*	69.19 *(22.50 - 112.80)*	127.14 *(52.30 - 178.70)*
Net pay (mTVD)		25.04 *(8.55 - 41.73)*	30.11 *(9.45 - 45.71)*	17.90 *(6.72 - 25.95)*	73.29 *(41.25 - 102.10)*	43.48 *(28.95 - 60.45)*	45.05 *(17.10 - 74.30)*	88.74 *(46.20 - 116.77)*
Net pay connectivity (%)		0.88	0.87	0.91	0.90	0.92	0.91	0.92
TOC (wt%)		3.00 *(0.85 - 6.06)*	2.64 *(0.60 - 4.84)*	2.59 *(0.69 - 4.75)*	2.75 *(0.60 - 6.06)*	4.10 *(2.16 - 6.86)*	3.60 *(1.04 - 6.05)*	3.86 *(1.04 - 6.86)*
Maturity (%Ro)		3.44 *(3.01 - 4.18)*	3.36 *(2.52 - 4.20)*	3.62 *(2.69 - 4.60)*	3.48 *(2.52 - 4.60)*	2.88 *(2.16 - 3.91)*	2.78 *(2.09 - 3.50)*	2.84 *(2.09 - 3.91)*
Mineralogy	**SiO_2 (%)**	82.3 *(66.9 - 91.0)* biogenic	82.5 *(72.0 - 92.0)* biogenic	80.2 *(70.0 - 91.3)* biogenic	81.9 *(66.9 - 92.0)* biogenic	90.3 *(81.9 - 97.1)* biogenic	85.3 *(69.5 - 96.8)* biogenic	87.8 *(69.5 - 97.1)* biogenic
	CaO+MgO (%)	8.4 *(2.6 - 21.4)*	4.8 *(1.5 - 8.4)*	5.3 *(1.4 - 12.0)*	6.3 *(1.4 - 21.4)*	2.8 *(0.2 - 12.1)*	3.1 *(0.2 - 8.7)*	2.9 *(0.2 - 12.1)*
	Al_2O_3 (%)	8.8 *(4.0 - 22.3)*	12.8 *(6.5 - 22.7)*	14.5 *(7.2 - 21.4)*	11.8 *(4.0 - 22.7)*	6.9 *(2.7 - 13.5)*	11.7 *(3.0 - 24.3)*	9.3 *(2.7 - 24.3)*
	Stiffness rank	0.81	0.81	0.80	0.81	0.87	0.83	0.85
Porosity (%)		0.98 *(0.12 - 1.71)*	1.93 -	1.66 *(1.39 - 1.94)*	1.21 *(0.12 - 1.94)*	4.43 *(2.99 - 6.04)*	3.23 *(2.86 - 3.59)*	4.21 *(2.86 - 6.04)*

Net pay zones (delineated on Fig. 5 by black strip log bars) are thick and continuous in the Kotaneelee field and in Beaver YT G-01 along strike to the south, exhibiting very high reservoir homogeneity (e.g., 0.98 in the Exshaw-Patry shale in Kotaneelee YT B-38). Net pay strip logs that display as thin, discontinuous bars correspond to relatively high heterogeneity, for example in the Horn River Group of Merrill YT L-60 (0.78) or Beavercrow YT K-02 (0.75). On average, net pay connectivity indices are greater than 0.87 in both plays.

TOTAL ORGANIC CARBON

TOC values in Horn River Group shales range between 0.6-6.1 wt% (Table 2). Average TOC values decrease up-section in this play, with the highest recorded in the Evie Formation (3.0 wt%) and lowest in the Muskwa Formation (2.6 wt%). In general, the average TOC for Horn River Group per well increases to the northwest (Fig. 7a) from 1.7 wt% in North Beaver River YT I-27 to 3.9 wt% in Merrill YT L-60. TOC concentrations in the Exshaw-Patry shale play exhibit a similar range (1.0-6.9 wt%), however both shales within this play exhibit higher average TOCs than any of the Horn River Group formations, with the highest average (4.1 wt%) and maximum concentration recorded in the Patry shale. In contrast to the older Horn River Group, TOC values in the Exshaw-Patry shale play decrease from east to west in the basin (Fig. 7b).

Wireline logs from both plays indicate that intervals of elevated TOC typically exhibit high gamma ray (>100 API). Hydrocarbon presence is also suggested in these intervals by higher than background resistivity (>10 Ωm) values and a density curve that approaches or crosses the neutron curve on a RhoB or DPhi/NPhi log (Fig. 3). Cross-plots of TOC vs. S1 + S2 used to interpret conventional source rocks indicate that Yukon shales in Liard basin are of good quality (*i.e.*, TOC greater than 2 wt%: Peters and Cassa 1994) but low generative potential (Fig. 8). Unconventional reservoir potential is also supported in these shales with most TOC values greater than 2 wt% (Zou, 2013). Spatial relationships in organic matter quality are cryptic in Liard; however, shales from Kotaneelee YT I-48, Beaver YT G-01 and Merrill YT L-60 appear to consistently plot closest to or

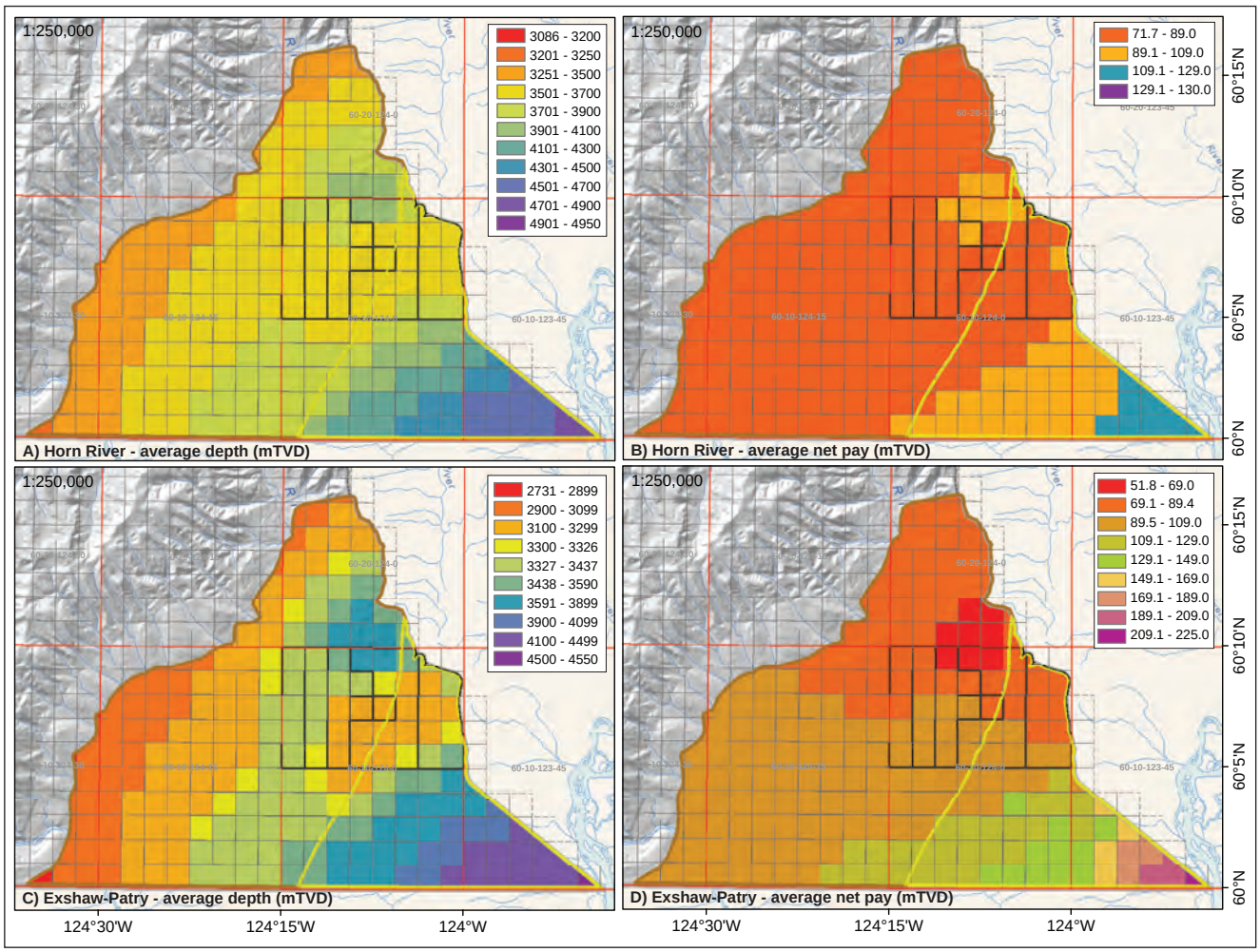

Figure 6. *Gridded, tract-by-tract data (in mTVD) for Yukon's portion of Liard basin (see text and NEB, 2016, for discussion of tract sizes and grid methods).* ***(A)*** *Average depth to top Horn River Group.* ***(B)*** *Average net pay thickness of the Horn River Group.* ***(C)*** *Average depth to top Exshaw-Patry shale.* ***(D)*** *Average net pay thickness of the Exshaw-Patry shale. See Figure 12 for map legend.*

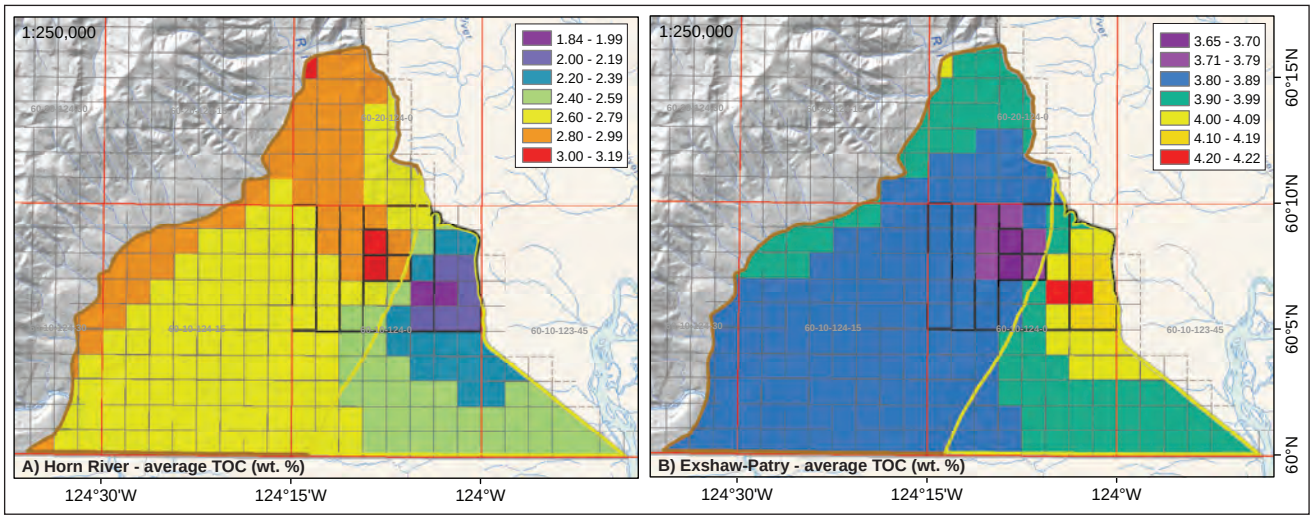

Figure 7. *Gridded, tract-by-tract TOC data (in wt%) for Yukon's portion of Liard basin (see text and NEB, 2016, for discussion of tract sizes and grid methods).* ***(A)*** *Average Horn River Group TOC.* ***(B)*** *Average Exshaw-Patry shale TOC. See Figure 12 for map legend.*

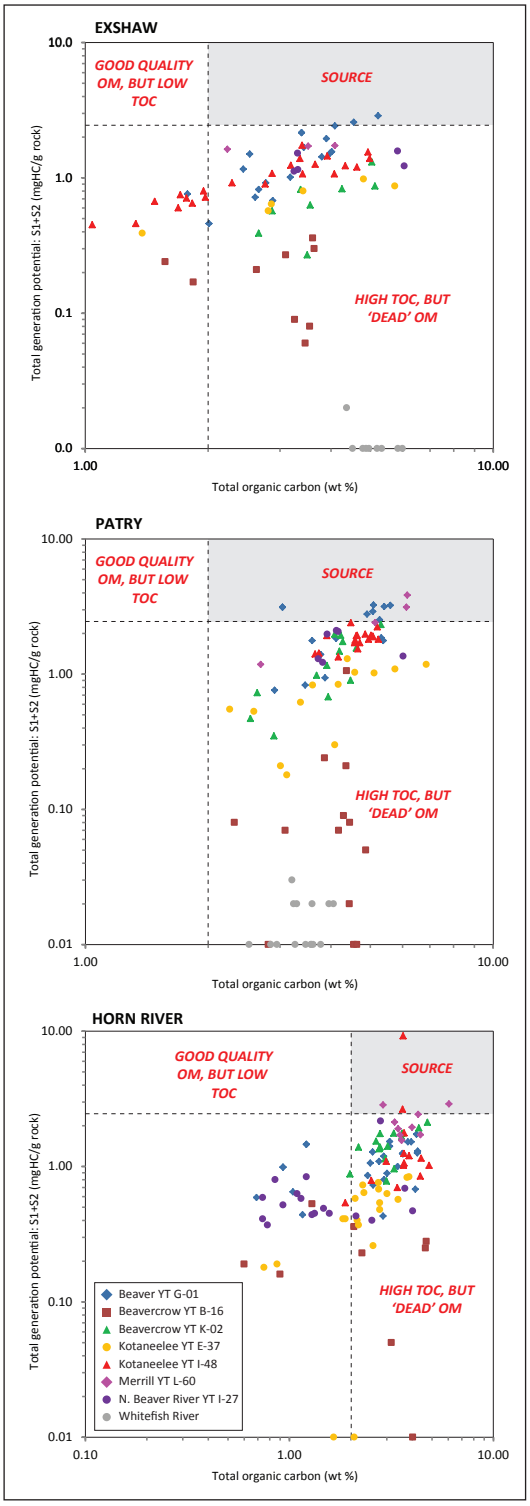

Figure 8. *Organic richness (TOC content) and total generative potential of the Exshaw, Patry and Horn River shales. The TOC lower boundary is here set at 2 wt% to represent good conventional source rock quality (c.f., Peters and Cassa, 1994) and potential unconventional reservoir quality (c.f., Zou, 2013).*

within the source window. Yukon basin data obtained from Beavercrow YT B-16 and the Whitefish River outcrop display very low to zero total generative potential despite elevated TOC values. The Patry shale exhibits the best overall quality relative to the overlying Exshaw Formation or older Horn River Group shales.

VITRINITE REFLECTANCE

Maturity profiles generated from vitrinite reflectance data support the low S1 and S2 values obtained from RockEval analysis, with both shale plays being highly mature and well within or past the dry gas window (based on a dry gas preservation limit of 3.0 %R_o; Dow, 1977) (Fig. 9; Table 2). Within each shale play, the Otter Park and Exshaw formations are the least mature (3.36 %R_o and 2.78 %R_o respectively), with maturity typically increasing towards the south of the basin in the Horn River shale and to the north in the Exshaw-Patry shale. Overall, maturity values for individual shales within these plays do not vary significantly from the overall play mean (Horn River = 3.48 %R_o, Exshaw-Patry = 2.84 %R_o).

MINERALOGY AND GEOCHEMISTRY

All Horn River Group and Exshaw-Patry shales are silica-rich (Table 2), with average SiO_2 concentrations between 80.2% (Muskwa Formation) to 90.3% (Patry shale) when plotted proportionally on SiO_2-Al_2O_3-(CaO + MgO) ternary diagrams (Fig. 10a,b). Overall, a dominance of biogenic silica (as opposed to detritally-derived silica) is indicated by the shallow, negative SiO_2-Zr correlation trend (*e.g.*, Fraser and Hutchison, 2017; Blood *et al.*, 2013; Wright *et al.*, 2010; Fig. 10c). Carbonate content is low, even in the Otter Park Formation, and average CaO + MgO proportions range from 2.8% in the Patry shale to 8.4% in the Evie Formation (Table 2). Al_2O_3 (used as a proxy for clay) proportions range up to 24.3% in the Exshaw Formation, with values consistently greater than 10% in the Otter Park, Muskwa and Exshaw formations.

The high SiO_2 and very low Al_2O_3 composition of these shales indicates a high fraction of stiff minerals (high Young's Modulus and low Poisson's Ratio) that comprise the matrix volume of the rock (Figs. 4 and 10d). The very high overall fraction of stiff minerals corresponds well to the black, siliceous lithology of these prospective shale plays. Average shale stiffness mirrors average shale silica trends, with the Muskwa Formation being the least stiff (0.80) and the Patry shale the most (0.87). The moderate positive correlation (R^2 = 0.33) that exists between stiffness

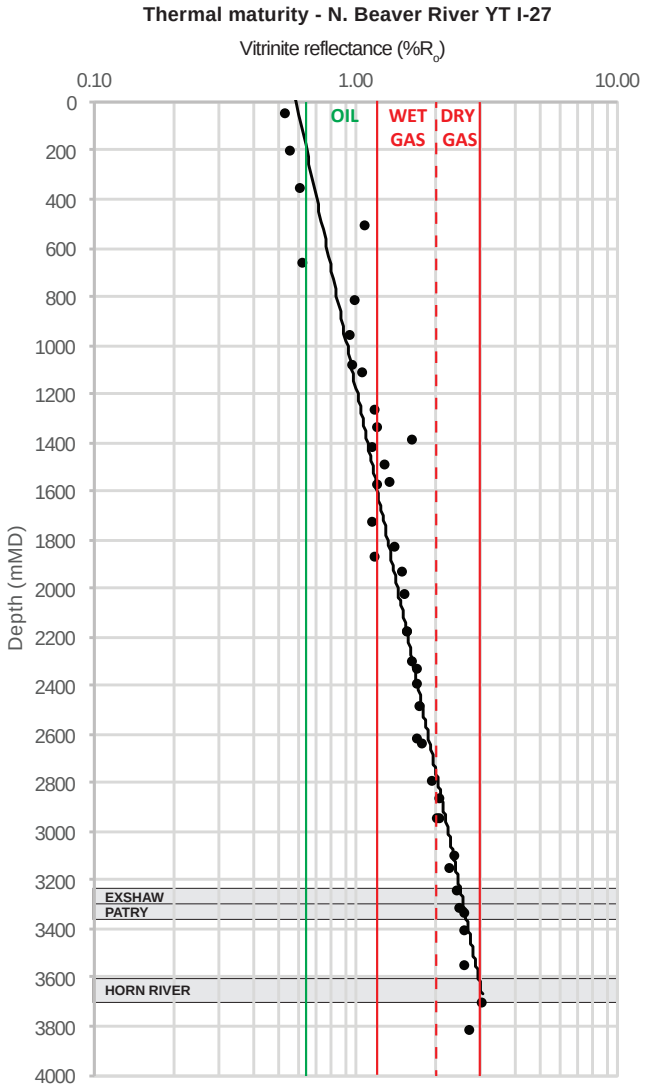

Figure 9. *Vitrinite reflectance maturity profile for North Beaver River YT I-27 in Yukon's Liard basin. Both shale plays of interest plot within the dry gas generation zone (R_o >1.35: Peters and Cassa, 1994) but below the wet gas floor (R_o >2.0: Dow, 1997).*

rank and TOC initially suggests zones of elevated TOC (and therefore enhanced unconventional reservoir quality) will respond well to artificial stimulation during production. Intra-play mineralogical stiffness is more variable in the Exshaw-Patry shale (0.73-0.95) than in the Horn River Group (0.70-0.89), and stiffness and TOC visually covary within these shale units (*see* Fig. 4).

POROSITY

Cuttings samples have a corrected porosity range from 1.4 to 3.6% with the highest porosity in the Exshaw Formation, and an overall average porosity of 2.2% (*see* Hutchison, 2016, for methodology). Pore size for the entire sample set ranged from <3 to 1900 nm, with peak pore sizes between 3 and 38 nm. Pore size distribution is similar for the two Exshaw samples and the two Muskwa samples, and the Exshaw samples exhibited the greatest intrusion. A strong correlation exists between depth and cuttings porosity (R^2=0.81), and initial data suggest that intra-shale porosity decreases with increasing depth (Fig. 11a).

Plugs from the Evie Formation had lower stressed helium porosity values throughout the testing (average 0.9%) relative to the Patry shale (4.4%) in Kotaneelee YT E-37. The three Patry plugs show a general trend of decreasing pore compressibility as depth increases (Fig. 11b), with porosity reductions between low and high confining pressure conditions approximately 40% for samples T1 and T2 but only 8% for the deepest T3 sample. Pore compressibility was higher in the deeper Evie Formation plugs, with significant differences observed between the two samples (T4=44%, T5=93%).

DISCUSSION

YUKON RESERVOIR POTENTIAL

Reservoir net pay continuity between individual shale stratigraphic units in the Horn River Group, and between the Exshaw Formation and Patry member confirms that the basin's potential is best illustrated by combining these units into two 'productive' shale plays – the Horn River shale (Evie, Otter Park and Muskwa formations) and the Exshaw-Patry shale (*e.g.*, Table 2). However, the stratigraphic breakdown of these plays into their constituent units in this study (as opposed to the higher-level assessment by the NEB in 2016) has also resulted in a more precise resolution of 'sweet spot' reservoir intervals for targeting during initial exploration.

Within the Horn River play in Yukon, the available data suggest the Otter Park Formation exhibits the best unconventional gas reservoir potential (Table 2), with average net pay thicknesses in excess of 30 m, TOC contents ranging from 0.6 to 4.8 wt%, and porosities approaching 2%. In Yukon, the Otter Park Formation exhibits lithological and petrophysical characteristics more like those of the prospective under and overlying Evie and

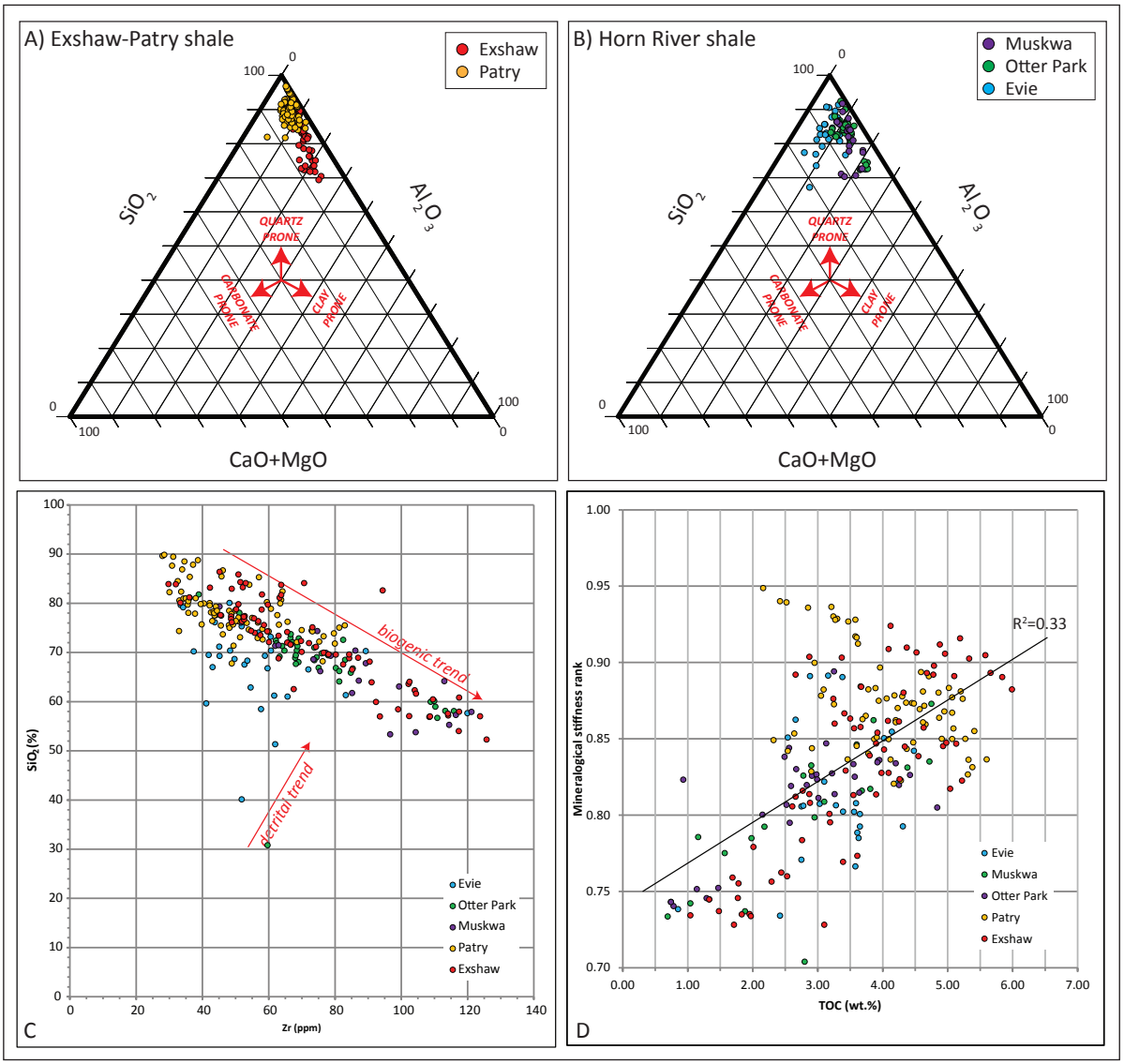

Figure 10. ***(A and B*** *Shale proxy-mineralogical ternary diagrams for the Exshaw-Patry and Horn River plays respectively.* ***(C)*** *The silica is biogenic in origin as shown by the inverse correlation between SiO_2 and Zr.* ***(D)*** *Correlation between TOC and stiffness rank.*

Muskwa formations; differing markedly to those made from the same formation towards the southeast of Liard basin and in the Horn River basin. In these locations in BC, the Otter Park consists of calcareous to clay-rich sediments with relatively low TOC (2.2 wt%; Ayranci *et al.*, 2015) that were deposited within transitional to oxygenated shallow water environments adjacent to the Slave Point and Upper Keg River Formation shelf-break and platform carbonates (*e.g.*, Johnson and Johnson, 2012).

In Yukon, deeper, more distal depositional environments, as suggested by darker black colouration, higher TOC, biogenic silica and pyrite content and low carbonate, highlight the potential for noticeable lateral facies variability in the Horn River play (*c.f.*, Ayranci *et al.*, 2015), with reservoir properties ultimately controlled by water depth, oxygenation, sediment input and proximity to basin margin (*e.g.*, Bohacs *et al.*, 2005). Whilst a detailed lithogeochemical appraisal is beyond the scope of this initial report, redox-sensitive trace elemental data were collected for some of the wells included in this study (*see* Fig. 4) that could be used in future to investigate such depositional controls in Yukon and supplement similar redox studies conducted on this stratigraphy in BC (*e.g.*, Harris *et al.*, 2017). Furthermore, these results

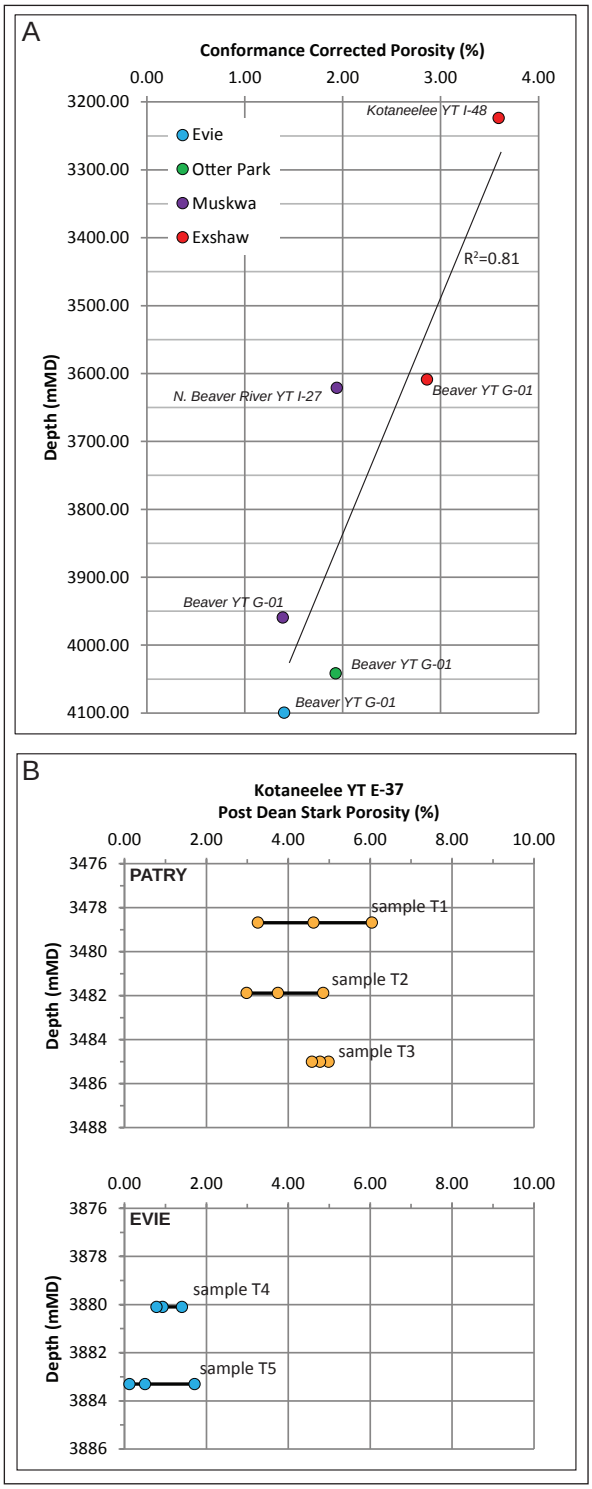

Figure 11. ***(A)*** *Porosity measured from MICP analysis on cuttings, and* ***(B)*** *from stressed helium analysis on core from the Evie and Patry shales in Kotaneelee YT E-37.*

suggest initial caution is required in extrapolating analogous reservoir properties for the Horn River play from areas of relatively dense well-control into the more frontier, deeper-water basin. The key for unlocking the accurate potential of Yukon's Liard will stem only from future exploration in the territory, especially due to the significant depth challenges of accessing this play in BC (Johnson *et al.*, 2016).

In the Exshaw-Patry play, the upper part of the Patry member and the lower member of the Exshaw Formation offer the best reservoir potential for gas; with reservoir quality deteriorating up-section into the upper Exshaw Formation (Fig. 4). The Patry member exhibits average net pay thicknesses of 43.5 m, in addition to the highest average net pay connectivity, TOC content, silica versus clay and carbonate proportion, mineralogical stiffness and porosity of the study (Table 2), and offers the best potential for significant gas volumes within the combined Exshaw-Patry play. Hydrocarbon presence is also suggested in these intervals in Yukon by higher than background resistivity (>10 Ωm) values and a density curve that typically crosses the neutron curve on a RhoB or DPhi/NPhi log plot (*see* Fig. 4).

These observations compare favorably to the cored Exshaw-Patry interval in BC well b-023-K, where Ferri *et al.* (2015) document the highest TOC (~8 wt%), porosity (~9%) and gas saturation (~80%) associated with resistivities ranging between 20 and 60 Ωm across the middle to upper Patry shale. In particular, Patry shale porosities are comparable to those obtained from this interval in the Apache Patry b-023-K well in northeastern BC where they average 4-9% (Ferri *et al.*, 2015). The Patry b-023-K well also displays the same trend as Yukon for decreasing porosity with depth, in which samples from the principal gas-prone zone in the middle to upper Patry shale (9%) yield higher porosities than those towards the base of the unit (4-6% in BC, 4.4% average in Yukon).

There are significant volumes of gas to be found in these frontier Yukon plays - recently illustrated by the NEB (2016) assessment of the Exshaw-Patry shale play of the entire Liard basin as the ninth largest unconventional marketable gas resource in the world, and the second largest in Canada. The NEB (2016) unconventional resource assessment indicates a total expected gas in place volume of 68 Tcf (47 Tcf from the Exshaw-Patry shale and 21 Tcf from the Horn River). Using an expected recovery factor of approximately 17% in Yukon, the

NEB (2016) calculates dry expected ultimate P50 recoveries of 7.6 Tcf from the Exshaw-Patry shale in Yukon's portion of the basin (the Horn River marketable gas was not calculated in this assessment). The entire basin's total 219 Tcf of marketable gas is estimated to extend Canada's gas supplies for a further 68 years (based on the country's 2014 consumption of 3.2 Tcf – Statistics Canada, 2014), and more significantly for Yukon itself, the 7.6 Tcf from this play alone would deliver approximately 1800 years of the territory's 2014 energy usage (Statistics Canada, 2014).

YUKON'S SHALE RESOURCE DISTRIBUTION

The small GIP and marketable volumes in Yukon relative to the Northwest Territories and British Columbia are due to the small basin area chosen for this jurisdiction for assessment rather than an indication of poor reservoir quality or significant geological or extraction risks in the deformed zone (risks estimated at 10% *vs.* no risk for the undeformed zone; NEB, 2016). The assessed area covers approximately one tenth of the basin's areal extent in Yukon, and although these Middle Devonian-Mississippian plays are typically present across the entire basin, exposure at surface and intense folding and faulting on the Liard Plateau impart significant challenges to exploration and extraction of this gas based on today's technology and economics. Favourable Exshaw-Patry reservoir data from: Merrill YT L-60 (4.28 wt% average TOC, 73.35 mTVD net pay); Beavercrow YT K-02 (3.87 wt% average TOC, 69.30 mTVD net pay); and the Whitefish River outcrop (4.08 wt% average TOC) confirm the play's geological extension west of the currently defined deformed zone in Yukon's Liard basin.

It is important to note, however, that the resource in Yukon is not uniformly spread within the territory (Fig. 12). Exshaw-Patry marketable P50 gas volumes per tract area (3.2 km^2 in

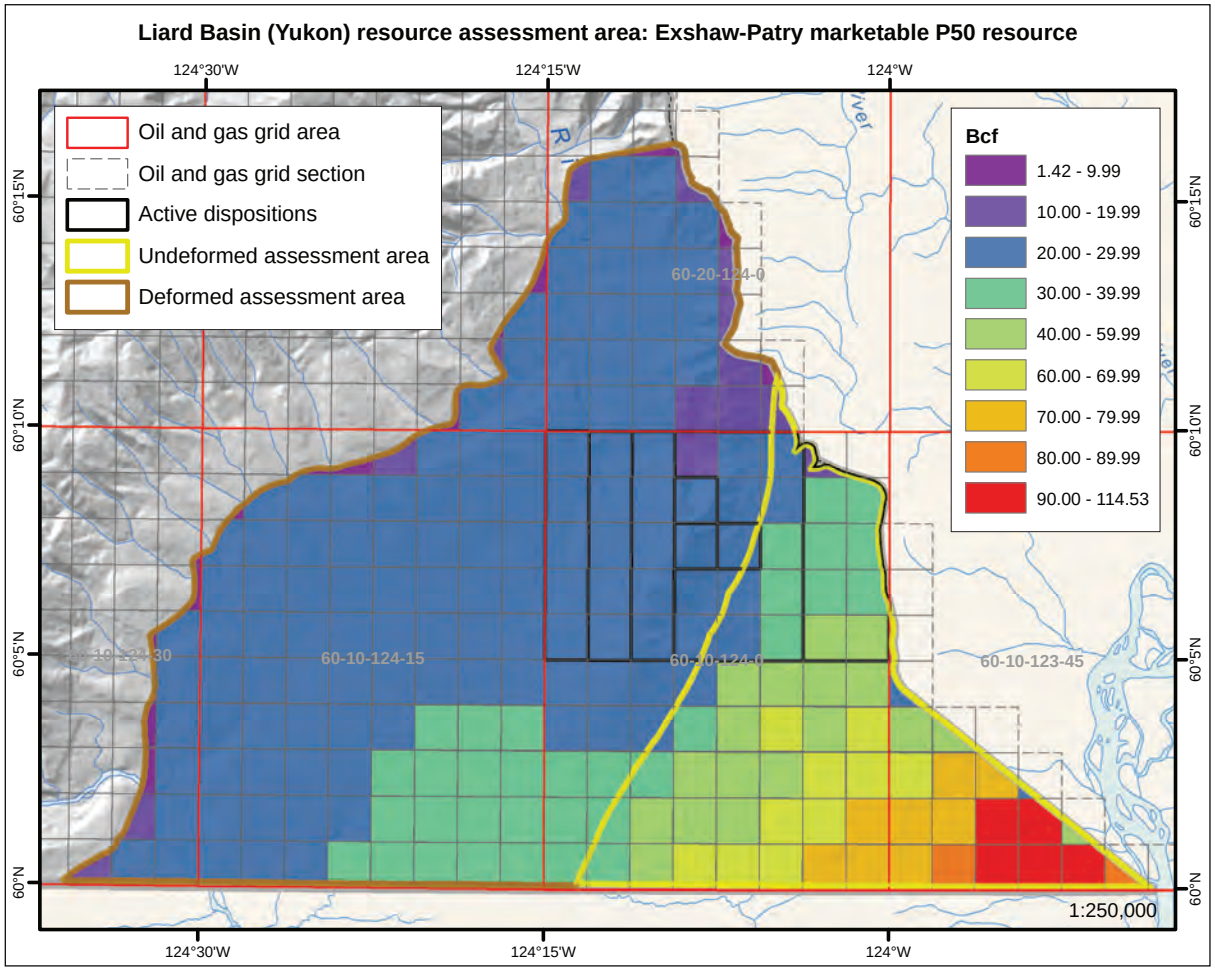

Figure 12. *Gridded, tract-by-tract P50 marketable gas resource for Yukon's portion of Liard basin (see text and NEB, 2016, for discussion of tract sizes and grid methods).*

Yukon) calculated by the NEB (M. Johnson, 2016, personal communication) suggest a relatively flat resource spread until the 70th percentile of tracts (as ranked by Bcf/tract) is reached, at which point the resource volumes start increasing significantly (Fig. 13). In addition, 50% of Yukon's Exshaw-Patry cumulative marketable resource is also reached at approximately the 70th percentile, suggesting that resource percentage occurs in only 30% of the area assessed in Yukon. The Exshaw-Patry reservoir exhibits relatively consistent depths and net pay thicknesses across the deformed zone in Yukon (where well-control exists). However, the NEB (2016) modelled the thickness and depth to increase dramatically towards the southeast of the territory into the core of the basin, with the result that these combined effects increase the reservoir pressure and therefore the volumes of gas able to be stored per assessed tract of land. Apart from this qualitative inference based on overburden pressures increasing with depth, quantitative models predicting regional shale reservoir pore pressure regimes in the basin are not yet able to be built in Yukon using the currently archived historical well or drilling data (*see* Green, 2016). In summary, resource distribution data suggest that the largest potential areal recoveries of marketable gas will be derived from wells spudded in the undeformed zone as close to the BC and NWT borders and the basin's core as possible.

Two further shale gas plays have been identified as secondary exploration targets in Yukon: the interbedded dark grey siliceous shales and black cherts of the middle member of the Fort Simpson Formation (Figs. 3 and 4); and the shale member of the Banff Formation. The middle member of the Fort Simpson exhibits very good TOC contents (averaging 2.59 wt%), and, in Kotaneelee YT B-38 at least, a thick and homogeneous net pay interval (Fig. 5). The Banff Formation's shale member ranges from 100.4 to 504.0 mTVD in thickness across the study area; however, the brown to grey, silty, calcareous lithology and relatively subdued TOC contents (1.39 wt%) initially suggest low reservoir quality. Despite this, significant gas shows were reported during drilling of the Kotaneelee YT L-38 well: gas readings of up to 8074 units over a sustained background of 175 units confirm the potential of this play (Wasylyk, 2005). In summary, these observations suggest that there is the ultimate potential for up to four stacked shale gas plays to be present in the southeast of Yukon's Liard basin.

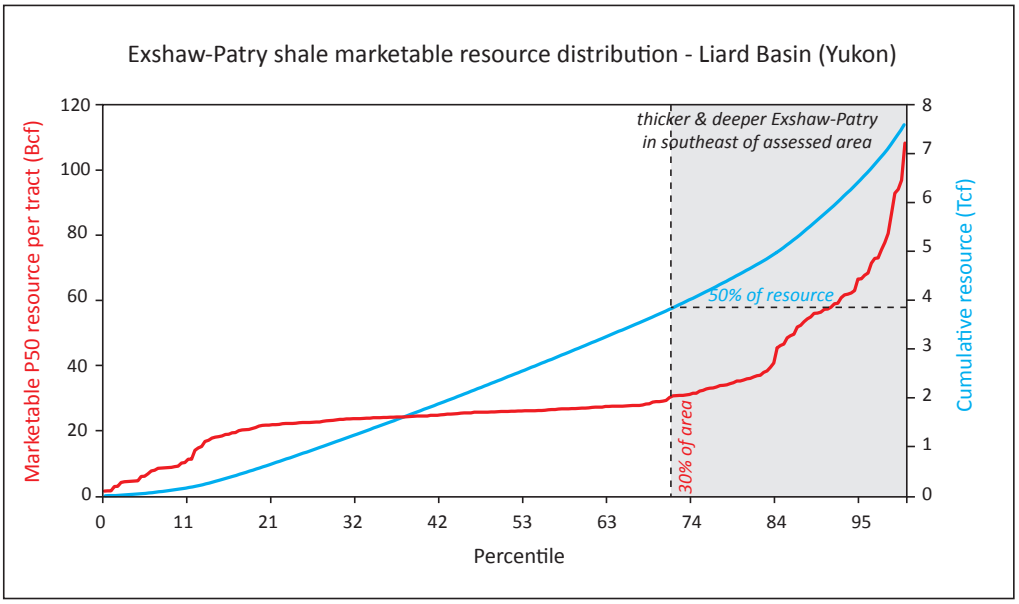

Figure 13. *Exshaw-Patry marketable P50 resource distribution in Yukon's Liard basin (data courtesy of the National Energy Board=M. Johnson, personal communication, 2016).*

CONCLUSION

Organic-rich Upper Devonian-Mississippian black shale formations are one of the most prospective unconventional exploration targets in the Western Canada Sedimentary basin. With an assessed GIP of 68 Tcf and 7.6 Tcf of marketable gas, this paper reports the first shale gas appraisal of these strata in Yukon's Liard basin (and the appraisal in the territory itself). Wireline log reinterpretation has resolved the previously undifferentiated Besa River Formation shales into four potentially stacked shale plays, with the best prospectivity in Yukon occurring in the Horn River shale play (Otter Park Formation) and upper Patry/lower Exshaw units of the Exshaw-Patry shale play. Resource distribution assessments estimate approximately 50% of Yukon's Exshaw-Patry cumulative marketable resource in 30% of its area, with the best potential for significant volumes located in the southeast of the territory's undeformed zone where play burial depths and thicknesses increase towards the basin's depocentre.

ACKNOWLEDGEMENTS

Yukon data presented here are derived, for the most part, from a collaborative, multi-jurisdictional study of shale reservoir potential in Liard basin initiated in 2012 and currently involving: Yukon Geological Survey; Northwest Territories Geological Survey; British Columbia Ministry of Natural Gas Development; British Columbia Oil & Gas Commission; National Energy Board; and Natural Resources Canada (Geological Survey of Canada). Those colleagues within the project and those who have contributed their time and provided technical input and advice through the years are numerous, and special mention must go to Tiffani Fraser, Fil Ferri, Mike Johnson, Kathryn Fiess, Jonathan Rocheleau, Mark Hayes, Jeff Johnson and Galina Doubrovina. Tiffani Fraser, Richard Fontaine, Bill Dwyer, Leyla Weston, Michele Campbell and Aleksandra Pertrusic assisted in subsurface sample preparation. Rock-Eval/TOC and vitrinite reflectance analyses were funded in part by Natural Resources Canada's Program of Energy Research & Development (PERD), coordinated by Margot McMechan and carried out by Rachel Robinson, Pat Webster and Julito Reyes at the Geological Survey of Canada's Organic Petrology Laboratory in Calgary. Gemma Hildred of Chemostrat Canada Ltd. provided assistance with calculating the log shifts in well I-48, and Liudmila LeBarge drafted the grid maps from NEB data. The author is indebted to Leanne Pyle, Fil Ferri, Maurice Colpron and Tiffani Fraser for their constructive reviews of earlier versions of this manuscript.

REFERENCES

Adams, C., Janicki, E. and Balogun, A., 2015. British Columbia Oil & Gas Industry Activity Report 2014. British Columbia Ministry of Natural Gas Development, Oil and Gas Geoscience Reports, 2015, p. 1-39.

Ayranci, K., Dong, T. and Harris, N., 2015. Paleo-environmental interpretations and sequence stratigraphy of the Horn River Group, British Columbia, Canada. Presented at the 2015 Gussow Conference, http://www.cspg.org/cspg/documents/Conference%20Website/Gussow/2015/Gussow2015_Abstract_Ayranci.pdf [accessed 26 April 2017].

Bohacs, K.M., Grabowski Jr., G.J., Carroll, A.R., Mankiewicz, P.J., Miskell-Gerhadt, K., Schwalbach, J.R., Wegner, M.B. and Simo, J.A., 2005. Production, destruction, and dilution – the many paths to source-rock development. *In:* Deposition of organic-carbon-rich sediments: models, N.B. Harris, (ed.), Society for Sedimentary Geology, Special Publication, vol. 82, 61-101.

Blood, R., Lash, G. and L. Bridges, 2013. Biogenic silica in the Devonian shale succession of the Appalachian basin, USA. American Association of Petroleum Geologists Search and Discovery Article #50864 (2013), http://www.searchanddiscovery.com/pdfz/documents/2013/50864blood/ndx_blood.pdf.html [accessed 26 April 2017].

Creaser, R.A., Sannigrahi, P., Chacko, T. and Selby, D., 2002. Further evaluation of the Re-Os geochronometer in organic-rich sedimentary rocks: a test of hydrocarbon maturation effects in the Exshaw Formation, Western Canada Sedimentary basin. Geochimica et Cosmochimica, vol. 66, p. 3441-3452.

Dow, W.G. 1977. Kerogen studies and geological interpretations. Journal of Geochemical Exploration, vol. **7**, p. 79-99.

Fallas, K.M., Lane, L.S. and Pigage, L.C., 2014. Geology La Biche River Yukon-Northwest Territories. Natural Resources Canada, Canadian Geoscience Map 144, 1 sheet, doi: 10.4095/294606.

Ferri, F., Hickin, A.S and Huntley, D.H., 2011. Besa River Formation, western Liard basin, British Columbia (NTS 094N): geochemistry and regional correlations. British Columbia Ministry of Energy and Mines, Geoscience Reports 2011, p. 1-18.

Ferri, F., Hickin, A.S and Reyes, J., 2012, Horn River basin – equivalent strata in Besa River Formation shale, northeastern British Columbia (NTS 094K/15). British Columbia Ministry of Energy and Mines, Geoscience Reports 2012, p. 1-15.

Ferri, F., McMechan, M., Fraser, T., Fiess, K., Pyle, L. and Cordey, F., 2013. Summary of field activities in the western Liard basin, British Columbia. British Columbia Ministry of Natural Gas Development, Oil and Gas Geoscience Reports 2013, p. 13-31.

Ferri, F., McMechan, M. and Creaser, R., 2015. The Besa River Formation in Liard basin, British Columbia. British Columbia Ministry of Natural Gas Development, Oil and Gas Geoscience Reports 2015, p. 1-27.

Fraser, T.A. and Hogue, B.C., 2007. List of wells and formation tops, Yukon Territory, version 1.0. Yukon Geological Survey, Open File 2007-05.

Fraser, T.A. and Hutchison, M.P., 2017. Lithogeochemical characterization of the Middle-Upper Devonian Road River Group, Canol and Imperial formations on Trail River, east Richardson Mountains, Yukon: age constraints and a depositional model for fine-grained strata in the Lower Paleozoic Richardson Trough. Canadian Journal of Earth Sciences, vol. 54, p. 731-765.

Fraser, T.F., Ferri, F., Fiess, K. and Pyle, L., 2012. Besa River Formation in Liard basin, southeast Yukon: Report on 2012 reconnaissance fieldwork. *In:* Yukon Exploration and Geology 2012, K.E. MacFarlane, M.G. Nordling and P.J. Sack, (eds.), Yukon Geological Survey, p. 37-46.

Green, S., 2016. Pressure data assessment, Liard basin, Yukon. Yukon Geological Survey, Miscellaneous Report 16.

Harris, N.B., Dong, T. and Ayranci, K., 2017. High resolution stratigraphic variability in black shale geochemistry: Horn River Group, British Columbia. American Association of Petroleum Geologists Search and Discovery Article #90291 (2017), http://www.searchanddiscovery.com/abstracts/html/2017/90291ace/abstracts/2611981.html [accessed 26 April 2017].

Hutchison, M.P., 2016. Analytical methods and non-interpretative data compilation for unconventional shale plays of Yukon's Liard basin. Yukon Geological Survey, Open File 2016-33.

Hutchison, M.P. and Fraser, T.A., 2016. Frontier shale gas plays of Yukon's Liard basin, Canada. Presented at the Canadian Society of Petroleum Geologists GeoConvention 2016 (abstract missing from online archive).

Johnson, E.G. and Johnson, L.A., 2012. Hydraulic fracture water usage in northeast British Columbia: locations, volumes and trends. British Columbia Ministry of Energy and Mines, Geoscience Reports 2012, p. 41-64.

Johnson, M., Doubrovina, G., Ferri, F., Hayes, M., Johnson, J., Fiess, K., Rocheleau, J. and Hutchison, M., 2016. The unconventional gas resources of Devonian-Mississippian shales in the Liard basin of British Columbia, Yukon Territory, and the Northwest Territories. Presented at the 10th British Columbia Unconventional Gas Technical Forum.

Mossop, G.D., Wallace-Dudley, K.E., Smith, G.G. and Harrison, J.C., 2004. Sedimentary basins of Canada. Geological Survey of Canada, Open File 4673, 1 sheet, doi 10.4095/215559.

Nadjiwon, L.M., 2001. Facies analysis, diagenesis and correlation of the Middle Devonian Dunedin and Keg River formations, northeastern BC. MSc thesis, University of Waterloo.

NEB, 2001. Petroleum resource assessment of the Liard Plateau, Yukon Territory, Canada: Oil & Gas Resources Branch, Department of Economic Development, Government of the Yukon.

NEB, 2016. The unconventional gas resources of Mississippian-Devonian shales in the Liard basin of British Columbia, the Northwest Territories, and Yukon. National Energy Board Energy Briefing Note.

Noble, J.P.A. and Ferguson, R.D., 1971. Facies and faunal relations at edge of Early-Mid Devonian carbonate shelf South Nahanni River area, N.W.T. Bulletin of Canadian Petroleum Geology, vol. 19, p. 570-588.

Peters, K.E. and Cassa, M.R., 1994., Applied source-rock geochemistry. *In:* The petroleum system. From source to trap, L.B. Magoon and W.G. Dow (eds.), American Association of Petroleum Geologists, p. 93-120.

Pyle, L.J., Rocheleau, J., Fiess, K.M., Fraser, T.A. and Ferri, F., 2016. Petroleum potential, lithogeochemical, and mineralogical data from Devonian and Carboniferous sections in Liard basin, Northwest Territories. Northwest Territories Geological Survey, Open Report 2016-007.

Richards, B.C., Barclay, J.E., Bryan, D., Hartling, A., Henderson, C.M. and Hinds, R.C., 1994. Carboniferous strata of the Western Canada Sedimentary basin. *In:* Geological Atlas of the Western Canada Sedimentary basin, G.D. Mossop and I. Shetsen (eds.), Canadian Society of Petroleum Geologists and Alberta Research Council, http://www.ags.aer.ca/publications/atlas-of-the-western-canada-sedimentary-basin [accessed 28 March 2016].

Richards, B.C., Ross, G.M. and Utting, J., 2002. U Pb geochronology, lithostratigraphy and biostratigraphy of tuff in the upper Famennian to Tournaisian Exshaw Formation: evidence for a mid-Paleozoic magmatic arc on the northwestern margin of North America. *In:* Carboniferous and Permian of the World, L.V. Hills, C.M. Henderson and E.W. Bamber (eds.), Canadian Society of Petroleum Geologists Memoir, vol. 19, p. 158-207.

Rocheleau, J., Fiess, K.M., Pyle, L.J., Ferri, F. and Fraser, T.A., 2014. Source rock characterization of the Carboniferous Golata Formation and Devonian Besa River Formation outcrops, Liard basin, Northwest Territories. Canadian Society of Petroleum Geologists GeoConvention 2014, http://www.geoconvention.com/archives/2014/301_GC2014_Source_Rock_Characterization_of_Carboniferous_Golata_Fm.pdf [accessed 26 April 2017].

Selby, D. and Creaser, R.A., 2005. Direct radiometric dating of the Devonian-Carboniferous timescale boundary using the Re-Os black shale geochronometer. Geology, vol. 33, p. 545-548.

Statistics Canada, 2014. Report on Energy Supply and Demand in Canada (CANSIM table 57-003-X). Statistics Canada, http://www5.statcan.gc.ca/-pub/57-003-x/57-003-x2016002-eng.htm [accessed 14 November 2016].

Wasylyk, P., 2005. Geological wellsite report – Devon et al Kotaneelee L-38, L-38/ST1, L-38A, L-38A/ST3. Devon Canada Corporation. Available from Oil & Gas Resources Branch, Government of Yukon.

Wright, A.M., Ratcliffe, K.T., Zaitlin, B.A. and Wray, D.S., 2010. The application of chemostratigraphic techniques to distinguish compound incised valleys in low-accommodation incised-valley systems in a foreland-basin setting: an example from the Lower Cretaceous Mannville Group and Basal Colorado Sandstone (Colorado Group), Western Canadian Sedimentary basin. SEPM Special Publication, vol. 94, p. 93-107.

Zou, C., 2013. Unconventional petroleum geology. Elsevier, 384 p.

Evidence for limited glaciation in northern Kluane Range, southwestern Yukon, with implications for surficial geochemical exploration

K.E. Kennedy
Yukon Geological Survey

Kennedy, K.E., 2018. Evidence for limited glaciation in northern Kluane Range, southwestern Yukon, with implications for surficial geochemical exploration. *In:* Yukon Exploration and Geology 2017, K.E. MacFarlane (ed.), Yukon Geological Survey, p. 89-102.

ABSTRACT

Preliminary investigation of surficial geology in northern Kluane Range has resulted in new interpretations of Pleistocene ice cover including extensive unglaciated terrain and restricted glaciation during the Last Glacial Maximum. Two glacial limits are identified: a higher limit recording the most extensive glaciation of the area; and a lower limit that records younger, less extensive glaciation. This paper describes Pleistocene limits of the Donjek Glacier and the distribution of surficial materials in the upper Quill, Maple, and Wade creek drainages. The source and transport mechanism of surface materials has particular significance for surficial geochemistry sampling programs and implications for mineral exploration are addressed.

* *kristen.kennedy@gov.yk.ca*

INTRODUCTION

Preliminary results from 1:50 000-scale surficial geologic mapping in northern Kluane Range include new interpretations of glacial limits and descriptions of surficial material textures and distributions. The study area (Fig. 1) is characterized by steep, mountainous terrain and bedrock is commonly well exposed along canyons, ridges and high elevation summits. However, mid to low-elevation slopes of moderate steepness are largely covered with deposits of weathered bedrock, till, glaciofluvial and glaciolacustrine materials. Determining the provenance and composition of these materials can inform new surficial geochemical (*e.g.*, soil, stream sediment, till) exploration programs and help interpret results from earlier programs.

GEOLOGY AND MINERAL DEPOSITS

Northern Kluane Range is a high-relief landscape surrounded by relatively subdued topography in Shakwak Trench to the east and the Duke Depression to the south and west. The range is bound by the Denali fault to the northeast and the Duke River fault to the southwest, forming a wedge of Late Paleozoic to Middle Mesozoic rocks that widens to the northwest (Israel and van Zeyl, 2005). A variety of mineral deposit types likely exist in the study area (Yukon MINFILE, 2017; Fig. 2), with regional occurrences including porphyry Cu-Mo-Au (Amp and Cork), possible Besshi-type massive sulphide (Musketeer and Burwash), and the well-known Ni-Cu-PGE ultramafic complexes (Wellgreen, Linda, Jaquot, Quill). Additionally, placer gold (and minor platinum) deposits are found

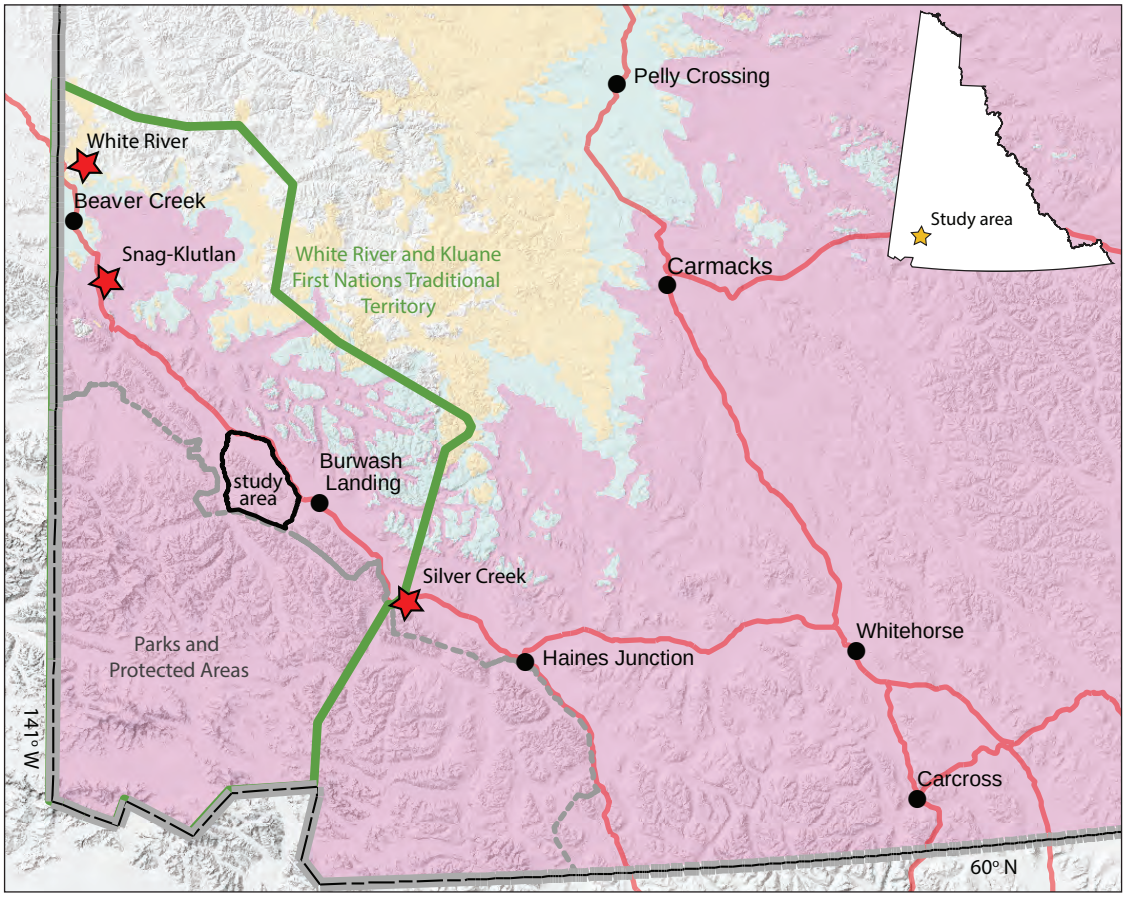

Figure 1. *Location of the study area (outlined in black) in SW Yukon. The study area is in the Traditional Territory of the White River and Kluane First Nations (outlined in green), adjacent to Kluane National Park and Asi Keyi Territorial Park (outlined in grey). Locations of glacial history studies mentioned in text are marked with red stars. Regional glacial limits by Duk-Rodkin (1999) are shown in pink (least extensive), blue (intermediate extent), and yellow (most extensive). Yellow (most extensive) limits of the St. Elias Lobe mapped by Duk-Rodkin (1999) have not been confirmed by subsequent authors (i.e., Turner et al., 2013) working in southwestern Yukon.*

in most streams draining the study area and may be associated with native gold in bedrock, paleo-placer gold in Cenozoic conglomerate units, and/or gold transported by glacial processes (YGS, 2010; van Loon and Bond, 2014; Kennedy and van Loon, 2017).

GLACIAL HISTORY

The Quaternary in southwestern Yukon has been marked by cyclical advance and retreat of valley glaciers originating in the St. Elias Mountains, which have, during extended cold periods, coalesced and filled the broad Shakwak Trench, advancing up to 125 km to the north and northeast (Fig. 1; Duk-Rodkin, 1999). The coalescing glaciers formed the St. Elias lobe within the northern sector of the Cordilleran Ice Sheet (CIS). At Silver Creek, a tributary to the south end of Kluane Lake, Turner *et al.* (2016) identified at least five Middle to Late Pleistocene advances of the northern Cordilleran Ice Sheet. The three most recent advances identified at Silver Creek correlate well with glacial deposits in the Snag-Klutlan and White River areas north of the study area (Fig. 1; Rampton, 1971; Turner *et al.*, 2013).

The build up of the St. Elias lobe appears to have been out of phase with overall global ice volumes and advances of the CIS in central Yukon (Turner *et al.*, 2013). Central Yukon saw maximum advances of ice prior to marine isotope stage (MIS) 6 (Pre-Reid glaciations; Ward *et al.*, 2008; Westgate *et al.*, 2008), and limited advances in MIS 4 (Gladstone Glaciation; Ward *et al.*, 2007). The most

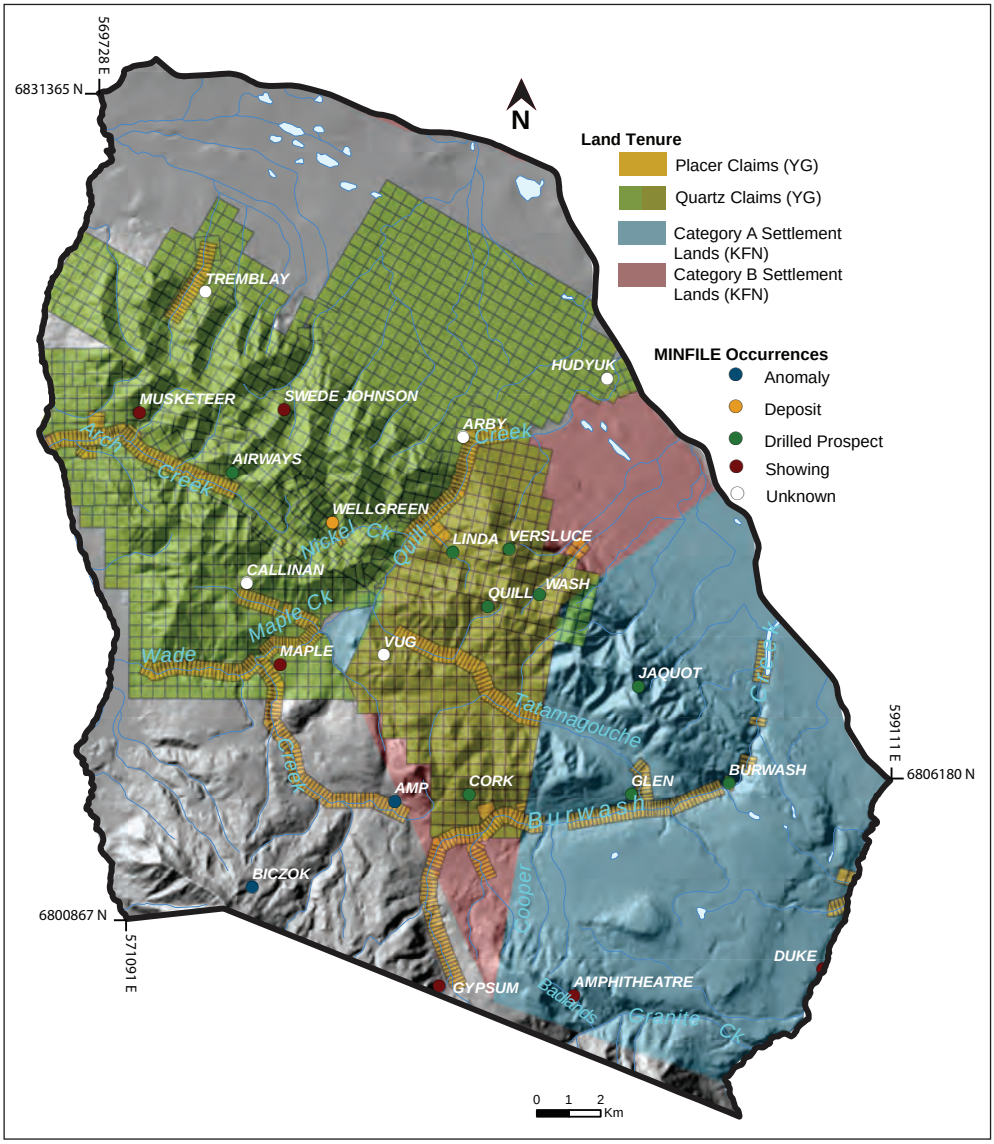

Figure 2. *Land tenure and locations of MINFILE occurrences in the study area.*

extensive advance of the St. Elias lobe occurred in MIS 6 (Reid Glaciation), with a very similar extent achieved in MIS 4 (Gladstone Glaciation), suggesting constraints on precipitation in the St. Elias Mountains remained similar through the Pleistocene (Turner *et al.*, 2013). The pre-Reid (prior to MIS 6) extent of the St. Elias lobe suggested by Duk-Rodkin (1999; yellow limit in Fig. 1) has not been confirmed by subsequent mapping (Bond *et al.*, 2008; Lipovsky and Bond, 2013) and paleoenvironmental studies (Turner *et al.*, 2013) which found the most extensive limit to correlate with mapped MIS 6 (Reid Glaciation) limits.

PREVIOUS WORK

Regional-scale (1:250 000) glacial limit mapping and compilation work by Duk-Rodkin (1999) used glacial landforms to reconstruct paleo ice-flow directions and suggested three sources of ice during regional glaciations in the study area: (1) locally-sourced alpine glaciers; (2) advances of the Donjek Glacier and its tributaries along the western edge; and (3) advances of glaciers occupying the Shakwak Trench, including a glacier in the Duke River valley which may have advanced over the Burwash Upland (Fig. 3). This mapping suggests high elevation peaks in the study area may have been unglaciated during the most recent advance, but were completely inundated by ice in earlier advances (Duk-Rodkin, 1999). Glacial limits of ~1200-1400 m above sea level (a.s.l.) were suggested in earlier work related to 1:100 000-scale surficial geological mapping of a large part of the study area (Rampton, 1980; 1981), however, no surficial mapping was completed for Arch, Wade, or Maple creeks.

GLACIAL LIMIT MAPPING

Glacial limit mapping in 2017 focused on limits associated with advance of the Donjek Glacier along the northwestern margin of the study area. Glacial limits associated with Duke and Shakwak glaciers will be investigated in 2018. During periods of advance of the St. Elias lobe, the Donjek Glacier thickened considerably, inundating and flowing up valleys draining the northern Kluane Range. Two distinct ice limits are mapped along the eastern margin of the Donjek valley and extend into the drainages of Arch, Wade, Maple and Quill creeks (Fig. 4). The limits are highest in the western part of the map area, where

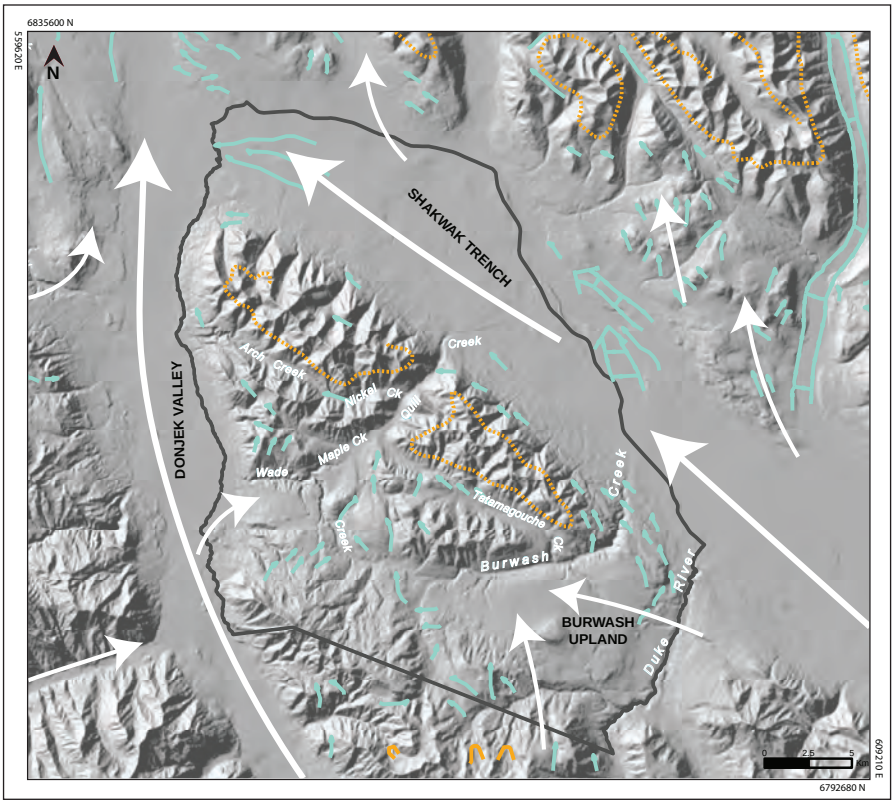

Figure 3. *Regional glacial limits (yellow lines) and meltwater channels (blue arrows) from existing glacial limits mapping (Duk-Rodkin, 1999). Generalized flow directions are represented by white arrows and suggest Donjek Valley and Shakwak Trench glaciers flowed up tributary valleys in the study area.*

the Donjek Glacier flowed along the mountain front, and descend in elevation eastward toward terminus positions in the valley bottoms of the Kluane Range.

Both higher all-time limits and younger lower elevation limits may be composite features consisting of multiple ice advances that reached similar extents, and/or recessional limits. All-time limits in the study area are identified through a combination of erratic and landform mapping. Extra-basinal pebbles and cobbles are identified along ridges and spurs in the study area (Fig. 5), and their elevations are used to correlate discontinuous and subdued landforms. Landforms preserved at the all-time limit are typically rounded in appearance, and have been eroded by subsequent colluvial and/or glaciofluvial processes. The limit is best marked by meltwater channels along spurs (Fig. 6) and rare ice marginal features preserved on high elevation valley floors. There is no age associated with the all-time limit in the study area but it may correlate with one or both of the MIS 6 all-time limit or the similarly extensive MIS 4 limit documented by Turner *et al.* (2013) on the White River and mapped to the north by Lipovsky and Bond (2013).

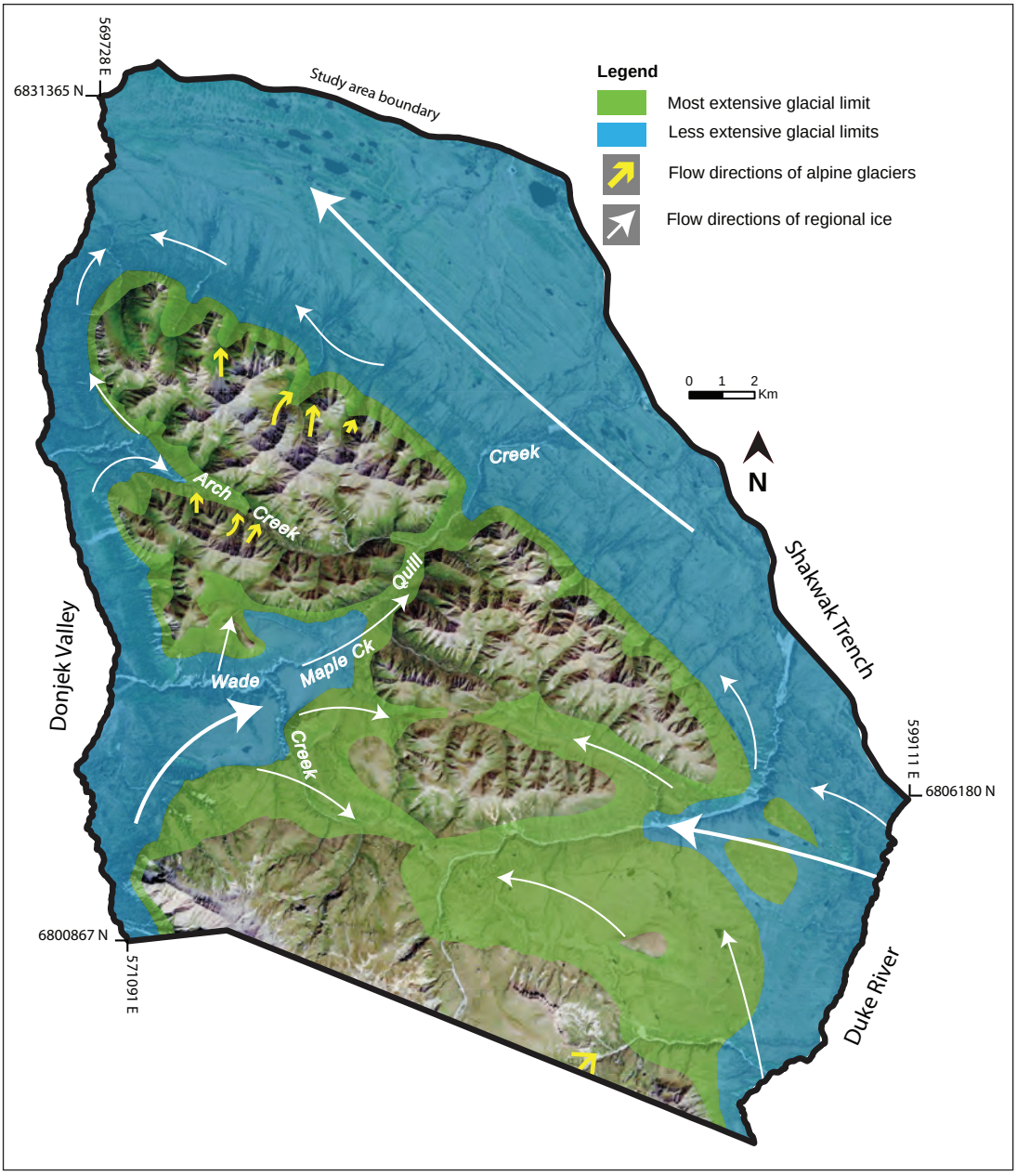

Figure 4. *Preliminary glacial limits for the study area, including draft limits for the Donjek Glacier, and tentative limits for glaciers occupying Shakwak Trench.*

Landforms associated with the lower limit are typically well preserved, and are best marked by glaciofluvial features including kame terraces and meltwater channels (Fig. 6). Up-valley flowing ice from the Donjek Glacier would have impounded the drainages of Wade, Maple and Arch creeks (*see* Fig. 4), creating glacial lakes and redirecting meltwater and stream flow over former drainage divides. Landforms characteristic of glacial lakes and streams include broad glaciofluvial deltas and terraces (Fig. 7), often overlying glaciolacustrine silt and sand. There are no ages associated with low elevation limits in the study area, but they may correlate with one or both of the most recent regional glaciations (MIS 4 or MIS 2).

WADE CREEK GLACIAL LIMITS

In the Wade Creek valley, glacial limits suggest ice during the most extensive glaciation entered the valley as a broad off-shoot of the Donjek Glacier. It would have measured ~8 km across at the mountain front where it entered the Wade Creek valley and narrowed rapidly as it flowed up the valley and across the narrow drainage divide (Fig. 4).

Northward flow of the trunk glacier in the Donjek valley resulted in a higher northern limit (~1550 m a.s.l.) and lower southern limit (~1450 m a.s.l.) at the mouth of the Wade Creek valley, with the ice surface achieving a level cross-valley profile ~5 km up valley at an elevation of ~1400 m a.s.l. The main body of ice flowed up the Maple Creek valley, crossing the divide at 1150 m a.s.l., and flowing down Quill Creek valley to its terminus position at the confluence of Nickel and Quill creeks, where it measured ~500 to 700 m wide at an elevation of ~1100 m a.s.l. (Fig. 8). Moraines associated with glaciation in the Shakwak Trench are preserved at the terminus position, and it is possible Donjek ice coalesced with Shakwak ice in this location.

All-time ice also advanced eastward into upper Wade Creek and a NE-flowing unnamed tributary to Maple Creek (Fig. 8). Ice entered these valleys at elevations of ~1450-1500 m a.s.l., and flowed ~3 to 5 km upstream before terminating at ~1350 m a.s.l. It is possible that Donjek ice in these tributaries coalesced with Shakwak ice flowing up Burwash and Tatamagouche valleys during this most extensive glaciation.

Figure 5. *Example of an erratic cobble (circled) marking the all-time glacial limit in the study area.*

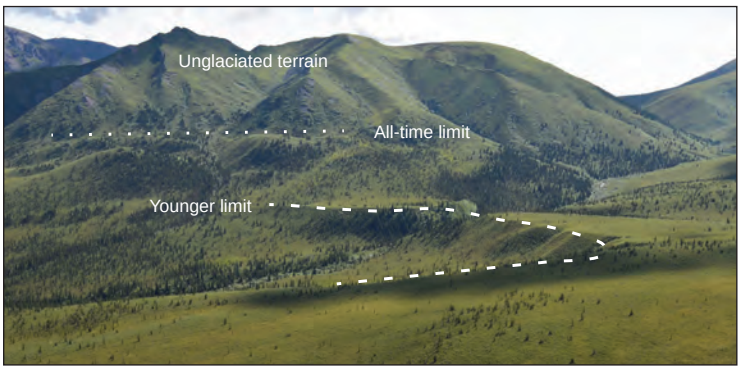

Figure 6. *Both the all-time limit and a more recent glacial limit are visible in this tributary to Maple Creek. The older, higher elevation, limit is marked by a meltwater channel with subdued morphology. The younger limit is marked by an ice-contact, or possibly glaciolacustrine, delta with well-defined morphology.*

Figure 7. *Maple Creek is characterized by a broad flat valley bottom filled with glacial materials (view west toward the Donjek River). The modern stream is cutting through thick surficial sediments (see Fig. 14) before becoming entrenched in a bedrock canyon just above its confluence with Wade Creek.*

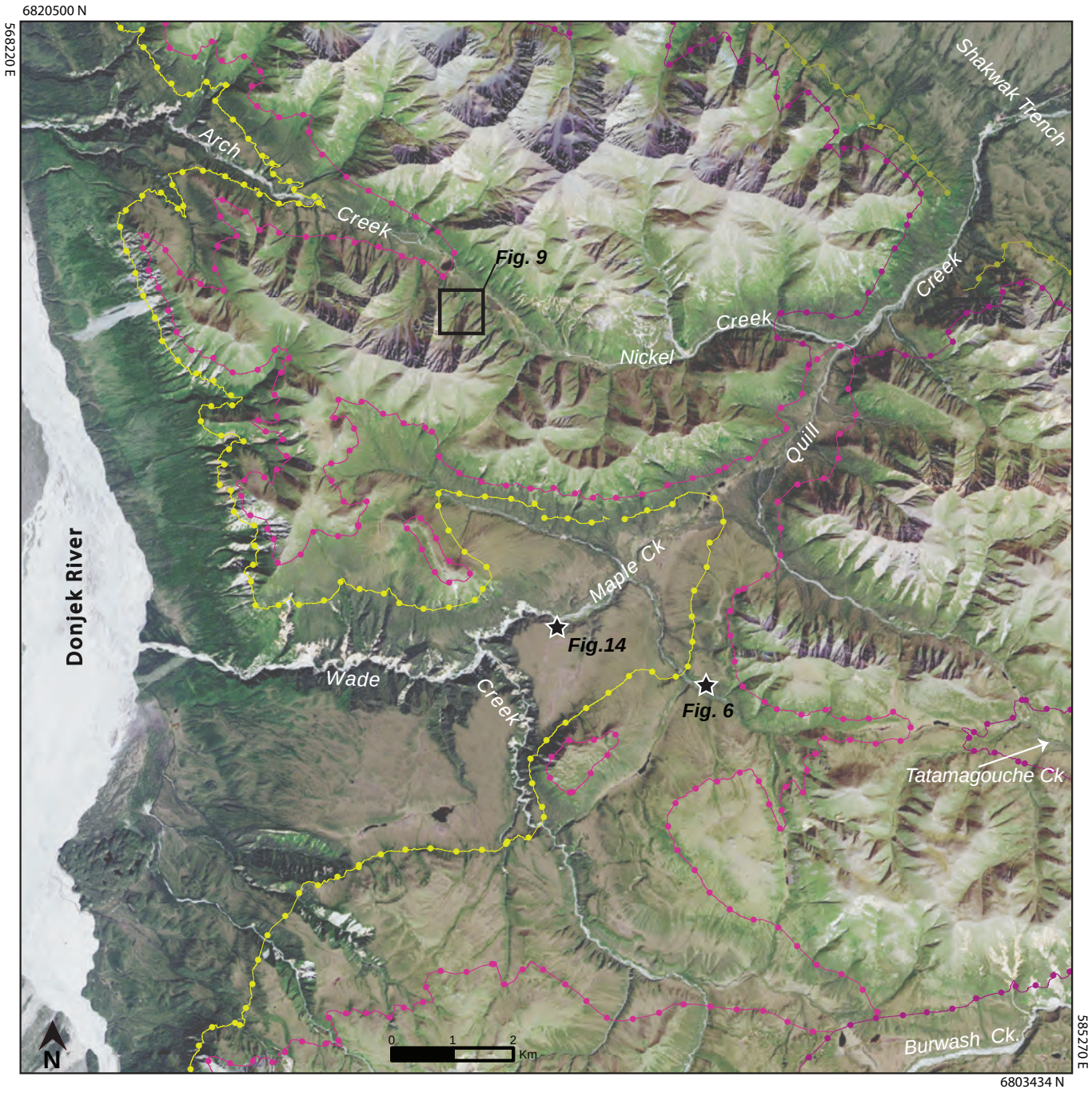

Figure 8. *Glacial limits in the western part of the study area. Pink lines indicate higher, all-time limits, and yellow lines indicate lower, more recent limits. Darker shades of pink and yellow are limits associated with glaciers in the Shakwak Trench.*

Younger, lower elevation limits in Wade Creek valley are considerably less extensive than all-time limits, terminating ~3 km SW of the all-time limit (Fig. 8). The lower limit also has an asymmetrical profile at the mountain front, entering the Wade Creek valley at ~1300-1250 m a.s.l., and descending to its terminus position at 1150 m a.s.l. near the modern divide of the Maple and Quill creek drainages. The lower limit did not advance into tributary valleys, and these limits are marked with large, well-preserved ice-contact glaciofluvial terraces and kames (*i.e.*, Fig. 6).

ARCH CREEK GLACIAL LIMITS

Donjek Glacier ice entering Arch Creek valley during the most extensive glaciation was more constrained than in Wade Creek valley. Only ~3.5 km wide at the mountain front, ice was unable to advance as far into the narrower Arch Creek valley. Surface elevations of ~1400 m a.s.l. at the mouth of Arch Creek descend over ~5 km to a terminus elevation of ~1300 m a.s.l. during the most extensive glaciation (Fig. 8). This left much of the Nickel Creek valley unglaciated, and it likely served as a conduit for glacial meltwater flowing toward Shakwak Trench.

Younger, low elevation limits in the Arch Creek valley are even more restricted compared to earlier glaciations (Fig. 8). Limits are largely found at ~1200-1250 m a.s.l., however stacked moraines from ~1100 to 1200 m a.s.l. may record recessional features, and/or separate advances that achieved very similar limits. Ice thicknesses during the most recent glaciation were likely insufficient to redirect meltwater through Nickel valley, and ice contact features along the limit record ice marginal damming and redirection of flow northward along the margin of the Donjek Glacier.

Alpine glaciers occupied some north and northeast-facing cirques in the Arch Creek valley during the Quaternary (Fig. 4). Moraines are poorly preserved and glaciers appear to have been limited to high alpine valleys. Alpine moraines are preserved in an unglaciated reach of the Arch/Nickel valley where cirque glaciers extended onto the valley floor (Fig. 9).

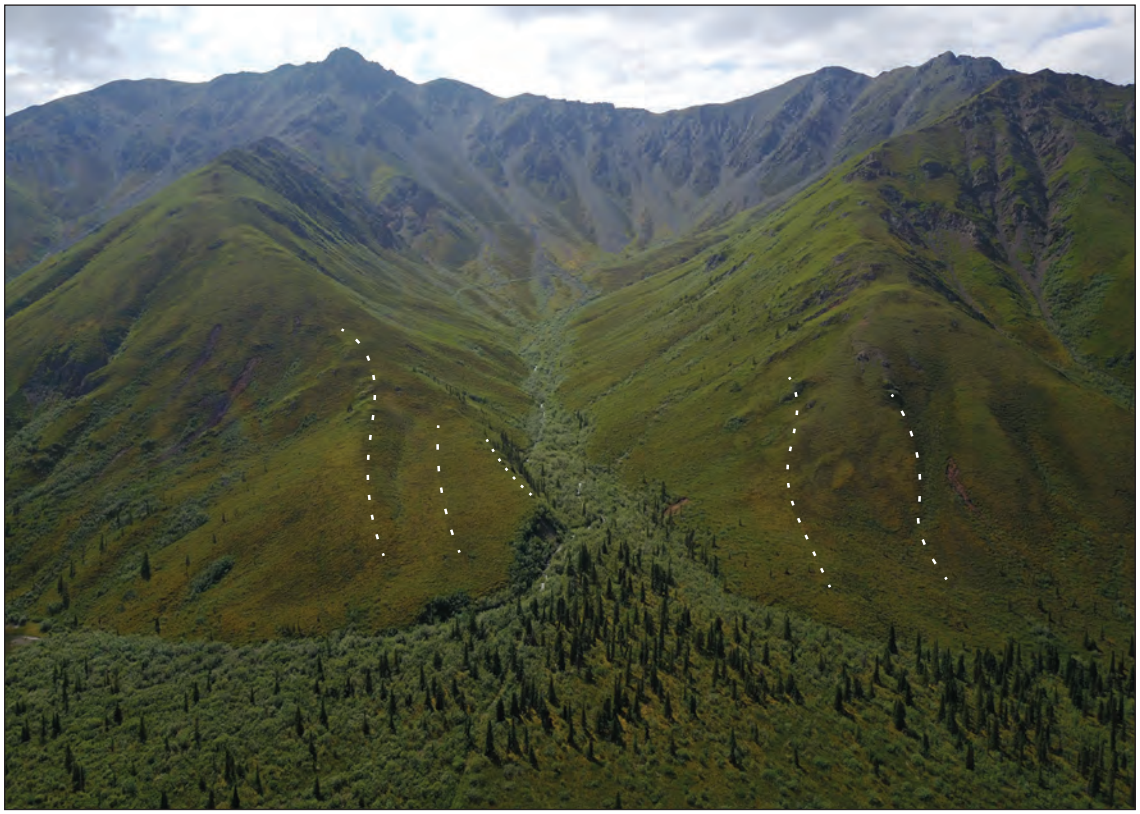

Figure 9. *Alpine moraines (dashed lines) preserved in a small north-facing cirque in the divide between Arch and Nickel creeks, beyond the all-time limits of the Donjek Glacier in Arch Creek (location shown on Fig. 8).*

SURFICIAL MATERIALS

The distribution of surficial materials is controlled by the limits of glaciation and the relative steepness of slopes in any particular setting in the study area. Colluviation (the movement of materials through the action of gravity) is, by far, the most active surficial process on-going today. Together with steep, high-energy streams in the study area, the landscape in the Kluane Ranges is capable of moving unconsolidated surficial materials quickly off slopes and out of the study area.

While many streams currently occupy channels incised into bedrock, thick surficial cover is preserved in the broad, relatively flat-bottomed upper reaches of Arch, Wade, Maple, and Quill creeks (Fig. 7). A typical valley profile, from unglaciated uplands to bedrock entrenched stream, is presented in Figure 10 and described below.

UNGLACIATED TERRAIN

Much of the high elevation terrain in the study area remained unglaciated throughout the Quaternary (*see* Fig. 4). On the steepest slopes, freshly weathered bedrock surfaces may be covered with thin to moderate thicknesses (0-1 m) of weathered bedrock and weathered bedrock colluvium as a veneer or mantle of variable thickness (*see* Fig. 10).

Moderate slope angles typically have distinctive cryoplanation or pediment surfaces that are unique to unglaciated terrain (Fig. 11). These surfaces often have thin veneers or blankets of weathered bedrock colluvium overlying bedrock. In the study area, where rates of erosion and uplift are high, some raised surfaces retain fluvial and colluvial sediments deposited at the time they were formed (Fig. 12).

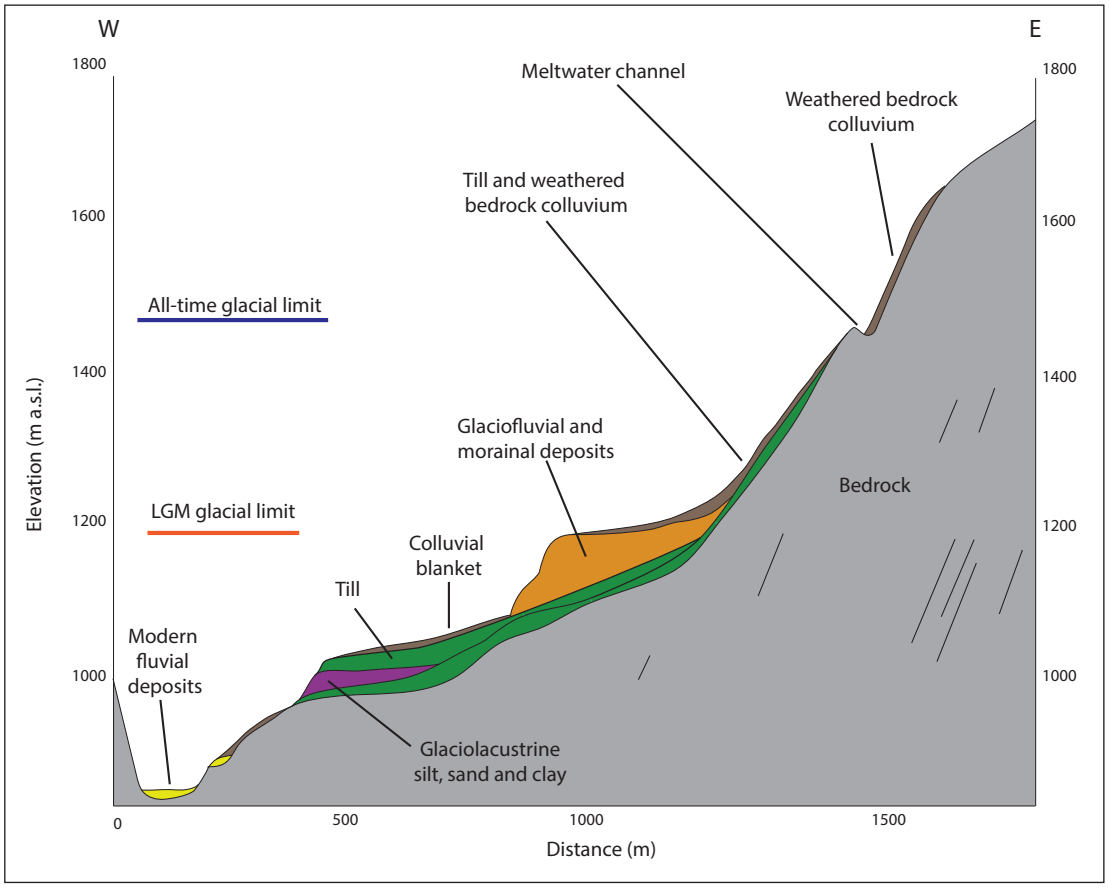

Figure 10. *Idealized valley profile illustrating the distribution of sediments in Maple and Wade creeks.*

Figure 11. *Typical subdued morphology of unglaciated terrain with flat cryoplanation terraces (black arrows) and pediments (white arrows) marking erosional surfaces that likely pre-date the Quaternary period.*

Figure 12. *Paired terraces (arrows) across upper Quill Creek record former base level and retain gravel deposited above the modern valley floor.*

Glaciers and glacial meltwater affected all of the trunk streams in the study area, and glacial meltwater would have flowed through some unglaciated valley bottoms that were outside the limit of glaciation. Modern stream sediments in all these valleys likely contain extra-basinal sediments. In contrast, where fluvial terraces are found along these unglaciated valley bottoms, the sediments are likely representative of the upslope basin and contain no foreign materials.

UPPER GLACIATED SLOPES

Upper glaciated slopes in the study area are defined as being between the all-time glacial limit and the lower glacial limit (*see* Figs. 4 and 10). While glaciogenic materials are present on these slopes, they are typically thin and incorporated into more abundant deposits of locally-derived weathered bedrock colluvium. On moderate to gentle slopes (SE side of the Wade Creek valley, much of Maple and upper Quill creeks) mixed morainal and colluvial materials thicken downslope from thin veneers to blankets (>1 m) of sediment (Fig. 13). On steeper slopes, or where there has been significant base level change (much of Arch Creek valley, NW side of Wade Creek valley) only thin remnants of glaciogenic sediments are preserved.

Materials related to alpine glaciation are limited to high and mid-elevation landscape positions near their source areas. Deposits from alpine glaciers are derived entirely of local bedrock material with little or no input of extra-basinal material. A dissected alpine moraine in the Arch Creek valley (Fig. 9) comprises ~3.5 m of interbedded diamict and fluvial sediments over bedrock in the creek bottom.

LOWER GLACIATED SLOPES AND VALLEY BOTTOMS

Low-elevation slopes and valley bottoms in the study area are defined as being at, or below, the lower glacial limit (*see* Figs. 4 and 10). These landscape positions are likely to have very thick (>40 m) deposits of glaciogenic materials including blankets and ridges of moraine, glaciofluvial terraces and glaciolacustrine blankets, all of which can be covered by,

Figure 13. *Uniform angular clasts visible in a colluvial apron on an upper glaciated slope. These slopes are within the all-time glacial limit, but very little morainal material is preserved, particularly on north-facing slopes where mass wasting is active.*

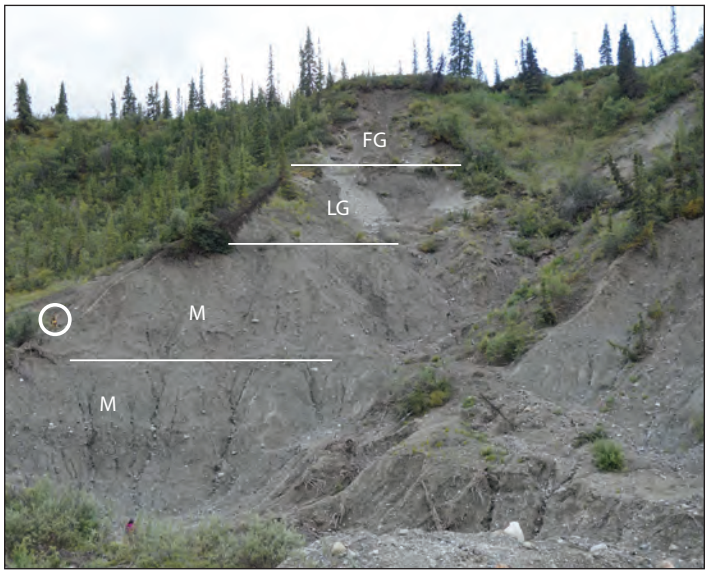

Figure 14. *Thick deposits of glacial materials recording at least two phases of advance and retreat of the Donjek Glacier into lower Maple Creek (FG – glaciofluvial; LG – glaciolacustrine; M – morainal). Exposed sediments are 60 m thick (person circled for scale) and the location of the exposure is shown in Fig. 8.*

and/or incorporated with locally-derived colluvial and fluvial materials. Permafrost and peat blankets are common in low elevation landscape positions, particularly on north-facing slopes where the permafrost table can be immediately below surface vegetation.

Valleys draining toward the Donjek Glacier were affected by impoundments and diversions of regional streams and meltwater during glaciations. In particular, upper Maple Creek valley is characterized by a wide, flat, valley bottom that likely represents one or more phases of glaciolacustrine deposition (Fig. 7). Valley-fill may record many glacial episodes (Fig. 14), and surface materials are unlikely to be representative of underlying, up-slope, or up-valley bedrock.

While the Donjek Glacier advanced in similar configurations throughout the Quaternary, interglacial streams draining toward the Donjek River likely formed entirely or partially new channels after each glaciation. This migration of paleo-valleys has created significant buried topography in valley bottoms that is largely masked by deposits of the last glaciation (Fig. 15). The lower reaches of Arch, Maple and Wade creeks have bedrock entrenched reaches as well as reaches of thick glaciogenic sediments, resulting in highly mixed stream sediments that aren't representative of bedrock in upstream drainages. Modern stream sediments on the lower, bedrock entrenched, reaches of Arch and Wade creeks comprise extremely coarse-grained (boulders >2 m diametre are common) gravel deposits that overlie bedrock. Gravel deposits are relatively thin (a few metres), but represent significant reworking and concentration of both local bedrock and transported glaciogenic materials.

Figure 15. *Paleo-topography on lower Wade Creek is masked by thick glacial fill that forms a flat surface above the creek. Dashed line follows the approximate bedrock surface.*

MASS WASTING

Mass wasting of surface materials through detachment slides is prevalent on mid-elevation slopes (Fig. 16). Mass wasting is more active on north-facing slopes where permafrost is common at depths of 0.5 to 1 m below the surface. North-facing slopes typically have a thin cover of colluvium on steep slopes and thicker blankets of well-mixed colluvium and morainal material at breaks in slope where materials accumulate. Bedded colluvial deposits are shown in Figure 17, where thin bands of resedimented

tephra mark individual events. Detachments typically occur in the upper ~1 m of seasonally thawed materials (active layer), and underlying perennially frozen (permafrost) sediments comprise local weathered bedrock and minor morainal materials in a silty matrix.

IMPLICATIONS FOR MINERAL EXPLORATION

Weathered bedrock and colluvium in unglaciated terrain are ideal materials for soil geochemical sampling programs (e.g., Fig. 11). The new glacial limits for the study area highlight significant regions of unglaciated terrain marginal to the valleys of Wade, Maple and Arch creeks (Figs. 4 and 8). Some of these unglaciated areas include lower slopes and valley bottoms. On steeper slopes, soil geochemical anomalies may be displaced from their source due to colluvial processes. These same processes can be used advantageously in high-elevation basins when soil sampling. For example, talus aprons can be a used to target upslope mineralization on otherwise difficult to access alpine environments.

Stream sediment geochemistry should work well in high-elevation basins above the glacial limits. When collecting stream sediment samples in the unglaciated region, care should be taken to stay upstream of glacial deposits related to up-valley advancing ice. In addition, glacial meltwater may have emptied into an unglaciated valley resulting in the deposition of foreign sediments. Raised fluvial terraces in the unglaciated area are rare, but could be interesting targets for stream sediment sampling.

Upper glaciated slopes are generally good targets for soil geochemistry sampling. Where slope angles are steep, moraine deposition would have been limited and is likely partially eroded. In regions of mixed moraine and colluvium, slope material thickness and composition should be assessed to determine the degree to which local materials are present. Soil sampling should avoid thicker deposits of moraine where valley slopes become gentler and are susceptible to accumulation of glacial sediment. Stream sediment geochemistry in this environment can be effective depending on the concentration of foreign sediment in a stream bed.

Figure 16. *Surface detachments on a north-facing slope at the divide between Arch and Nickel creeks. Detachments are commonly 0.5-1.5 m thick, 10-30 m wide, and ~200 m long. Detached materials are comprised of weathered bedrock and colluvium that slides on permafrost or bedrock detachment surfaces.*

Figure 17. *Thin white bands of tephra mark individual mass wasting events on this mid-elevation slope. The entire active layer (above the dashed line) comprises bedded colluvial deposits. Below the permafrost table, sediments are comprised of local weathered bedrock and minor morainal materials.*

Lower glaciated slopes and valley bottoms are the most complicated landscape type for designing and undertaking surficial geochemical sampling programs. Significant lateral and vertical changes in surficial cover can introduce far-travelled materials into areas that appear to be dominated by local bedrock. Quaternary fill in valley bottoms comprises primarily glacially-transported material with significant and complex transport vectors that do not represent local bedrock conditions. As a result, soil geochemical sampling should only be conducted where surficial mapping has identified areas of thin morainal or colluviated morainal cover over bedrock. In these areas, ice transport directions need to be factored into geochemical interpretations. Stream sediment geochemistry in valley bottoms should only be considered where significant local bedrock is being eroded into the fluvial system.

Modern stream sediments in bedrock and sediment entrenched reaches of Wade and Arch creek are favourable placer mining targets because of the significant volumes of material that have been concentrated into relatively thin modern deposits, and the potential for modern valleys to intersect with enriched paleo-valleys (Kennedy and van Loon, 2017). Glacial moraine or lacustrine sediments in upper Maple Creek (Fig. 7) can act as false bedrock surfaces where placer gold can accumulate, but entrenchment of the stream (and related concentration of surface materials) decreases quickly toward the drainage divide.

CONCLUSIONS

New glacial limit mapping near the Donjek River in the Kluane Ranges indicates that Quaternary glaciation of the region was restricted. Extensive regions of unglaciated terrain persisted throughout the Quaternary in an area that was formerly thought to be predominantly glaciated. As suggested by Rampton (1981), the lee of the Icefields Range would have received limited moisture during full glacial conditions, and high cirques in the Kluane Ranges were unable to accumulate large volumes of ice.

Extensive glaciers emanating from the Icefields Range fed the St. Elias lobe in southwestern Yukon, and although the Donjek and Shakwak glaciers advanced into Kluane Ranges, most of the ice flowed freely to the Shakwak Trench, and ultimately, Wellesley basin. The combination of restricted moisture in the lee of the Icefields Range, and free (unrestricted) drainage of glaciers into Shakwak Trench likely existed along a large region of the Kluane Ranges, and there may be significantly more unglaciated terrain than has been mapped to date.

The unique ice configuration in the study area resulted in episodes of up-valley flowing glaciation. Thick accumulations of valley-bottom glacial materials, drainage diversions and drainage impoundments are all characteristic of up-valley flowing ice, and are present in the lower drainages of Arch, Maple and Wade creeks.

Mid and high-elevation slopes are dominated by weathered bedrock materials, and glacial deposits on upper slopes may have undergone substantial reworking into local colluvial materials. The permafrost table controls mass wasting on many slopes in the study area, and increases in active layer thicknesses related to climate warming are likely to increase the magnitude of mass wasting events, creating thicker deposits of colluvium on mid-elevation slopes.

Mineral exploration programs undertaking surficial sediment geochemistry sampling programs, or employing existing geochemistry data, need to consider the sediment genesis in the area of investigation. Unglaciated environments are generally mantled by locally sourced weathered bedrock, weathered bedrock colluvium, and fluvial deposits that provide an excellent sampling medium. Within the glacial limits, there is considerable variation in the amount of glaciogenic cover. Much of the variation is associated with topographic position, however, the surficial geology map (*in prep.*) should be referenced to avoid terrain overlain by thick deposits of far-travelled glaciogenic sediment.

ACKNOWLEDGEMENTS

This project took place in the Traditional Territories of the White River and Kluane First Nations. Much of the field work occurred on Kluane First Nation settlement land and would not have been possible without their support. Conversations with a wide variety of people working in the region have benefitted the project greatly. In particular, Geordan Clark of Kluane Mineral Resources is thanked for his enthusiasm and engagement, and for sharing exploration results and insight. Jeff Bond, Steve Israel, and Sydney van Loon are all thanked for their collaboration in the field and contributions to glacial limit mapping, bedrock setting, and placer understanding, respectively. Sarah Ellis provided exceptional assistance in the field and office. Reviews of this paper by Jeff Bond resulted in many improvements.

REFERENCES

Bond, J.D., Lipovsky, P.S. and von Gaza, P., 2008. Surficial geology investigations in Wellesley basin and Nisling Range, southwest Yukon. *In:* Yukon Exploration and Geology 2007, D.S. Emond, L.R. Blackburn, R.P. Hill and L.H. Weston (eds.), Yukon Geological Survey, p. 125-138.

Duk-Rodkin, A., 1999. Glacial Limits Map of Yukon, Yukon Geological Survey, Geoscience Map 1999-2; *also known as GSC Open File 3694*.

Israel, S. and Van Zeyl, D.P., 2005. Preliminary geology of the Quill Creek map area, southwest Yukon parts of NTS 115G/5, 6 and 12. *In:* Yukon Exploration and Geology 2004, D.S. Emond, L.L. Lewis and G.D. Bradshaw (eds.), Yukon Geological Survey, p. 129-146.

Kennedy, K.E. and van Loon, S., 2017. Preliminary investigations of placer gold settings in Arch Creek, Kluane district, southwestern Yukon. *In:* Yukon Exploration and Geology 2016, K.E. MacFarlane and L.H. Weston (eds.), Yukon Geological Survey, p.103-115.

Lipovsky, P.S. and Bond, J.D., 2013. Surficial geology of Onion Creek (115J/02), Yukon (1: 50000 scale). Yukon Geological Survey, Energy, Mines and Resources, Government of Yukon, Open File 2013-8.

Rampton, V.N., 1971. Late Pleistocene glaciations of the Snag-Klutlan area, Yukon Territory. Arctic, vol. 24, p. 277-300.

Rampton, V.N., 1980. Surficial geology and geomorphology, Burwash Landing, Yukon Territory. Geological Survey of Canada, Preliminary map 6-1978.

Rampton, V.N., 1981. Surficial materials and landforms, Kluane National Park, Yukon Territory. Geological Survey of Canada, Paper 79-24, 37 p. (includes maps 13-1979 and 14-1979).

Turner, D.G., Ward, B.C., Bond, J.D., Jensen, B.J.L., Froese, D.G., Telka, A.M., Zazula, G.D. and Bigelow, N.H., 2013. Middle to Late Pleistocene ice extents, tephrochronology and paleoenvironments of the White River area, southwest Yukon. Quaternary Science Reviews, vol. 75, p. 59–77.

Turner, D.G., Ward, B.C., Froese, D.G., Lamothe, M., Bond, J.D. and Bigelow, N.H., 2016. Stratigraphy of Pleistocene glaciations in the St Elias Mountains, southwest Yukon, Canada. Boreas, vol. 45, p. 521-536.

Ward, B.C., Bond, J.D., Froese, D. and Jensen, B., 2008. Old Crow tephra (140±10 ka) constrains penultimate Reid glaciations in central Yukon Territory. Quaternary Science Reviews, vol. 27, p. 1909–1915.

Ward, B.C., Bond, J.D. and Gosse, J.C., 2007. Evidence for a 55–50 ka (early Wisconsin) glaciation of the Cordilleran ice sheet, Yukon Territory, Canada. Quaternary Research, vol. 68, p. 141–150.

Westgate, J.A., Preece, S.J., Froese, D.G., Pearce, N.J.G., Roberts, R.G., Demuro, M., Hart, W.K. and Perkins, W., 2008. Changing ideas on the identity and stratigraphic significance of the Sheep Creek tephra beds in Alaska and the Yukon Territory, northwestern North America. Quaternary International, vol. 178, p. 183–2.

Yukon Geological Survey (YGS), 2010. Yukon Placer Database – Geology and mining activity of placer occurrences. Yukon Geological Survey, CD-ROM.

Yukon MINFILE, 2017. Yukon MINFILE – A database of mineral occurrences. Yukon Geological Survey, http://data.geology.gov.yk.ca [accessed May 2017].

Van Loon and J.D. Bond (compilers), 2014. Yukon Placer Mining Industry 2010 to 2014. Yukon Geological Survey, 230 p.

Mod property, VMS mineralization in the western part of the Yukon-Tanana terrane? (Yukon MINFILE 105B 028, 029, 031)

T. Liverton
Consultant, Watson Lake, Yukon

S. Casselman
Yukon Geological Survey

Liverton, T. and Casselman, S., 2018. Mod Property, VMS Mineralization in the Western Part of the Yukon-Tanana terrane? (Yukon MINFILE 105B 028, 029, 031). *In:* Yukon Exploration and Geology 2017, K.E. MacFarlane (ed.), Yukon Geological Survey, p. 103-109.

ABSTRACT

Base metal-silver prospects have been known to exist in the upper Swift River region since 1946. These prospects, occurring in Yukon-Tanana terrane, have been previously described as isolated skarn occurrences and have hitherto received limited prospecting attention. Exploration work at the Mod property in 2016 has indicated that the sulphide mineralization is deformed (hence it predates the adjacent Cretaceous Seagull batholith) and that it demonstrates textures that are not consistent with a skarn origin. If, indeed, this mineralization is of exhalative origin then a large region of Yukon-Tanana terrane becomes prospective for mineralization similar to that of the Finlayson VMS district.

* *scott.casselman@gov.yk.ca*

INTRODUCTION

The Mod property contains three MINFILE occurrences: MOD (105B 031), TBMB (or Munson, 105B 029) and Bom (105B 028) which are located in the headwaters of the Swift River and are hosted in Yukon-Tanana terrane (Fig. 1). Base metal-silver prospects in the upper Swift River were discovered in 1946 during prospecting by Hudson Bay Mining and Smelting following the route for the Alaska Highway. A limited amount of diamond drilling was performed in 1947; in the 1960s Boswell River Mines undertook an aeromagnetic survey and several small-scale geochemical surveys. The TBMB to MOD trend, the southernmost of two known trends, has received limited excavation and structural mapping since then (McLeod and Sevensma, 1969; D'el-Rey Silva *et al.*, 2001a,b). The prospects are contained in metavolcanic and metasedimentary units of the Yukon-Tanana terrane that have been regionally metamorphosed and deformed with an overprint of thermal metamorphism from the mid-Cretaceous Seagull batholith. Consequently, the gangue mineralogy of the mineralization is of calc-silicates: either chlorite-epidote or diopside dominant. Based on the metamorphic overprint, these occurrences have previously been described as skarns. However, fieldwork since 2015 has revealed that the geological setting and sulphide mineralogy and textures are more consistent with an exhalative origin. If, indeed, this mineralization is of exhalative origin, then an underexplored region of many tens of kilometres strike length within the Yukon-Tanana terrane southwest of Tintina fault becomes prospective for VMS-style mineralization.

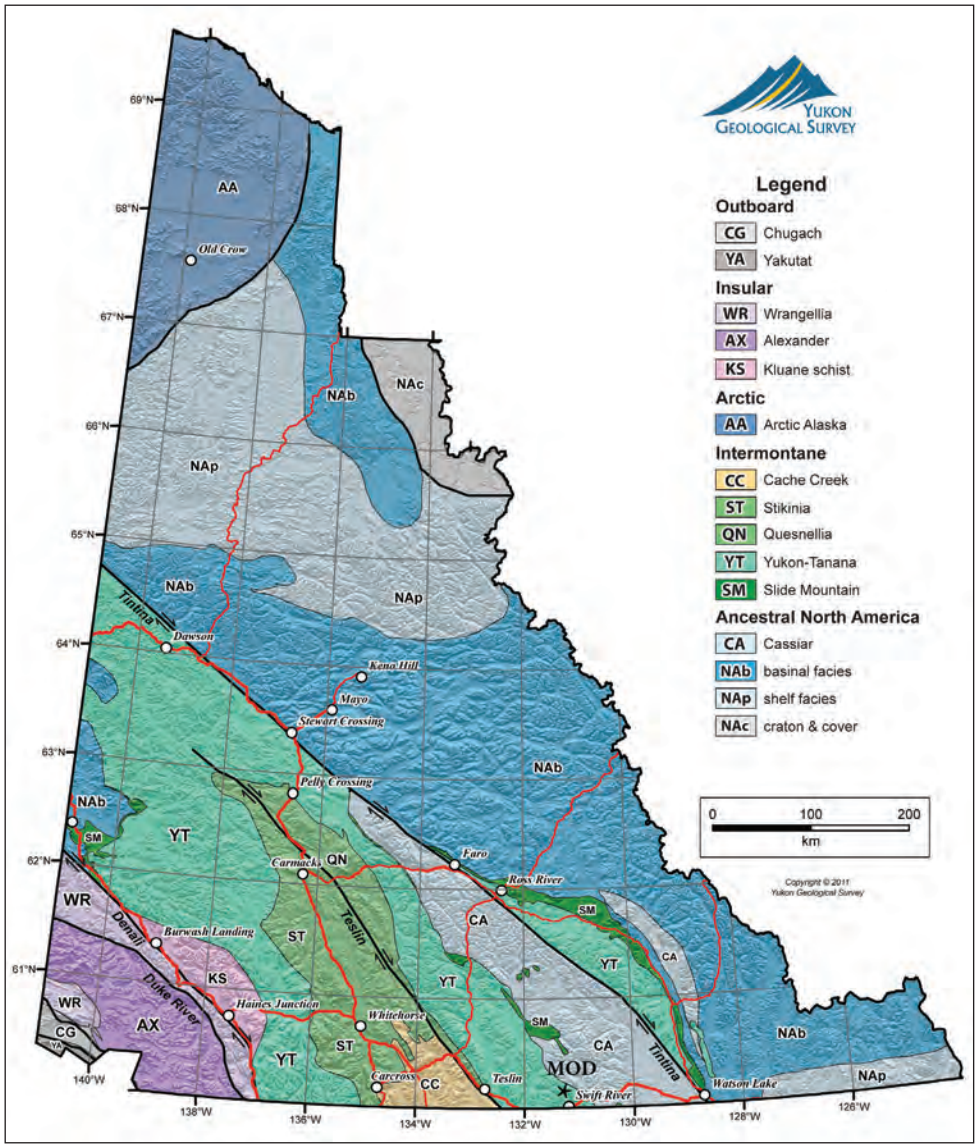

Figure 1. *Terrane map of Yukon (after Colpron and Nelson, 2011) showing location of the Mod property in the Yukon-Tanana terrane, southwest of Tintina fault.*

REGIONAL GEOLOGY

The upper Swift River basin contains metasedimentary and metavolcanic strata that have been assigned to the Snowcap and Finlayson assemblages of the Yukon-Tanana terrane (Colpron *et al.*, 2016). These relationships were originally mapped by Roots (D'el-Rey Silva *et al.*, 2000a,b) and have been compiled by Colpron (2016). These rocks are in fault contact on the northern side of the drainage basin with lower Paleozoic strata of displaced North American continental assemblages (Cassiar terrane). The Yukon-Tanana rocks are intruded by a Jurassic diorite-granodiorite sill of approximately 1 km in thickness, approximately 3 km to the north of the MOD-TBMB trend, and by a mid-Cretaceous granite stock, satellite to the Seagull batholith, 1 km north (Fig. 2). The units in proximity to the MOD-TBMB showings contain metamorphosed volcanic rocks, marble, siltstone, felsic and basic tuff, sandstone, greywacke, chert and phyllite of the Snowcap assemblage. Immediately south of the prospect, siliciclastic rocks of the Finlayson assemblage are in fault contact with the Snowcap assemblage.

PROPERTY GEOLOGY

Figure 3 presents a compilation of the detailed geology of the vicinity of the TBMB and MOD properties produced (D'el-Rey Silva *et al.*, 2000a,b). This map shows that at least two generations of folding have been recognized (D'el-Rey Silva *et al.*, 2000a,b). Tight F_2 folds are overturned to the northeast and have wavelengths in the order of 600 m. A marble unit adjacent to the obvious mineralization is traceable between the TBMB, MOD and Bound occurrences, with some obvious, but relatively minor, displacement by faults. Sphalerite mineralization is known to the northeast of the TBMB trenches, as well as weak copper-gold mineralization associated with the metavolcanics, but these occurrences require further mapping to elucidate their extent.

Chlorite-amphibole gangue mineral assemblages are seen at the TBMB (2.8 km NW of the MOD) and diopside/hedenbergite-epidote at the MOD occurrence. A leucogranite stock, satellite to the Seagull batholith, crops out in the canyon 1 km to the NE of the MOD and a

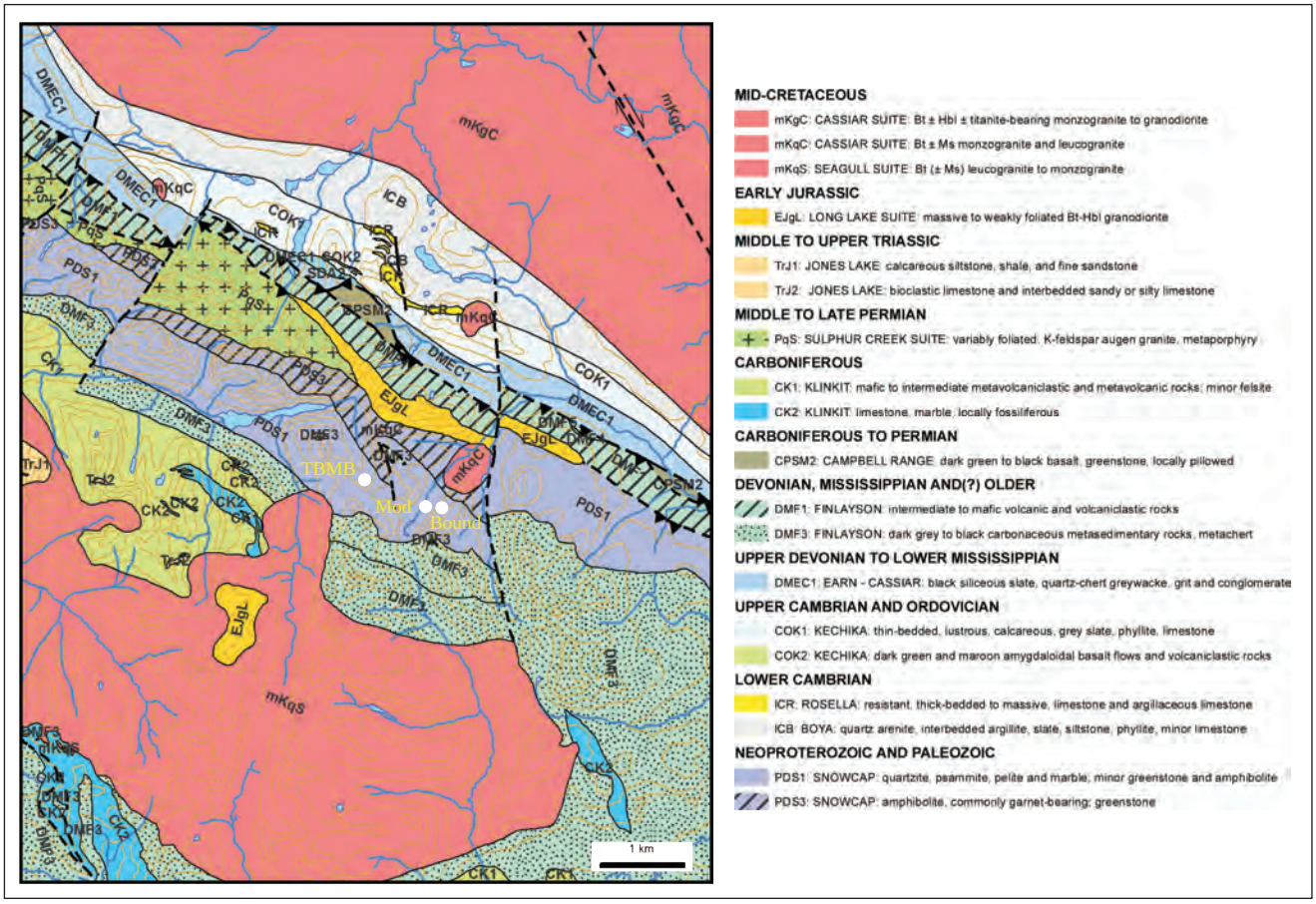

Figure 2. *Regional geology of the area around the Mod property (after Yukon Geological Survey, 2017); mKqS- Seagull Suite, mKqC- Cassiar Suite, EJgL- Long Lake Suite, PqS- Sulphur Creek Grp, DMF1- Ram Creek Fm, DMF3- Swift River Fm, DMEC1- Earn Grp, COK1- Kechika Grp, PDS1, 3- Snowcap Grp.*

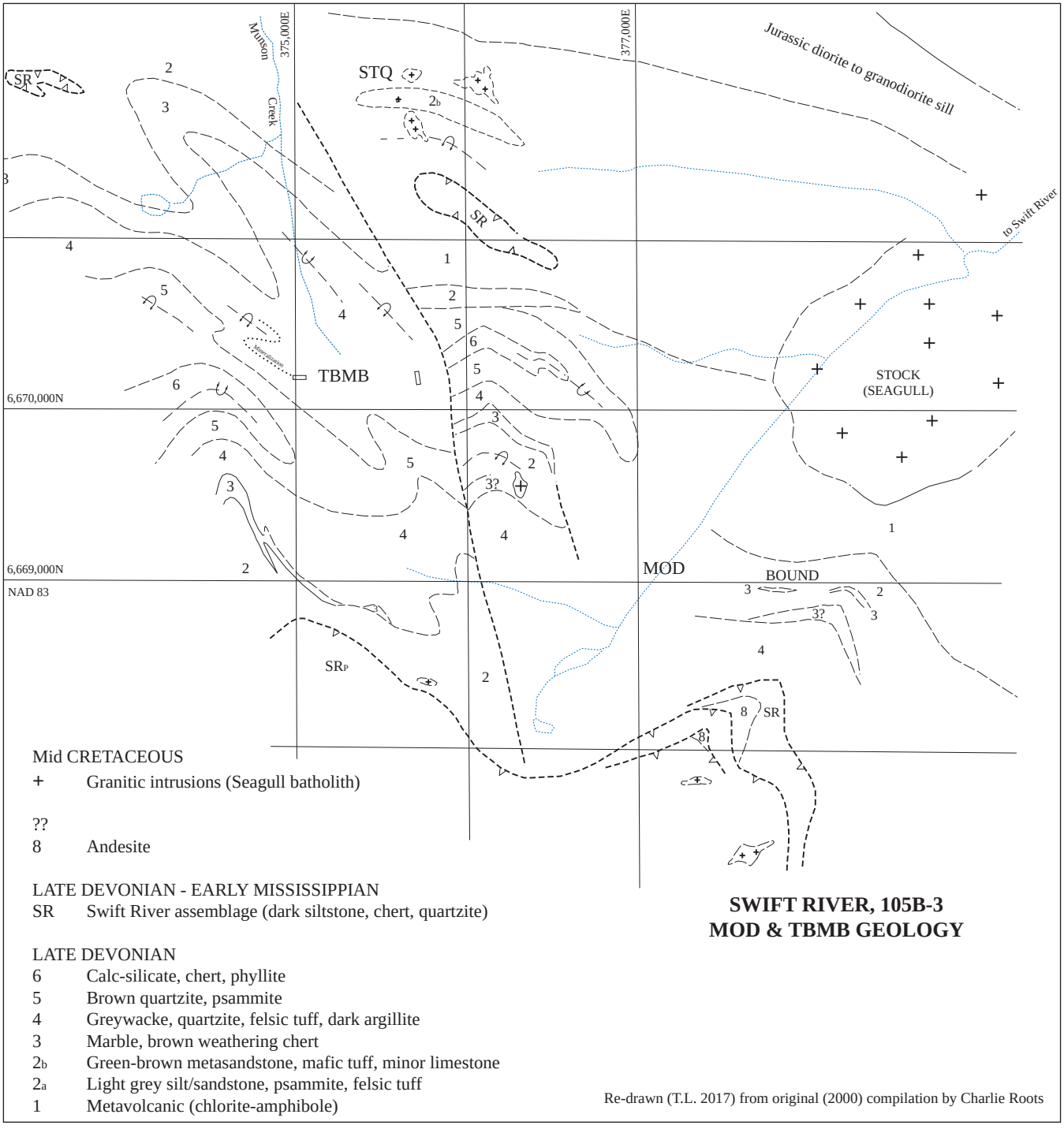

Figure 3. *Property-scale geology from mapping by Charlie Roots and Tim Liverton in 2000.*

further stock (the STQ) is exposed in a cirque 2 km NW of the TBMB. It is likely, therefore, that the batholith underlies the whole TBMB-MOD region and that this intrusion has produced the calc-silicate mineral assemblages seen in carbonate and the volcanic rocks.

MINERALIZATION

The MOD showing is exposed for a stike length of 170 m in two bulldozer cuts. Two locations, 140 m apart and 25 m vertically apart, have been cleaned to expose 2.2 m true thickness of sulphide in the northwestern ('lower') showing and 8.4 m thickness at the 'upper' showing. Mineralization may be traced to the southeast to the top of the ridge. Some 800 m along strike sphalerite-magnetite mineralization is found adjacent to a marble horizon at the Bound occurrence.

The sulphide mineralization is layered on a decimetre scale and foliation is obvious in thin section (Figs. 4 and 5a,b). Pyrrhotite forms one layer of 20 cm thickness at either exposure. The sulphides are laminated into pyrrhotite, sphalerite/tetrahedrite, sphalerite/magnetite, and galena-rich layers which is consistent with the mineralization being of exhalative origin. Slabs cut from the pyrrhotite show disjointed folds and intrusion of the sulphide into extension fractures in the calc-silicate gangue layer. This is typical of the 'durchbewegung' texture of deformed sulphides. Mixed sulphide layers contain sphalerite, often with tetrahedrite along its grain boundaries, with galena, euhedral magnetite crystals and rare arsenopyrite. Centimetre-scale folding of the mixed sulphides shows varying plunge directions (Figs. 6 and 7).

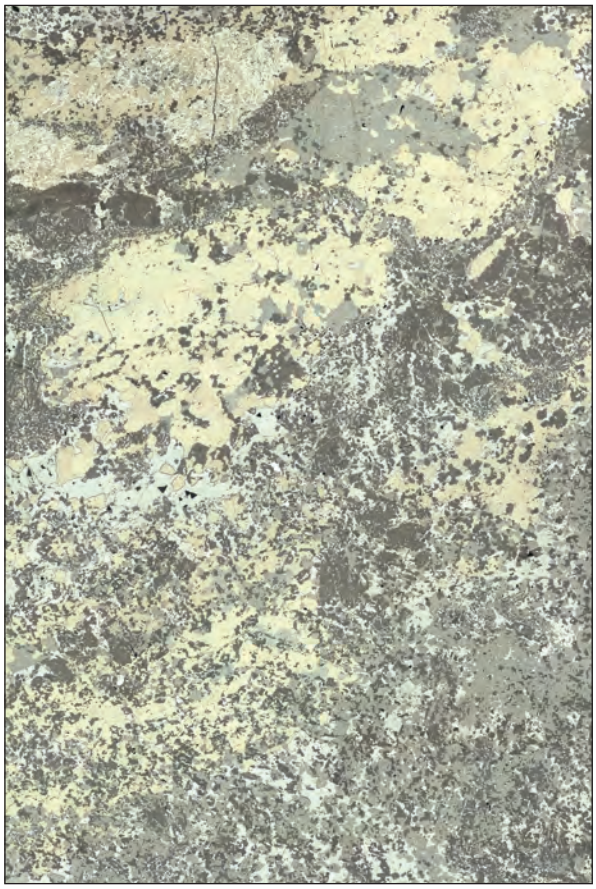

Figure 4. *Photomicrograph showing detail (plane polarized reflected light) of the region outlined in Fig. 7. The width of the image is approximately 22 mm.*

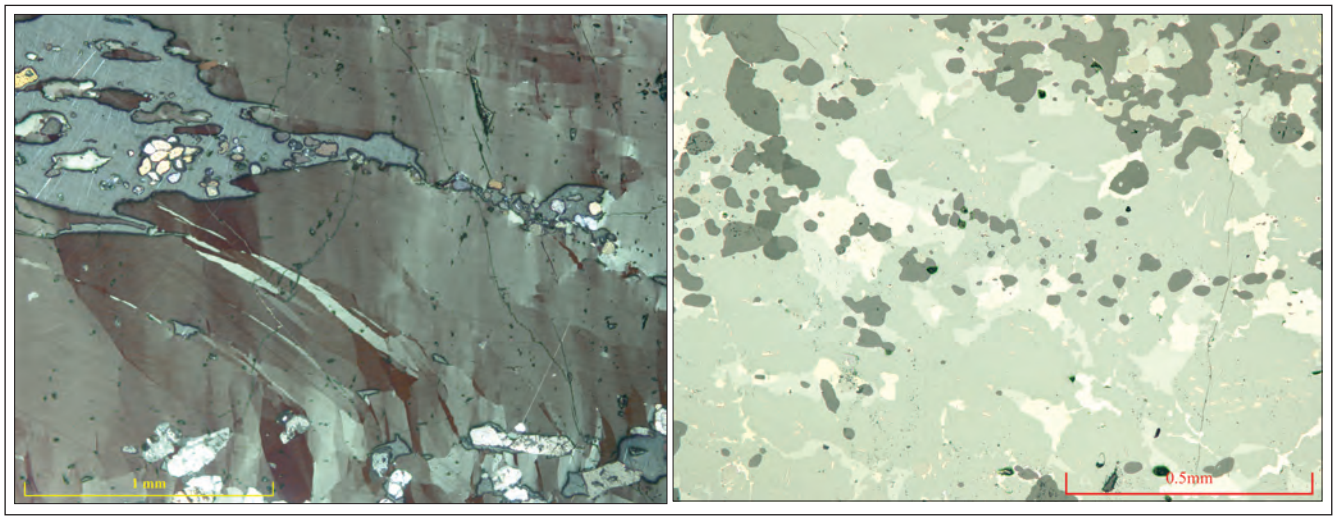

Figure 5. ***(a)*** *Polished thin section, polarizers at 85° showing deformation twinning in pyrrhotite (reflected light).* ***(b)*** *Zinc-rich mineralization from the upper showing. Plane polarized reflected light. Sphalerite is mid grey; tetrahedrite is a lighter grey; pyrrhotite is yellow; magnetite is brownish grey (crystals in upper R.H. corner); gangue is black.*

Channel sampling of the lower showing yielded an average grade of 7.49% Zn, 5.12% Pb and 8.4 oz/ton Ag over 2.2 m true thickness. The upper showing has not been systematically channel sampled, however ~10 kg blocks of coarse galena gave an assay of 41.6% Pb and 62.7 oz/ton Ag, and the fine-grained pyrrhotite-bearing sulphide assayed 5.61% Zn, 3.19% Pb and 7.8 oz/ton Ag.

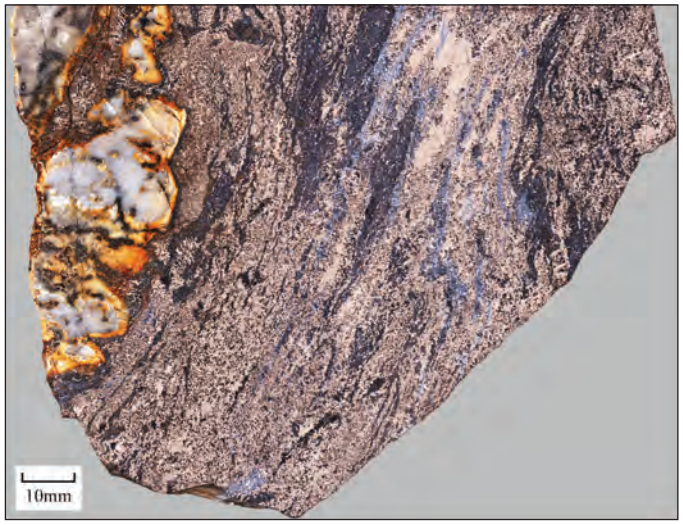

Figure 6. *Ground slab of folded, layered pyrrhotite-galena from the upper showing with durchbewegung texture. Pyrrhotite is bronze, galena bluish grey, calc-silicate/ carbonate gangue black.*

DISCUSSION AND CONCLUSIONS

The finely laminated and highly deformed nature of the sulphides at the Mod property is inconsistent with this mineralization being a skarn produced by the Seagull batholith. The deformation has preceded the thermal metamorphism that produced calc-silicate gangue minerals. Skarns are known to have layered magnetite/pyrrhotite or pyrite mineralogy, but not with the textures shown by the Mod mineralization. Layered skarns (wrigglite: Kwak and Askins, 1981a,b) have discrete monomineralic layering (see also Liverton, 2016, his Figs. 11c, 12b,c). The geological setting at the Swift River area is prospective for VMS formation: the area is underlain by an abundance of basinal metasedimentary rocks and felsic meta-volcanic rocks. The authors are of the belief that the mineralization is likely to be of exhalative origin that was coeval with deposition of the volcano-sedimentary units that are part of the Yukon-Tanana terrane. The mineralization at Mod appears to be of VMS-origin, making this a significant new region that is comparable to the Finlayson district and is prospective for Zn-Pb-Ag VMS deposits. Detailed mapping, rock geochemistry and petrography are recommended to test this model.

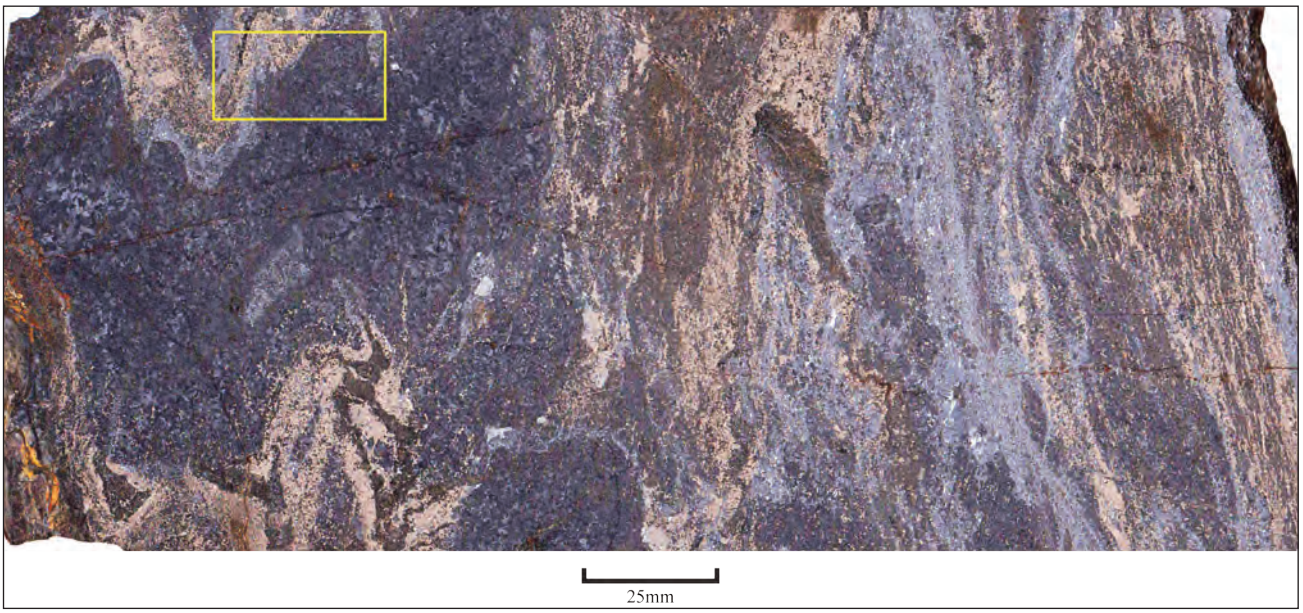

Figure 7. *Slab of layered, mixed sulphides showing folding. The fold at the top left plunges (upward) at 40° to the section plane. The approximate corresponding location for Figure 4 is outlined in yellow.*

REFERENCES

Colpron, M. and Nelson, J.L., 2011. A digital atlas of terranes for the northern Cordillera: Yukon Geological Survey, www.geology.gov.yk.ca/bedrock_terrane.html [accessed May 15, 2013].

Colpron, M., Israel, S., Murphy, D.C., Pigage, L.C. and Moynihan, D. (compilers), 2016. Yukon Bedrock Geology Map. Yukon Geological Survey, Open File 2016-1, map and legend.

D'el-Rey Silva, L.J.H., Liverton, T., Paradis, S. and Roots, C., 2001a. A structural analysis of the upper Swift River area (105B/3), Yukon, Part I: Dan Zn occurrence and implications for sulphide mineralization. *In:* Yukon Exploration and Geology 2000, D.S. Emond and L.H. Weston (eds.), Exploration and Geological Services Division, Yukon, Indian and Northern Affairs Canada, p. 289-300.

D'el-Rey Silva, L.J.H., Liverton, T., Roots, C. and Paradis, S., 2001b. A structural analysis of the upper Swift River area (105B/3), Yukon, Part II: The TBMB claims and implications for the regional geology. *In:* Yukon Exploration and Geology 2000, D.S. Emond and L.H. Weston (eds.), Exploration and Geological Services Division, Yukon, Indian and Northern Affairs Canada. p. 301-310.

Kwak, T.A.P. and Askins, P.W. 1981a. Geology and genesis of the F-Sn-W (-Be-Zn) skarn (wrigglite) at Moina Tasmania. Economic Geology, vol. 76, p. 439-467.

Kwak, T.A.P. and Askins, P.W. 1981b. The nomenclature of carbonate replacement deposits, with emphasis on Sn-F-(-Be-Zn) 'wrigglite' skarns. Journal of the Geological Society of Australia, vol. 28, p. 123-136.

Liverton, T., 2016. A-type granite plutons and tin skarns in southeast Yukon: Mindy prospect and surrounding granite of 105C/9. *In:* Yukon Exploration and Geology 2015, K.E. MacFarlane and M.G. Nordling (eds.), Yukon Geological Survey, p. 151-164.

McLeod, J.W. and Sevensma, P.H., 1969. Boswell River Mines Ltd., Dan Group, Summary of 1968 Work Program. Yukon Energy, Mines and Resources Assessment Report 018616.

Yukon Geological Survey, 2017. Yukon Digital Bedrock Geology. Yukon Geological Survey, http://www.geology.gov.yk.ca/update_yukon_bedrock_geology_map.html [accessed December, 2017].

Re-evaluating the chronostratigraphic framework for felsic volcanic and intrusive rocks of the Finlayson Lake region, Yukon-Tanana terrane, Yukon

M.J. Manor* and S.J. Piercey
Department of Earth Sciences, Memorial University of Newfoundland

Manor, M.J. and Piercey, S.J., 2018. Re-evaluating the chronostratigraphic framework for felsic volcanic and intrusive rocks of the Finlayson Lake region, Yukon-Tanana terrane, Yukon. *In:* Yukon Exploration and Geology 2017, K.E. MacFarlane (ed.), Yukon Geological Survey, p. 111-127.

ABSTRACT

The Finlayson Lake district contains >30 Mt of volcanogenic massive sulphide (VMS) mineralization, but has not been the focus of field-based research since the mid-2000s. We present herein preliminary fieldwork on Yukon-Tanana terrane (YTT) host rocks that are the groundwork for future petrologic, isotopic, and geochronologic studies of the stratigraphy and crustal evolution of the VMS deposits and YTT rocks in the Finlayson Lake region and other peri-Laurentian terranes of the northern Cordillera. During the summer of 2017, we logged seven drill holes that intersected the stratigraphic hanging walls and footwalls of the mafic-hosted Fyre Lake and felsic-hosted Kudz Ze Kayah and GP4F VMS deposits. The stratigraphic results generally reveal finely laminated to bedded mafic or felsic volcaniclastic rocks that are interbedded with clastic rocks or cut by intrusive rocks and reflect changes in depositional environments and tectonomagmatic regimes in the Late Devonian to Early Mississippian.

* *mjmanor@mun.ca*

INTRODUCTION

The Finlayson Lake district contains >30 Mt of polymetallic (Zn-Pb-Cu-Co-Au-Ag) volcanogenic massive sulphide (VMS) mineralization that has been discovered since the mid-1990s (Hunt, 1997; Peter *et al.*, 2007). Current exploration and development has been focused at the Kudz Ze Kayah Zn-Pb-Cu deposit and has resulted in a NI 43-101 compliant total geological resource of 19.2 Mt at 6.3% Zn, 1.9% Pb, 0.9% Cu, 148 g/t Ag, and 1.4 g/t Au (BMC Minerals Ltd.). Regional mapping and U-Pb ages completed in the late 1990s and early 2000s have defined stratigraphic domains and a tectonostratigraphic framework for the Kudz Ze Kayah and other VMS deposits in the district (Grant, 1997; Murphy and Piercey, 1999a,b; Murphy *et al.*, 2006); however, the petrological relationships and precise timing of sulphide deposition relative to nearby subvolcanic intrusions is not well understood.

Modern, high-precision U-Pb geochronology has been useful in constraining the of age of stratigraphic sequences, timing of mineralization, and relationships between intrusive and extrusive rocks in various VMS deposits worldwide (*e.g.*, Corfu *et al.*, 1989; Barrie *et al.*, 2002; Mortensen *et al.*, 2008; Piercey *et al.*, 2008; Rosa *et al.*, 2009; Eyuboglu *et al.*, 2014; Ross *et al.*, 2014). In addition, more recent studies have combined isotopic geochemistry with mineral-scale petrology to address critical knowledge gaps related to the fertility and prospectivity of mineral belts, and intrinsic parameters of the magmas that supply heat and/or metals to VMS deposits (*e.g.*, Wolverine VMS deposit; Piercey *et al.*, 2017). The integration of modern geochronological and geochemical techniques can also constrain the timing and petrological evolution of VMS-associated rocks, which may be useful to discriminate prospective from less prospective stratigraphic sequences globally (*e.g.*, Piercey, 2011).

In this paper, we provide new stratigraphic data for VMS mineralization in the Finlayson Lake district. This revised stratigraphic framework forms the basis for additional geochronological and lithogeochemical sampling undertaken in 2017. We present a compilation of mainly U-Pb zircon ages from the current geochronological database (Appendix 1) to evaluate the constraints on stratigraphic horizons that host mineralization in the district. This assessment sheds light on the overall paucity of robust U-Pb ages throughout the region, especially those in the Cleaver Lake and Money Creek thrust sheets, and the need for updated ages utilizing modern high-precision chemical abrasion-thermal ionization mass spectrometry (CA-TIMS) U-Pb techniques to better constrain the stratigraphic boundaries for VMS-bearing horizons. We also present new graphic logs from the Fire Lake, Kudz Ze Kayah, and Wind Lake formations, subject of detailed U-Pb sampling in 2017, and describe the research plan for future work in the region.

GEOLOGICAL SETTING

The Finlayson Lake region is an Upper Devonian to Lower Mississippian fault-bounded sliver of the peri-Laurentian Yukon-Tanana and Slide Mountain terranes located in southeastern Yukon (Fig. 1; Tempelman-Kluit, 1979; Mortensen and Jilson, 1985; Murphy *et al.*, 2006). The Yukon-Tanana stratigraphy comprises variably deformed,

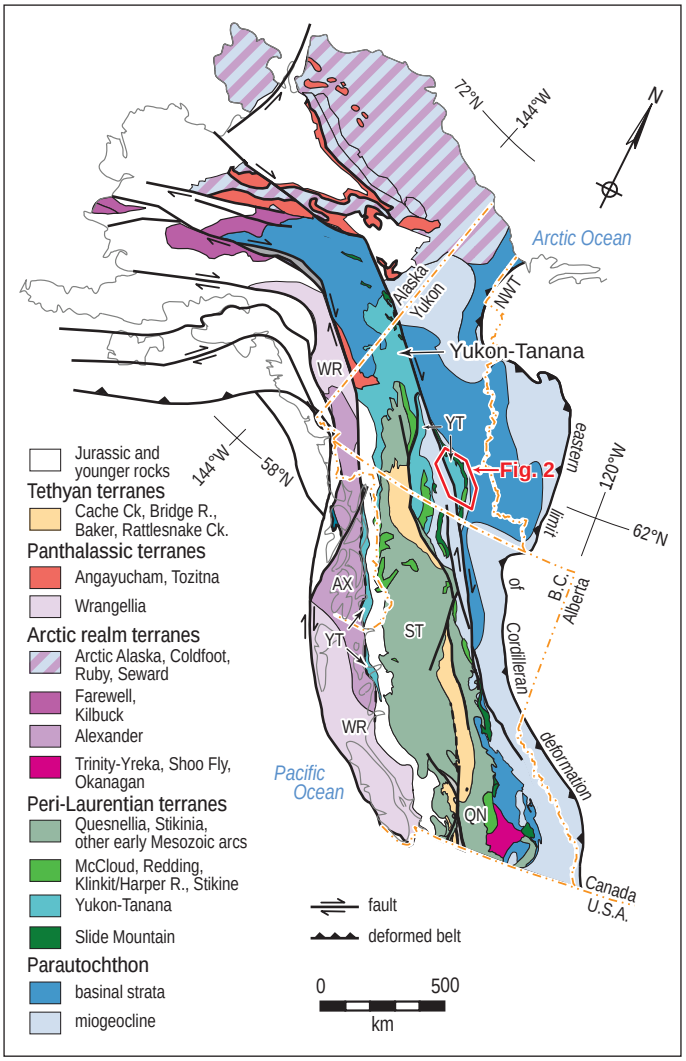

Figure 1. *Terranes of the northern Cordillera in British Columbia, Yukon and Alaska (modified after Colpron and Nelson, 2011). AX = Alexander, QN = Quesnellia, ST = Stikinia, YT = Yukon-Tanana, WR = Wrangellia.*

pervasively metamorphosed, and stratigraphically-intact volcanic, plutonic, and sedimentary rocks that were deposited or intruded above a pre to Late Devonian continental basement (*i.e.*, North River formation and Snowcap assemblage; Colpron *et al*., 2006; Murphy *et al*., 2006; Piercey and Colpron, 2009). The Yukon-Tanana rocks are separated from juvenile mafic volcanic rocks and basinal sedimentary rocks of the Slide Mountain terrane by the Jules Creek transform fault (Murphy *et al*., 2006). The combined Yukon-Tanana and Slide Mountain rocks were thrust onto Laurentian continental margin strata, including Selwyn basin, along the Jurassic-Early Cretaceous Inconnu thrust following final accretion (Figs. 2 and 3; Murphy *et al*., 2002). Rocks of the Yukon-Tanana terrane presently located in the Finlayson Lake district were subsequently displaced ~430 km south of the main part of the terrane along the Tintina strike-slip dextral fault in the Eocene (Fig. 1; Gabrielse *et al*., 2006).

Rocks of the Yukon-Tanana terrane in the Finlayson Lake region comprise three fault-bounded stratigraphic successions confined to distinct structural panels: the Cleaver Lake, Money Creek, and Big Campbell thrust sheets, respectively (Figs. 2 and 3). The Cleaver Lake thrust sheet includes Upper Devonian to Lower Mississippian basalt and minor rhyolite, chert, and greywacke of the Cleaver Lake formation, which are intruded by Early Mississippian Simpson Range granitoid rocks and juxtaposed with ultramafic-mafic components from the Money and North klippen (Tempelman-Kluit, 1979; Piercey and Murphy, 2000; Murphy *et al*., 2006). Rocks in the Money Creek thrust sheet comprise pre-Upper Devonian sedimentary rocks of the North River formation (also basement to the Big Campbell thrust sheet discussed below) that are stratigraphically overlain by predominantly felsic volcanic and deep marine sedimentary rocks of the Waters Creek formation and intruded by Simpson Range granitoid rocks. Intermediate to felsic volcanic, volcaniclastic, and epiclastic rocks of the Tuchitua River formation unconformably overlie the Waters Creek formation (Fig. 3). The Big Campbell thrust sheet contains North River formation metasiliciclastic rocks that precede Upper Devonian volcanism of the Grass Lakes group, which is unconformably overlain by the sedimentary and volcanic rocks of the Lower Mississippian Wolverine Lake group (Figs. 2, 3 and 4). The base of the Grass Lakes group consists of bimodal mafic and lesser felsic volcanic and volcaniclastic rocks of the Fire Lake formation that are associated with ultramafic-mafic rocks. These are overlain by felsic volcanic-volcaniclastic rocks of the Kudz Ze Kayah (KZK) formation, which have been intruded by Late-Devonian-Early Mississippian Grass Lakes granitoid rocks, and mafic volcanic rocks of the Wind Lake formation (Murphy, 1998; Murphy *et al*., 2006). The Mississippian Wolverine Lake group unconformably overlies the Grass Lakes group and typically includes conglomerate to sandstone and felsic volcanic rocks that are capped by an extensive exhalite horizon and basalt (Figs. 3 and 4; Murphy and Piercey, 1999a, b; Bradshaw *et al*., 2001, 2008; Murphy *et al*., 2002).

The Big Campbell thrust sheet is host to most VMS deposits in the district. Mineralization is of variable style and hosted in different stratigraphic packages that reflect the dynamic mid-Paleozoic tectonomagmatic history of the district (Piercey *et al*., 2001, 2006; Nelson *et al*., 2006; Peter *et al*., 2007). The Kudz Ze Kayah Zn-Pb-Cu and GP4F Zn-Pb deposits (Kudz Ze Kayah formation) are hosted by felsic volcanic host rocks of the Kudz Ze Kayah formation, whereas the Fyre Lake Cu-Co-Au and Ice Cu ± Zn deposits are part of mafic-dominated successions (Fire Lake and Campbell Range formations, respectively), and the Wolverine Zn-Pb-Cu-Ag-Au deposit is hosted by the volcano-sedimentary sequence of the Wolverine Lake group, which contains abundant shale and iron formation (Figs. 3 and 4; Piercey *et al*., 2001, 2016; Sebert *et al*., 2004; Peter *et al*., 2007; Bradshaw *et al*., 2008).

PREVIOUS WORK

LITHOGEOCHEMISTRY AND RADIOGENIC ISOTOPES

A number of studies over the past 30 years have contributed to the growing database of geochemical data in the Finlayson Lake region. The earliest work by Mortensen (1992) and Grant (1997) focused on U-Pb and radiogenic isotopic data for granitoid and other rocks in the district, and both illustrate that continental crustal material played a significant role in the formation of magmatic rocks throughout the region, and that basin sediments contained significant contributions from Precambrian crustal material. Integrated mapping, lithogeochemical, and radiogenic isotopic work on the felsic and mafic rocks in the district was undertaken Piercey (2001). Subsequent investigations of the felsic rocks revealed a distinct divide between typical calc-alkalic, I-type arc rocks and HFSE-REE-enriched, A-type back-arc rocks (Piercey *et al*., 2001; 2003) that are both interpreted to have extensive crustal contamination from Precambrian basement domains.

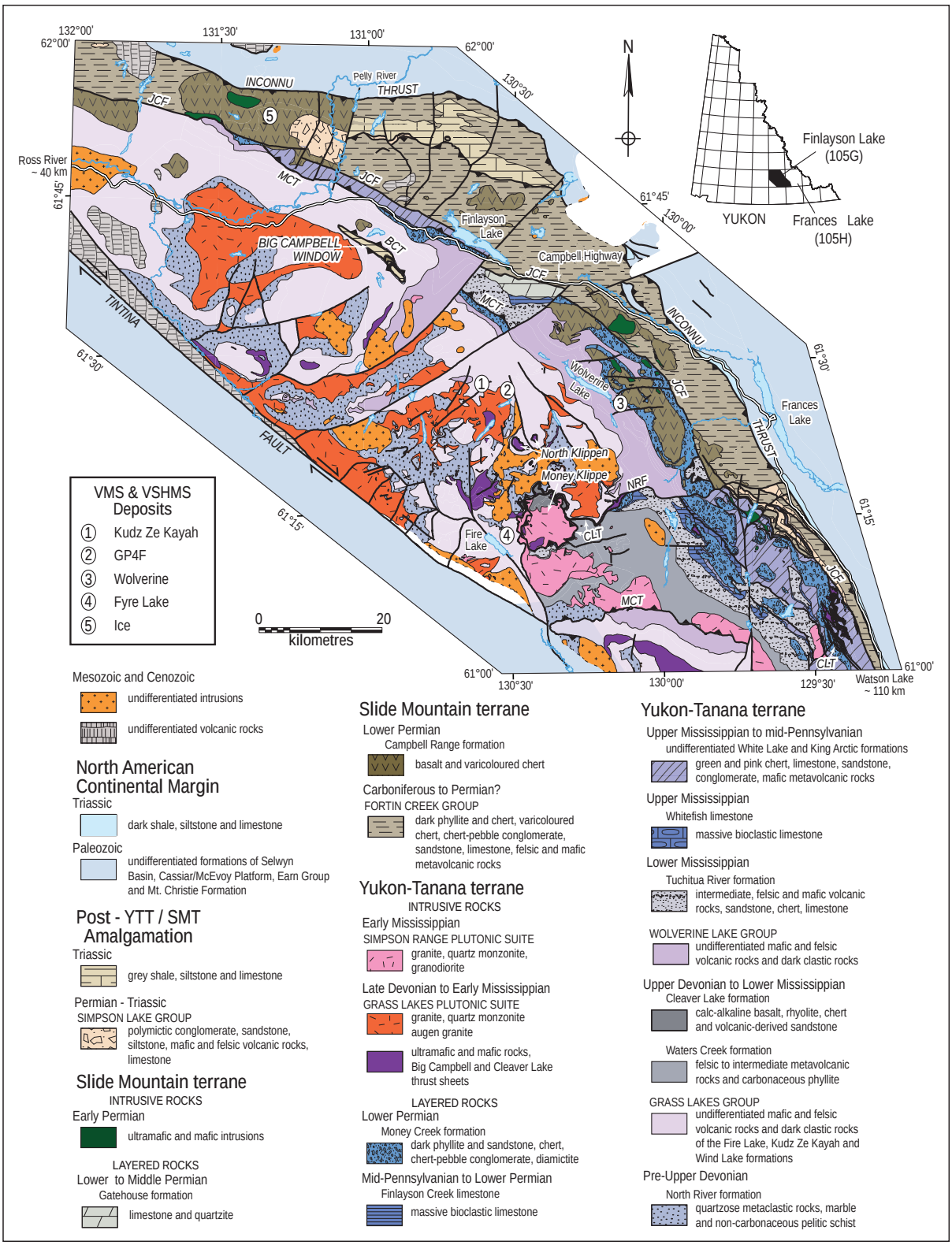

Figure 2. *Regional geologic setting of the Finlayson Lake region, Yukon-Tanana terrane (modified after Murphy et al., 2006). Numbers indicate locations of VMS deposits in the region. BCT=Big Campbell thrust; CLT=Cleaver Lake thrust; JCF=Jules Creek fault; MCT=Money Creek thrust; NRF=North River fault; VMS=volcanogenic massive sulphide; VSHMS=volcanic sediment-hosted massive sulphide.*

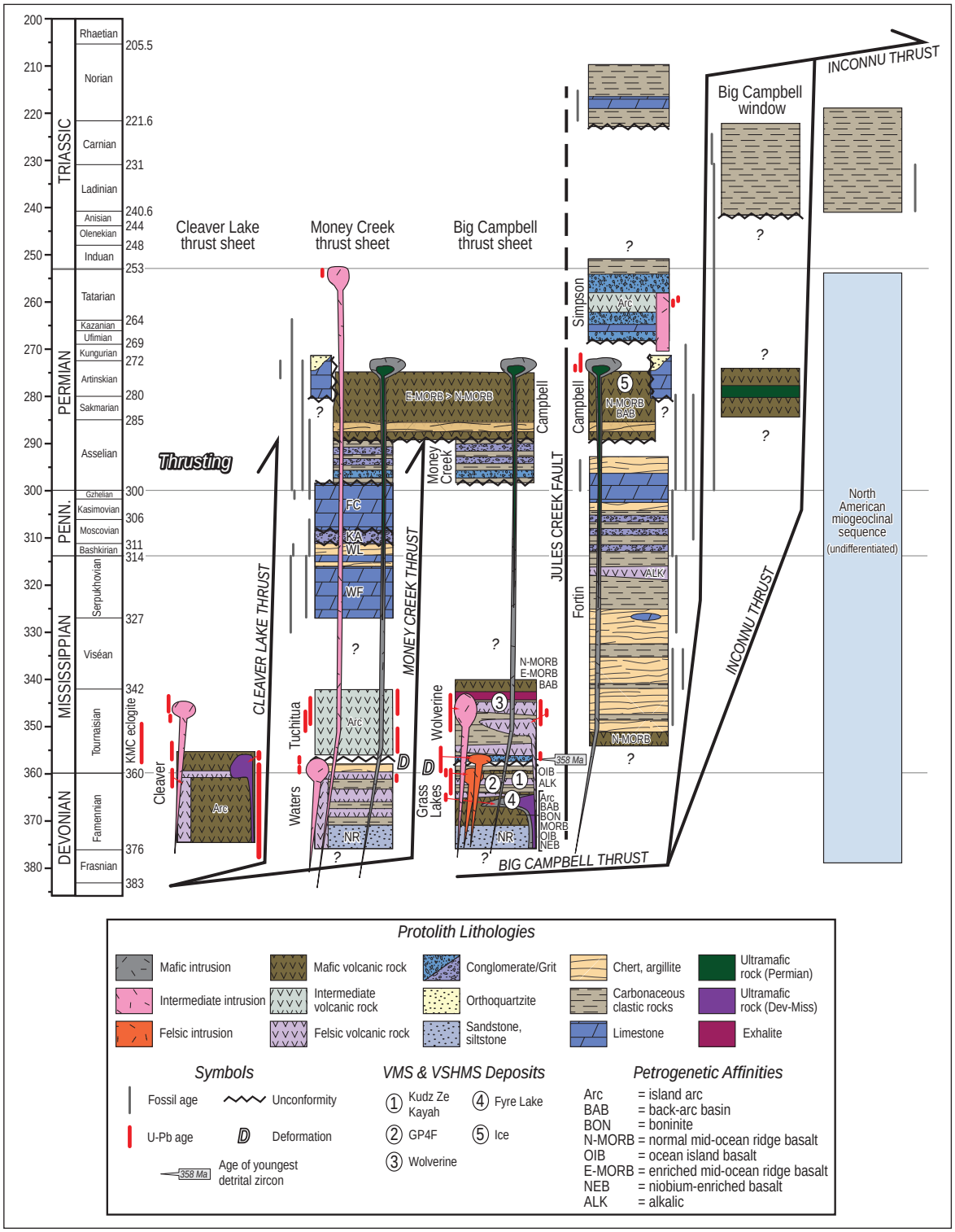

Figure 3. *Composite chronostratigraphic columns for the Finlayson Lake region with locations of VMS prospects, U-Pb zircon and fossil ages, and petrogenetic affinities (modified after Murphy et al., 2006). KMC = Klatsa Metamorphic Complex; NR = North River formation; Dev = Devonian; Miss = Mississippian.*

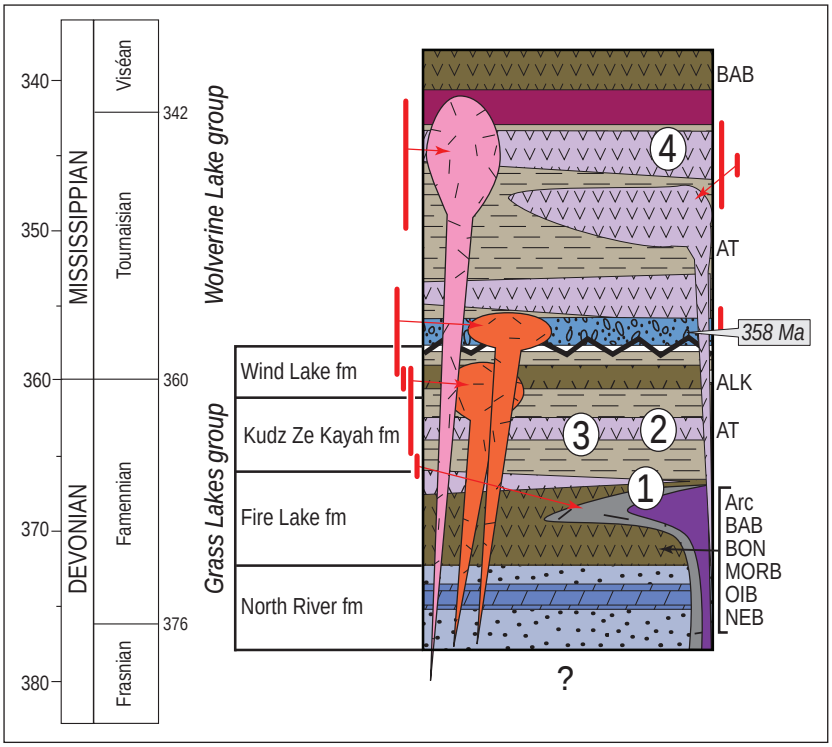

Figure 4. *Stratigraphic column for the Big Campbell thrust sheet (modified after Piercey et al., 2016). Petrogenetic affinity abbreviations as in Figure 3. Existing age constraints are indicated by red bars.*

Associated mafic volcanic rocks in this arc-back-arc setting exhibit petrogenetic affinities of alkalic ocean island basalt (OIB), low-Ti tholeiite to boninite, back-arc basin basalt (BABB), enriched mid-ocean ridge basalt (E-MORB; *e.g.*, Fire Lake formation; Piercey *et al.*, 2002a,b; 2004), enriched and normal mid-ocean ridge basalt (E-, N-MORB) and back-arc basin basalts (BABB; *e.g.*, Wolverine Lake group and Campbell Range basalts, Slide Mountain terrane; Piercey *et al.*, 2002c). The evolved Nd isotopic signature of felsic rocks (*i.e.*, $\varepsilon Nd_{(t)} < 0$) in the district indicate significant Precambrian crustal contributions during evolution of the northern Cordillera (Piercey *et al.*, 2001, 2003). Conversely, juvenile isotopic compositions in mafic rocks (*i.e.*, $\varepsilon Nd_{(t)} > 0$) represent components of mantle-derived material and shifts in tectonomagmatic affinities; however, these rocks are interpreted as minor additions to a predominantly evolved Cordilleran crust (Piercey *et al.*, 2004, 2012).

U-PB GEOCHRONOLOGY

Numerous studies have presented new geochronological data to constrain the age of stratigraphy in the Finlayson Lake region and its relationship to the rest of the Yukon-Tanana terrane (Mortensen, 1983, 1992, 2004, unpublished data; Grant, 1997; Piercey, 2001; Devine *et al.*, 2006; Murphy *et al.*, 2006; and Piercey *et al.*, 2008; Appendix 1; Fig. 5). While the first U-Pb ages for the Finlayson Lake district illustrated the host rocks were Paleozoic (*ca.* 360-351 Ma; Mortensen, 1983), they are excluded from discussion here for consistency because analyses were completed prior to the introduction of air-abrasion sample preparation (Krogh, 1982). Thirty-seven ages are reported for the Finlayson Lake region; analyses include air abrasion-isotope dilution-thermal ionization mass spectrometry (ID-TIMS) U-Pb zircon (n = 33), ID-TIMS U-Pb titanite (n = 1), sensitive high-resolution ion microprobe (SHRIMP) U-Pb zircon (n = 3), and $^{40}Ar/^{39}Ar$ white mica (n = 1) geochronology (Appendix 1; Fig. 5). Ages range from the Early Devonian (*ca.* 375 Ma) to the Late Permian (*ca.* 255 Ma; Figs. 3 and 5). Re-evaluation of these data indicate that the U-Pb analyses only broadly define the age of host stratigraphy and the timing of seafloor VMS formation (Fig. 5). In evaluating historic data, we assigned each age an objective rating (*i.e.*, uncertain, poor, good, moderate, excellent) based on the number of concordant *vs.* discordant fractions, inheritance and Pb-loss reported for these samples (Appendix 1).

Historic samples from the district provide a rough framework for magmatism, volcanism and sedimentation (Appendix 1). In the Big Campbell thrust sheet, these ages provide reasonable constraint for the Wolverine Lake group (*ca.* 356 to 346 Ma) and a possible upper limit of the Fire Lake formation (*ca.* 365 Ma), but do not define critical boundaries for VMS-bearing rocks of the Kudz Ze Kayah formation (Fig. 5). Ages determined for the Money Creek thrust sheet are relatively well-defined with clear breaks between the Waters Creek (*ca.* 360 Ma) and Tuchitua (*ca.* 352 to 347 Ma) formations, with Simpson Lake granitoid rocks intruding the Waters Creek formation at *ca.* 357 Ma. The Cleaver Lake thrust sheet contains the *ca.* 360 to 356 Ma Cleaver Lake formation and two intervals of magmatic activity represented by the Simpson Range plutonic suite (*ca.* 355 Ma and *ca.* 347 Ma). Despite a broad range of U-Pb ages presented here, new age analyses are needed to tighten the constraints on stratigraphic boundaries and timing of mineralization, which will provide an improved framework for future exploration in the district.

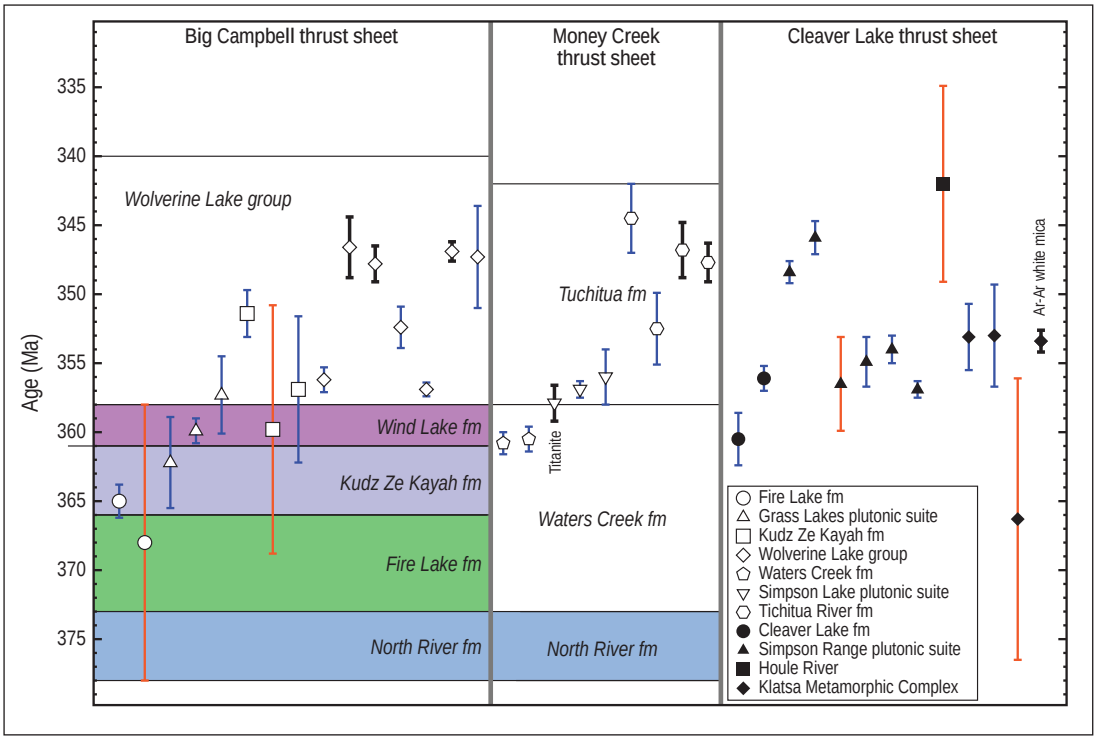

Figure 5. *Compilation of U-Pb zircon geochronology for rocks in the Finlayson Lake region. Ages from Mortensen (1992); Grant (1997); Piercey (2001); Mortensen (2004, unpublished data); Devine et al. (2006); Murphy et al. (2006); and Piercey et al. (2008; as in Appendix 1). Bold, black error bars indicate analyses of excellent quality; blue error bars are of moderate to good quality; and red bars indicate uncertain or poor quality that cannot discriminate between stratigraphic units.*

2017 FIELD STUDIES

The primary goals of the 2017 fieldwork were to map and sample the stratigraphy in the Finlayson Lake region, specifically the Big Campbell thrust sheet and deposit-bearing stratigraphy, for the purposes of: 1) refining the ages of stratigraphic horizons that host VMS deposits; and 2) determining the role of felsic magmatism in crustal growth of the northern Cordillera and, if possible, the formation of VMS deposits in the Yukon-Tanana terrane. Fieldwork was based out of the Kudz Ze Kayah exploration camp (BMC Minerals Ltd., 2017). Focused sampling of outcrop and drill core, combined with detailed stratigraphic logging, was completed on seven drill holes from the Kudz Ze Kayah (n=4), GP4F (n=1), and Fyre Lake (n=2) VMS deposits, with holes that intersected the stratigraphic hanging wall and footwall of each deposit (Figs. 6 and 7). Twelve U-Pb geochronology and 71 lithogeochemistry samples were collected at selected outcrops and from drill core intervals both above and below ore lenses. For the purposes of this paper, we will only discuss the stratigraphic results relevant to sampling for U-Pb geochronology.

STRATIGRAPHY

Grass Lakes group

Fire Lake formation

Two drill holes (FL96-39 and FL97-109) from the Fire Lake formation, where both intersected the Fyre Lake VMS lenses, were logged. Both sections contain a footwall sequence of bedded and variably deformed mafic volcaniclastic rocks (*e.g.*, mafic ash to lapilli tuff) associated with sulphide-magnetite lenses, (*e.g.*, Sebert *et al.* 2004). Drill hole FL96-39 contains two stacked, ~10-15 m sulphide lenses that are separated by ~35 m of mafic tuffaceous rocks with minor felsic material. The stratigraphic hanging wall to the sulphide lenses presents a transition from interbedded argillite, siltstone, and sandstone with mafic tuffaceous rocks grading into a fining-upwards sequence dominated by finely laminated to bedded black, grey, and/or white clastic rocks and argillite interpreted as turbidite deposits (Fig. 6).

Kudz Ze Kayah formation

Outcrop and drill holes from the Kudz Ze Kayah (n=3; K15-299, K15-301, K16-372) and nearby GP4F (n=1; K15-302) VMS deposits are dominated by felsic volcaniclastic rocks and lesser sedimentary rocks, which contrast with the mafic rocks of the Fire Lake (below) and Wind Lake formations (above; Fig. 4). Rocks that comprise the Kudz Ze Kayah deposit are primarily felsic volcaniclastic rocks with crosscutting intermediate to felsic intrusive rocks (rarely they have mafic compositions) throughout the hanging wall and footwall to the Kudz Ze Kayah VMS lenses (*e.g.*, BMC Minerals Ltd., 2017).

The Kudz Ze Kayah deposit is contained within the >500 m thick Kudz Ze Kayah formation, which consists of a deeper footwall of fining-upwards sequences dominated by felsic crystal tuff to lapilli tuff intercalated with either laminated clastic pelitic rocks, felsic tuff with argillite, or rare mafic tuffaceous rocks; locally massive to amygdaloidal felsic volcanic rocks comprise parts of the footwall. In the GP4F deposit, the stratigraphic footwall consists of feldspar-blue quartz-eye crystal tuffs that are interbedded with finely laminated pelitic rocks near the contact with massive sulphides. The immediate hanging wall stratigraphy of the GP4F deposit contains variably lapilli and crystal-rich tuffaceous rocks that are interbedded with finely laminated biotite-calcite-rich pelitic rocks immediately above the GP4F sulphide zone. In the uppermost part of the Kudz Ze Kayah formation, the rocks are dominantly felsic tuffs to lapilli tuffs that dip shallowly to the north and are transitional with overlying mafic tuffs of the overlying Wind Lake formation.

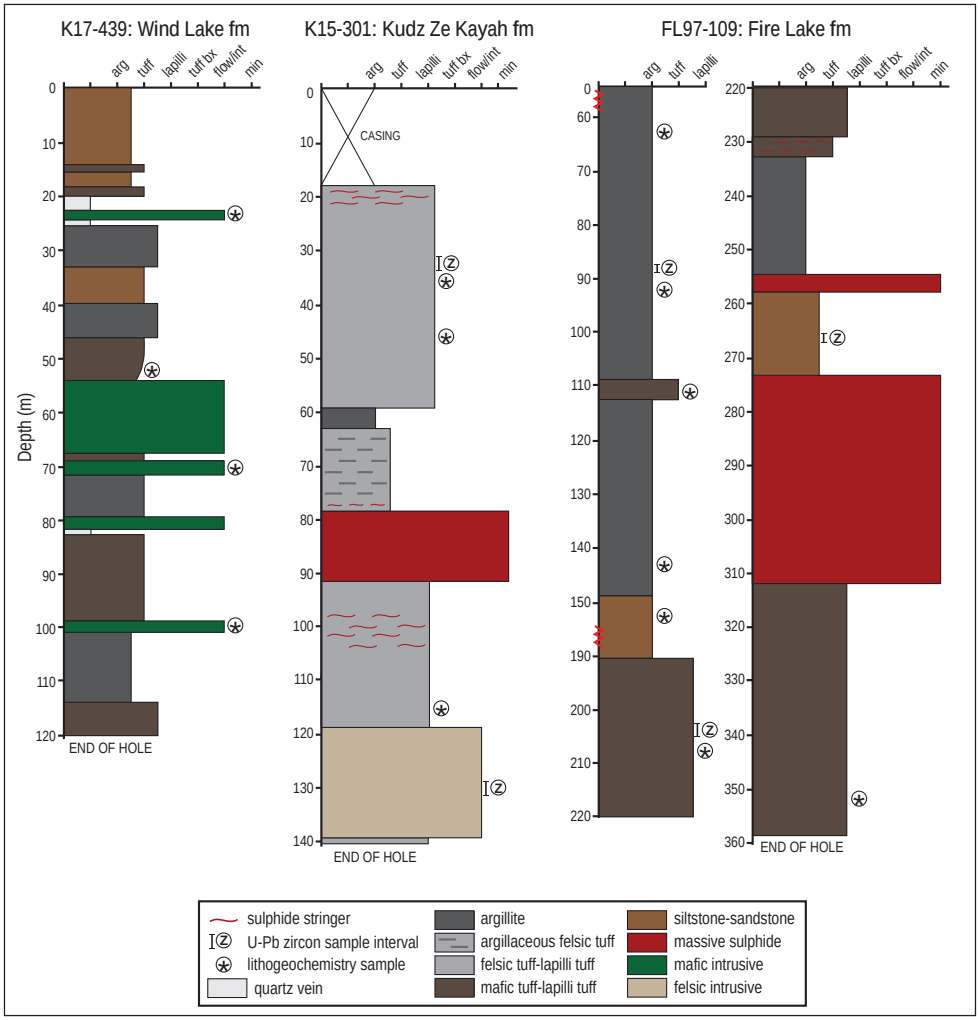

Figure 6. *Detailed stratigraphic logs and sampling locations for three representative drill holes through stratigraphy in the Wind Lake, Kudz Ze Kayah, and Fire Lake formations. Note the change in scale (red zig-zag line) for hole FL97-109, where units of the same lithology were shortened at 0-60 m and 150-190 m. Abbreviations: arg=argillite; bx=breccia; int=intrusion; min=mineralization.*

Both the Kudz Ze Kayah and GP4F deposits are cut by mafic and felsic intrusive rocks (dikes?) that are locally up to 30 m thick; some of the mafic intrusive rocks are potentially correlative with the Wind Lake formation. The lower and upper contacts of the Kudz Ze Kayah formation are cut by intrusive rocks of the Late Devonian-Early Mississippian Grass Lakes plutonic suite, which are shown to have comparable age and geochemical characteristics to rocks of the Kudz Ze Kayah formation (Piercey *et al.*, 2003).

Wind Lake formation

The Wind Lake formation overlies the Kudz Ze Kayah formation and represents a geochemical transition to dominantly mafic volcaniclastic rocks and argillaceous to quartz-rich sedimentary rocks (*e.g.*, Murphy, 1998; Murphy *et al.*, 2006; Fig. 6). Drill hole K17-439 shows dominantly mafic rocks that include interbedded, finely laminated mafic tuffaceous rocks with argillite that transitions uphole to greater abundances of siltstone, wacke, and lesser clastic material intercalated with mafic tuff and argillite (Fig. 6). Abundant biotite-rich mafic intrusive rocks have sharp contacts with tuffaceous rocks (*i.e.*, dikes or sills) and are thickest (~13.5 m) at the transition from mafic volcaniclastic rocks to coarser grained clastic to argillaceous rocks up section in the Wind Lake formation.

Grass Lakes plutonic suite

Rocks of the Late Devonian to Early Mississippian Grass Lakes plutonic suite intrude the entire Grass Lakes group stratigraphy, are texturally heterogeneous, and range from feldspar-quartz augen granites to feldspar-dominant porphyries with minor blue quartz eyes (*e.g.*, Murphy *et al.*, 2006; Figs. 4 and 7d,i). Both varieties are variably foliated and deformed with feldspar crystal modes between 10 and 40 vol.% and that have grain sizes between 2 and 30 mm.

Wolverine Lake group

The lowermost rocks of the Wolverine Lake group crop out approximately 80 m east of Grass Lakes granite outcrops and across an angular unconformity (Murphy and Piercey, 1999b; Murphy *et al.*, 2002). These rocks are strongly foliated quartz and feldspar-bearing felsic rocks (porphyry?) that contain relatively homogenous, 3-5 mm quartz and feldspar crystals (Fig. 7c).

SAMPLE DESCRIPTIONS

Grass Lakes group

Fire Lake formation

Two U-Pb geochronology samples from FL97-109 are sedimentary rocks (sand beds in siltstone, 17MM-043; siltstone between sulphide lenses, 17MM-049; Fig. 7j,l) that will be treated as detrital samples and analyzed using laser ablation-inductively coupled plasma-mass spectrometry (LA-ICP-MS) techniques, with the potential for follow-up CA-TIMS analyses to constrain maximum depositional ages. Sample 17MM-047 is a siliceous band (tuff?) intercalated with mafic volcaniclastic rocks where CA-TIMS methods will be utilized to constrain the upper limits of sulphide mineralization in the Fyre Lake deposit (Figs. 6 and 7k).

Kudz Ze Kayah formation

Sampling for U-Pb geochronology was restricted to outcrop and holes K15-301 (intersects massive sulphides) and K16-372 (footwall; Figs. 6 and 7b,e-h). A beige, blue quartz-eye felsic volcaniclastic rock (ash to local lapilli tuff) was collected ~5 m below the inferred Wind Lake formation contact to constrain the upper limit and last major phase of felsic volcanism in the hanging wall of the Kudz Ze Kayah formation (17MM-002; Fig. 7b). Approximately 50 m above the massive sulphides, a green to grey, felsic ash to lapilli tuff, with local lapilli stone is interpreted to record the minimum age for mineralization (17MM-031; Figs. 6 and 7e). Three additional intrusive rocks interpreted to cut primary stratigraphy were collected in the footwall of the Kudz Ze Kayah deposit (17MM-034, 17MM-060, and 17MM-061; Fig. 7f-h).

Wind Lake formation

One U-Pb sample (17MM-001) was collected from an outcrop approximately 300 m above the Kudz Ze Kayah contact. Here, a 40-cm section of beige to orange, foliated and locally laminated felsic ash tuff is intercalated with chlorite-rich mafic tuff and interpreted to represent the upper limit of volcanic activity for the Wind Lake formation (Fig. 7a).

Figure 7. *Field photographs of 2017 sampling locations for U-Pb zircon geochronology in the Big Campbell thrust sheet, Finlayson Lake region.* ***(a)*** *17MM-001: Wind Lake formation, felsic ash tuff interbedded with mafic ash tuff ~300 m above contact with Kudz Ze Kayah formation (413749E, 6815933N);* ***(b)*** *17MM-002: Kudz Ze Kayah formation, blue quartz-eye felsic volcaniclastic intercalated with ash tuff, ~ 5 m below the Wind Lake formation contact (413907E, 6815182N);* ***(c)*** *17MM-004: Wolverine Lake group, massive and foliated quartz-feldspar porphyry (429446E, 6812106N);* ***(d)*** *17MM-005: Grass Lakes plutonic suite, foliated and deformed, massive alkali feldspar-quartz augen granite (429291E, 6812095N);* ***(e)*** *17MM-031: Kudz Ze Kayah hanging wall (50 m above massive sulphides), felsic lapilli to ash tuff with local lapilli stone;* ***(f)*** *17MM-034: Kudz Ze Kayah footwall, quartz-sericite altered massive rhyolite intrusive;* ***(g)*** *17MM-060: biotite-chlorite altered mafic dike cross-cutting KZK footwall;* ***(h)*** *17MM-061: quartz-feldspar porphyry with rare blue quartz eyes that cuts KZK footwall;* ***(i)*** *17MM-062: Grass Lakes plutonic suite, quartz-feldspar porphyry;* ***(j)*** *17MM-043: Fyre Lake hanging wall, grey siltstone with intercalated sandy beds;* ***(k)*** *17MM-047: Fire Lake hanging wall, siliceous bands interbedded in mafic tuff; and* ***(l)*** *17MM-049: Fire Lake formation, siltstone between sulphide lenses. Hammer (35 cm) for scale in (a)-(d). Coordinates for specific locations noted in (a)-(d) above are UTM Zone 9N, NAD 83.*

Grass Lakes plutonic suite

Two U-Pb samples were collected from this unit. Sample 17MM-005 is a foliated and deformed to massive alkali feldspar-quartz augen granite from just below the inferred Wolverine Lake group unconformity (Fig. 7d; Murphy and Piercey, 1999b,c). Sample 17MM-062 is a quartz-feldspar porphyry with blue quartz eyes from the base of the Kudz Ze Kayah formation, at 580 m depth in drill hole K16-372 (Fig. 7i).

Wolverine Lake group

U-Pb sample 17MM-004 was collected from outcrop where it is interpreted to be the lowermost, thus oldest, rocks of the Wolverine Lake group (Fig. 7c). This will test the existing detrital zircon data by Murphy *et al*. (2006) which indicated a maximum depositional age of 358 Ma for a basal conglomerate of the Wolverine Lake group (Figs. 3 and 4).

FUTURE RESEARCH

CHEMICAL ABRASION ID-TIMS U-PB ZIRCON GEOCHRONOLOGY

A review of historical U-Pb zircon dates reveals a knowledge gap when defining the chronostratigraphic framework for VMS mineralization in the Finlayson Lake region.

Air abrasion treatment of zircon was the typical sample preparation technique used for these samples from the 1980s to 2000s, a method which removed the U+Th-rich rims of zircon to lessen the effects Pb-loss and produce more concordant and thus geologically significant ages (Krogh, 1982). Recent advances in chemical abrasion techniques (CA-TIMS) have increased our ability to remove high U+Th domains within the internal structure of zircon by thermal annealing and stepwise chemical leaching (Mattinson, 2005). The result is increased precision down to 0.1% (or better) and capability to analyze closed-system zircon with relatively low levels of initial U and Th (Mattinson, 2005; Schmitz and Kuiper, 2013). Utilization of the CA-TIMS method on felsic rocks of the Finlayson Lake region will considerably increase our confidence in the chronostratigraphic framework for mineralization, the timing of mineralization, and the duration of magmatic activity. These results will provide key information that may aid future exploration in the region.

LITHOGEOCHEMISTRY, BULK ROCK AND *IN SITU* HF-ND ISOTOPES

Rocks in the Finlayson Lake region display a wide range of geochemical characteristics and petrogenetic affinities that reflect distinct tectonic regimes during the Late Paleozoic (Piercey *et al*., 2001, 2002a,b, 2003, 2004, 2006, 2012). New drill core, most notably from the ongoing projects of BMC Minerals Ltd. at Kudz Ze Kayah and GP4F, has allowed us to access previously unavailable parts of the Grass Lakes group stratigraphy for ancillary geochemical sampling. A subset of the samples will be analyzed for major and trace element lithogeochemical analysis to properly place these rocks in a petrogenetic context. In addition, whole-rock Hf-Nd radiogenic isotopic analyses will be undertaken to complement existing Nd isotopic data (*e.g.*, Piercey *et al*. 2003). At a smaller scale, we will also begin a comprehensive mineral separation program to remove zircon, monazite, and apatite from select samples for *in situ* laser ablation split stream (LASS) Lu-Hf and U-Pb (zircon) and Sm-Nd and U-Pb (monazite, apatite) isotopic analyses at Memorial University of Newfoundland. Integration of these methods will aim to link new field observations with lithogeochemical and *in situ* analyses to evaluate petrogenetic processes and the intensive parameters of magma generation (*e.g.*, temperature of emplacement, redox state, sulphur budget) and the extent of mantle *vs.* crustal contributions to formation of felsic rocks (both VMS-bearing and barren suites). Isotopic analyses of felsic rocks will provide new insight in evolved magmatism and crustal growth in Paleozoic terranes of the northern Cordillera, and add to the existing regional framework for direct comparison and refinement of tectonic models for the Finlayson Lake region and the Yukon-Tanana terrane.

CONCLUSIONS

1) The level of exposure in the Finlayson Lake region, coupled with stratigraphically controlled drill core, provide exceptional opportunities to study the age and geochemistry of the VMS stratigraphy of the Finlayson Lake region and test existing tectonic and metallogenic models for the district.

2) New high-precision chemical abrasion ID-TIMS U-Pb zircon geochronology is needed to constrain the VMS-bearing and barren stratigraphy, and timing of VMS mineralization in the district.

3) New stratigraphic logging has allowed us to accurately place U-Pb and lithogeochemical samples in stratigraphic context relative to VMS mineralization.

4) Future work will include high-precision U-Pb zircon geochronology, *in situ* and whole-rock radiogenic isotopic techniques, and major and trace element lithogeochemistry to address the petrology of felsic rocks and their relation to crustal growth of the northern Cordillera.

ACKNOWLEDGEMENTS

We acknowledge BMC Minerals for providing us the opportunity to study and sample drill core from the Kudz Ze Kayah, GP4F and Fyre Lake VMS deposits. Thanks to Robin Black, Neil Martin and Darcy Baker for logistical and financial support while at KZK camp during the summer of 2017. Mark Baknes, Roger Hulstein, Ron Voordouw, Trent Newkirk, Dillon Hume, and other employees with BMC Minerals Ltd. and Equity Exploration Consultants Ltd., are also thanked for insightful discussions on the geology of KZK and the region. Flights to field sites would not have been possible without the excellent pilots from Trans North Helicopters. We are grateful for a thorough and constructive review by Maurice Colpron, and editorial support by Karen MacFarlane. Support for this project was provided by BMC Minerals (No. 1) Ltd., Yukon Geological Survey, Targeted Geoscience Initiative 5 (TGI-5) program of the Geological Survey of Canada, and an NSERC Discovery Grant to Stephen Piercey.

REFERENCES

Barrie, T.C., Amelin, Y. and Pascual, E., 2002. U-Pb geochronology of VMS mineralization in the Iberian Pyrite belt. Mineralium Deposita, vol. 37, p. 684-703. doi: 10.1007/s00126-002-0302-7.

BMC Minerals Ltd., 2017. Kudz Ze Kayah polymetallic project prefeasibility information booklet May 2017, http://bmcminerals.com/wp-content/uploads/2017/06/BMC%20KZK%20Polymetallic%20Project%20prefeasability%20Bk%202017%20Final%20sml.pdf, [accessed November 2017].

Bradshaw, G.D., Peter, J.M., Paradis, S. and Rowins, S.M., 2001. Geological characteristics of the Wolverine volcanic-hosted massive sulphide deposit, Finlayson lake district, Yukon Territory, Canada. *In:* Yukon Exploration and Geology 2000, D.S. Emond and L.H. Weston (eds.), Exploration and Geological Services Division, Yukon Region, Indian and Northern Affairs Canada, p. 269-288.

Bradshaw, G.D., Rowins, S.M., Peter, J.M. and Taylor, B.E., 2008. Genesis of the wolverine volcanic sediment-hosted massive sulfide deposit, Finlayson Lake District, Yukon, Canada: Mineralogical, mineral chemical, fluid inclusion, and sulfur isotope evidence. Economic Geology, vol. 103, p. 35-60. doi: 10.2113/gsecongeo.103.1.35.

Colpron, M. and Nelson, J., 2011. A digital atlas of terranes for the Northern Cordillera. Yukon Geological Survey, www.geology.gov.yk.ca.

Colpron, M., Nelson, J.L. and Murphy, D.C., 2006. A tectonostratigraphic framework for the pericratonic terranes of the northern Canadian Cordillera. *In*: Paleozoic Evolution and Metallogeny of Pericratonic Terranes at the Ancient Pacific Margin of North America, Canadian and Alaskan Cordillera, M. Colpron and J.L. Nelson (eds.), Geological Association of Canada, Special Paper 45, p. 1-23.

Corfu, F., Krogh, T.E., Kwok, Y.Y. and Jensen, L.S., 1989. U-Pb zircon geochronology in the southwestern Abitibi greenstone belt, Superior Province. Canadian Journal of Earth Sciences, vol. 26, p. 1747-1763. doi: 10.1139/e89-148.

Devine, F., Carr, S.D., Murphy, D.C., Davis, W.J., Smith, S. and Villeneuve, M., 2006. Geochronological and geochemical constraints on the origin of the Klatsa metamorphic complex: Implications for Early Mississippian high-pressure metamorphism within Yukon-Tanana terrane. *In*: Paleozoic Evolution and Metallogeny of Pericratonic Terranes at the Ancient Pacific Margin of North America, Canadian and Alaskan Cordillera, M. Colpron and J.L. Nelson (eds.), Geological Association of Canada, Special Paper 45, p. 107-130.

Eyuboglu, Y., Santosh, M., Yi, K., Tuysuz, N., Korkmaz, S., Akaryali, E., Dudas, F.O. and Bektas, O., 2014. The Eastern Black Sea-type volcanogenic massive sulfide deposits: Geochemistry, zircon U-Pb geochronology and an overview of the geodynamics of ore genesis. Ore Geology Reviews, vol. 59, p. 29-54. doi: 10.1016/j.oregeorev.2013.11.009.

Gabrielse, H., Murphy, D.C. and Mortensen, J.K., 2006. Cretaceous and Cenozoic dextral orogen-parallel displacements, magmatism, and paleogeography, north-central Canadian Cordillera. *In*: Paleogeography of the North American Cordillera: Evidence For and Against Large-Scale Displacements, J.W. Haggart, R.J. Enkin and J.W.H. Monger (eds.), Geological Association of Canada, Special Paper 46, p. 255-276.

Grant, S.L., 1997. Geochemical, radiogenic tracer isotopic, and U-Pb geochronological studies of Yukon-Tanana terrane rocks from the Money klippe, southeastern Yukon, Canada. Unpublished MSc thesis, University of Alberta, Edmonton, Canada, 177 p.

Hunt, J.A., 1997. Massive sulphide deposits in the Yukon-Tanana and adjacent terranes. *In*: Yukon Exploration and Geology 1996, Exploration and Geological Services Division, Yukon, Indian and Northern Affairs Canada, p. 35-45.

Krogh, T.E., 1982. Improved accuracy of U-Pb zircon ages by the creation of more concordant systems using an air abrasion technique. Geochimica et Cosmochimica Acta, vol. 46, p. 637-649, doi: 10.1016/0016-7037(82)90 165-X.

Mattinson, J.M., 2005. Zircon U-Pb chemical abrasion ("CA-TIMS") method: Combined annealing and multi-step partial dissolution analysis for improved precision and accuracy of zircon ages. Chemical Geology, vol. 220, p. 47-66, doi: 10.1016/j.chemgeo.2005.03.011.

Mortensen, J.K., 1983. Age and evolution of the Yukon-Tanana terrane, southeastern Yukon Territory. Unpublished PhD dissertation, University of California, Santa Barbara, 115 p.

Mortensen, J.K., 1992. Pre-Mid-Mesozoic tectonic evolution of the Yukon-Tanana Terrane, Yukon and Alaska. Tectonics, vol. 11, p. 836-853, doi: 10.1029/91TC01169.

Mortensen, J.K. and Jilson, G.A., 1985. Evolution of the Yukon-Tanana terrane: evidence from southeastern Yukon Territory. Geology, vol. 13, p. 806-810, doi: 10.1130/0091-7613(1985)13<806:EOTYTE>2.0.CO;2.

Mortensen, J.K., Hall, B.V., Bissig, T., Friedman, R.M., Danielson, T., Oliver, J., Rhys, D.A., Ross, K.V. and Gabites, J.E., 2008. Age and paleotectonic setting of volcanogenic massive sulfide deposits in the Guerrero terrane of central Mexico: Constraints from U-Pb age and Pb isotope studies. Economic Geology, vol. 103, p. 117-140, doi: 10.2113/gsecongeo.103.1.117.

Murphy, D.C., 1998. Stratigraphic framework for syngenetic mineral occurrences, Yukon-Tanana Terrane south of Finlayson Lake: A progress report. *In*: Yukon Exploration and Geology 1997, C.F. Roots (ed.), Exploration and Geological Services Division, Yukon Region, Indian and Northern Affairs Canada, p. 51-58.

Murphy, D.C. and Piercey, S.J., 1999a. Geological map of parts of Finlayson Lake (105G/7, 8 and parts of 1, 2, and 9) and Frances Lake (parts of 105H/5 and 12) map areas, southeastern Yukon. Exploration and Geological Services Division, Yukon Region, Indian and Northern Affairs Canada, Open File 1999-4, 1:100 000 scale.

Murphy, D.C. and Piercey, S.J., 1999b. Geological map of Wolverine Lake area, Pelly Mountains (NTS 105G/8), southeastern Yukon. Exploration and Geological Services Division, Yukon Region, Indian and Northern Affairs Canada, Open File 1999-3, 1:50 000 scale.

Murphy, D.C. and Piercey, S.J., 1999c. Finlayson project: Geological evolution of Yukon-Tanana Terrane and its relationship to Campbell Range belt, northern Wolverine Lake map area, southeastern Yukon. *In*: Yukon Exploration and Geology 1998, C.F. Roots and D.S. Emond (eds.), Exploration and Geological Services Division, Yukon Region, Indian and Northern Affairs Canada, p. 47-62.

Murphy, D.C., Colpron, M., Roots, C.F., Gordey, S.P. and Abbott, J.G., 2002. Finlayson Lake Targeted Geoscience Initiative (southeastern Yukon), Part 1: Bedrock geology. *In*: Yukon Exploration and Geology 2001, D.S. Emond, L.H. Weston and L.L. Lewis (eds.), Exploration and Geological Services Division, Yukon Region, Indian and Northern Affairs Canada, p. 189-207.

Murphy, D.C., Mortensen, J.K., Piercey, S.J., Orchard, M.J. and Gehrels, G.E., 2006. Mid-Paleozoic to early Mesozoic tectonostratigraphic evolution of Yukon-Tanana and Slide Mountain terranes and affiliated overlap assemblages, Finlayson Lake massive sulphide district, southeastern Yukon. *In*: Paleozoic Evolution and Metallogeny of Pericratonic Terranes at the Ancient Pacific Margin of North America, Canadian and Alaskan Cordillera, M. Colpron and J.L. Nelson (eds.), Geological Association of Canada, Special Paper 45, p. 75-106.

Nelson, J.L., Colpron, M., Piercey, S.J., Dusel-Bacon, C., Murphy, D.C. and Roots, C.F., 2006. Paleozoic tectonic and metallogenic evolution of the pericratonic terranes in Yukon, northern British Columbia and eastern Alaska. *In*: Paleozoic Evolution and Metallogeny of Pericratonic Terranes at the Ancient Pacific Margin of North America, Canadian and Alaskan Cordillera, M. Colpron and J.L. Nelson (eds.), Geological Association of Canada, Special Paper 45, p. 323-360.

Peter, J.M., Layton-Matthews, D., Piercey, S.J., Bradshaw, G.D., Paradis, S. and Bolton, A., 2007. Volcanic-hosted massive sulphide deposits of the Finlayson Lake District, Yukon. *In*: Mineral Deposits of Canada: A Synthesis of Major Deposit-Types, District Metallogeny, the Evolution of Geological Provinces, and Exploration Methods, W.D. Goodfellow, (ed.), Geological Association of Canada, Mineral Deposits Division, Special Publication No. 5, p. 471-508.

Piercey, S.J., 2001. Petrology and tectonic setting of felsic and mafic volcanic and intrusive rocks in the Finlayson Lake volcanic-hosted massive sulphide (VHMS) district, Yukon, Canada: A record of mid-Paleozoic arc and back-arc magmatism and metallogeny. Unpublished PhD dissertation, University of British Columbia, Vancouver, Canada, 324 p.

Piercey, S.J., 2011. The setting, style, and role of magmatism in the formation of volcanogenic massive sulfide deposits. Mineralium Deposita, vol. 46, p. 449-471, doi: 10.1007/s00126-011-0341-z.

Piercey, S.J. and Colpron, M., 2009. Composition and provenance of the Snowcap assemblage, basement to the Yukon-Tanana terrane, northern Cordillera: Implications for Cordilleran crustal growth. Geosphere, vol. 5, p. 439-464, doi: 10.1130/GES00505.S3.

Piercey, S.J. and Murphy, D.C., 2000. Stratigraphy and regional implications of unstrained Devono-Mississippian volcanic rocks in the Money Creek thrust sheet, Yukon-Tanana Terrane, Southeastern Yukon. *In*: Yukon Exploration and Geology 1999, D.S. Emond and L.H. Weston (eds.), Exploration and Geological Services Division, Yukon Region, Indian and Northern Affairs Canada, p. 67-78.

Piercey, S.J., Paradis, S., Murphy, D.C. and Mortensen, J.K., 2001. Geochemistry and paleotectonic setting of felsic volcanic rocks in the Finlayson Lake volcanic-hosted massive sulfide district, Yukon, Canada. Economic Geology, vol. 96, p. 1877-1905, doi: 10.2113/gsecongeo.96.8.1877.

Piercey, S.J., Mortensen, J.K., Murphy, D.C., Paradis, S. and Creaser, R.A., 2002a. Geochemistry and tectonic significance of alkalic mafic magmatism in the Yukon-Tanana terrane, Finlayson Lake region, Yukon. Canadian Journal of Earth Sciences, vol. 39, p. 1729-1744, doi: 10.1139/E02-090.

Piercey, S.J., Murphy, D.C., Mortensen, J.K. and Paradis, S., 2002b. Boninitic magmatism in a continental margin setting, Yukon-Tanana terrane, southeastern Yukon, Canada. Geology, vol. 29, p. 731-734, doi: 1130/0091-7613(2001)029<0731:BMIACM>2.0.CO;2.

Piercey, S.J., Paradis, S.J., Peter, J.M. and Tucker, T.L., 2002c. Geochemistry of basalt from the Wolverine volcanic-hosted massive-sulphide deposit, Finlayson Lake district, Yukon Territory. Geological Survey of Canada, Current Research 2002-A3, 11 p.

Piercey, S.J., Mortensen, J.K. and Creaser, R.A, 2003. Neodymium isotope geochemistry of felsic volcanic and intrusive rocks from the Yukon-Tanana Terrane in the Finlayson Lake Region, Yukon, Canada. Canadian Journal of Earth Sciences, vol. 40, p. 77-97, doi: 10.1139/e02-094.

Piercey, S.J., Murphy, D.C., Mortensen, J.K. and Creaser, R.A., 2004. Mid-Paleozoic initiation of the northern Cordilleran marginal backarc basin: Geologic, geochemical, and neodymium isotope evidence from the oldest mafic magmatic rocks in the Yukon-Tanana terrane, Finlayson Lake district, southeast Yukon, Canada. Bulletin of the Geological Society of America, vol. 116, p. 1087-1106, doi: 10.1130/B25162.1.

Piercey, S.J., Nelson, J.L., Colpron, M., Dusel-Bacon, C., Simard, R.-L. and Roots, C.F., 2006. Paleozoic magmatism and crustal recycling along the ancient Pacific margin of North America, northern Cordillera. In: Paleozoic Evolution and Metallogeny of Pericratonic Terranes at the Ancient Pacific Margin of North America, Canadian and Alaskan Cordillera, M. Colpron and J.L. Nelson (eds.), Geological Association of Canada, Special Paper 45, p. 281-322.

Piercey, S.J., Peter, J.M., Mortensen, J.K., Paradis, S., Murphy, D.C. and Tucker, T.L., 2008. Petrology and U-Pb geochronology of footwall porphyritic rhyolites from the wolverine volcanogenic massive sulfide deposit, Yukon, Canada: Implications for the genesis of massive sulfide deposits in continental margin environments. Economic Geology, vol. 103, p. 5-33, doi: 10.2113/gsecongeo.103.1.5.

Piercey, S.J., Murphy, D.C. and Creaser, R.A., 2012. Lithosphere-asthenosphere mixing in a transform-dominated late Paleozoic backarc basin: Implications for northern Cordilleran crustal growth and assembly. Geosphere, vol. 8, p. 716-739, doi: 10.1130/GES00757.1.

Piercey, S.J., Gibson, H.L., Tardif, N. and Kamber, B.S., 2016. Ambient redox and hydrothermal environment of the Wolverine volcanogenic massive sulfide deposit, Yukon: Insights from lithofacies and lithogeochemistry of Mississippian host shales. Economic Geology, vol. 111, p. 1439-1463, doi: 10.2113/econgeo.111.6.1439.

Piercey, S.J., Beranek, L.P. and Hanchar, J.M., 2017. Mapping magma prospectivity for Cordilleran volcanogenic massive sulphide (VMS) deposits using Nd-Hf isotopes: Preliminary results. In: Yukon Exploration and Geology 2016, K.E. MacFarlane and L.H. Weston, (eds.), Yukon Geological Survey, p. 197-205.

Rosa, D.R.N., Finch, A.A., Andersen, T. and Inverno, C.M.C., 2009. U-Pb geochronology and Hf isotope ratios of magmatic zircons from the Iberian Pyrite Belt. Mineralogy and Petrology, vol. 95, p. 47-69, doi: 10.1007/s00710-008-0022-5.

Ross, P.S., McNicoll, V.J., Debreil, J.A. and Carr, P., 2014. Precise U-Pb geochronology of the Matagami mining camp, Abitibi greenstone belt, Quebec: Stratigraphic constraints and implications for volcanogenic massive sulfide exploration. Economic Geology, vol. 109, p. 89-101, doi: 10.2113/econgeo.109.1.89.

Schmitz, M.D. and Kuiper, K.F., 2013. High-precision geochronology. Elements, vol. 9, p. 25-30, doi: 10.2113/gselements.9.1.25.

Sebert, C., Hunt, J.A. and Foreman, I.J., 2004. Geology and lithogeochemistry of the Fyre Lake copper-cobalt-gold sulphide-magnetite deposit, southeastern Yukon. Yukon Geological Survey, Open File 2004-17, 46 p.

Tempelman-Kluit, D.J., 1979. Transported cataclasite, ophiolite and granodiorite in Yukon: Evidence of arc-continent collision. Geological Survey of Canada, Paper 79-1, 27 p.

Appendix 1. *Geochronology compilation from the Finlayson Lake region, Yukon.*

Sample[1]	Thrust Sheet	Unit	Age (Ma)	Error (2σ)	Analysis Comments	Quality	Method[2]	Reference
HD-35	Big Campbell	Fire Lake formation	365	1.2	3-point discordant array	Moderate	ID-TIMS	Murphy et al. (2006)
96DM-065	Big Campbell	Fire Lake formation	366.3	10.2	Highly discordant	Poor	ID-TIMS	Murphy et al. (2006)
98DM-088	Big Campbell	Grass Lakes plutonic suite	362.2	3.3	3-point weighted Pb-Pb of Pb-loss discordia	Moderate	ID-TIMS	Murphy et al. (2006)
GG-19	Big Campbell	Grass Lakes plutonic suite	359.9	0.9	1 concordant fraction; Pb-loss and inheritance	Good	ID-TIMS	Murphy et al. (2006)
96DM-119	Big Campbell	Grass Lakes plutonic suite	357.3	2.8	4-point Pb-loss discordia with Pb-Pb weighted age	Moderate	ID-TIMS	Murphy et al. (2006)
FV-49	Big Campbell	Kudz Ze Kayah formation	351.4	1.7	Uncertain	Uncertain	ID-TIMS	Mortensen, unpublished data (2004)
FV-16	Big Campbell	Kudz Ze Kayah formation	359.8	9	Uncertain	Uncertain	ID-TIMS	Mortensen, unpublished data (2004)
P98-KZK2	Big Campbell	Kudz Ze Kayah formation	356.9	5.3	6-point discordia; Pb-loss and inheritence	Good	ID-TIMS	Piercey (2001)
FV-21	Big Campbell	Wolverine Lake group	356.2	0.9	1 concordant fraction; inheritance in 3 fractions	Good	ID-TIMS	Murphy et al. (2006)
P98-069A	Big Campbell	Wolverine Lake group	346.6	2.2	3 concordant fractions	Excellent	ID-TIMS	Piercey et al. (2008)
WW-00-01	Big Campbell	Wolverine Lake group	347.8	1.3	2 concordant fractions	Excellent	ID-TIMS	Piercey et al. (2008)
Sable	Big Campbell	Wolverine Lake group	352.4	1.5	2 concordant fractions; Pb-loss and inheritance	Moderate	ID-TIMS	Piercey et al. (2008)
Puck	Big Campbell	Wolverine Lake group	356.9	0.5	1 concordant fraction, potential inheritance	Good	ID-TIMS	Piercey et al. (2008)
GP4F-1	Big Campbell	Wolverine Lake group	346.9	0.7	2 concordant fractions; Pb-loss in 4 fractions	Excellent	ID-TIMS	Murphy et al. (2006)
98DM-GDR	Big Campbell	Wolverine Lake group	347.3	3.7	2-point discordia, Pb-Pb weighted age; Pb-loss array	Moderate	ID-TIMS	Murphy et al. (2006)
FV-27	Money Creek	Waters Creek formation	360.8	0.8	3-point discordia; inheritance	Moderate	ID-TIMS	Murphy et al. (2006)
Sample 2	Money Creek	Waters Creek formation	360.5	0.9	5-point discordia; inheritance	Moderate	ID-TIMS	Mortensen (1992)
SL-45*	Money Creek	Simpson Lake plutonic suite	357.9	1.3	2 condordant fractions	Excellent	ID-TIMS	Murphy et al. (2006)
TRP-22	Money Creek	Simpson Lake plutonic suite	356.9	0.6	1 concordant fraction	Good	ID-TIMS	Murphy et al. (2006)
ARG-32	Money Creek	Simpson Lake plutonic suite	356	2.0	4-point Pb-loss discordia with Pb-Pb weighted age	Moderate	ID-TIMS	Mortensen, unpublished data (2004)
01DM-238	Money Creek	Tichitua River formation	344.5	2.5	3-point discordia; inheritance	Moderate	ID-TIMS	Murphy et al. (2006)
PR-21	Money Creek	Tichitua River formation	352.5	2.6	1 concordant fraction	Good	ID-TIMS	Murphy et al. (2006)
03DM-022	Money Creek	Tichitua River formation	346.8	2.0	2 concordant fractions	Excellent	ID-TIMS	Murphy et al. (2006)
03DM-023	Money Creek	Tichitua River formation	347.7	1.4	3 concordant fractions	Excellent	ID-TIMS	Murphy et al. (2006)
QP-30	Cleaver Lake	Unnamed	360.5	1.9	Uncertain	Uncertain	ID-TIMS	Mortensen (1992)
ARG-32	Cleaver Lake	Unnamed	356.1	0.9	Pb-Pb discordia; Pb-loss	Moderate	ID-TIMS	Murphy et al. (2006)
SA-02	Cleaver Lake	Simpson Range plutonic suite	348.4	0.8	3-point lower intercept	Moderate	ID-TIMS	Murphy et al. (2006)
SG94-14	Cleaver Lake	Simpson Range plutonic suite	345.9	1.2	3-point discordia; inheritance	Moderate	ID-TIMS	Grant (1997)
SG94-11	Cleaver Lake	Simpson Range plutonic suite	356.5	3.4	2-point discordia; inheritance	Poor	ID-TIMS	Grant (1997)

Appendix 1 continued.

Sample[1]	Thrust Sheet	Unit	Age (Ma)	Error (2σ)	Analysis Comments	Quality	Method[2]	Reference
SA-28	Cleaver Lake	Simpson Range plutonic suite	354.9	1.8	Pb-Pb discordia; Pb-loss	Moderate	ID-TIMS	Murphy et al. (2006)
TRP-22	Cleaver Lake	Simpson Range plutonic suite	354	1.0	Uncertain	Uncertain	ID-TIMS	Mortensen, unpublished data (2004)
TRP-22	Cleaver Lake	Simpson Range plutonic suite	356.9	0.6	Uncertain	Uncertain	ID-TIMS	Mortensen, unpublished data (2004)
AG-48	Cleaver Lake	Hoole River orthogneiss	342	7.1	Uncertain	Uncertain	ID-TIMS	Mortensen, unpublished data (2004)
03FD039-2	Cleaver Lake	Klatsa Metamorphic Complex	353.1	2.4	Metamorphic overgrowths; inverse isochron; age of metamorphism	Moderate	SHRIMP	Devine et al. (2006)
03FD056-2	Cleaver Lake	Klatsa Metamorphic Complex	353	3.7	Metamorphic overgrowths; inverse isochron; age of metamorphism	Moderate	SHRIMP	Devine et al. (2006)
03FD231-1	Cleaver Lake	Klatsa Metamorphic Complex	368	10	Igneous cores; large errors	Poor	SHRIMP	Devine et al. (2006)
03FD039-2**	Cleaver Lake	Klatsa Metamorphic Complex	353.4	0.79	Ar-Ar white mica; plateau age; exhumation age	Excellent	Laser NG-MS	Devine et al. (2006)

Notes: 1 Analyses are U-Pb zircon geochronology unless noted: *=U-Pb titanite; **=$^{40}Ar/^{39}Ar$ white mica.
2 ID-TIMS = isotope dilution-thermal ionization spectrometry (air abrasion); SHRIMP = sensitive high-resolution ion microprobe; Laser NG-MS = laser noble gas mass spectrometry.

Stratigraphic affinity of late Neoproterozoic limestone in the vicinity of Tillei and McPherson lakes, 105H/13, 14, southeastern Yukon

D. Moynihan
Yukon Geological Survey

Moynihan, D., 2018. Stratigraphic affinity of late Neoproterozoic limestone in the vicinity of Tillei and McPherson lakes, 105H/13, 14, southeastern Yukon. *In:* Yukon Exploration and Geology 2017, K.E. MacFarlane (ed.), Yukon Geological Survey, p. 129-137.

ABSTRACT

The area around Tillei and McPherson lakes includes extensive exposure of a relatively thick, late Neoproterozoic limestone. The limestone is lithologically similar to the Espee Formation of the Ingenika Group, but is in geological continuity with the Hyland Group. The Hyland and Ingenika groups are age-equivalent sequences that were in close proximity before they were separated by Cenozoic dextral displacement on the Tintina fault. The area may therefore contain evidence for stratigraphic linkages between the two groups. The limestone is interpreted to have been deposited in a high-standing region outboard of the Hyland Group type-area. Further work is required to determine the extent to which late Neoproterozoic paleobathymetry aligns with Paleozoic platform/basin margins.

* *david.moynihan@gov.yk.ca*

INTRODUCTION

The oldest rocks exposed in the core of the Selwyn-Mackenzie fold belt (Gordey and Anderson, 1993; Fig. 1) belong to the Windermere Supergroup (Ross, 1991). This supergroup comprises Cryogenian-Terreneuvian rocks that were deposited during episodes of rifting that led to formation of the western Laurentian ancestral margin. The most extensive exposures of the Windermere Supergroup in southern Yukon are mostly Ediacaran-Terreneuvian rocks of the Hyland (Gordey and Anderson, 1993) and Ingenika groups (Mansy and Gabrielse, 1978; Fig. 1). These groups are restricted to opposite sides of the Tintina fault, but were in close proximity to one another prior to >430 km of dextral displacement during the Cenozoic (Gabrielse *et al.*, 2006).

Correlation between the two groups is hampered by a scarcity of fossils and volcanic rocks, but there are clear lithological similarities (Fig. 2), in particular the presence of a late Neoproterozoic limestone that separates mostly coarse clastic rocks from overlying varicoloured mudstone/siltstone. Limestone and dolostone comprise a relatively small part of the Hyland and Ingenika groups, but calcareous units form useful marker horizons that facilitate stratigraphic subdivision of the groups and recognition of the structural geometry.

The Hyland and Ingenika groups are overlain by contrasting Paleozoic sequences. The Ingenika Group underlies Paleozoic rocks of the Cassiar platform (Fritz *et al.*, 1991), while the Hyland Group was succeeded by deeper marine strata of the Selwyn basin (Gordey and Anderson, 1993; Fig. 1). Dextral displacement on the Tintina fault separated most of the Cassiar platform from its northernmost part. Its inferred northern extension, now located east of the Tintina fault, is called the McEvoy platform, and includes many of the same distinctive Paleozoic rocks as the main part of the Cassiar platform. Although Paleozoic rocks of the Cassiar platform have been identified on either side of the Tintina fault, the same is not true of the Ingenika Group.

Unresolved questions therefore include the following:

1. What is the extent of similarities/differences between the Hyland and Ingenika groups, and
2. If they are as similar as they appear to be, when did their depositional histories diverge?

Relatively thick Neoproterozoic limestone/dolostone in the region around Tillei and McPherson lakes (Figs. 3 and 4a) was first recognized by Roots *et al.* (1966), and the area was revisited during the summer of 2017 as part of an ongoing bedrock mapping project in the Hyland region of southeastern Yukon. The area is interesting because it includes the westernmost exposures of the Hyland Group in southeastern Yukon, and also lies in close proximity to Paleozoic rocks of the McEvoy platform. The area may therefore shed light on the relationship between upper parts of the Hyland and Ingenika groups. This paper provides a description of the limestone and adjacent units, outlines the stratigraphic position of the limestone, and discusses its implications for regional correlations.

REGIONAL STRATIGRAPHY

HYLAND GROUP

The Hyland Group, which was defined in the Little Nahanni River area (NTS 105I), comprises the Yusezyu Formation and the overlying Narchilla Formation (Gordey and Anderson, 1993; Fig. 2). The Yusezyu Formation is dominated by sandstone, conglomerate ('grit') and shale, with minor calcareous horizons, while the Narchilla Formation is mostly variably coloured (grey, black, green and maroon) mudstone with lesser sandstone. A discontinuous, <15 m-thick limestone (limestone member of Yusezyu Formation; Gordey and Anderson, 1993) typically marks the boundary between the two formations, and is stratigraphically equivalent to thicker limestone/dolostone of the Algae formation in the Niddery Lake area (NTS 105O; Cecile, 2000) and the Risky Formation of the Mackenzie and Ogilvie Mountains (Turner *et al.*, 2011). Moynihan (2016, 2017) recognized the presence of prominent limestone/marble horizons at deeper levels in the Yusezyu Formation in the upper Hyland area (NTS 105H), including distinctive fetid limestone, and a stratigraphically lower marble/calc-silicate layer up to 60 m thick (Hyland marble of Moynihan, 2016; Fig. 2). There are few age constraints on the Hyland Group but based on trace fossils, the Precambrian-Cambrian boundary is low within the Narchilla Formation (Hofmann *et al.*, 1994).

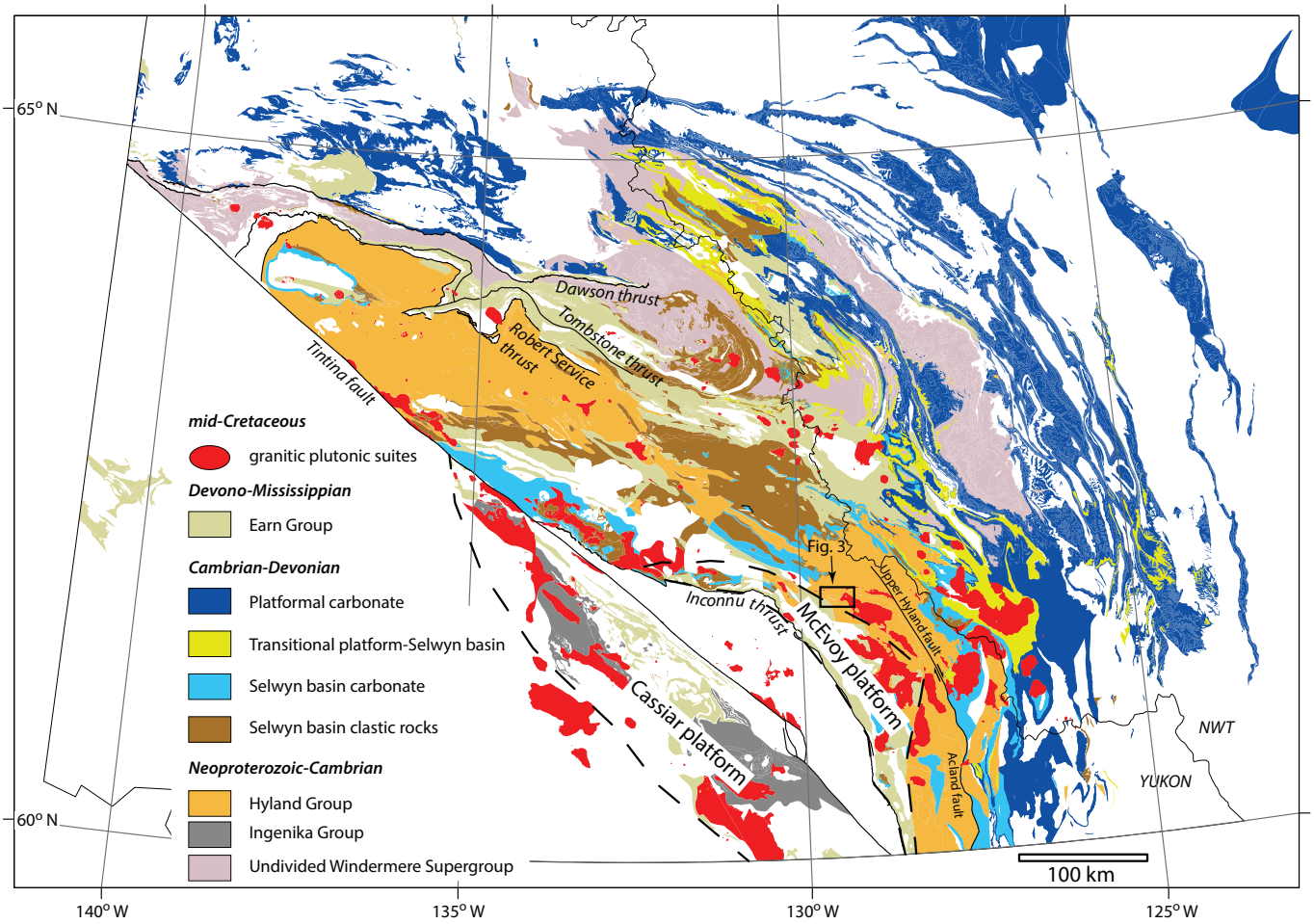

Figure 1. *Neoproterozoic – lower Paleozoic rocks within the arcuate Selwyn-Mackenzie fold and thrust belt, in Yukon and NWT (Colpron et al., 2016). The Hyland Group crops out extensively in the core of the fold belt east of the Tintina fault. Rocks of the same age west of the Tintina fault belong to the Ingenika Group. Prior to Cenozoic dextral displacement on the Tintina fault, the Hyland and Ingenika groups were continuous with one another.*

INGENIKA GROUP

The oldest part of the Ingenika Group (Mansy and Gabrielse, 1978) is the Swannell Formation, which comprises resistant sandstone/conglomerate and shale. This is overlain by the less resistant, generally finer-grained Tsaysdiz Formation, followed by the Espee Formation – a thick cliff-forming cryptograined limestone-dolostone unit that is characterized by abundant pisoliths/oolites and ferrodolomite nodules in its type area (Mansy and Gabrielse, 1978). The youngest part of the Ingenika Group is represented by the Stelkuz Formation, which includes varicoloured, typically green and maroon shale, with lesser limestone and sandstone.

STRATIGRAPHY OF THE TILLEI AND MCPHERSON LAKES AREA

Neoproterozoic-Cambrian rocks, including the thick limestone-dolostone exposures in the area (Fig. 3) were assigned to the Hyland Group by Gordey and Makepeace (2001). Deepest stratigraphic levels are exposed in the eastern part of the area illustrated in Figure 3, where they form the core of an overturned antiform. These rocks, which correlate with parts of the middle/lower Yusezyu Formation (as defined in Moynihan, 2017) are dominated by medium to thick-bedded sandstone and grit, interlayered with brown-weathering mudstone/phyllite. They form relatively resistant topography, and sandstone-rich sections impart a ribbed appearance to hillslopes. These rocks are overlain by a distinctive fetid

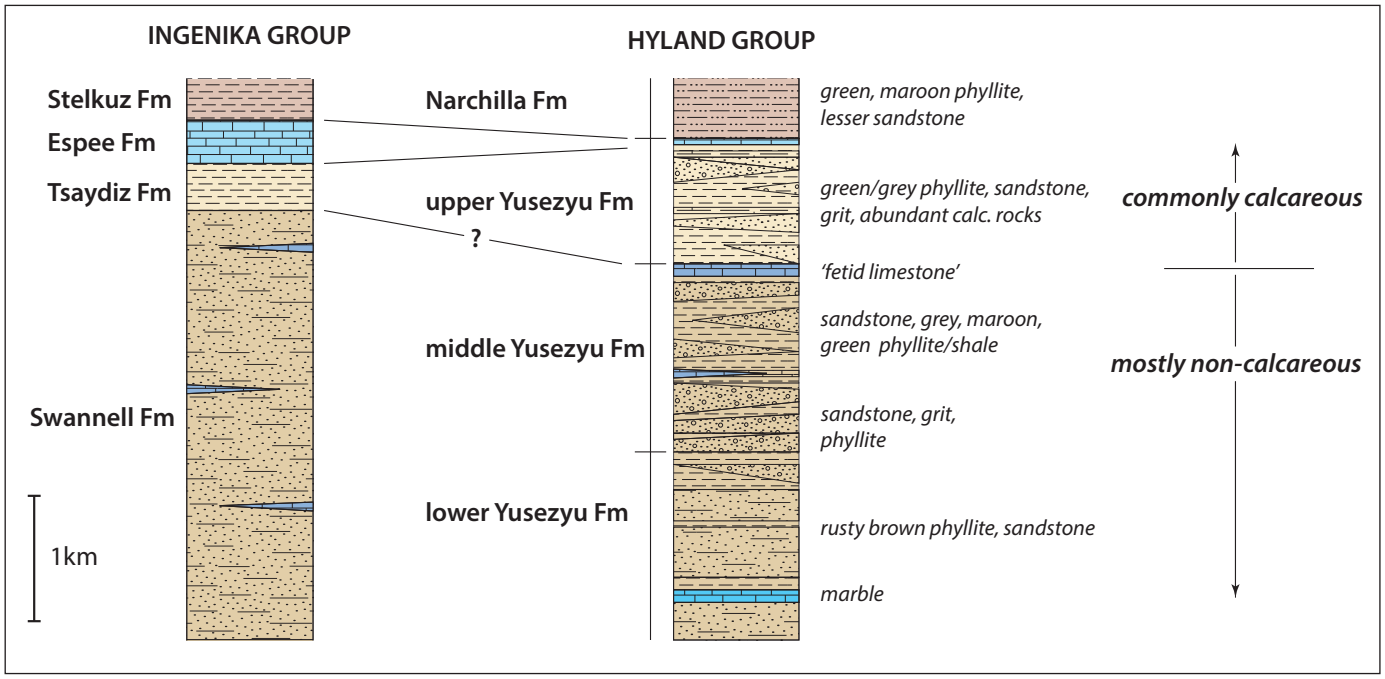

Figure 2. *Generalized stratigraphy of the Hyland and Ingenika groups; information from Mansy and Gabrielse (1978) and Moynihan (2017).*

limestone (*see* Moynihan 2017), followed by the upper part of the Yusezyu Formation, which includes sandstone, conglomerate, minor limestone and abundant mudstone/phyllite, including a thick interval of green (locally maroon) mudstone/phyllite above the fetid limestone.

The latest Neoproterozoic limestone-dolostone is a resistant (cliff-forming) unit that is dominated by pure, pale grey weathering, pale to medium grey limestone (Fig. 4b,c). The limestone is mostly blocky and forms coarse talus with irregular-shaped blocks generally >5 cm in diameter. Creamy-brown dolomite nodules (ferrodolomite?; generally ~2-4 mm in diameter; Fig. 4c) are common throughout the limestone, and locally form clusters. Bedding is rarely discernible, but banding is common in regions of higher metamorphic grade/strain. In these areas, tectonic foliation wraps dolomite nodules and clusters, giving rise to a streaky, marbled appearance; locally ferrodolomite clusters form porphyroclasts in a matrix of recrystallized calcite marble.

East of Tillei Lake, there is a large region of brecciated dolostone adjacent to a N-S striking late normal fault. Elsewhere, between Tillei and McPherson Lakes, dolostone is commonly developed in the upper part of the unit. The dolostone is a cream to creamy-brown colour with sucrosic texture and local rust-stained sections (Fig. 4d). Space-filling sparry calcite is common and zebra dolostone is locally developed.

The upper contact of the limestone unit was observed in two areas. East of Tillei Lake, where it is isoclinally infolded with the overlying phyllite (Fig. 4e), the contact between the limestone and overlying fine clastic unit consists of a zone, 1-5 m thick comprising clasts, pods and lenses of limestone in a green phyllite matrix (Fig. 4f). Lenses are up to 1 m thick and are composed exclusively of tightly packed pisoids/ooids (Fig. 4g). Limestone ooids/pisoids weather grey while dolomitized equivalents are orange-brown. In the north of the area, a pisolitic layer was not observed at the contact, but there is a 3-5 m thick interval within the overlying shale (Fig. 4h) that consists of abundant limestone pods and lenses within green phyllite (Fig. 4i).

The thickness of the limestone is difficult to estimate due to the effects of folding; nevertheless it is clear that there is significant variation in its thickness. In the northernmost part of the study area the limestone is approximately 10 to 30 m thick, while between Tillei and McPherson lakes it may exceed 100 m in true (stratigraphic) thickness.

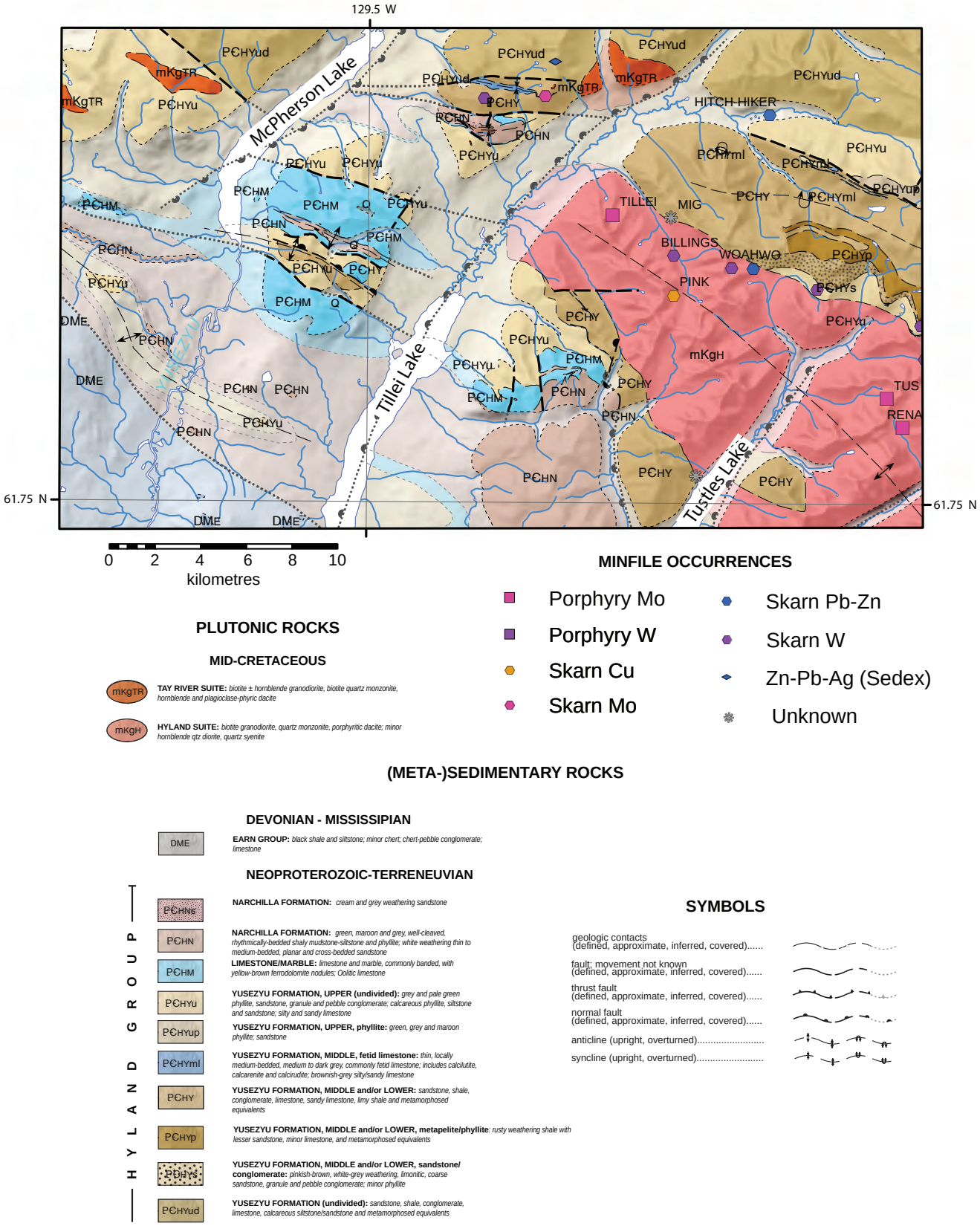

Figure 3. *Geological map of the study area, showing extensive exposure of late Neoproterozoic limestone in the region around Tillei and McPherson lakes, SE Yukon (NTS 105H/13, 14). SEDEX=sedimentary exhalative.*

DISCUSSION

DEPOSITIONAL ENVIRONMENT

The limestone in the study area is homogeneous and clean, devoid of siliciclastic rocks or structures indicative of deep marine deposition. The only macroscopically visible textures preserved in the limestone are the dense ooids/pisoliths that form layers, pods and lenses at, or near, the base of the overlying shale; these layers are interpreted to have formed in a platformal environment before being reworked into overlying shale. While sedimentological interpretation of the limestone is inhibited by the level of deformation/recrystallization, it is reasonable to infer that the clean, homogeneous, relatively thick limestone unit was deposited in a shallow marine environment.

STRATIGRAPHIC CORRELATIONS

The limestone around Tillei and McPherson lakes is in the same stratigraphic position as the limestone member at the top of the Yusezyu Formation, but differs in its character and depositional environment. The upper limestone member of the Yusezyu Formation in the Hyland River and Little Nahanni River region (Gordey and Anderson, 1993) includes interbedded shale and limestone conglomerate, and exhibits sedimentary structures indicative of deposition by turbidity currents below wave base. Lithologically, the limestone in the Tillei and McPherson lakes area has more in common with the Espee Formation, including the ubiquitous presence of distinctive cream-brown ferrodolomite nodules and oolitic/pisolitic limestone.

Given the continuity of Neoproterozoic-early Cambrian rocks in the area with the type area of the Hyland Group, and similarities with the Espee Formation, the study area appears to represent a link between the Hyland and Ingenika groups. Rocks underlying the limestone are similar to those of the Swannell and Tsaydiz formations, just as overlying rocks resemble the Stelkuz Formation. Distinction between the Hyland and Ingenika groups in this area may therefore be a question of nomenclature rather than substance. The fetid limestone marker unit extends throughout the study area and is a distinctive part of the Hyland Group; the linkages proposed here could be confirmed if this marker unit were to be recognized elsewhere in the Ingenika Group.

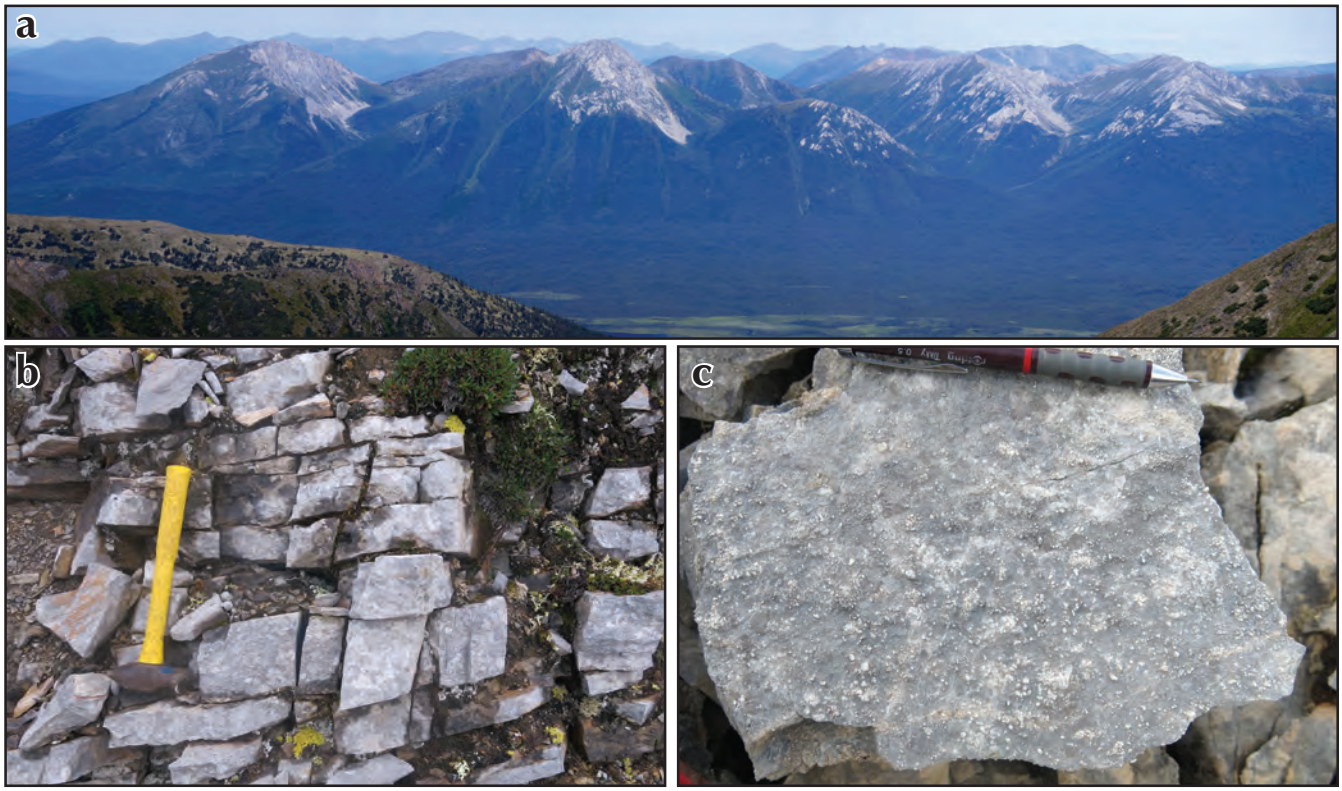

Figure 4. *Field photographs:* ***(a)*** *panorama looking NW across Tillei Lake towards exposures of cliff-forming, late Neoproterozoic limestone; relief is approximately 1000 m;* ***(b)*** *faint lamination visible in blocky, medium grey weathering limestone; hammer for scale;* ***(c)*** *dolomite nodules weather out from the surface of grey limestone. Nodules are commonly creamy-brown on broken surfaces; pencil for scale;* **continued on next page.**

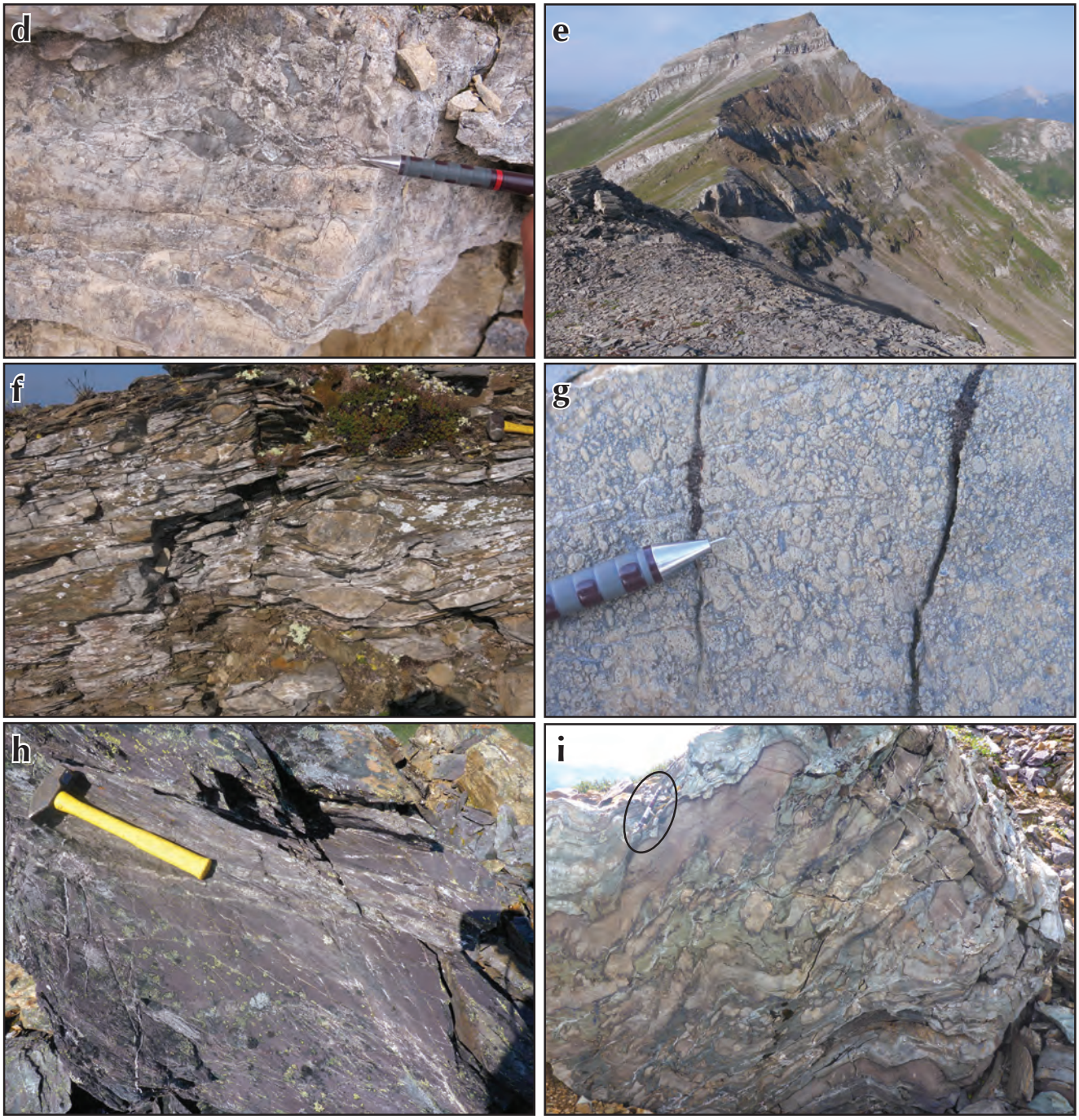

Fig. 4 continued - (d) *sparry calcite-filled vugs in cream-coloured, sugary-textured dolostone; pencil for scale;* ***(e)*** *isoclinally folded upper contact between limestone and stratigraphically overlying shale; SE of Tillei Lake; relief is approximately 300 m;* ***(f)*** *pods and lenses of pisolitic limestone in matrix of green shale. This layer marks the transition between the limestone and overlying shale-dominated unit. Hammer in upper right for scale;* ***(g)*** *densely-packed, concentrically zoned ooliths and pisoliths at the top of the late Neoproterozoic limestone unit; pencil for scale;* ***(h)*** *cleaved, maroon mudstone and siltstone; hammer for scale; and* ***(i)*** *limestone lenses and pods in a green mudstone matrix; pencil for scale (circled).*

REGIONAL VARIATION IN THE THICKNESS AND CHARACTER OF THE LATE NEOPROTEROZOIC LIMESTONE

There is considerable variations in the thickness and character of the late Neoproterozoic limestone throughout eastern Yukon. Although thin to non-existent in the type area of the Hyland Group (Gordey and Anderson, 1993), and thin (<15 m) east of the Hyland River (Moynihan, 2016), it is thicker in the study area, and in parts of the Sheldon Lake-Tay River area (NTS 105J, K; Gordey, 2013). Thick-bedded, fine-crystalline limestone is up to 250 m thick between the South Macmillan and Ridell rivers, while planar and cross-laminated limestone, interbedded with maroon and green shale is 40-50 m thick near Dragon Lake (Gordey, 2013). In the Niddery Lake (NTS 105O; Cecile, 2000) and Nadaleen River areas (NTS 106C; Moynihan, 2014), the equivalent limestone – the Algae Formation – is more than 400 m thick in places.

Further work, including detailed facies analysis is required to interpret the implications of variations in thickness and rock types for paleogeography; however, a reasonable interpretation of available information is that, rather than a simple SW-deepening basin (*c.f.*, Gordey and Anderson, 1993), there was heterogeneous bathymetry in eastern Yukon during the latest Neoproterozoic. The type area of the Hyland Group likely occupied a paleogeographic low, while the current study area, along with the Ingenika Group and parts of the Sheldon Lake-Tay River area were deposited in a higher-standing regions. The extent to which latest Neoproterozoic bathymetry aligns with the depositional environments that developed during the Paleozoic (*i.e.*, Selwyn basin and Cassiar/McEvoy platform) remains to be determined.

CONCLUSIONS

Late Neoproterozoic limestone/dolostone in the region around McPherson and Tillei lakes is stratigraphically equivalent to the upper limestone member of the Yusezyu Formation (Hyland Group), and the Espee Formation of the Ingenika Group. The limestone is interpreted to have been deposited in a shallow water environment on a high-standing region outboard of the Hyland Group type-area. The study area provides evidence for correlations between the Ingenika and Hyland groups of the Windermere Supergroup.

AKNOWLEDGEMENTS

Thanks to Jessie Thomson-Gladish for assistance during the 2017 field season. Thanks also to Golden Predator Ltd. for providing logistical support, and to Maurice Colpron for reviewing an earlier version of the manuscript.

REFERENCES

Cecile, M.P., 2000. Geology of the northeastern Niddery Lake map area, east-central Yukon and adjacent Northwest Territories. Geological Survey of Canada, Bulletin 553, 120 p.

Colpron, M, Israel, S., Murphy, D., Pigage, L. and Moynihan, D., 2016. Yukon bedrock geology map. Yukon Geological Survey, Open File 2016-1, scale 1:1 000 000.

Gabrielse, H., Murphy, D.C. and Mortensen, J.K., 2006, Cretaceous and Cenozoic dextral orogeny-parallel displacements, magmatism, and paleogeography, north-central Canadian Cordillera. *In:* Paleogeography of the North American Cordillera: Evidence for and against large-scale displacements, J.W. Haggart, R.J. Enkin and J.W.H. Monger (eds.). Geological Association of Canada, Special Paper 46, p. 255-276.

Fritz, W.H., Cecile, M.P., Norford, B.S., Morrow, D. and Geldsetzer, H.H., 1991. Cambrian to Middle Devonian assemblages. *In:* Geology of the Cordilleran Orogen in Canada, H. Gabrielse and C.J. Yorath (eds.). Geological Survey of Canada, Geology of Canada, no. 4, p. 151-218.

Gordey, S. P and Makepeace, A.J., 2001. Bedrock Geology, Yukon Territory. Yukon Geological Survey, Open File 2001-1; *also Geological Survey of Canada, Open File 3754*, scale 1: 1 000 000

Gordey, S.P. and Anderson, R.G., 1993. Evolution of the Northern Cordilleran miogeocline, Nahanni map area (105I), Yukon and Northwest Territories. Geological Survey of Canada, Memoir 428, 214 p.

Gordey, S.P., 2013. Evolution of the Selwyn basin region, Sheldon Lake and Tay River map areas, central Yukon. Geological Survey of Canada, Bulletin 599, 176 p.

Hofmann, H.J., Cecile, M.P. and Lane, L.S., 1994. New occurrences of Oldhamia and other trace fossils in the Cambrian of the Yukon and Ellesmere Island, Arctic Canada. Canadian Journal of Earth Sciences, vol. 31, p. 767-782.

Mansy, J.L. and Gabrielse, H., 1978. Stratigraphy, terminology and correlation of Upper Proterozoic rocks in Omineca and Cassiar Mountains, north-central British Columbia. Geological Survey of Canada, Paper 77-19, 17 p.

Moynihan, D., 2014. Bedrock Geology of NTS 106B/04, Eastern Rackla Belt. *In:* Yukon Exploration and Geology 2013, K.E. MacFarlane, M.G. Nordling and P.J. Sack (eds.), Yukon Geological Survey, p. 147-167.

Moynihan, D., 2016. Stratigraphy and structural geology of the upper Hyland River area (parts of 105H/8, 105H/9), southeast Yukon. *In:* Exploration and Geology 2015, K.E. MacFarlane and M.G. Nordling (eds.), Yukon Geological Survey, p. 187-206.

Moynihan, D., 2017. Progress report on geological mapping in the upper Hyland River region of southeastern Yukon (parts of NTS 105H/08,09,10,15,16 and 105I/02). *In:* Yukon Exploration and Geology 2016, K.E. MacFarlane and L.H. Weston (eds.), Yukon Geological Survey, p. 163-180.

Roots, E.F., Roddick, J.A. and Blusson, S.L., 1966. Geology, Frances Lake, Yukon Territory and District of Mackenzie. Geological Survey of Xanada, Preliminary Map 6-1966, scale 1:250000.

Ross, G.M., 1991. Tectonic setting of the Windermere Supergroup revisited. Geology, vol. 19, p. 1125-1128.

Turner, E.C., Roots, C.F., MacNaughton, R.B., Long, D.G.F., Fischer, B.J., Gordey, S.P., Martel, E. and Pope, M.C., 2011. Chapter 3. Stratigraphy. *In:* Geology of the central Mackenzie Mountains of the Northern Canadian Cordillera, Sekwi Mountain (105P), Mount Eduni (106A), and northwestern Wrigley Lake (95M) map areas, Northwest Territories, E. Martel, E.C. Turner and B.J. Fischer (eds). NWT Geoscience Office, NWT Special Volume 1, 423 p.

The structural framework for Carlin-type gold mineralization in the Nadaleen trend, Yukon

A. Steiner*, K. Hickey
Mineral Deposit Research Unit (MDRU), University of British Columbia

A.B. Coulter
Archer Cathro (1981) and Associates Limited

Steiner, A., Hickey, K. and Coulter, A.B., 2018. The structural framework for Carlin-type gold mineralization in the Nadaleen trend, Yukon. *In:* Yukon Exploration and Geology 2017, K.E. MacFarlane (ed.), Yukon Geological Survey, p. 139-149.

ABSTRACT

Structure imparts a significant control on the distribution of Carlin-type gold mineralization recently discovered in the Nadaleen trend, Yukon. An improved understanding of the structural framework for gold mineralization is essential for continued exploration success and interpreting ore fluid controls. Structural observations from the Osiris cluster of the Nadaleen trend indicate that NW-verging F_1 folds were refolded in response to later SSW-NNE directed contraction. F_2 folds have a subvertical ESE-striking axial plane with subvertically plunging axes on steep F_1 limbs and subhorizontal fold axes in shallow F_1 limbs. F_2 folds have a pervasive axial planar cleavage that is recognized regionally. The steeply dipping Osiris and Nadaleen faults appear to cut all folds. Mineralization is spatially associated with later NW-striking faults in the Conrad zone. Much of the folding within the mineralized Conrad limestone is synsedimentary and its geometry reflects its emplacement as an olistostrome.

* *astein@eoas.ubc.ca*

INTRODUCTION

The Nadaleen trend is an array of Carlin-type gold showings within the eastern extent of ATAC Resources Limited's Rackla Gold property in eastern-central Yukon (Fig. 1; Tucker *et al.*, 2013). It is generally considered to encompass the Osiris cluster in the east, including the Osiris, Sunrise, Ibis and Conrad ore zones, and gold occurrences within the Orion area, including the Pyramid showing and the Anubis cluster (Fig. 1b). Gold mineralization occurs in thin arsenic-rich rims on pyrite and is associated with decalcified and silicified host limestone (Tucker *et al.*, 2013; Tucker, 2015). Siliciclastic rocks are locally mineralized proximal to faults and along lithological contacts between mineralized limestone and adjacent siliciclastic rocks. In all host rocks, mineralization is spatially associated with realgar and orpiment, as well as enrichments in As, Sb, Hg and Tl (Tucker *et al.*, 2013). A deposit overview including examples of mineralization is provided by Coulter *et al.* (2018). Lithology and associated porosity and permeability exert a stratigraphic control in which mineralization is preferentially concentrated within some units and along lithological contacts at all scales. Gold distribution is also controlled by structures, with mineralization occurring in folded rock units, and proximal to fault zones at the deposit scale. At smaller scales, mineralization can be observed in stylolites, veins, minor faults, fault gouges, fracture sets and mesoscopic (metre or tens of metre-scale) fold hinges. A detailed structural understanding of the region is essential for considering structural controls on mineralization and identifying ore fluid pathways.

Building on previous work by Palmer and Kuiper (2017) and Tucker (2015), this paper presents the preliminary results of a new study to assess the role structure played in controlling fluid flow and the spatial distribution of gold mineralization along the Nadaleen trend. It summarizes field observations from the summer of 2017 during which the structure of the Osiris cluster was assessed through detailed surface geological mapping, examination of drill core, and 3D geological modelling. We present an updated geological map of the Osiris cluster, as well as structural observations and initial interpretations.

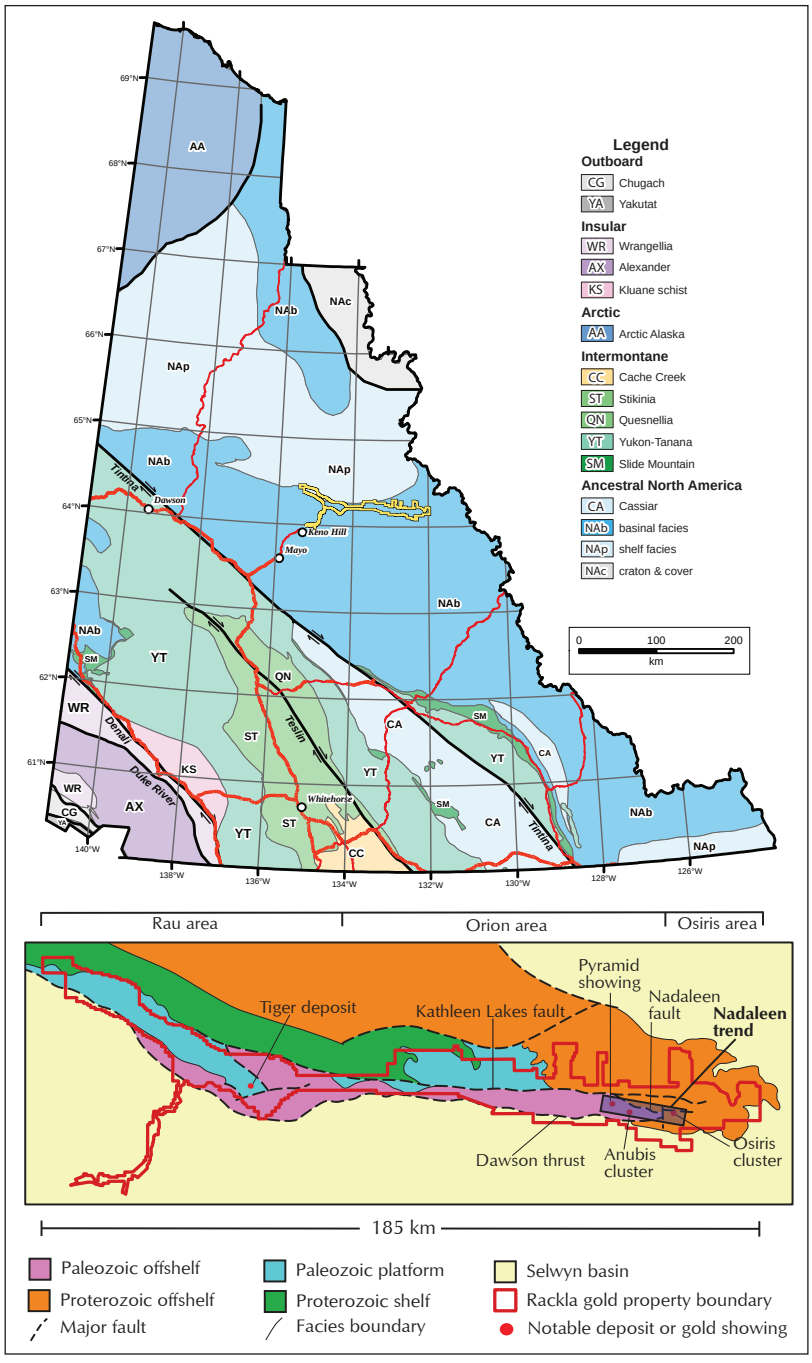

Figure 1. ***(a)*** *Terrane map of Yukon with ATAC Resources Ltd.'s Rackla Gold property outlined in yellow (after Colpron and Nelson, 2011).* ***(b)*** *Property map with overview geology and the locations of major faults and gold showings (after Colpron et al., 2013). The Nadaleen trend is highlighted in blue.*

SUMMARY OF REGIONAL AND DEPOSIT GEOLOGY

The Nadaleen trend is bound to the north by the Kathleen Lakes fault and to the south by the eastern terminus of the Dawson thrust (Colpron, 2012; Moynihan, 2014). It comprises sedimentary rocks of off-shelf slope to basinal facies that are interpreted as a zone of transitional facies at the interface between the Mackenzie Platform to the north and the Selwyn basin to the south (Colpron, 2012). The Osiris cluster is underlain by Neoproterozoic rocks of the Windermere Supergroup with volumetrically minor mafic intrusive rocks (Tucker *et al.*, 2013), while the Orion area is largely underlain by Palaeozoic sedimentary rocks ranging from Cambrian to Permian in age (Fig. 1b). The Osiris cluster (Fig. 2) is situated in the footwall of the Nadaleen fault, which juxtaposes the Cryogenian Ice Brook Formation against the Nadaleen formation (Fig. 3; Moynihan, 2016).

The Nadaleen formation forms the oldest package of rocks within the Osiris cluster (Moynihan, 2016). The lowermost unit of this formation comprises a thinly bedded silty limestone bound on both sides by a heterogeneous and somewhat chaotic siliciclastic package of sandstone, mudstone and gravel conglomerate. This package is overlain by a black shale unit, which is in turn is overlain by interleaved limestone, rudstone and siliciclastic shale. The Stenbraten member at the top of the Nadaleen formation is a grey argillite that has irregular colour bands of maroon and green in its upper strata. The Gametrail Formation, comprising variably dolomitized silty, quartz-rich limestone and interleaved rudstone, overlies the Nadaleen formation. A calcareous breccia defines the boundary between the Gametrail Formation and overlying Blueflower Formation. The Lower member of the Blueflower Formation is a distinctive thinly bedded brown calcarenite with local conglomerate beds. The overlying Middle member is a well-bedded siltstone with minor limestone beds. This member is overlain by the dolomitized Algae Formation and the maroon coloured Narchilla Formation argillite. Three intrusive igneous rock units have been recognized within the Osiris cluster. The hornblende-rich Osiris gabbro is exposed along Osiris ridge and has been dated as 465.6±4.4 Ma (Tucker, 2015). Two altered dikes have been observed in drill core and in discontinuous surface exposures. They are plagioclase and carbonate-rich with minor pyroxene (Tucker *et al.*, 2013) and have been dated as 74.4±1.0 Ma (Tucker, 2015). More details of Osiris cluster rocks can be found in the map legend (Fig. 2), stratigraphic column (Fig. 3) and in Coulter *et al.* (2018).

The Osiris cluster is generally characterized by steep, homoclinal bedding with monoclines and isolated macroscopic (hundreds of metres in scale or larger) folds. Carbonate units are folded on the mesoscopic and macroscopic scale with only local development of any associated cleavage, and without many smaller scale folds. Less competent argillaceous units accommodate deformation through widespread folding and pervasive cleavage development. Although exposure along ridge-tops is generally excellent for structural analysis, thinly to moderately bedded units tend to be *ex-situ* to some extent as a result of frost-heave and gravitational creep.

SYN-SEDIMENTARY STRUCTURES

Abundant examples of soft sediment deformation and dewatering structures are readily observed in drill core (Fig. 4) from the Nadaleen trend. Examples of soft-sediment structures include soft-sediment folding (Fig. 4a), dewatering dish structures (Fig. 4b), interrupted bedding (Fig. 4b) and convoluted bedding (Fig. 4c). Grain flows (Fig. 4d) and turbidites are also common and are indicative of gravitational instability during deposition. Many of these features, particularly dewatering structures, soft-sedimentary folding and gravity flow deposits, are also observed in surface exposures. Interpreted allochthonous rafts and olistoliths can be observed in the Ice Brook Formation, as well as the Blueflower Formation and the Conrad siliciclastics in the Nadaleen formation (Aitken, 1989, 1991). Mesoscopic synsedimentary slump folds are common in the Osiris cluster and throughout the Orion area. Slump folds are identified within the Upper Osiris limestone, the Conrad siliciclastics and the Conrad limestone (Fig. 5) using the following criteria (after Bradley and Hanson, 1998): 1) folds are anomalous in the wider structural context; 2) folds are disharmonic and variable; 3) folds truncate against one another with no indication of strain along the truncation surface; 4) folds are bound by homoclinal strata or strata recognizable as being tectonically folded from regional events and map contacts do not follow folds; and 5) folds are spatially associated with soft-sediment deformation structures. The best examples of slump folds can be found in the Conrad limestone at 630540 mE, 7112470 mN (Fig. 5; all grid references are relative to the NAD83, UTM8N).

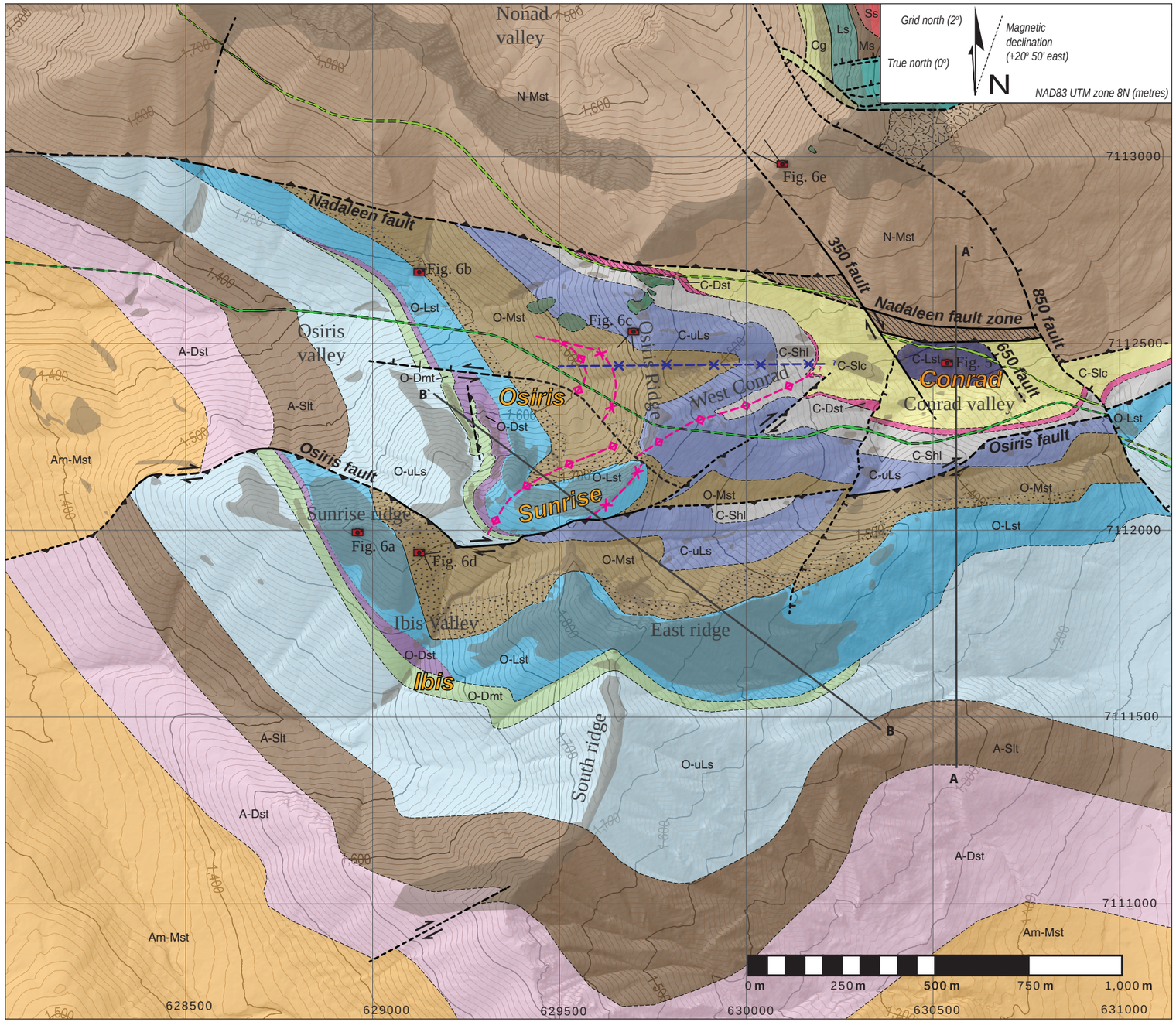

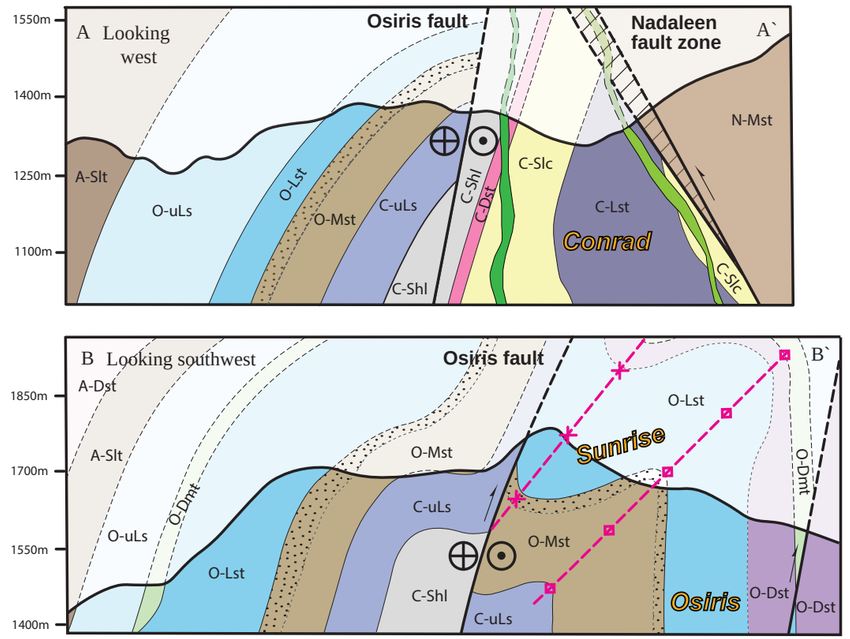

No vertical exaggeration, map scale equal to figures 2a and 2b

Figure 2. *Geology map of the Osiris cluster with geographical names, major fold axial traces, cross section lines and the Osiris, Sunrise, Ibis and Conrad ore zones indicated, and cross sections. Geologic map with overlay showing structural measurements and stereonets and map legend on next page.*

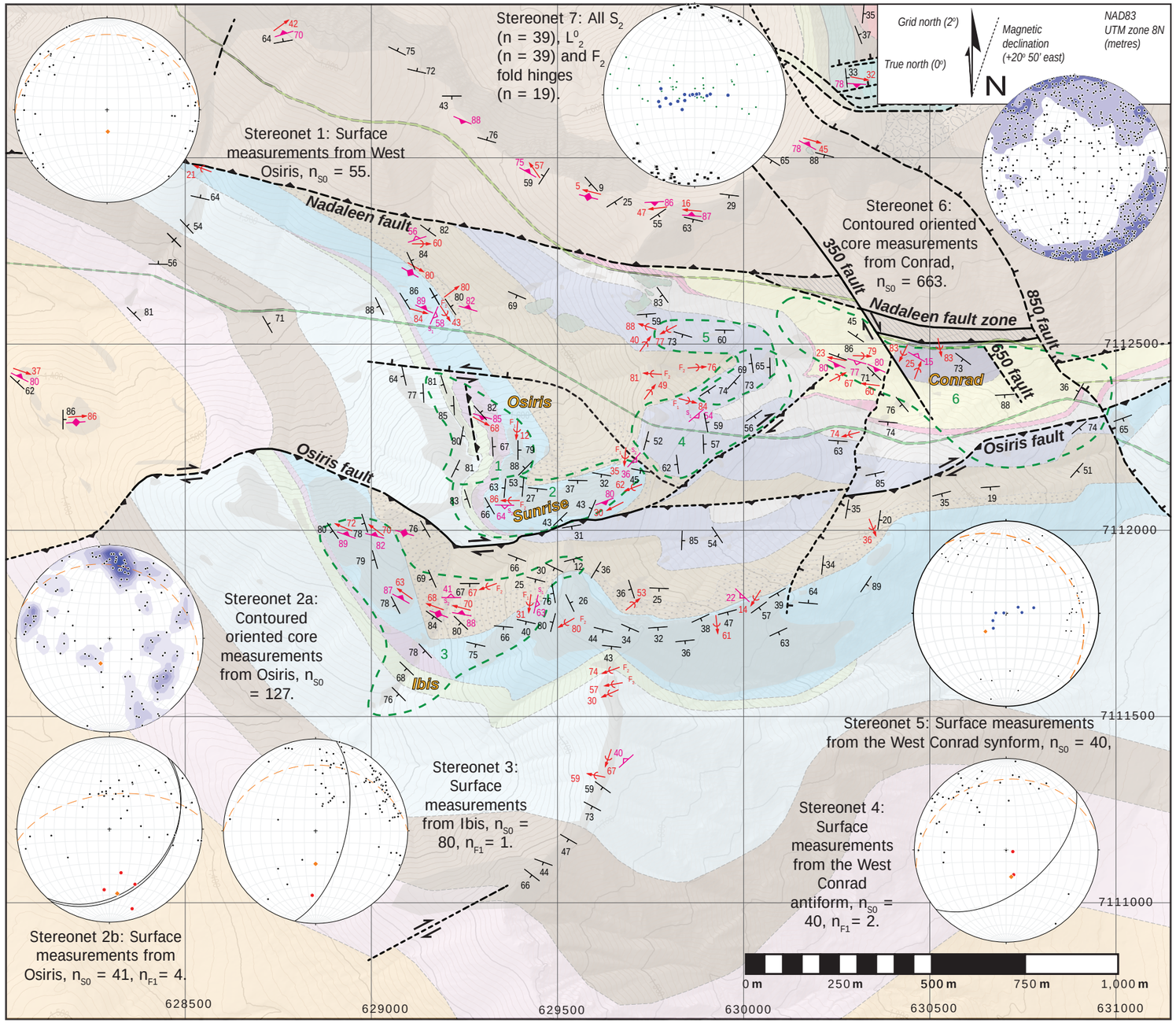

Stereonet symbols

- Area from which data on corresponding stereonet was obtained
- Calculated best fit girdle
- F_1 axial plane
- Pole to S_0
- F1 fold axis
- F2 fold axis
- Pole to best fit girdle
- Pole to S2
- Intersection axis, L02

MAP UNITS

Ediacaran - Cambrian
Narchilla Formation

Amon mudstone, Am-Mst. Grey and maroon thinly bedded mudstone with thicker interbeds of siltstone and fine sandstone.

Ediacaran - Algae Formation

Atum dolostone, A-Dst. Cream to light grey silty or sandy dolostone with minor rudstone interbeds.

Ediacaran - Blueflower Formation

Atum siltstone, A-Slt. Thinly bedded to laminated brown siltstone with interbeded sandy limestone.

Upper Osiris limestone, O-uLs. Thinly bedded sandy limestone with calcareous breccias and rare sandstone interbeds. Distinctive terracotta colour. Readily frost-heaved and creeped.

Ediacaran - Gametrail Formation

Osiris diamictite, O-Dmt. Orange weathering, generally recessive carbonate breccia. Angular clasts of dolostone and limestone supported in a carbonate matrix which is locally dolomitized.

Osiris dolostone, O-Dst. Dolomitized version of Osiris Limestone (see below).

Osiris limestone, O-Lst. Variably bedded and laminated limestone, flat-pebble rudstone and carbonate breccia, often partially dolomitized. Dolomitic beds weather orange while limestone beds weather pale grey. Dark grey when fresh with extensive stylolites. Limestones are silty and locally show manganese dentritic weathering. Abundant soft-sediment deformation. Maroon coloured at its base.

Ediacaran - Nadaleen formation

Osiris mudstone, stippled where maroon coloured. O-Mst. Grey, thinly bedded mudstone and siltstone. Alternating maroon and green coloured layers at top generally follow bedding. Often pencil fractured with small scale folds.

Upper Conrad limestone, C-uLs. Interbedded calcareous breccia, limestone and siliclastic shale. Breccias comprise gravel to cobble sized limestone clasts thatfine upwards in a limestone matrix. Extensive 'beefy' calcite veining.

Conrad shale, C-Shl. Recessive grey to black shale with abundant small scale folds.

Conrad dolostone, hatched where not dolomitised, C-Dst. Pale grey silica dolostone cut by abundant black quartz veins. Not fully dolomitized near Nadaleen fault.

Conrad siliciclastics, C-Slc. Chaotic, interbedded sandstone, mudstone, siltstone and gravel conglomerates. Conglomerates are matrix supported, irregular and lensoidal. Minor calcareous sandstones. Abundant soft-sediment deformation.

Conrad limestone, C-Lst. Thinly bedded silty limestone. Abundant calcite veins and stylolites. Dark-grey weathering and black when fresh. Abundant soft-sediment deformation. Minor dolomitized zones.

Cryogenian - Ice Brook Formation

Unclassified Nonad mudstone, patterned where diamictite, N-Mst. Interbedded mudstone and siltstone with minor sandstone. Large rafts of dolostone and conglomerate. Weathers along S2. Abundant soft-sediment deformation. Diamictites are polymict with clasts of sandstone, mudstone and limestone supported in a blue-grey clay matrix.

Upper sandstone, Ss. Poorly sorted, generally coarse grained orange-weathering sandstone.

Upper mudstone, Ms. Dark grey to black laminated claystone and siltstone.

Nonad limestone, Ls. Dominantly grey granular limestone with isolated coarse quartz clasts. Buff-weathering. Interbedded with trough cross-bedded siltstone and black mudstone.

Cryogenian - Twitya Formation

Quartz gravel conglomerate, Cg. Locally with minor feldspar clasts. Interbedded with sandstone and black mudstone.

Intrusive rocks

North Conrad dike. Altered mafic dike. Pale grey when fresh and orange weathering. 74.4Ma (Tucker, 2015).

South Conrad dike. Altered mafic dike. Pale grey-green when fresh and orange weathering. 74.4Ma (Tucker, 2015).

Osiris gabbro. Altered hornblende-rich gabbro. Green colour when fresh, black weathering. 465.6Ma (Tucker, 2015).

Fault rocks

Nadaleen fault zone. Sheared cataclasite comprising clasts from the Nonad mudstone, Conrad siliciclastics and Conrad limestone.

Map symbols

- Observed contact
- Inferred contact
- Exposure
- Fault - observed
- Fault - approximate location
- Fault - inferred
- Reverse motion - triangles on up-thrown block
- Normal motion - ticks on down-thrown block
- Lateral motion
- F1 axial trace (syncline)
- F_1 axial trace (anticline)
- F_2 axial trace (syncline)
- Photo location for figures
- Strike and dip of inclined bedding
- Strike of vertical bedding
- Strike and dip of inclined cleavage (S_2)
- Strike of vertical cleavage (S_2)
- Plunge and trend of bedding-cleavage intersection lineation (L^0_2)
- Strike and dip of axial plane (S1)
- Strike and dip of axial plane (S2)
- Strike and dip of axial plane (unknown or syn-sedimentary fold)
- Plunge and trend of minor fold axis (F1)
- Plunge and trend of minor fold axis (F2)
- Plunge and trend of minor fold axis (unknown or syn-sedimentary fold)

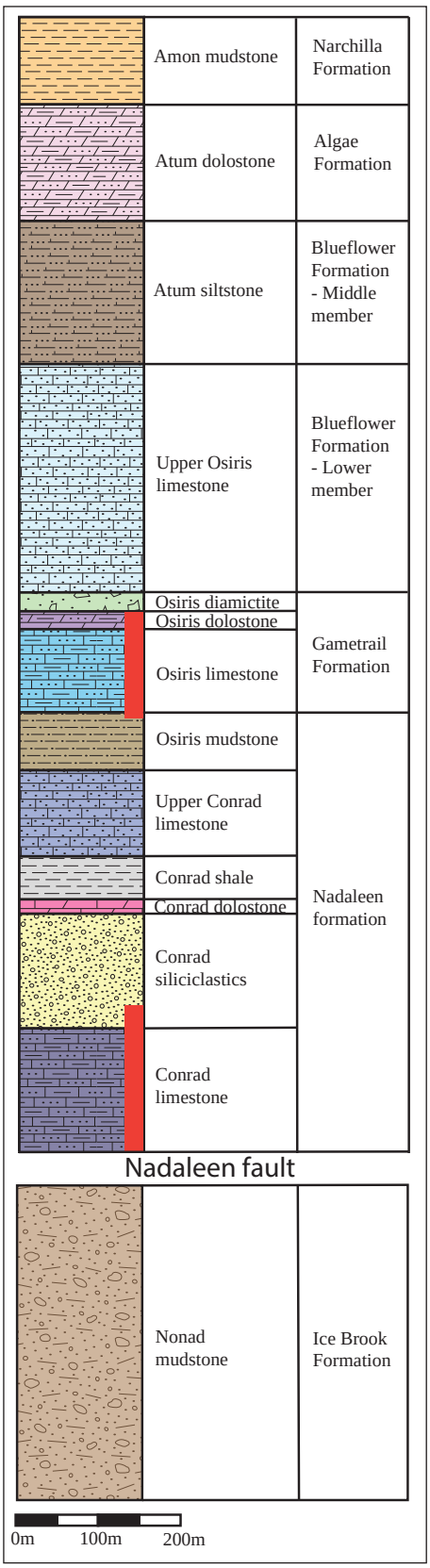

Figure 3. *Stratigraphic succession of sedimentary rocks in the Osiris cluster. Mineralized intervals are shown in red. Regional correlation is after Moynihan (2016).*

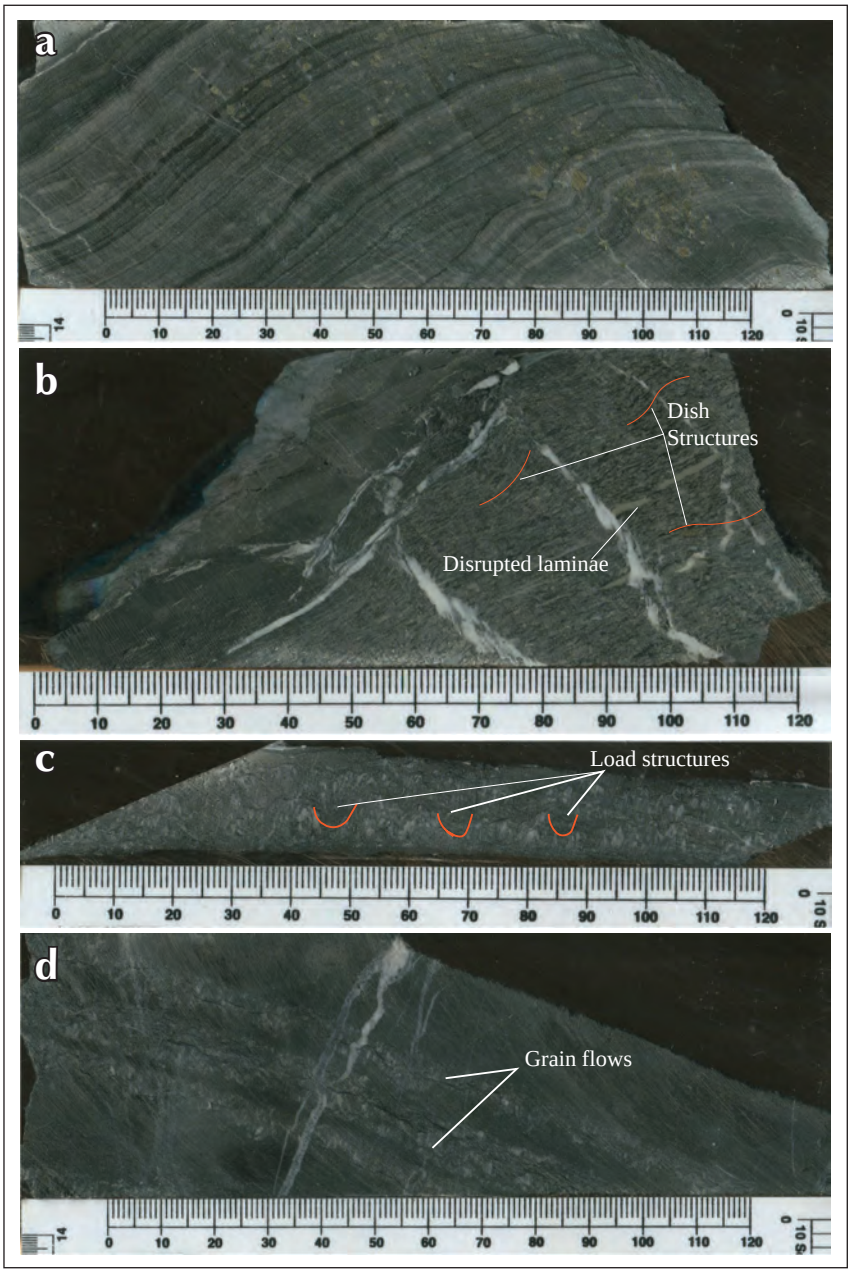

Figure 4. *Core photographs of sedimentary structures in the Conrad limestone.* ***(a)*** *Synsedimentary folding;* ***(b)*** *interrupted laminae with dish structures;* ***(c)*** *convoluted bedding with small-scale slumps and load casts; and* ***(d)*** *grain flows with interrupted laminae. Scale in millimetres.*

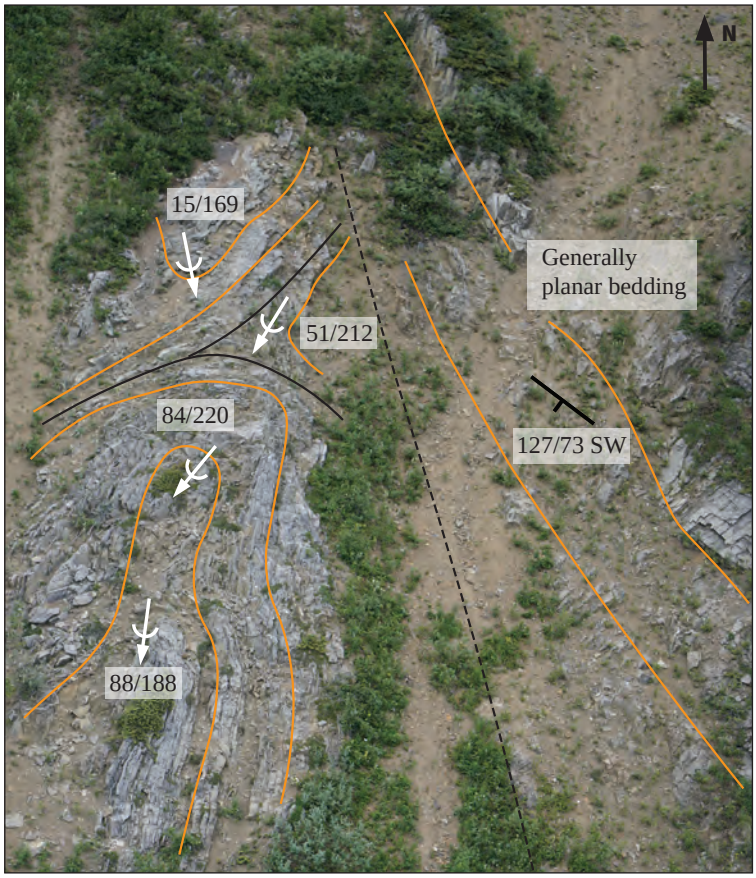

Figure 5. *Annotated oblique aerial view of a steep exposure of Conrad limestone with interpreted soft-sediment slump folds. Bedding formlines are represented in orange whereas black lines represent observed (solid) or inferred (dashed) truncation surfaces. Fold hinges (shown in white) are denoted by plunge/trend and a representative value for generally homoclinal bedding to the east is in the form strike/dip/dip direction. Note the variance in fold hinge plunge. Field of view is ~12 m across.*

STRUCTURAL GEOLOGY

FOLIATIONS

A well-developed S_2 foliation is present in all argillaceous rocks and is locally developed in limestone units (Fig. 6a). This fabric is best observed along the western extent of the Sunrise ridge within the Osiris limestone (629000 mE, 7112010 mN), and in the Ice Brook Formation immediately north of the Nadaleen fault where the foliation forms a prominent weathering surface. S_2 strikes ESE with a subvertical dip and has been recognized throughout the Orion area and elsewhere regionally (Moynihan, 2014), suggesting it can serve as a regional marker foliation. S_2 is axial planar to vertically plunging F_2 folds (described below; Fig. 6b) and crosscuts macro scale F_1 folds. Across the Osiris cluster, intersection lineations of S_2 with bedding exhibit considerable variation in plunge (Fig 2b; Stereonet 7), indicating pre-F_2 folding occurred on a large scale. No S_1 fabric was identified in the field, although the intersection of S_2 and a weakly developed bedding parallel fissility has resulted in pervasive conchoidal pencil fracturing of argillaceous rocks and this commonly obscures the identification of any potential pre-S_2 fabrics.

FOLDING

Two phases of mesoscopic to macroscopic folding have affected the Osiris cluster. F_1 folds are primarily developed on the macroscopic scale with the Osiris antiform-synform fold pair (Fig. 6c), and the West Conrad anticline being the most prominent examples of large F_1 folds in the Osiris cluster. F_1 folds have a steep to moderate southerly plunge and steep to moderately southeast-dipping axial planes. Where least affected by F_2 folding, these large F_1 folds typically have one subvertically dipping limb and one shallow to moderate dipping limb (*e.g.*, the Osiris antiform-synform fold pair, Fig. 6c). Although parasitic mesoscopic F_1 folds are not common, they can be readily observed adjacent to the Osiris ridge (629700 mE, 7112185 mN) and in the Ibis valley (629440 mE, 7111800 mN). Comparable scale F_1 folds are also observed in the Mississippian limestone in the Orion area.

F_2 folds overprint F_1 folds and are characterized by axial planes that dip steeply to the south. S_2 is typically developed as an axial plane foliation to F_2 folds (Fig. 6b). Mesoscopic F_2 folds are well developed on the Sunrise ridge (629325 mE, 7112075 mN), and along the Osiris ridge and at West Conrad. Examples of macroscopic F_2

folds are the West Conrad synform and the West Osiris synform (Fig. 2, Stereonets 1 and 5). The F_2 fold axes and intersection lineations between bedding and S_2 vary from a shallow to steep plunge within S_2 (Fig. 2, Stereonet 7). The most prominent examples of F_2 folds have a steep to subvertical plunge that likely represent folding of the steeply dipping limbs of macroscopic F_1 folds.

In the Ibis valley and along the East ridge, subhorizontal upright monoclinal warps in bedding are developed on a macroscopic scale (Fig. 6d; cross sections in Fig. 2). A similar monoclinal warp is evident in drill core through the Sunrise zone (Fig. 2, Stereonet 2a). The dominant bedding attitude at depth is steep to the south, compared to a 30-40° southerly dip at the surface (Fig. 2, Stereonet 2b). The monocline overprints the Osiris antiform-synform F_1 fold pair and is interpreted as being a product of F_2 folding of an F_1 shallow limb. An upright subhorizontal macroscopic F_2 fold can be observed on the western bluffs of the Nonad valley (Fig. 6e). Similar upright, subhorizontal, open to close folds that we interpret as being F_2 structures can be recognized on regional maps (Moynihan, 2016; Colpron, 2012) and are particularly clear in aerial photographs of the Orion area. The regions characterized by shallow plunging F_2 monoclines and F_2 folds likely represent folding of shallow dipping F_1 fold limbs and/or regions largely unaffected by F_1 folding.

Palmer and Kuiper (2017) identified a macroscopic antiform in the Ibis area. This fold was mapped as having a steep SE-dipping limb and a steep SW-dipping limb, but this is inconsistent with field observations made in this study (Fig. 2, Stereonet 3). Our data indicate the fold is an open antiformal flexure with a gentle interlimb angle of greater than 130°. We interpret this as being an F_1 structure and we correlate it with the Osiris antiform on the north side of the Osiris fault (*see* below). We suggest that the tighter 'fold-shaped' map pattern at Ibis is largely a function of shallow topography near the Osiris fault owing to the presence of an F_2 monocline (Fig. 6d) and the interaction with topography creating a pronounced 'V-in-the-valley' (Fig. 2).

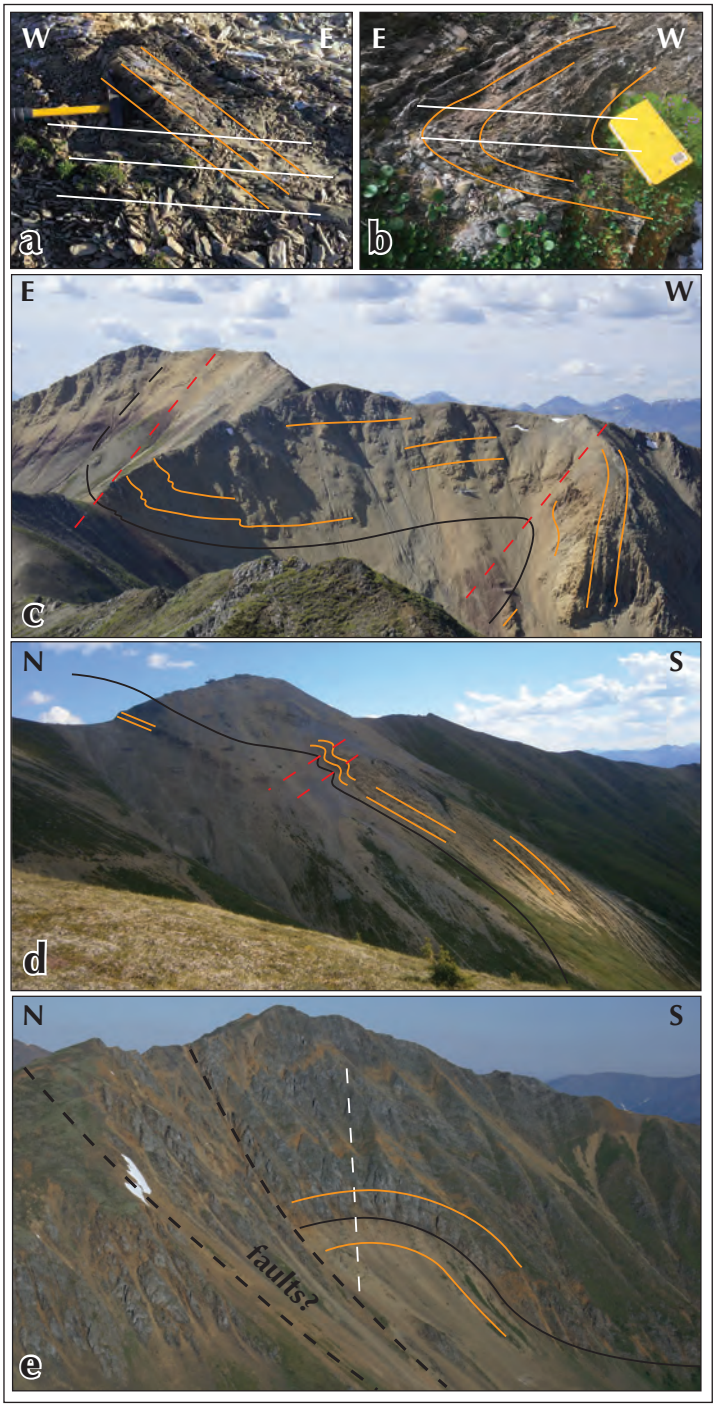

Figure 6. *Annotated field photographs. Bedding formlines are shown in orange, unit contacts in black, faults in dashed black, F_1 axial traces in red dashed, S_2 cleavage in white and F_2 axial traces in dashed white. Photo locations shown in Figure 2.* ***(a)*** *Bedding-cleavage on Sunrise ridge. Hammer shaft is 37 cm;* ***(b)*** *S_2 axial planar to an F_2 fold. Notebook spine is 19 cm;* ***(c)*** *Osiris F_1 antiform-synform pair. Wavelength pictured is ~325 m;* ***(d)*** *F_2 monocline at Ibis. Field of view is ~650 m across; and* ***(e)*** *upright F_2 fold hinge, Nonad valley. Field of view is ~500 m across.*

FAULTS

The Osiris cluster is cut by a number of significant faults that generally strike E, W or NW. The largest fault in terms of lateral extent is the Nadaleen fault, which can be traced west at least as far as the Pyramid gold showing, approximately 16 km west of the Osiris cluster (Fig. 1b; Moynihan, 2016). It has a net reverse displacement, placing Cryogenian rocks of the Ice Brook Formation on top of Ediacaran rocks within the Osiris cluster, where it strikes WNW. In Orion, it strikes NW and juxtaposes Paleozoic rocks to the south against Ediacaran rocks to the north. Drilling in the Conrad zone has constrained the Nadaleen fault to dip 60° to the north and also identified a large brittle shear zone known as the Nadaleen fault zone. This is a zone of sheared cataclasite, 60 m wide at its thickest, which occurs approximately between the 350 and 650 faults. Drill core data from Conrad indicate that there is no increase in thickness of sedimentary units towards the fault plane, nor are any rollover structures developed. As such, we suggest the Nadaleen fault did not initiate as a synsedimentary structure. Rather, it initiated after the deposition of these rocks constraining its age to Paleozoic or younger. The Nadaleen fault is not folded and is interpreted to cut all folds.

The other large fault within the study area is the Osiris fault, which is an E striking structure that cuts through the centre of the Osiris cluster (Fig. 2). Drill core data from the Sunrise ore zone indicates that the fault dips to the south at ~70°, although its strike varies significantly along its length. Correlation of the anticlinal flexure at Ibis in the hanging wall to the fault with the Osiris antiform in the footwall, constrains net slip on the fault to have been oblique, with a dextral-reverse sense. The Sunrise zone of gold mineralization forms a plane that is subparallel to the Osiris fault, but is offset ~50 m down into the footwall. Drill core through the Osiris fault and the Sunrise zone define a continuous brittle shear zone comprising intensely fractured rock, fault gouge, sheared material and high vein density between them suggesting that the Sunrise zone might represent fluid flow through the high–permeability damage zone on the periphery of a wide, multi-cored Osiris fault zone (Faulkner *et al.,* 2010). The Osiris fault cuts both F_1 and F_2 folds, restricting its age to post-folding.

The other dominant orientation of faults in the Osiris cluster are the NW-striking 350, 650 and 850 faults. These structures were targeted by diamond drilling for the first time in the summer of 2017. All three faults are spatially associated with mineralization and are interpreted as potential fluid conduits during mineralization. The 350 fault has a dextral strike separation in plan view while the 650 and 850 faults have an apparent normal offset to the east. Drill data indicate displacement of both Conrad dikes across the 350 fault, indicating post-74.4 Ma slip. Drilling has not yet identified any significant offset across the 650 or 850 faults.

INTERNAL GEOMETRY OF THE CONRAD LIMESTONE

Extensive diamond drilling in the Conrad ore zone has shown that the Conrad limestone has a 3D lenticular geometry with depth; the strike length and unit thickness both decrease upwards as it approaches the Nadaleen fault (*see* cross section A-A`; Fig. 2). It is also bound on either side by a siliciclastic package that is thought to represent the same stratigraphic horizon - the Conrad siliciclastic unit. One possible explanation for this geometry is that the Conrad limestone is the core of an upright anticline, with a subvertical E-striking axial plane that is double plunging to the east and west (ATAC Resources Ltd., 2017). This geometry is anomalous in the wider tectonic context as it requires a tight interlimb geometry that is not observed in macroscopic folds elsewhere.

We propose that the Conrad limestone is an olistostrome and that its geometry is primarily a function of its emplacement morphology. We infer this from the abundance of slump folding and soft-sediment deformation within the Conrad limestone (Figs. 4 and 5), the inconsistency between structural measurements and outcrop pattern (Fig. 2; Stereonet 6), and the repeated Conrad siliciclastic unit on either side of the Conrad limestone. Furthermore, the Conrad limestone is not correlated with any part of the Nadaleen formation elsewhere regionally (Moynihan, 2016). The apparent double plunging nature of the Conrad limestone is a function partly of its lenticular emplacement shape and apparent normal dip-slip motion along the 650 and 850 faults that cut across it. As an olistostrome, the Conrad limestone would have been emplaced during deposition of the Conrad siliciclastics. The provenance of the Conrad limestone is currently unknown.

FOLD EVOLUTION

The geometry of various parts of the Osiris cluster can be explained using the following fold evolution model (Fig. 7). NW-SE directed bulk shortening produced NW-verging F_1 folds with a subvertical limb and a shallow limb (Fig. 7a,b). This was later refolded in response to SSW-NNE directed contraction (Fig. 7b). F_2 folds formed with S_2 as an axial planar cleavage. In steep F_1 limbs, these folds have subvertical plunges while in shallow limbs they have subhorizontal plunges and form large wavelength monoclines, although upright F_2 hinges are observed elsewhere regionally. F_1 folds hinges were steepened towards the south (Fig. 7c). Folding is cut by both the Osiris fault and the Nadaleen fault, indicating that these faults likely formed post-folding. However, they may be longer-lived structures that were recurrently active during folding. Later NW striking faults in the Conrad ore zone are spatially associated with mineralization and, if they all developed contemporaneously with the 350 fault, are constrained to post dike emplacement at 74.4 Ma. This model is consistent with observations by Palmer and Kuiper (2017), who proposed a similar model in which SSW-directed tilting came prior to folding and justified this with the lack of evidence for a prior E-W fold event elsewhere. We propose that the observations outlined in this contribution are evidence for such a prior event, at least locally.

FUTURE WORK

This study forms the structural context within which ore fluid pathways into, out of, and within the Nadaleen trend will be assessed. Future work will focus on mapping fluid conduits using isotopic, thermal and mineralogical proxies for fluid alteration including $\delta^{18}O$ isotopes, clumped isotopes, apatite fission track thermochronology and illite crystallinity. The aim is to recognize fluid pathways on three scales: 1) identifying where fluids enter and exit the Nadaleen trend as a whole; 2) assessing the macroscopic structures controlling the distribution of ore zones; and 3) identifying small scale structures (stylolites, veins, minor faults) that are fluid conduits into mineralized horizons. This will be coupled with additional structural studies, including investigation of fault kinematics, analysis of fabrics in oriented thin-sections and assessing deformation age constraints through geochronology of intrusive rocks. Understanding the deformation context in which ore fluid pathways formed will help identify possible mineralizing structures elsewhere and explain the distribution of mineralized zones.

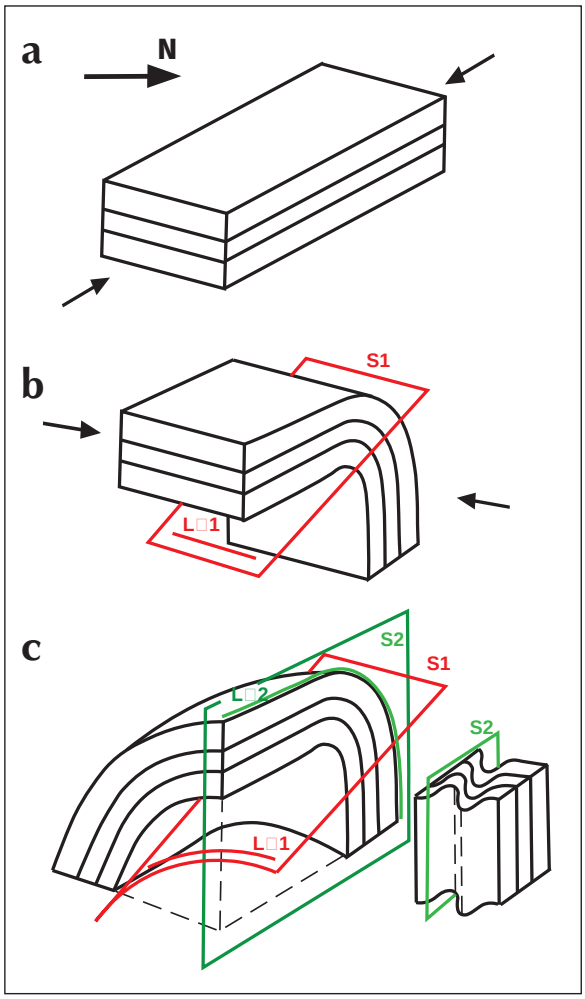

Figure 7. *Fold evolution within the Osiris cluster.* ***(a)*** *NW-SE directed contraction of subhorizontal beds;* ***(b)*** *Formation of F_1 folds with a shallow limb, steep limb and an axial plane shown in red. L^0_1 is the intersection lineation of S_0 and S_1. Later NNE-SSW directed compression; and* ***(c)*** *refolding of F_1 folds. Shallow limbs are refolded into F_2 monoclines while steep limbs are refolded to steeply plunging F_2 folds with subvertical south-dipping axial planes (shown in green). L^0_1 is folded so that it has a variable plunge towards the south. L^0_2 is the intersection lineation of S_0 and S_2.*

ACKNOWLEDGEMENTS

This work was conducted as part of Andrew Steiner's MSc thesis at the University of British Columbia. We would like to thank Julia Lane of ATAC Resources Ltd. for all of her logistical support, Daniel Schrader for his assistance in the field, and to Barrick Gold Corporation for their expertise and support during a busy field season. This project is funded by Natural Resources Canada through their Targeted Geoscience Initiative (TGI), the Mitacs Accelerate Program, the Society of Economic Geologists Foundation's Graduate Student Fellowship and ATAC Resources Ltd. Thank you to Jim Mortensen and Patrick Sack for their feedback when reviewing this paper.

REFERENCES

Aitken, J.D., 1989. Uppermost Proterozoic formations in central Mackenzie Mountains, Northwest Territories. Geological Survey of Canada, Bulletin 368.

Aitken, J.D., 1991. The Ice Brook Formation and Post-Rapitan, Late Proterozoic glaciation, Mackenzie Mountains, Northwest Territories. Geological Survey of Canada, Bulletin 404.

ATAC Resources Ltd., 2017. Osiris Project. http://www.atacresources.com/projects/rackla/osirus-cluster [accessed 26th Nov. 2017].

Bradley, D. and Hanson, L., 1998. Paleoslope Analysis of Slump Folds in the Devonian Flysch of Maine. The Journal of Geology, vol. 106, p. 305-318.

Colpron, M., 2012. Preliminary observations on the geology of the Rackla belt, Mount Ferrell map area (NTS 106C/3), central Yukon. *In:* Yukon Exploration and Geology 2011, K.E. MacFarlane and P.J. Sack (eds.), Yukon Geological Survey, p. 27-43.

Colpron, M., Moynihan, D., Israel, S., and Abbott, G., 2013. Geological map of the Rackla belt, east-central Yukon (NTS 106C/1-4, 106D/1). Yukon Geological Survey, Open File 2013-13, 1:50 000 scale, 5 maps and legend.

Colpron, M. and Nelson, J.L., 2011. A Digital Atlas of Terranes for the Northern Cordillera. Accessed online from Yukon Geological Survey, www.geology.gov.yk.ca [accessed 26th Nov. 2017].

Coulter, A. B., Lane, J. and Steiner, A., 2018. Osiris cluster Carlin-type gold, east-central Yukon. *In:* Yukon Exploration and Geology 2017, K.E. MacFarlane (ed.), Yukon Geological Survey, p. 65-74.

Faulkner, D.R., Jackson, C.A.L., Lunn, R.J., Schlische, R.W., Shipton, Z.K., Wibberley, C.A.J. and Withjack, M.O., 2010. A review of recent developments concerning the structure, mechanics and fluid flow properties of fault zones. Journal of Structural Geology, vol. 32, p. 1557-1575.

Moynihan, D., 2014. Bedrock Geology of NTS 106B/04, Eastern Rackla Belt. *In:* Yukon Exploration and Geology 2013, K.E. MacFarlane, M.G. Nordling, and P.J. Sack (eds.), Yukon Geological Survey, p. 147-167.

Moynihan, D., 2016. Bedrock geology compilation of the eastern Rackla belt, NTS 105N/15, 105N/16, 105O/13, 106B/4,106C/1,106C/2, east-central Yukon. Yukon Geological Survey, Open File 2016-2, 1:75 000 scale.

Palmer, J.C. and Kuiper, Y.D., 2017. Structural geology of the eastern Nadaleen trend, Yukon Territory, Canada: Implications for recently discovered sedimentary rock-hosted gold. Ore Geology Reviews, vol. 80, p. 48-60.

Tucker, M.J., 2015. Geology, Mineralization and Geochronology of the Conrad Zone Carlin-type gold prospect, East-Central Yukon Territory, Canada. Unpublished MSc thesis, University of British Columbia, 213 p.

Tucker, M.J., Hart, C.J.R. and Carne, R.C., 2013. Geology, alteration, and mineralization of the Carlin-type Conrad zone, Yukon. *In:* Yukon Exploration and Geology 2012, K.E. MacFarlane, M.G. Nordling, and P.J. Sack (eds.), Yukon Geological Survey p. 163-178.

New investigations of basal Laberge Group stratigraphy, Whitehorse trough, central Yukon

L.H. van Drecht and L.P. Beranek
Department of Earth Sciences, Memorial University of Newfoundland

van Drecht, L.H. and Beranek, L.P., 2018. New investigations of basal Laberge Group stratigraphy, Whitehorse trough, central Yukon. *In:* Yukon Exploration and Geology 2017, K.E. MacFarlane (ed.), Yukon Geological Survey, p. 151-163.

ABSTRACT

The tectonic evolution of the Whitehorse trough in central Yukon is largely preserved by the Early to Middle Jurassic Laberge Group, an ~3000-m thick succession of synorogenic clastic strata that unconformably overlies arc and arc marginal rocks of the Lewes River Group. A two-year project was initiated to test a Sinemurian to Toarcian transgression of basal Laberge Group strata westward across the Whitehorse trough and examine the regional relationships between the timing of Jurassic exhumation, sedimentation, and terrane accretion in the northern Canadian Cordillera. Field studies in 2017 targeted basal Laberge Group strata at seven locations in central Yukon. At each field locality, basal Laberge Group strata are known or inferred to unconformably overlie the Povoas formation and multiple units of the Aksala formation. Pre-Early Jurassic unconformities may indicate variable basin topography due to the complex internal stratigraphy of the Lewes River Group, or that regional exhumation and erosion affected the Whitehorse trough prior to Laberge Group sedimentation.

* *lberanek@mun.ca*

INTRODUCTION

The early growth of the northern Canadian Cordillera is marked by the late Paleozoic to mid-Mesozoic accretion of the Intermontane terranes to the western Laurentian margin, crustal thickening in the Cordilleran hinterland, and initial subsidence in the Alberta foreland basin (*e.g.,* Cant and Stockmal, 1989; Colpron *et al.*, 2007, 2015; Nelson *et al.*, 2013). This early growth is in part recorded by the Whitehorse trough, a sedimentary basin that developed on top of the Intermontane terranes in a transitional forearc to wedge-top setting during the Early to Middle Jurassic closure of the Cache Creek Ocean (Nelson *et al.*, 2013; Colpron *et al.*, 2015). The Whitehorse trough is regionally extensive and spans more than 600 km from the Carmacks region of central Yukon (Fig. 1) to the Dease Lake region of northern British Columbia. The northern apex of the trough near Carmacks is characterized by proximal, marginal marine to fluvial strata of the Tanglefoot formation, whereas the central part of the trough near Whitehorse consists of distal, deep-marine mass-flow deposits of the Richthofen formation, suggesting a deepening of the basin towards the south (*e.g.,* Dickie and Hein, 1995; Tempelman-Kluit, 1984; Lowey, 2004; Lowey *et al.*, 2009). Laberge Group strata unconformably overlie several Upper Triassic units of the Lewes River Group (Stikinia; Cairnes, 1910; Tempelman-Kluit, 1984; Dickie and Hein, 1995; Lowey, 2004, 2008; Colpron *et al.,* 2007), which likely reflects the lateral discontinuity of Carnian-Rhaetian rock units in central Yukon (Bordet, 2016a,b, 2017) and/or exhumation of the Intermontane terranes (*e.g.,* Knight *et al.*, 2013; Joyce *et al.,* 2015; Colpron *et al.,* 2015), creating topography within the Whitehorse trough prior to Early Jurassic sedimentation.

Previous studies of the Whitehorse trough have mostly focused on the sedimentology and depositional setting of the Laberge Group (*e.g.*, Hart and Radloff, 1990; Dickie and Hein, 1995; Lowey *et al.*, 2008; Bordet, 2016a), but relatively few studies (Hart *et al.*, 1995) have examined the stratigraphic responses of Jurassic exhumation and erosion or tested relationships between the timing of exhumation, sedimentation and terrane accretion. Recently, Colpron *et al*. (2015) investigated these relationships and hypothesized a westward younging of basal Laberge Group strata across the Whitehorse trough, which may indicate that subsidence followed exhumation and uplift of its western shoulder. A two-year project was initiated in summer 2016 to test the hypotheses of Colpron *et al.* (2015) and constrain the field geology and detrital zircon (U-Pb and Hf isotope) signatures of Laberge Group strata in central Yukon. The objectives of the 2016 field season, summarized by van Drecht *et al.* (2017), focused on the physical stratigraphy and depositional setting of Laberge Group rock units at four localities. The objectives of the 2017 field season, presented in this report, were to identify the contact relationships between basal Laberge Group and underlying Lewes River Group strata in the Mandanna Lake, Conglomerate Mountain, Fish Lake, Takhini subdivision, King Lake, Mount Byng and Mount Slim areas to test the westerly transgression of basal strata hypothesized by Colpron *et al.* (2015). Forthcoming detrital zircon U-Pb and Hf isotope studies will use these stratigraphic constraints to more fully define the provenance and paleodrainage history of Laberge Group rock units and provide new insights on the evolution of the Intermontane terranes.

TECTONIC SETTING

The Intermontane terranes (Yukon-Tanana, Stikinia and Quesnellia) were in proximity to western Laurentia by the Early Triassic (Beranek and Mortensen, 2011) and later imbricated following the Late Triassic-Early Jurassic closure of the Cache Creek Ocean (Mihalynuk *et al.*, 1994). The most widely accepted model to explain the imbrication and subsequent geometry of the Intermontane terranes involves the counterclockwise bending and subsequent entrapment of oceanic rock units assigned to the Cache Creek terrane (Mihalynuk *et al.*, 1994; Logan and Mihalynuk, 2014; Colpron *et al.*, 2015). Late Triassic to Early Jurassic crustal thickening and pluton emplacement in central Yukon was accompanied by rapid exhumation of the Yukon-Tanana, Stikinia and Quesnellia terranes (*e.g.*, Johnston *et al.*, 1996). Lower to Middle Jurassic synorogenic strata of the Laberge Group were likely sourced from exhumed plutons and basement rocks assigned to Stikinia.

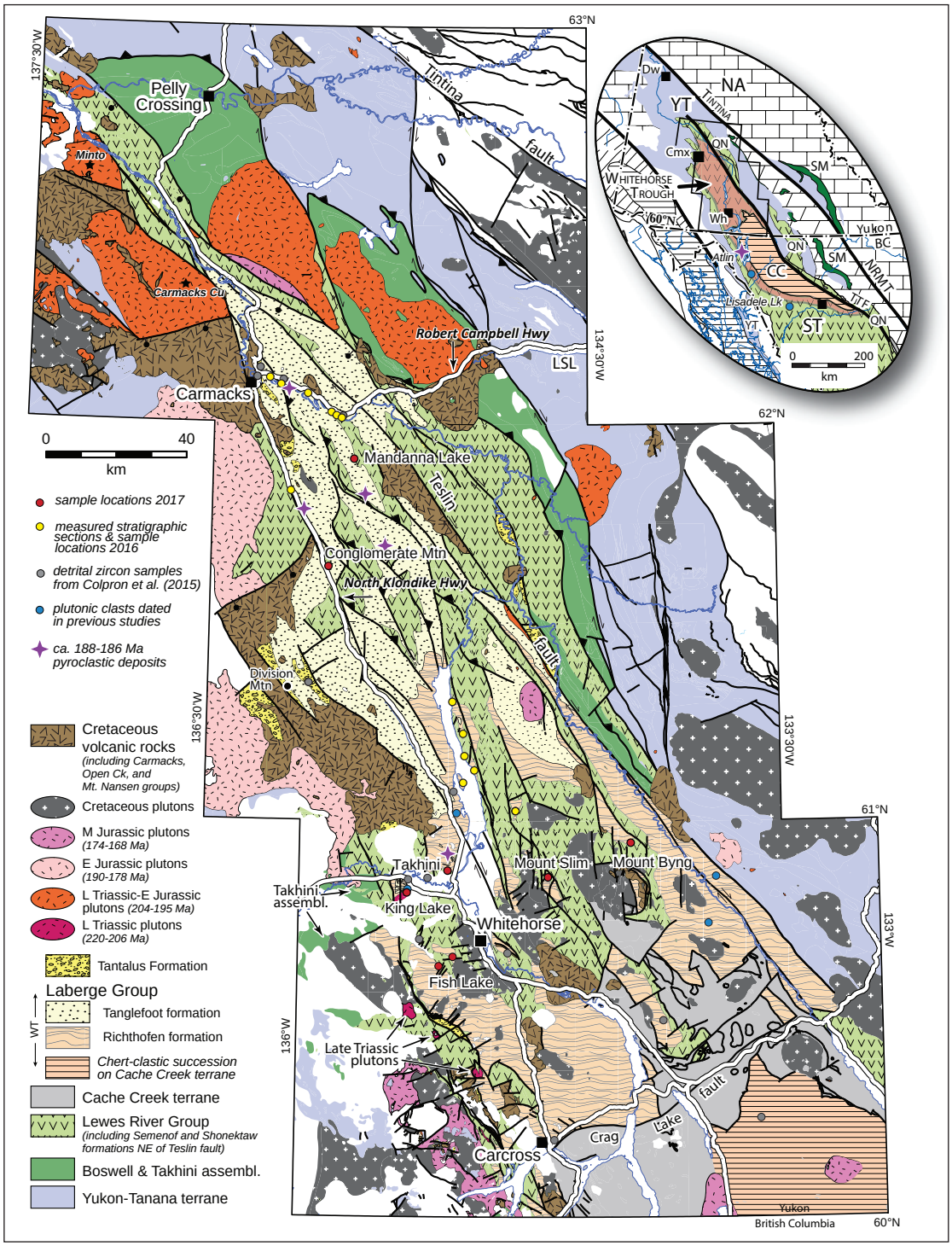

Figure 1. *Regional geology of the Whitehorse trough area modified from Colpron (2015). Locations of 2016 field sites are shown by yellow dots and 2017 field sites are shown by red dots. Field locations on the Robert Campbell Highway represent measured stratigraphic sections. Locations at Mandanna Lake, Conglomerate Mountain, Takhini, King Lake, Fish Lake, Mount Byng, and Mount Slim indicate sampling locations. Grey and blue dots denote detrital zircon sample locations of (Colpron et al. 2015) and previously dated plutonic clasts (Hart et al., 1995). The inset shows the location of the Whitehorse trough relative to the Intermontane terranes of the northern Canadian Cordillera. Abbreviations: CC-Cache Creek terrane; CMx-Carmacks; Dw-Dawson; LSL- Little Salmon Lake; NA-rocks of ancestral North America; NRMT-Northern Rocky Mountain Trench Fault; QN-Quesnellia; SM-Slide Mountain terrane; ST-Stikinia; TTF-Teslin-Thibert fault; Wh-Whitehorse; YT-Yukon-Tanana terrane.*

STRATIGRAPHIC FRAMEWORK

LEWES RIVER GROUP

The stratigraphy of the Lewes River Group is complex due to lateral facies changes from west to east across central Yukon (Wheeler, 1961; Bordet 2016a, 2017). The Povoas formation is the lowermost unit of the Lewes River Group and consists of Carnian basalt and andesite, volcanic breccia, tuff and agglomerate (Fig. 2; Tempelman-Kluit, 1984, 2009). The overlying Carnian-Rhaetian Aksala formation records a break in regional magmatism and is characterized by micritic limestone, fossiliferous limestone, calcareous mudstone-sandstone, lithic sandstone, argillite and calcareous conglomerate (Tozer, 1958; Tempelman-Kluit, 1984; Bordet, 2016a, 2017). Tozer (1958) divided these Upper Triassic rocks into seven limestone units that are regionally interbedded with, or laterally equivalent to Norian-Rhaetian clastic strata, whereas Tempelman-Kluit (1984) divided these rocks into the Casca (lithic sandstone, argillite and conglomerate), Hancock (limestone), and Mandanna members (maroon weathering lithic sandstone, mudstone and conglomerate). Recent mapping by Bordet (2016a,b, 2017) broadly supports the interpretations of Tozer (1958) and argues for the presence of several Norian and younger carbonate units within the Lewes River Group, which implies that not all Upper Triassic carbonate strata are equivalent to the Rhaetian Hancock member. In this paper, the Casca and Hancock members of Tempelman-Kluit (1984) are referred to as green lithic sandstone and limestone of the Aksala formation, respectively, to more accurately reflect the revised stratigraphy of Bordet (2016b, 2017). The Mandanna member nomenclature is used as per Templeman-Kluit (1984) because it does not crop out in the updated map area of Bordet (2016b) and accurately represents the upper Aksala formation.

LABERGE GROUP

The Lower to Middle Jurassic Laberge Group is a 3000 m-thick sedimentary succession that was first described in central Yukon along the shoreline of Lake Laberge (Dawson, 1887). The Laberge Group is divided into the Sinemurian-Bajocian Tanglefoot and Richthofen formations and Pliensbachian Nordenskiöld dacite (Fig 2; Tempelman-Kluit, 1984; Dickie and Hein, 1995; Lowey, 2004). Post-Bajocian fluvio-deltaic rocks of the Tantalus Formation unconformably overlie the Laberge Group in central Yukon (Fig. 2; Hart and Radloff, 1990; Dickie and Hein, 1995; Colpron *et al.*, 2015).

The Tanglefoot formation (Fig. 2) consists of interbedded sandstone and mudstone, mass-flow conglomerate, pebbly sandstone, and coal with abundant terrestrial plant and marginal marine fossils. The Tanglefoot formation is restricted to the northern apex of the Whitehorse trough and was deposited in a proximal marginal marine to fluvial setting (Lowey, 2004; Hutchison, 2017). The type area for this formation is located at Tanglefoot Mountain, north of Lake Laberge (Lowey, 2004) and good exposures are also present along the Robert Campbell Highway (Fig. 1; van Drecht *et al.*, 2017).

The Richthofen formation (Fig. 2) consists of graded siltstone, very fine grained sandstone with mudstone couplets, mass-flow conglomerate, pebbly sandstone, massive sandstone, volcaniclastic rocks and minor limestone (Lowey, 2004; Lowey *et al.,* 2009). Richthofen formation strata are restricted to the central part of the trough and were deposited in a distal mass-flow setting.

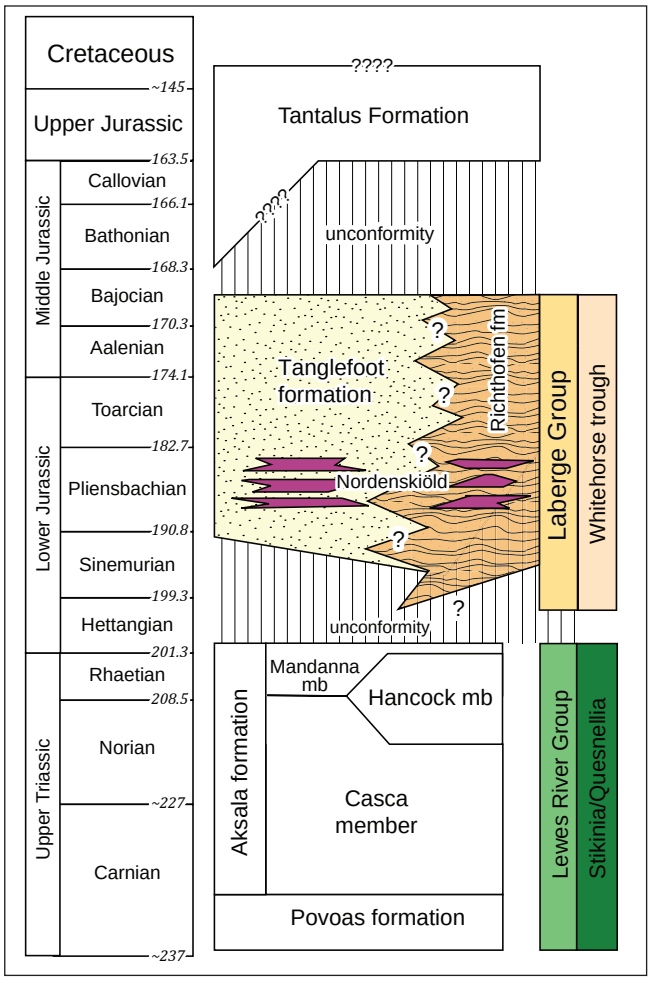

Figure 2. *Schematic stratigraphy of Stikinia, Quesnellia and the Whitehorse trough complied by Colpron et al. (2015).*

The type area is located at the Lake Laberge campground along the western shoreline of Lake Laberge (Tempelman-Kluit, 1984; Lowey, 2004). Good exposures of the Richthofen formation can also be seen along the eastern shoreline of Lake Laberge and flanks of Mount Laurier.

Well-rounded, cobble to boulder, clast to matrix-supported, mass-flow conglomerate units occur throughout the Richthofen and Tanglefoot formations (Hart *et al.*, 1995). Sinemurian conglomerate units comprise volcanic and sedimentary (predominantly limestone) clasts, whereas Pliensbachian and younger strata contain a larger proportion of plutonic rock clasts that imply the unroofing of a nearby arc complex (Dickie and Hein, 1995; Hart *et al.*, 1995; Shirmohammad *et al.*, 2011). In northern British Columbia, Pliensbachian and younger strata of the Whitehorse trough also include metamorphic clasts, which have not been observed in Yukon prior to this field season (Dickie and Hein, 1995; Shirmohammad *et al.*, 2011). Laberge Group conglomerate units were likely deposited as debris flows, sheet floods and bar deposits (Dickie and Hein, 1988). Paleocurrent indicators (flute casts, wavy stratification, bar-swash lamination) suggest that sediment transport was from west to east, transverse to the north-to-south deepening direction of the Whitehorse trough as indicated by longitudinal facies changes (Dickie and Hein, 1988, 1995; Hart *et al.*, 1995; Lowey, 2004, Lowey *et al.,* 2008).

The Nordenskiöld dacite consists of epiclastic and primary dacitic tuffs and flows (Tempelman-Kluit, 1984) that have been mapped at three stratigraphic levels in the Laberge Group and represent volcanic episodes at 188.1 ± 0.4 Ma, 187. 2 ± 0.4 Ma and 186.5 ± 0.3 Ma (Colpron *et al.*, 2007). Zircon U-Pb ages of the Nordenskiöld dacite indicate active volcanism during deposition of the Laberge Group (Colpron and Friedman, 2008).

CONTACT RELATIONSHIPS

Numerous workers, including Cairnes (1910), Cockfield and Bell (1926), Bostock and Lees (1938), Wheeler (1961), Tempelman-Kluit (1984), and Hart and Radloff (1990), have described the contact relationship between the Lewes River and Laberge groups in central Yukon. The contact has been described as a conformity (Bostock and Lees, 1938; Tempelman-Kluit, 1984; Hart and Radloff, 1990), an unconformity (Lowey, 2008), a disconformity (Hart and Radloff, 1990), an angular unconformity (Cockfield and Bell, 1926; Wheeler, 1961; Lowey, 2008), or as changing from a disconformity on the western margin of the basin to a conformity in the central region (Wheeler, 1961). Lowey (2008) proposed that the contact is an unconformity that spans the entire Whitehorse trough, typically marked by basal conglomerate in the Richthofen and Tanglefoot formations.

2017 FIELD STUDIES

The 2017 field season focused on describing the contact relationships between the Lewes River and Laberge groups at Mandanna Lake, Conglomerate Mountain, Fish Lake, Takhini subdivision, King Lake, Mount Byng and Mount Slim (Fig. 1). In the northern apex of the trough, the Tanglefoot formation overlies massive limestone and maroon weathering sandstone of the upper Aksala formation at Mandanna Lake and Conglomerate Mountain. In the central part of the trough the Richthofen formation overlies massive limestone and green sandstone of the Aksala formation and gabbro of the Povoas formation at Fish Lake, King Lake, Mount Byng and Mount Slim.

TANGLEFOOT FORMATION

Mandanna Lake

The Laberge Group overlies limestone of the Aksala formation to the southwest of Mandanna Lake (Fig. 1; zone 08V, 459834 E, 6857184 N, NAD83), ~30 km southeast of Carmacks (Colpron *et al.,* 2007). Basal Laberge Group strata at this locality consist of massive, brown, cobble to pebble, clast to matrix-supported, polymictic conglomerate of the Tanglefoot formation. Conglomerate clasts are dominantly felsic plutonic and volcanic rocks with lesser amounts of sedimentary rocks. Clasts are subrounded to rounded, poorly sorted and range in size from 2 to 20 cm (Fig. 3a). Dark blue-grey, massive, medium to coarse-grained, poorly sorted sandstone underlies the ~3 m-thick conglomerate unit and dips to the northeast (Fig. 3b). This outcrop represents probable basal Laberge Group as limestone crops out west of this locality, but the contact is covered and not directly observed. The contact is inferred to be unconformable.

Conglomerate Mountain

Tanglefoot formation conglomerate overlies maroon weathering sandstone of the upper Aksala formation at Conglomerate Mountain, ~110 km north of Whitehorse along the North Klondike Highway (Fig. 1; zone 08V, 453930 E, 6833117 N, NAD83). At this locality, maroon weathering, medium to coarse-grained, poorly sorted,

massive to burrowed sandstone of the Mandanna member dips towards the southeast (Fig. 5a,b). A thick unit of massive, brown, matrix to clast-supported, polymictic cobble to boulder conglomerate of the Tanglefoot formation overlies the Mandanna member (Fig. 4a). The overlying conglomerate is composed of subrounded to rounded, poorly sorted, volcanic and plutonic clasts with minor sedimentary clasts that range in size from 0.3 to 127 cm (Fig. 5c). Felsic plutonic rocks make up the greatest fraction of the boulder-sized clasts, whereas volcanic and sedimentary clasts make up finer clast sizes. The matrix is buff coloured, medium to coarse-grained, poorly sorted sandstone (Fig. 5d). The contact at Conglomerate Mountain is covered but interpreted to be unconformable.

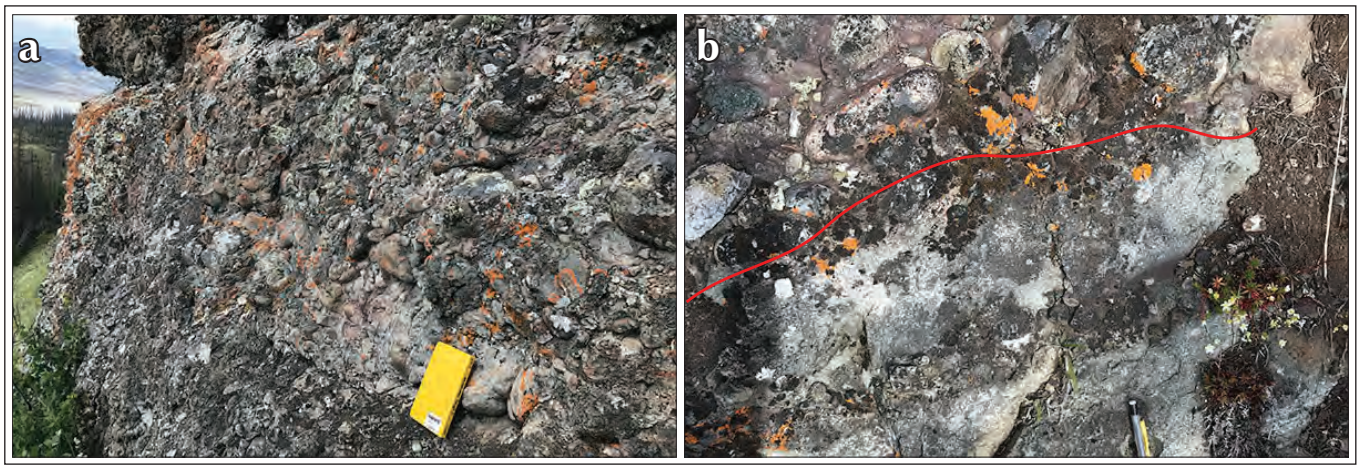

Figure 3. *Field photographs of the Tanglefoot formation at Mandanna Lake.* ***(a)*** *Poorly sorted cobble to boulder conglomerate; and* ***(b)*** *annotated photo of the contact between conglomerate (top) and medium to coarse-grained sandstone (bottom).*

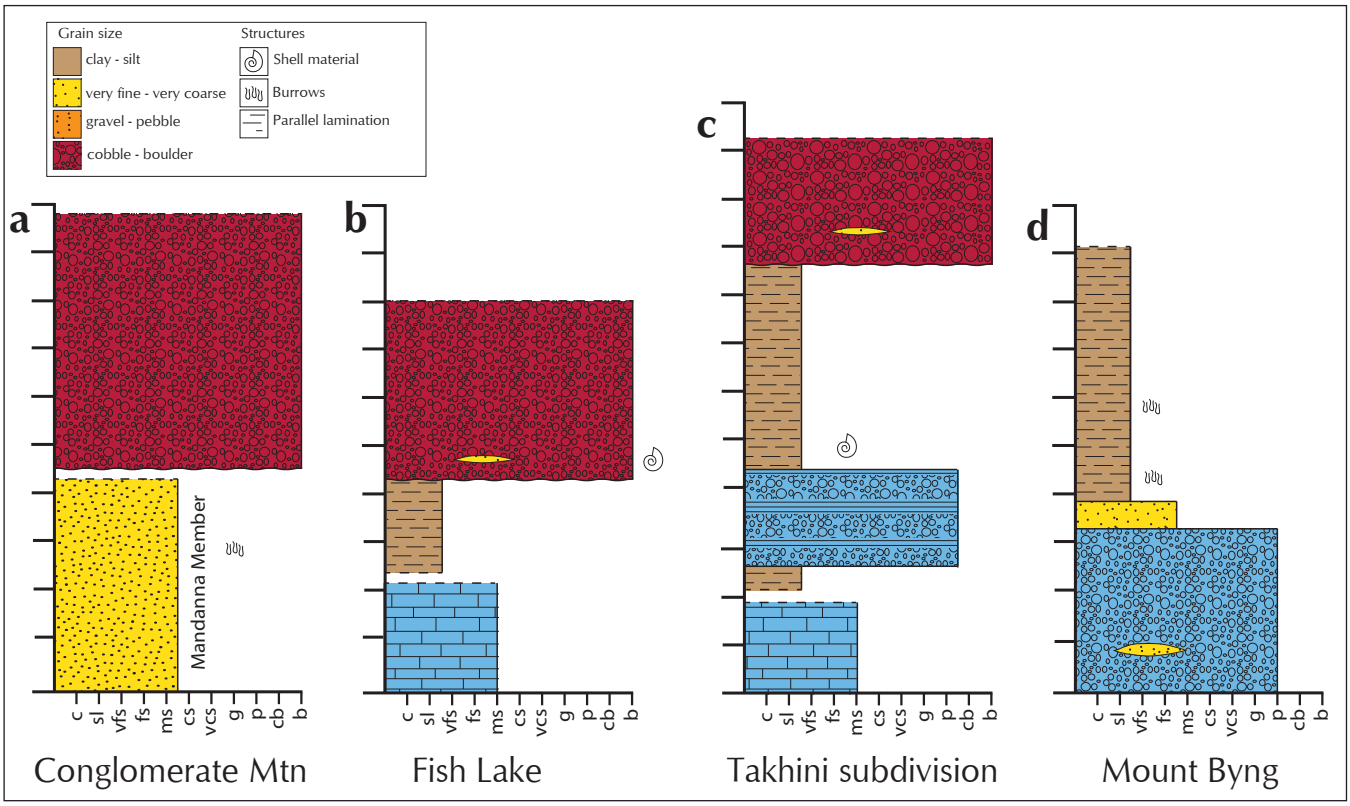

Figure 4. *Schematic stratigraphy at* ***(a)*** *Conglomerate Mountain,* ***(b)*** *Fish Lake,* ***(c)*** *Takhini subdivision, and* ***(d)*** *Mount Byng. Grain size abbreviations: c=clay, sl=silt, vfs=very fine grained, fs=fine-grained, ms=medium-grained, cs=coarse-grained, vcs=very coarse grained, g=granule, p=pebble, cb=cobble, b=boulder.*

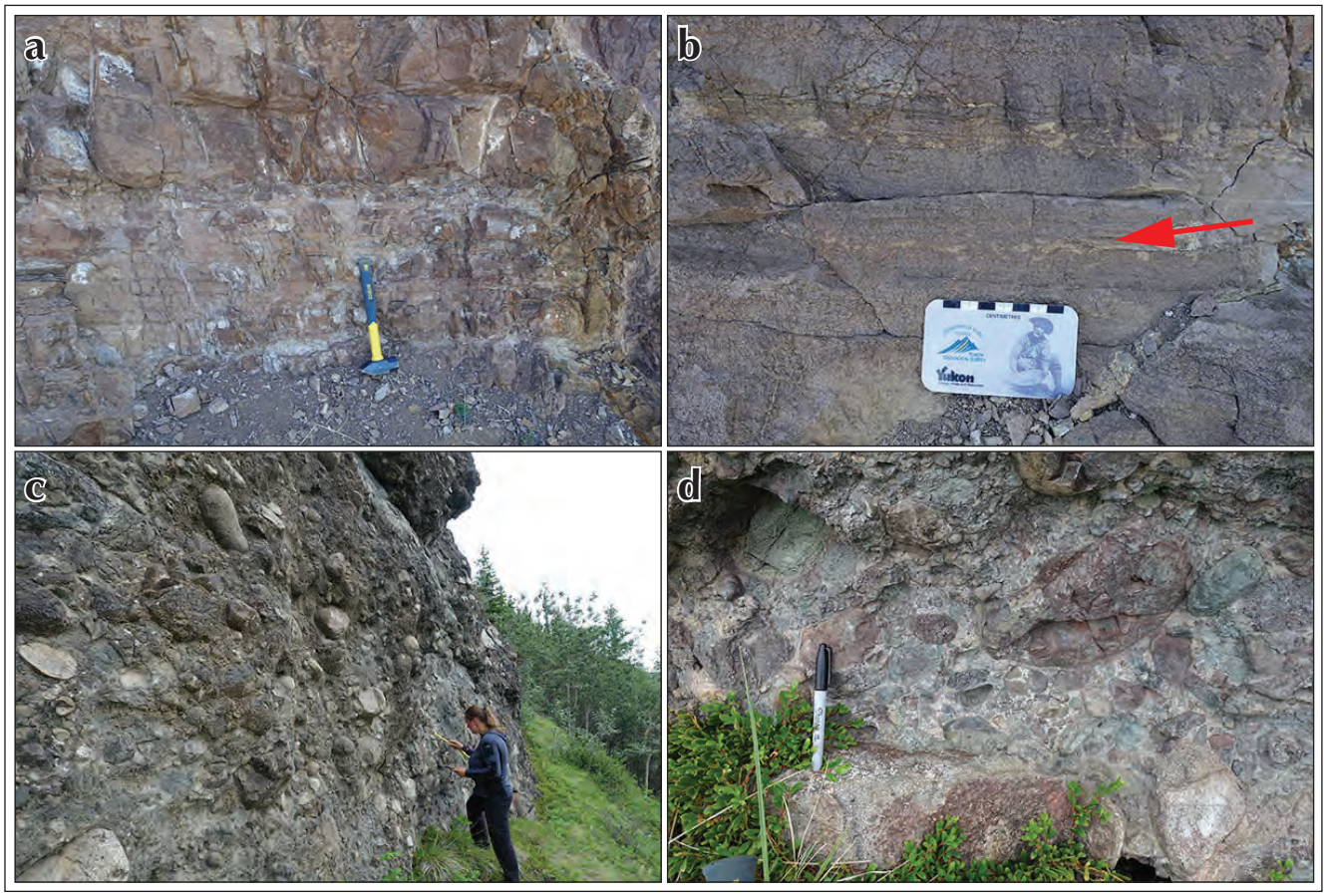

Figure 5. *Field photographs of the Tanglefoot formation at Conglomerate Mountain.* ***(a)*** *Medium to coarse-grained, poorly sorted, massive Mandanna formation sandstone;* ***(b)*** *example of burrows in the Mandanna formation;* ***(c)*** *outcrop scale photo of Laberge Group polymictic pebble to boulder conglomerate; and* ***(d)*** *fresh surface of Laberge Group polymictic pebble to boulder conglomerate.*

RICHTHOFEN FORMATION

Fish Lake

Basal Laberge Group strata crop out in the Fish Lake area ~16 km southwest of Whitehorse and are inferred to overlie the Mandanna member sandstone and Aksala formation limestone (Fig. 1; zone 08V, 485805 E, 6721676 N, NAD 83). At this locality, the contact is covered and not directly observed; basal strata are inferred by the proximity to limestone. The ridge west of Fish Lake comprises massive, brown, matrix-supported, pebble to cobble, poorly sorted, polymictic conglomerate that overlies dark blue, very fine to fine-grained sandstone of the Richthofen formation (Fig. 4b). Conglomerate units at this locality consist of subrounded to rounded clasts of felsic plutonic, volcanic and metamorphic rocks that range in size from 1 to 8 cm (Fig. 6a). Plutonic and volcanic clasts are the most abundant; three foliated mafic rock clasts were also observed (Fig. 6b,c). A recrystallized ammonite (Fig. 6d) from a dark blue, medium-grained sandstone lens near the contact with the Lewes River Group was collected for biostratigraphic analysis. Fine-grained maroon clasts are also present in the sandstone lens, which likely indicates proximity to the Mandanna member, although it does not crop out at this locality. Along the southern end of the ridge, very fine grained, dark blue Richthofen formation sandstone with buff coloured laminae underlies the conglomerate and is locally intruded by rhyolite dikes. Basal Laberge Group strata also crop out along the eastern side of Fish Lake (Fig. 1; zone 08V, 488343 E, 6724611 N, NAD 83). This locality is characterized by pebble to cobble, subrounded to rounded, poorly sorted, polymictic (felsic plutonic and volcanic) conglomerate with fine to medium-grained sandstone lenses, comparable to strata immediately west. The contact at Fish Lake is interpreted to be unconformable.

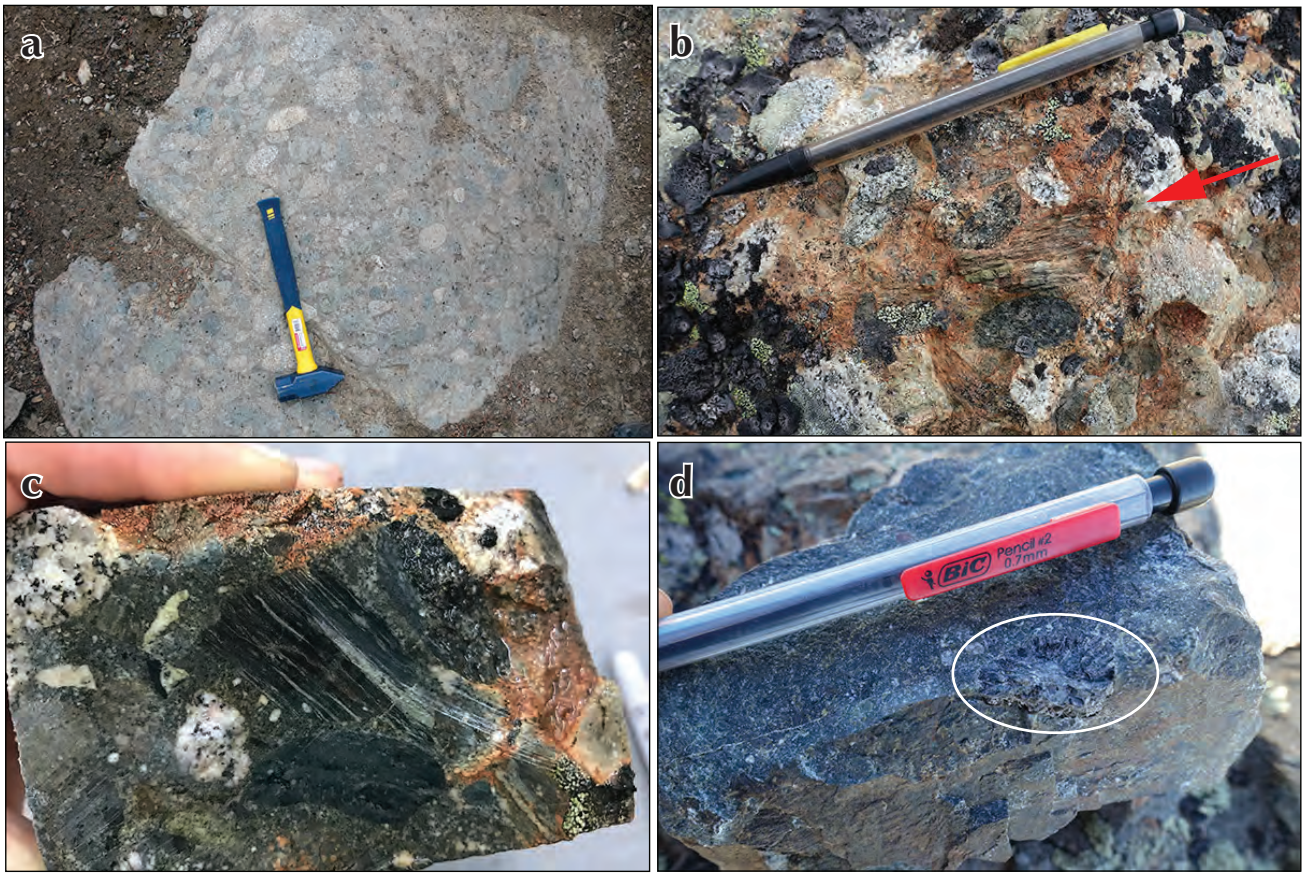

Figure 6. *Field photographs of the Richthofen formation at Fish Lake.* ***(a)*** *Laberge Group polymictic pebble to cobble conglomerate;* ***(b)*** *foliated mafic clast in the conglomerate annotated by red arrow;* ***(c)*** *fresh surface of the same clast from b; and* ***(d)*** *ammonite fossil in dark blue medium-grained sandstone lens.*

Takhini subdivision

Basal Laberge Group strata overlie limestone of the Askala formation in the Takhini subdivision area (Figs. 1 and 4c; zone 08V, 488086 E, 6748844 N, NAD 83). The base of this section consists of monomictic limestone conglomerate and laminated limestone (Fig. 7a). Conglomeratic beds range from 14 to 28 cm thick, whereas laminated beds range from 7 to 10 cm thick. Conglomerate clasts are white to dark blue in a dark blue carbonate matrix (Fig. 7a). The limestone unit is overlain by dark blue, very fine to fine-grained, mudstone/sandstone couplets and pebble to cobble, rounded to subrounded, poorly sorted conglomerate of the Richthofen formation (Fig. 7b) that is intruded by fine-grained intermediate dikes. Ammonite and gastropod fossils occur in very fine to fine-grained sandstone beds directly overlying limestone beds. The contact at Takhini subdivision is interpreted as unconformable.

King Lake

Basal Laberge Group strata crop out near King Lake ~20 km northwest of Whitehorse (Fig. 1). At this locality, crystal (quartz, feldspar) lithic tuff of the Nordenskiöld dacite nonconformably overlies Late Triassic gabbro of the Povoas formation (zone 08V, 474374 E, 6742564 N, NAD 83; Fig. 8a,b). Poorly sorted, polymictic pebble to cobble conglomerate of the Richthofen formation (Fig. 8c) overlies the tuff and is the dominant lithology that makes up the prominent ridges around King Lake. Subrounded to rounded clasts range from 1 to 8 cm. Conglomerate units at this locality are very weathered and typically not well exposed, but the clasts appear to be volcanic and felsic plutonic rocks.

Figure 7. *Field photographs of the Richthofen formation at Takhini subdivision.* ***(a)*** *Monomictic limestone conglomerate and laminated limestone; and* ***(b)*** *contact between dark blue very fine to fine-grained sandstone and mudstone couplets and pebble to boulder conglomerate.*

Figure 8. *Field photographs of the Richthofen formation at King Lake.* ***(a)*** *Contact between Nordenskiöld dacite crystal lithic tuff and Povoas formation gabbro;* ***(b)*** *fresh surface of crystal lithic tuff; and* ***(c)*** *Laberge Group polymictic pebble to cobble conglomerate.*

Mount Byng

Northeast of Mount Byng, the Richthofen formation overlies limestone that is currently mapped as undifferentiated Aksala formation (Fig. 4d; zone 08V, 539547 E, 6757952 N, NAD 83; Hart and Radloff, 1990). The base of this section consists of light grey-blue, pebble to cobble, poorly sorted, clast to matrix-supported, limestone conglomerate (Fig. 9a). Subrounded to rounded limestone clasts that range in size from 1 to 7 cm are the most abundant components in the conglomerate. Subrounded to rounded, pebble-sized, dark grey volcanic porphyry clasts are less abundant. The limestone unit is overlain by dark grey-blue, very fine to fine-grained Richthofen formation sandstone with buff coloured laminations. Richthofen formation strata at this location are comparable to those in other areas of the Whitehorse trough and typically characterized by fining-up mudstone and sandstone couplets (Fig. 9b) with rare burrows. Couplets range in thickness from 0.5 to 3 cm, with very fine grained material making up darker coloured beds and the fine-grained sand characterizing buff coloured beds. Contacts between beds are often wavy and buff coloured beds locally pinch and swell (Fig. 9c). The contact between the Laberge Group and Lewes River Group at Mount Byng is interpreted to be unconformable.

Mount Slim

Basal Laberge Group strata crop out at two localities southeast of Mount Slim, located ~20 km northeast of Whitehorse. In this area, the Richthofen formation overlies volcaniclastic sandstone and limestone of the Aksala formation. At the first locality, dark grey mudstone and buff coloured sandstone couplets of the Richthofen formation overlie green, fine to medium-grained sandstone mapped as the Casca member (Fig. 1; zone 08V, 517754 E, 6746129 N, NAD 83; Hart and Radloff, 1990; Fig 10a). Nearby dikes give the weathered surface of Richthofen formation strata a rusty, red-brown colour. At the second locality, the Richthofen formation unconformably overlies grey-blue limestone of the Aksala formation (zone 08V, 514475 E, 6751661 N, NAD 83). Dark grey, 0.2 to 2 cm unlined burrows are abundant at this locality and typically occur in buff-coloured beds (Fig. 10b,c). Smaller burrows are parallel to bedding, whereas larger burrows are vertical (Fig. 10b,c). Burrowed mudstone and sandstone couplets at this location resemble Richthofen formation strata described along the eastern shore of Lake Laberge during the 2016 field season (van Drecht *et al.*, 2017). The contacts between the Laberge Group and Lewes River Group in the Mount Slim area are interpreted to be unconformable.

Figure 9. *Field photographs of the Richthofen formation at Mount Byng.* ***(a)*** *Pebble to cobble limestone conglomerate;* ***(b)*** *Richthofen formation mudstone and sandstone couplets; and* ***(c)*** *example of wavy contacts between mudstone and sandstone couplets.*

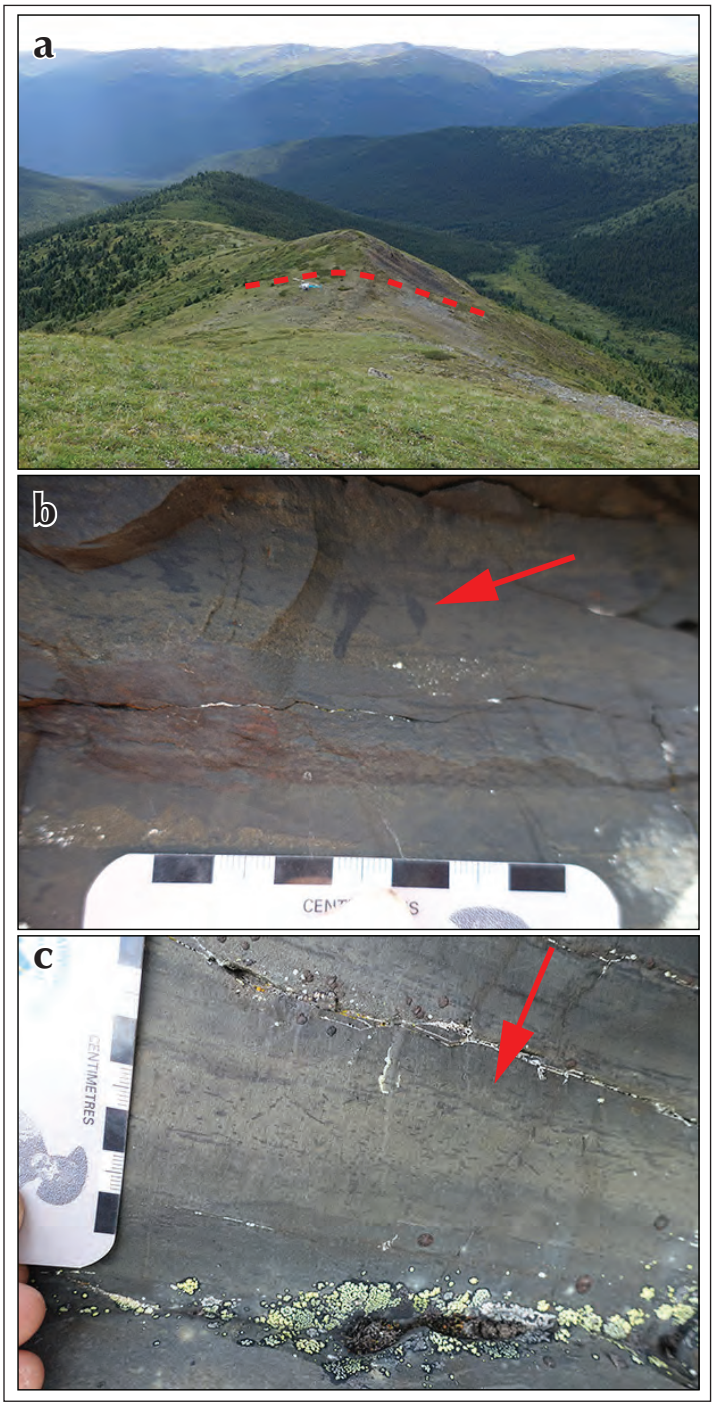

Figure 10. *Field photographs of the Richthofen formation at Mount Slim.* ***(a)*** *Rusty, red weathering Richthofen formation (near helicopter; above red line) overlying sandstone of the Askala formation (foreground; below red line);* ***(b)*** *vertical burrows in Richthofen formation mudstone and sandstone couplets; and* ***(c)*** *horizontal burrows in Richthofen formation mudstone and sandstone couplets.*

CONCLUSIONS

The Laberge Group-Lewes River Group contact observed at various locations during summer 2017 is apparently unconformable, which is consistent with a period of latest Triassic-earliest Jurassic erosion and/or nondeposition across the Whitehorse trough (*e.g.,* Lowey, 2008). The Laberge Group overlies multiple Carnian to Rhaetian units of the Lewes River Group, likely due to a combination of the complex internal stratigraphy and/or exhumation of the Whitehorse trough shoulders, creating topography prior to Early Jurassic sedimentation in central Yukon. The Lewes River Group is interpreted as a volcanic arc complex that formed a topographic high and was fringed by reef buildups and shallow lagoons (Bordet, 2017). The complex paleotopography created by the Late Triassic volcanic arc was further enhanced by the widespread exhumation and erosion, suggested by the unconformable relationships with the overlying Laberge Group. Variable paleotopography within the Lewes River Group in the latest Triassic-earliest Jurassic likely influenced paleodrainage pathways during Early to Middle Jurassic Laberge Group deposition.

In the northern apex of the trough, basal Tanglefoot formation rocks overlie the Norian-Rhaetian carbonate sequences of the Aksala formation at Mandanna Lake and Rhaetian Mandanna member at Conglomerate Mountain. In the central region of the trough, basal Richthofen formation rocks overlie carbonate sequences of the Aksala formation at Takhini subdivision and Fish Lake as well as clastic rocks of the Aksala formation at Mount Slim and the Carnian Povoas formation at King Lake. This suggests that latest Triassic-earliest Jurassic exhumation and erosion of the Lewes River Group may have been greater on the western flank of the trough to expose mafic volcanic rocks of the Povoas formation, prior to Laberge Group sedimentation. The contact between the Povoas formation gabbro and basal Laberge Group strata at King Lake may also suggest that exhumation was followed by rapid subsidence, allowing basal Laberge Group strata to transgress west.

Proximal Tanglefoot formation strata at Mandanna Lake and Conglomerate Mountain are consistent with deposition in a submarine mass-flow fan setting. Distal strata of the Richthofen formation described at Fish Lake, Takhini subdivision, King Lake, Mount Byng and Mount Slim are indicative of turbiditic facies and consistent with deposition in a distal submarine fan setting. Although rare, the foliated mafic rock clasts at Fish Lake suggest that

these Laberge Group units may represent Pliensbachian or younger conglomeratic beds, as metamorphic rock fragments are only observed in such strata in northern British Columbia (Shirmohammad *et al.,* 2011). This may indicate a potentially younger depositional age for basal strata at this locality, relative to basal strata in the western region of the trough. It is uncertain whether limestone conglomerate at the Takhini subdivision and Mount Byng field localities belong to the uppermost Lewes River Group or basal Laberge Group.

Stratigraphic constraints and detrital zircon U-Pb and Hf isotope studies of samples collected during the 2016 and 2017 field seasons will be used to test the Sinemurian to Toarcian transgression of basal Laberge Group strata westward across the Whitehorse trough. Isotopic studies will also be used to more fully define the depositional age, provenance and paleodrainage history of Laberge Group rock units and provide new insights on the evolution of the Intermontane terranes in the northern Canadian Cordillera.

ACKNOWLEDGEMENTS

Field logistics for this project were supported by the Yukon Geological Survey. We are grateful to Maurice Colpron for helpful field discussions and Pia Blake and Alexina Boileau for field assistance. TRK provided excellent helicopter support. Esther Bordet provided valuable discussions and constructive comments that improved this manuscript. Karen MacFarlane provided helpful editorial comments.

REFERENCES

Beranek, L.P. and Mortensen, J.K., 2011. The timing and provenance record of the Late Permian Klondike orogeny in northwestern Canada and arc-continent collision along western North America. Tectonics, vol. 30, TC5017, doi: 10.1029/2010TC002849.

Bordet, E., 2016a. Preliminary results on the Middle Triassic-Middle Jurassic stratigraphy and structure of the Teslin Mountain area, southern Yukon. *In:* Yukon Exploration and Geology 2015, K.E. MacFarlane and M.G. Nordling (eds.), Yukon Geological Survey, p. 43-61.

Bordet, E., 2016b. Bedrock geology map of the Teslin Mountain and East Lake Laberge areas, parts of NTS 105E/2, 3 and 6. Yukon Geological Survey, Open File 2016-38, scale 1:50000.

Bordet, E., 2017. Updates on the Middle Triassic-Middle Jurassic stratigraphy and structure of the Teslin Mountain and east Lake Laberge areas, south-central Yukon. *In:* Yukon Exploration and Geology 2016, K.E. MacFarlane and L.H. Weston (eds.), Yukon Geological Survey, p. 1-24.

Bostock, H.S. and Lees, E.J., 1938. Laberge map-area, Yukon. Geological Survey of Canada, Memoir 217, 32 p.

Cairnes, D.D., 1910. Preliminary memoir on the Lewes and Nordenskiöld rivers coal district, Yukon Territory. Geological Survey of Canada, Memoir 5, 70 p.

Cant, D.J. and Stockmal, G.S., 1989. The Alberta foreland basin: Relationships between stratigraphy and Cordilleran terrane-accretion events. Canadian Journal of Earth Sciences, vol. 26, p. 1964-1975.

Cockfield, W.E. and Bell, A.H., 1926. Whitehorse District, Yukon. Geological Survey of Canada, Memoir 150, 63 p.

Colpron, M., Gordey, S.P., Lowey, G.W., White, D. and Piercey, S.J., 2007. Geology of the northern Whitehorse trough, Yukon (NTS 105E/12, 13, and parts of 11 and 14; 105L/4 and parts of 3 and 5; parts of 115H/9 and 16; 115I/1 and part of 8) (1:150000 scale). Yukon Geological Survey, Open File 2007-6.

Colpron, M. and Friedman R.M., 2008. U-Pb zircon ages for the Nordenskiöld formation (Laberge Group) and Cretaceous intrusive rocks, Whitehorse trough, Yukon. *In*: Yukon Exploration and Geology 2007, D.S. Emond, L.R. Blackburn, R.P. Hill and L.H. Weston (eds.). Yukon Geological Survey, p. 139-151.

Colpron, M., Crowley, J.L., Gehrels, G., Long, D.G.F., Murphy, D.C., Beranek, L. and Bickerton, L., 2015. Birth of the northern Cordilleran orogeny, as recorded by detrital zircons in Jurassic synorogenic strata and regional exhumation in Yukon. Lithosphere, vol. 7, p. 541-562.

Colpron, M., Israel, S. and Hutchison, M., 2016. Tectonics of the Intermontane and Insular terranes, and development of Mesozoic synorogenic basins in southern Yukon: Carmacks to Kluane Lake. GAC®-MAC 2016 Whitehorse Field Trip Guidebook, June 4-6.

Dawson, G.M., 1887. Report on exploration in the Yukon District, N.W.T., and adjacent northern portion of British Columbia. Geological Survey of Canada, Annual Report, vol. 3, part B, 277 p.

Dickie, J.R. and Hein, R.J., 1988. Facies and depositional setting of Laberge conglomerates (Jurassic), Whitehorse Trough, Yukon. *In:* Yukon Geology Volume 2, J.G. Abbott (ed.), Exploration and Geological Services Division, Indian and Northern Affairs Canada, p. 26-32.

Dickie, J.R. and Hein, R.J., 1995. Conglomeratic fan deltas and submarine fans of the Jurassic Laberge Group, Whitehorse Trough, Yukon Territory, Canada: fore-arc sedimentation and unroofing of a volcanic arc complex. Sedimentary Geology, vol. 98, p. 263-292.

Hart, C.J.R. and Radloff, J.K., 1990. Geology of Whitehorse, Alligator lake, Fenwick Creek, Carcross and Part of Robinson Map Areas (105D/11, 6, 3, 2 & 7). Yukon Geological Survey, Open File 1990-4(G), scale 1:50 000.

Hart, C.J.R., Dickie, J.R., Ghosh, D.K. and Armstrong, R.L., 1995. Provenance constraints for Whitehorse Trough conglomerate: U-Pb zircon dates and initial Sr ratios of granitic clasts in Jurassic Laberge Group, Yukon Territory. *In:* Jurassic Magmatism and Tectonics of the North American Cordillera, D.M Miller and C. Busby (eds.), Geological Society of America Special Paper 299, p. 47-63.

Hutchison, M.P. 2017. Whitehorse trough: Past, present and future petroleum research – with a focus on reservoir characterization of the northern Laberge Group. Yukon Geological Survey, Open File 2017-2, 48 p.

Johnston, S.T., Mortensen, J.K. and Erdmer, P., 1996. Igneous and metaigneous age constraints for the Aishihik metamorphic suite, southwest Yukon. Canadian Journal of Earth Sciences, vol. 33, p. 1543-1555.

Joyce, N., Ryan, J.J., Colpron, M., Murphy, D.C. and Hart, C.J.R., 2015. Compilation of 40Ar/39Ar ages for southern Yukon. Geological Survey of Canada, Open File 7924.

Knight, E., Schneider, D.A. and Ryan, J.J., 2013. Thermochronology of the Yukon-Tanana terrane, west-central Yukon: Evidence for Jurassic extension and exhumation in the northern Canadian Cordillera. The Journal of Geology, vol. 121, p. 371-400.

Logan, J.M. and Mihalynuk, M.G., 2014. Tectonic controls on early Mesozoic paired alkaline porphyry deposit belts (Cu-Au ± Ag-Pt-Pd-Mo) within the Canadian Cordillera. Economic Geology, vol. 109, p. 827-858.

Lowey, G.W., 2004. Preliminary lithostratigraphy of the Laberge Group (Jurassic), south-central Yukon: Implications concerning the petroleum potential of the Whitehorse trough. *In:* Yukon Exploration and Geology 2003, D.S. Emond and L.L. Lewis (eds.), Yukon Geological Survey, p. 129-142.

Lowey, G.W., 2008. Summary of the stratigraphy, sedimentology and hydrocarbon potential of the Laberge Group (Lower-Middle Jurassic), Whitehorse trough, Yukon. *In*: Yukon Exploration and Geology 2007, D.S. Emond, L.R. Blackburn, R.P. Hill and L.H. Weston (eds), Yukon Geological Survey, p.179-197.

Lowey, G.W., Long, D.G.F., Fowler, M.G., Sweet, A.R. and Orchard, M.J., 2009. Petroleum source rock potential of Whitehorse trough: A frontier basin in south-central Yukon. Bulletin of Canadian Petroleum Geology, vol. 57, p. 350-386.

Mihalynuk, M.G., Nelson, J.A. and Diakow, L.J., 1994. Cache Creek terrane entrapment: Oroclinal paradox within the Canadian Cordillera. Tectonics, vol. 13, p. 575-595.

Nelson, J.L., Colpron, M. and Israel, S. 2013. The Cordillera of British Columbia, Yukon, and Alaska: Tectonics and Metallogeny (Chapter 3). *In:* Tectonics, Metallogeny and discovery: The North American Cordillera and similar accretionary settings, M. Colpron, T. Bissig, B.G. Rusk and J.F.H. Thompson (eds.), Society of Economic Geologist, Special Publication Number 17, p. 53-109.

Shirmohammad, F., Smith, P.L., Anderson, R.G. and McNicoll, V.J. 2011. The Jurassic succession at Lisadale Lake (Tulsequah map area, British Columbia, Canada) and its bearing on the tectonic evolution of the Stikine terrane. Volumina Jurassica, vol. 9, p. 43-60.

Tempelman-Kluit, D.J., 1984. Geology, Laberge (105E) and Carmacks (115I), Yukon Territory. Geologic Survey of Canada, Open File 1101, 10 p.

Tozer, E., 1958. Stratigraphy of the Lewes River Group (Triassic), central Laberge area, Yukon Territory. Geological Survey of Canada, Bulletin 43, 28 p.

van Drecht, L.H., Beranek, L.P. and Hutchison, M., 2017. Jurassic stratigraphy and tectonic evolution of the Whitehorse trough, central Yukon: Project outline and preliminary field results. *In:* Yukon Exploration and Geology 2016, K.E. MacFarlane and L.H. Weston (eds.), Yukon Geological Survey, p. 207-223.

Wheeler, J.O., 1961. Whitehorse map-area, Yukon Territory. Geological Survey of Canada, Memoir 312, 156 p.

YUKON GEOLOGICAL SURVEY

Yukon Geological Survey staff are located in two buildings in Whitehorse: the Elijah Smith Building at 300 Main Street, rooms 102 and 230, and the H.S. Bostock Core Library at Mile 918 on the Alaska Hwy.

BRANCH DIRECTOR

H.S. Bostock Core Library

Relf, Carolyn – Director, (867) 667-8892 carolyn.relf@gov.yk.ca

OPERATIONS

H.S. Bostock Core Library

Minor, Julie – Manager, Finance & Operations, (867) 667-8508 julie.minor@gov.yk.ca
Kirby, Midori – Administrative Assistant, (867) 667-3201 midori.kirby@gov.yk.ca

OUTREACH

H.S. Bostock Core Library

Weston, Leyla – Outreach Geologist, (867) 455-2808 leyla.weston@gov.yk.ca

REGIONAL GEOLOGY

H.S. Bostock Core Library

Colpron, Maurice – Head, Regional Geology, (867) 667-8235 maurice.colpron@gov.yk.ca
Bordet, Esther – Project Geologist, (867) 455–2804 esther.bordet@gov.yk.ca
Cobbett, Rosie – Project Geologist, (867) 455–2802 rosie.cobbett@gov.yk.ca
Fraser, Tiffani – Petroleum Geologist, (867) 667–3228 tiffani.fraser@gov.yk.ca
Israel, Steve – Project Geologist, (867) 667–5175 steve.israel@gov.yk.ca
Moynihan, David – Project Geologist, (867) 455–2805 david.moynihan@gov.yk.ca

SURFICIAL GEOLOGY

Elijah Smith Building

Bond, Jeff – Head, Surficial Geologist, (867) 667–8514 jeff.bond@gov.yk.ca
Kennedy, Kristen – Surficial Geologist, (867) 393–7188 kristen.kennedy@gov.yk.ca
Lipovsky, Panya – Surficial Geologist, (867) 667–8520 panya.lipovsky@gov.yk.ca
van Loon, Sydney – Placer Geologist, (867) 667-3408 sydney.vanloon@gov.yk.ca

MINERALS GEOLOGY

Elijah Smith Building

Casselman, Scott – Head, Minerals Geology, (867) 667–8195 scott.casselman@gov.yk.ca
Deklerk, Robert – MINFILE Geologist, (867) 667–3205 robert.deklerk@gov.yk.ca
Lewis, Lara – Economic Geologist, (867) 667–8518 lara.lewis@gov.yk.ca
Sack, Patrick – Economic Geologist, (867) 667–3203 patrick.sack@gov.yk.ca
Torgerson, Derek – Yukon Mineral Exploration Program, (867) 456–3828 derek.torgerson@gov.yk.ca

H.S. Bostock Core Library

Nicholson, Craig – Core Library Manager, (867) 393-6492 craig.nicholson@gov.yk.ca

EDITORIAL & TECHNICAL SERVICES

Elijah Smith Building

MacFarlane, Karen – Head, Technical Services, (867) 667–8519 karen.macfarlane@gov.yk.ca
Bruce, Olwyn – Geological Spatial Data Administrator, (867) 393–7186 olwyn.bruce@gov.yk.ca
Elliot, Brett – Geological Spatial Database Administrator, (867) 667–8481 brett.elliot@gov.yk.ca
Staffen, Bailey – GIS Technician/Web Manager, (867) 456–6801 bailey.staffen@gov.yk.ca